

HEALTH FUNCTIONALITY OF AGRICULTURAL PRODUCTS AND AGRICULTURAL BY-PRODUCTS

by

Samanthi Wathsala Pelpolage

A THESIS

Submitted in partial fulfilment of the requirements for the degree

DOCTOR OF PHILOSOPHY

The United Graduate School of Agricultural Sciences

Iwate University

Bioresources Science (Utilization of Bioresources)

Department of Life and Food Sciences

Obihiro University of Agriculture and Veterinary Medicine

2019

農産物および農産副産物の健康機能性について

Samanthi Wathsala Pelpolage

博士論文

岩手大学大学院連合農学研究科

生物資源科学専攻

生物資源利用学講座

帯広畜産大学所属

2019

Table of Contents

List of Figures	vi-viii
List of Tables	ix-x
Acknowledgement	xi-xii
Chapter 1 – Literature Review	
1.1. General Introduction	2-4
1.2. Plant indigestible matter (Dietary Fiber) – their biochemistry and sources	4-7
1.3. Plant indigestible matter in human nutrition- A colonic fermentation perspective	7-17
1.3.1. Principles and overview of colonic fermentation	7-10
1.3.2. Importance of short chain fatty acids in physiology	10-13
1.3.3. Diversity and differential benefits of prebiotic fibers	13-17
1.4. Gut microbiota, dietary fiber and health impairments	18-23
1.4.1. Gut microbial diversity	18-21
1.4.2. Dysbiosis and health disorders.....	21-23
1.5. Research statement and objectives.....	24
Chapter 2 - <i>In vitro</i> fermentation characteristics of Sorghum (<i>Sorghum bicolor</i> L. Moench) enzyme resistant fraction (ERF)	
2.1. Introduction.....	26-36
2.1.1. Structure and organization of the sorghum grain.....	26-27
2.1.2. Starch digestibility	27-31
2.1.3. Factors affecting the resistant starch content in sorghum.....	31-33
2.1.4. Fermentation potential of sorghum.....	33-34
2.1.5. Research statement, objectives and hypothesis	35-36
2.2. Material and Methods	37-51
2.1.1. Materials	37
2.2.2. Preparation of sorghum flour enzymes resistant fraction (ERF) by <i>in vitro</i> enzymatic digestion	37
2.2.3. Proximate composition analysis of the ERFs	38-40
2.2.4. <i>In vitro</i> intestinal fermentation model.....	41-42

2.2.5. Microbiological analyses	42-49
2.2.6. Short chain fatty acid analysis in fermenter media.....	49-50
2.2.7. Ammonia-nitrogen analysis	50-51
2.2.8. Statistical analysis.....	51
2.3. Results and Discussion	52-63
2.3.1. Proximate composition of ERFs and <i>in vitro</i> digestibility of sorghum flour	52
2.3.2. Microbiota composition in the fermenter media during the fermentation period.....	53-56
2.3.3. pH in the fermenter media	56-57
2.3.4. Short chain fatty acid production.....	57-61
2.3.5. Ammonia-nitrogen content	61-63
2.4. Implications and Conclusions to Chapter 2	64-65
Figures.....	66-77
Tables.....	78-86

Chapter 3 - Colonic fermentation characteristics of raw sorghum flour in murine models

3.1. Introduction.....	88-97
3.1.1. Sorghum protein digestibility	89-91
3.1.2. Protein metabolism in the colon	91-93
3.1.3. Confounding effects between carbohydrate and protein in a substrate on colonic fermentation	94-95
3.1.4. Research statement, objectives and hypothesis	96-97
3.2. Material and Methods	98-104
3.2.1. Preparation of experimental diets	98
3.2.2. Animal experimental design, maintenance and post-mortem excision of organs	98-99
3.2.3. Rat cecal bacterial DNA extraction, sequencing and analysis of 16S rRNA sequences	100
3.2.4. Rat cecal short chain and branched-chain fatty acid analysis.....	100
3.2.5. Ammonia-nitrogen analysis in cecal samples.....	100
3.2.6. Immunoglobulin A (IgA) in cecal samples.....	101-102
3.2.7. Mucin analysis in cecal samples	102-103
3.2.8. Serum biochemical analysis.....	103
3.2.9. Statistical analysis.....	103-104

3.3. Results and Discussion	105-117
3.3.1. Zoometric parameters, feed intake and organ weights	105-106
3.3.2. Microbial community DNA data	106-108
3.3.3. Cecal short chain fatty acid content and pH	108-110
3.3.4. Ammonia-nitrogen content and branched chain fatty acid content in the cecal content	110-112
3.3.5. Immunoglobulin A (IgA) content in cecal content.....	112-113
3.3.6. Mucin content in cecal content	114-115
3.3.7. Serum biochemical data.....	115-117
3.4. Implications and Conclusions to Chapter 3	118-119
Figures.....	120-130
Tables.....	131-139

Chapter 4 - Effect of cooking on the colonic fermentation potential of sorghum and potential physiological benefits

4.1. Introduction.....	141-149
4.1.1. Scientific background of cooking of starch	142-143
4.1.2. Effect of thermal processing on the native resistant starch contents and functionality	143-144
4.1.3. Effect of thermal processing on sorghum digestibility	145-147
4.1.4. Research statement, objectives and hypothesis	148-149
4.2. Materials and Methods.....	150-160
4.2.1. Preparation of experimental diets	150-151
4.2.2. Animal experimental design, care for laboratory animals and post-mortem excision of organs	151-152
4.2.3. Rat cecal bacterial DNA extraction, sequencing and analysis of 16S rRNA sequences	152
4.2.4. Rat cecal short chain and branched-chain fatty acid analysis.....	152-153
4.2.5. Determination of cecal ammonia-nitrogen content.....	153
4.2.6. Analysis of mucin content in rat cecal digesta.....	153-154
4.2.7. Analysis of cecal Immunoglobulin A (IgA) content.....	154
4.2.8. Fecal and liver lipid profile analysis	154-156
4.2.9. Histological procedure for mesenteric adipocyte staining	157-159

4.2.10. Serum biochemical analysis.....	159
4.2.11. Statistical analysis.....	160
4.3. Results and Discussion	161-172
4.3.1. Zoometric parameters, feed intake and organ weights	161-162
4.3.2. Microbial community DNA data	162-163
4.3.3. Cecal short chain fatty acid content and pH	163-165
4.3.4. Liver lipid profile and fecal moisture and dry matter contents, lipid and bile acid profiles	165-168
4.3.5. Ammonia-nitrogen content and branched chain fatty acid content in the cecal content	168-169
4.3.6. Immunoglobulin A (IgA) content in cecal content.....	169-170
4.3.7. Mucin content in cecal content	170-171
4.3.8. Serum biochemical data.....	171-172
4.4. Implications and Conclusions to Chapter 4	173
Figures.....	174-182
Tables.....	183-191
Chapter 5 - Colonic fermentation characteristics of soluble fiber fraction of sugarcane (<i>Saccharum officinarum</i> L.) bagasse	
5.1. Introduction – sugarcane bagasse and bagasse xylan	193-196
5.1.1. Beneficial effects of Xylooligosaccharides	196-197
5.1.2. Colonic fermentation potential of Xylooligosaccharides	197-199
5.1.3. Research statement, objectives and hypothesis	200
5.2. Materials and Methods.....	201-205
5.2.1. Preparation of experimental diets	201
5.2.2. Animal experimental design, care for laboratory animals and post-mortem excision of organs	201-202
5.2.3. Rat cecal bacterial population analyses	202-203
5.2.4. Rat cecal short chain fatty acid analysis	203
5.2.5. Ammonia-nitrogen analysis in cecal suspension	203
5.2.6. Analysis of mucin content in rat cecal digesta.....	204

5.2.7. Analysis of Immunoglobulin A (IgA) content.....	204
5.2.8. Serum biochemical analysis.....	204
5.2.9. Fecal total lipid analysis.....	204
5.2.10. Statistical analysis.....	204-205
5.3. Results and Discussion	206-220
5.3.1. Feed intake, zoometric parameters and organ parameters	206
5.3.2. Short chain fatty acids in cecal digesta.....	207-208
5.3.3. Cecal microbial community data	209-215
5.3.4. Cecal ammonia-nitrogen content	215-216
5.3.5. Cecal mucin content.....	216-218
5.3.6. Cecal immunoglobulin A (IgA) content	218-219
5.3.7. Fecal moisture and total lipid content.....	219-220
5.3.8. Serum biochemical data.....	220
5.4. Implications and Conclusions to Chapter 5	221-222
Figures.....	223-230
Tables.....	231-236
General Conclusions	237-238
References	239-254
Summary (English)	255-257
Summary (Japanese)	258-259

List of Figures

Figure 2.1. <i>In vitro</i> simulator fermenter apparatus	66
Figure 2.2. Gel electrophoresis bands for quality assurance PCR samples	67
Figure 2.3. Selected microbial population counts in the fermenter media during the 48 h fermentation period	68
Figure 2.4. (a) Box and whisker plots of (a) Shannon’s diversity index and (b) Observed species index (c) PCoA plot for the β -diversity of the microbial community data.....	69
Figure 2.5. (a) Rank test bar chart for relative abundance of microbial taxa at phylum level. Pie charts for microbial composition at (b) order (c) class (d) family levels, respectively. (e) Linear discriminant analysis (LDA) effect size (LEfSe) plot at genus level (f) Rank test plots for selected microbial genera	70-72
Figure 2.6. Variation in the pH in fermenter media during the 48 h fermentation period.....	73
Figure 2.7. Variation in the SCFA concentrations in fermenter media during the 48 h fermentation period	74
Figure 2.8. Variation in the SCFA production rate in fermenter media during the 48 h fermentation period	75
Figure 2.9. Variation in the SCFA molar ratio at 6, 12, 24 and 48 h sampling points in the fermenter media during the 48 h fermentation period.....	76
Figure 2.10. Variation in the ammonia-nitrogen production in the fermenter media during the 48 h fermentation period.....	77
Figure 3.1. Schematic representation of the animal experimental design	120
Figure 3.2. Placement of feeder, drinker in the animal cage	120
Figure 3.3. Preparation of feeder for individual animals during the experimental period.....	121
Figure 3.4. Preparation of biotinylated detection antibody (streptavidin-conjugated horseradish peroxidase (HRP) conjugated Goat anti-Rat IgA detection antibody; 1 mg/ml) in the ratio of 1:75000	

.....	121
Figure 3.5. Box and whisker plot of (a) Shannon’s diversity index and (b) Observed species index (c) Weighted UniFrac PCoA plot for the β -diversity (d) Clustered bar chart at OUT level of the microbial community data.....	122
Figure 3.6. (a) Rank test bar charts for the relative abundance of dominant microbial phyla in the rat cecal digesta and (b) Linear discriminant analysis (LDA) effect size (LEfSe) plot at genus level	123
Figure 3.7. Rank test bar charts for the relative abundance of selected microbial species in the rat cecal digesta	124
Figure 3.8. Short chain fatty acid concentrations in the cecal content of rats	125
Figure 3.9. pH in the cecal content of rats	126
Figure 3.10. Cecal ammonia-nitrogen content of rats.....	127
Figure 3.11. Cecal branched-chain fatty acid contents in rats	128
Figure 3.12. Cecal immunoglobulin A (IgA) content of rats.....	129
Figure 3.13. Cecal mucin content in rats	130
Figure 4.1. Microscopic view of the mesenteric adipocyte area of rats.....	174
Figure 4.2. Box and whisker plots of (a) Shannon’s diversity index and (b) Observed species index (c) Weighted UniFrac PCoA plot for the β -diversity	175
Figure 4.3. Clustered bar chart at genus level for cecal microbiota.....	176
Figure 4.4. Rank test bar charts for the relative abundance of selected microbial species in the rat cecal digesta	177
Figure 4.5. Short chain fatty acid concentrations in the cecal content of rats	178
Figure 4.6. Cecal pH of rats	179
Figure 4.7. Cecal ammonia-nitrogen content of rats.....	180

Figure 4.8. Cecal immunoglobulin A (IgA) content of rats.....	181
Figure 4.9. Cecal mucin content of rats	182
Figure 5.1. Short chain fatty acid concentrations in the cecal content of rats	223
Figure 5.2. Viable plate counts of (a) Anaerobes (b) Coliform in the cecal content of rats	224
Figure 5.3. Box and whisker plots of (a) Shannon’s diversity index and (b) Observed species index (c) Weighted UniFrac PCoA plot for the β -diversity	225
Figure 5.4. (a) Rank test bar charts for the relative abundance of dominant microbial phyla in the rat cecal digesta and (b) Linear discriminant analysis (LDA) effect size (LEfSe) plot at genus level	226
Figure 5.5. Rank test bar charts for the relative abundance of selected microbial species in the rat cecal digesta	227
Figure 5.6. Cecal ammonia-nitrogen content of rats.....	228
Figure 5.7. Cecal mucin content of rats	229
Figure 5.8. Cecal Immunoglobulin A (IgA) content of rats.....	230

List of Tables

Table 2.1. Proximate composition of the enzyme resistant fractions (ERFs) of the two sorghum flours	78
Table 2.2. The nutrient composition of the fermenter media of control and the two sorghum ERFs	79
Table 2.3. Polymerase chain reaction (PCR) mix composition for quality assurance PCR	80
Table 2.4. PCR conditions for total bacteria	81
Table 2.5. The composition of agarose gel mixture.....	82
Table 2.6. PCR reaction mix for first stage PCR during 16S sequencing library preparation.....	83
Table 2.7. PCR conditions for first stage PCR during 16S sequencing library preparation	84
Table 2.8. PCR reaction mix for second stage PCR during 16S sequencing library preparation	85
Table 2.9. PCR conditions for second stage PCR during 16S sequencing library preparation	86
Table 3.1. Different fractions of sorghum prolamin and their characteristics	131
Table 3.2. Proximate composition of sorghum flour	132
Table 3.3. Experimental diet composition	133
Table 3.4. Random groups of similar body weight at the end of the acclimatization period.....	134
Table 3.5. Cecal supernatant dilution for IgA analysis	135
Table 3.6. Standard preparation for IgA analysis.....	136
Table 3.7. Standard series preparation for mucin analysis.....	137
Table 3.8. Zoometric parameters, feed intake and organ weights of rats	138
Table 3.9. Serum biochemical parameters of rats	139
Table 4.1. Different cooking conditions for sorghum grains and resistant starch contents	183
Table 4.2. Proximate composition analysis of cooked sorghum flour	184

Table 4.3. Experimental diet compositions	185
Table 4.4. Similar body weight groups prepared after acclimatization period	186
Table 4.5. Zoometric parameters, feed intake and organ parameters of rats	187
Table 4.6. Liver lipid content and fecal moisture content and lipid content of rats.....	188
Table 4.7. Fecal bile excretion in rats	189
Table 4.8. Cecal branched-chain fatty acid content in rats	190
Table 4.9. Serum biochemical parameters at the end of the experimental period in rats	191
Table 5.1. Proximate composition of hydrothermally decomposed bagasse water soluble fraction	231
Table 5.2. Experimental diet composition	232
Table 5.3. Random groups prepared at the end of the acclimatization period.....	233
Table 5.4. Feed intake, zoometric parameters, organ weight parameters and cecal pH in rats	234
Table 5.5. Fecal fresh and dry weights, moisture content and total lipid content in rats	235
Table 5.6. Serum biochemical parameters at the end of the experimental period in rats	236

Acknowledgement

I would like to extend my sincere gratitude to the Ministry of Education, Culture, Sports, Science and Technology (MEXT) of Japan, for the indispensable financial support through the MEXT scholarship.

Secondly, I would like to acknowledge The United Graduate School of Agricultural Sciences-Iwate University and Obihiro University of Agriculture and Veterinary Medicine, for their academic and financial support during this period.

I would like to express my heartfelt gratitude to my major advisor Professor Michihiro Fukushima, for his understanding, patience, timely guidance, prodigious support and above all his belief in my credibility, the independency and opportunities bestowed upon me.

Secondly to my second advisor, Associate Professor Kyu-Ho Han, for his sincere guidance and understanding, assistance with experimental procedures, critical comments and encouraging suggestions on oral and written manuscripts, which incited me to improve my research work substantially.

Further, to my third supervisor, Associate Professor Nao Inoue, for her insightful comments, constructive suggestions, guidance on my oral presentation style and content, after every academic society meeting and mid-term evaluation.

My sincere thanks goes to Professor Ken-ichiro Shimada, Assistant Professor Naoki Fukuma, Dr. Hiroki Bochimoto (M.D.) and Assistant Professor Matthew Links, who assisted with respective research procedures with their specialized skills, knowledge, guidance and access to laboratories and research facilities.

Further, I would like to acknowledge Emeritus Professor Hiroshi Koaze, for his continuous assistance, guidance, encouragement and support until today, since the very first day I have known him.

I would like to thank my colleague, Mr. Ryuji Nagata for his continuous support throughout this journey of three years in various aspects, be it an experimental procedure or reserving a flight, train, bus, hotel during academic meetings we participated around Japan or filling official forms.

I would like to thank my fellow labmates, who are and were part of the Laboratory of Nutritional Biochemistry, including Ms. Yuka Goto and Mr. Atsushi Yoshida, for their hard work and commitment during the research work.

Further, I would like to acknowledge the International Students' Association (OUISA), Tokachi International Relations Center (TIRC) and the community of Obihiro town for their immense support regarding personal matters, sincerity and hospitality.

Last but not least, I would like to thank my parents, for their enormous dedications and eternal blessings since the day I was born and my husband and my daughter, for appreciating me, supporting me and the sacrifices they made, in every second for who I am today.

CHAPTER 1

Literature Review–Indigestible plant matter and gut microbiota diversity and fermentation of indigestible plant matter in the colon by gut microbiota

1.1. General Introduction

All forms of living beings on earth require a carbon source and an energy source for their growth, development and survival, through food or feed from plant or animal sources. All food/feed sources share a common nutrient make-up which differs in their relative compositions depending on the botanical source or raw material composition. All food/feed sources are composed of broad nutrient groups namely, carbohydrates, proteins, lipids (saturated/monounsaturated/polyunsaturated fat/cholesterol), vitamins and minerals (macro/micro nutrients) with respective functions for each nutrient. Generally, carbohydrates, lipids and/or proteins are known as energy sources, while proteins and minerals serve as building materials and vitamins, some trace minerals, amino acids and fatty acids are important for biochemical reactions as mediators, catalysts and cofactors.

The most important function of food is the provision of nutrients, thus food is a natural nutrient-bomb packaged in a peel, seed hull, shell or coat. For example, when a plate of rice is consumed, almost all nutrient groups enter the digestive system, which will be mechanically and biochemically degraded/digested and absorbed into blood along the gastrointestinal tract. Not all nutrients ingested via food/feed get digested and absorbed into body, the rest of the undigested part of food/feed get excreted in feces along with other bodily wastes. The types and sources of indigestible nutrients vary between different animal species and even individual animals. For example, cellulose is a type of carbohydrate well-known as an indigestible food component by humans, but digestible in ruminants. Further, gluten, a specialty protein in bread wheat is renounced to cause celiac disease due to its less digestibility in certain individual people and lactose intolerance also has a similar story! Thus, indigestibility of nutrients depends mainly on the genetic make-up of species of animals and individuals that determines their digestive capacity, in other words the availability/non-availability of certain enzymes that are responsible for digesting certain nutrients. Starting from the meiosis and decided during fertilization, an individual's genetic capacity is

decided for most of the cognitive and physiological functions in its lifetime, where digestibility is just one among thousands of such.

Being vertebrates and then mammals, omnivores and ruminants share a vast array of physiological, biological and biochemical similarities despite their gastrointestinal tract physiology and functions. These differences might have definitely served as a criteria for natural selection along the evolutionary path and at the same time might have been a merit for co-evolution with less inter-species competition over food sources. As one united group, most of the mammalian genomes are found not to encode most of the enzymes required for degrading complex polysaccharides, mainly the plant structural polysaccharides such as cellulose, hemicellulose, etc. Having mentioned that, now arises a question on how do the ruminants are able to digest cellulose! Ruminants, as the name implies have developed a specialized gastrointestinal anatomy and physiology (rumen), with a modified digestive function (rumination), attributed to their complex mutual dependence on symbiotic microbiota resides in the rumen, to access recalcitrant complex structural carbohydrates in the lush greens they ingest (microbial fermentation).

The major component in plant indigestible matter is the portion of dietary indigestible complex carbohydrates, which are known as dietary fiber. It consists of a wide array of heterogeneous and complex substances. According to Codex Alimentarius Commission, dietary fiber is defined as, polysaccharides made of ten or more monosaccharide units that cannot be hydrolyzed by the activity of endogenous human small intestinal enzymes and are fermented in the large intestine by the activity of intestinal microbiota (Fernández *et al.*, 2016). Due to their ability to be fermented by the gut microbiota, some of the dietary fibers are classified as prebiotic fibers. Dietary fibers that can be selectively fermented and result in specific modifications in the composition and/or activity of the gastrointestinal microbiota and subsequently exert benefits to the host health are classified as prebiotic fibers, thus all dietary fibers by extension, all generic fibers are not prebiotic (Fernández *et al.*, 2016). Thus, prebiotic fibers are an

important group of nutrients in the point of view of human nutrition. While, dietary fibers are of plant origin and non-starch polysaccharides makes up the majority, prebiotic fibers may include substances of bacterial or animal origin also, yet the most prebiotic fibers are also of plant origin.

1.2. Plant indigestible matter (Dietary Fiber) – their biochemistry and sources

Resistant starch

The stored carbohydrate polymers in the form of energy reserves and structural components in vast majority of plants are made of glucose polymers, where energy reserves in the form of starch were considered as completely digestible, until resistant starch (RS) was identified and currently RS is considered as a prebiotic fiber, due to its ability to be selectively fermented by bacteria and cause modifications to the gut bacteria composition and function. RS is the unavailable fraction of dietary starch, which is not digested even after 120 min of incubation with α -amylase and pullulanase under *in vitro* conditions (Sajilata *et al.*, 2006). Starch can be resistant due to many factors and according to the mode of their resistance, they are classified into four groups, namely, RS1, RS2, RS3 and RS4. Some of the factors that can make a starch unavailable for digestive enzymes are, physical protection by a coat that is hard to digest (whole and coarsely milled grains), crystallinity pattern of starch molecules within the granules such as B or C-type (raw potato), large granule size (potato), higher amylose:amylopectin ratio (high amylose corn starch), amylose chain length (degree of polymerization 10 to 100) and processing effects (retrogradation, cross-linking) (Sajilata *et al.*, 2006; Perera *et al.*, 2010).

RS1, composes the starches that are physically inaccessible (partially milled grains, seeds, vegetables), RS2 composes of ungelatinized starch, due to restricted accessibility to digestive enzymes and water due to the compact nature of the granule packing (high amylose corn starch), while RS3, composes of cooked and retrograded starch, which becomes resistant to digestion upon double helix formation in the leached amylose fraction and RS4 consists of chemically modified starches by cross-linking with substances such

as, sodium trimetaphosphate, sodium tripolyphosphate or epichlorohydrin or phosphoryl chloride, which become resistant to α -amylase (Sajilata *et al.*, 2006; Perera *et al.*, 2010).

Generally, RS also possesses similar physicochemical properties to starch, such as bland flavor, white color and fine particle size, yet in contrast to digestible starch, RS is known to possess a very high gelatinization temperature, lower water binding capacity and thus, incorporation of RS allows to process low-bulk high fiber products with improved texture, appearance and mouth feel compared to other fiber sources (Sajilata *et al.*, 2006). Further, due to its resistance to ileal digestion, it reduces the calorific value of foods.

Non-starch polysaccharides

Apart from the energy reserves, the major structural components in plants-cell wall material, accounts for the largest group of dietary fiber. Non-starch polysaccharides include cellulose, hemicellulose and pectic polysaccharides and they are found to consist up to 50% of the biomass of most annual and perennial plant species (Ebringerova *et al.*, 2005). The cell wall materials are heterogeneous in their ability when it comes to fermentation, depending on many factors. For example, cellulose, a polymer of glucose bound by β -(1,6) glycosidic bonds are insoluble in water and neither digested nor fermented in the humans, while they can be fermented in ruminants. Hemicelluloses, which are water soluble, can be converted into substances that can be fermented via biological, chemical and other processing methods. The structural diversity of the hemicelluloses has shown promising characteristics to be able to be used as a source of biopolymers either in their native or modified forms, for examples, xylans, mannans, β -glucans and xyloglucans (Ebringerova *et al.*, 2005).

Fructans

Apart from the glucose polymers, about 10% of vascular plants are known to store polysaccharides in the form of non-glucose based polymers, such as fructose-based polymers known as fructans, linked by β -(1,2) bonds consisting of 2 to more than 60 fructose moieties distinctly making two groups, fructooligosaccharides (2 to 10 moieties) and inulin (>10 moieties) (Kieffer *et al.*, 2016). These fructans also cannot be digested in the ileum, thus move to the colon and get fermented by the bacteria and exert many beneficial effects.

Inulin, a major prebiotic fiber is a colorless and sweet substance (10% sweetness compared to sucrose), which is moderately soluble in water with a low viscosity. Other than as an artificial sweetener, inulin has the ability to act as a fat replacer in low fat and non-fat products such as cheese and chocolate, to ameliorate the rheological, sensory and textural compromises of removing fat, such as rubbery texture, lack of taste, bitterness and odd color. Inulin is used in table spreads, butter, yoghurt, cream cheese and dairy drinks and it was found to improve the creaminess and smoothness in yoghurt and dairy drinks (Kieffer *et al.*, 2016). The major sources that are currently utilized to extract inulin are, chicory roots (*Cichorium intybus*), blue agave leaves (*Agave tequilana*), Jerusalem artichoke root (*Helianthus tuberosus*), asparagus stem (*Asparagus officinalis*), garlic bulbs (*Allium sativum*), artichoke flower (*Cynara scolimus*) and leek leaves (*Allium ampeloprasum*) (Kieffer *et al.*, 2016). The most common method of inulin extraction from these plants/plant parts is aqueous extraction at high temperatures.

Fructooligosaccharides are more soluble than inulin and also 35% more sweet compared to sucrose, attributed to its shorter length and higher fructose content compared to inulin. Further, fructooligosaccharides are known to possess a low glycemic index as they are not hydrolyzed by the pancreatic enzymes or gastric enzymes. Thus, fructooligosaccharides are important in processing low caloric food without compromises in food texture and taste and especially in diabetic diets. A combination

of inulin and fructooligosaccharides in extruded snacks and cereals are known to improve the crispiness, and improve the shelf life of bakery products due to increased water holding capacity. Fructooligosaccharides are produced either from inulin degradation or transfructosylation of sucrose (Kieffer *et al.*, 2016).

Milk oligosaccharides

Human milk oligosaccharides includes a diverse family of around 200 types of different combinations of five monosaccharides, namely, glucose, galactose, fucose, N-acetylglucosamine and N-acetylneuraminic acid and some of the major human milk oligosaccharides are 2'-fucosyl-lactose, lacto-N-tetraose and lacto-N-neotetraose (Kieffer *et al.*, 2016). These oligosaccharides in milk provide substrates for the gut microbiota of the new born until the introduction of solid food, thus responsible for the higher fecal *Bifidobacterium* abundance in infants.

Similar to human milk oligosaccharides, galactooligosaccharides found in mammals' milk (including humans), which are made of 2 to 10 galactose residues attached to a terminal glucose, have also exhibited prebiotic properties. These can be produced industrially also for the incorporation in infant formula from whey lactose. Galactooligosaccharides in infant formula are responsible for the maintenance and development of the early gut microbiota of completely formula-fed infants.

1.3. Plant indigestible matter in human nutrition-A colonic fermentation perspective

1.3.1. Principles and overview of colonic fermentation

Mainly dietary fiber (fermentable) and also proteins and peptides that escape ileal digestion are disintegrated by the versatile amylolytic and proteolytic enzyme repertoire of the microbial members inhabiting the colon, which overcasts the hosts' capabilities to unlock the indigestible substrates (Macfarlane and Macfarlane, 2012). Microbiota mediated hydrolysis of these indigestible substrates is

known as “colonic fermentation” in omnivores and herbivores (other than ruminants). This anaerobic catabolic process mainly produces, short-chain fatty acids (SCFAs) and gases, in particular, acetate, propionate, butyrate, ethanol, carbon dioxide, hydrogen, etc. (den Besten *et al.*, 2013). These SCFAs are known to mediate beneficial biochemical, biological and physiological processes in hosts, for example, regulating host energy metabolism, inhibiting carcinogen synthesis and pathogenic microbial activity, reducing the risk of developing colorectal cancers and improving gut physical and immunological barrier functions, highlighting their importance in the well-being of the host.

The indigestible carbohydrates reach the colon in different forms, such as polysaccharides, oligosaccharides and other resistant forms like resistant dextrin. Initial step in the colonic fermentation is converting these poly and oligomers into monomers by the microbial enzymatic activity of the specialized probiotic bacterial members. Upon disintegration into monomers, the resulting hexoses, pentoses, fucose and rhamnose participate in various pathways initiated or regulated by different enzymes, by extension different microorganisms, initially by the activity of lactic acid bacteria (*Bifidobacterium* and *Lactobacillus*). Major end products of these metabolic pathways mediated by microbial enzymes are lactate, pyruvate and acetate, which are later diversified into propionate and butyrate also (Fernández *et al.*, 2016). There are several well-characterized specific pathways for the biosynthesis of each individual SCFA (Koh *et al.*, 2016). Mainly, the hexoses and pentoses are known to be converted into phosphoenolpyruvate (either via glycolysis or pentose phosphate pathway), which later can be diverted into several other pathways yielding propionate and butyrate.

The major SCFA produced in the colon is acetate, which can be synthesized from pyruvate via acetyl-CoA pathway or Wood-Ljungdahl pathway, where these two pathways are led by distinct microbial members (Koh *et al.*, 2016). Between these two pathways, acetyl-CoA pathway is the major pathway, which is known to be a very common pathway among the majority of commensal bacteria, such as

Bacteroides spp., *Bifidobacterium* spp., *Prevotella* spp., *Ruminococcus* spp. and *Akkermansia muciniphila* (Koh *et al.*, 2016). On the other hand, Wood-Ljungdahl pathway is found to be carried out by *Blautia hydrogenotrophica*, *Clostridium* spp. and *Streptococcus* spp. via C₁-body branch/Eastern branch by reducing carbon dioxide to formate and via Western branch by reducing carbon dioxide to carbon monoxide, which is later methylated to produce acetyl-CoA (Koh *et al.*, 2016).

Propionate, the three-carbon SCFA can be produced via three pathways: starting from pyruvate via Acrylate pathway (precursor Lactate) and Succinate pathway (precursor Succinate) and starting from L-lactaldehyde via Propanediol pathway (Koh *et al.*, 2016). The major metabolic pathway through which rhamnose and fucose (deoxyhexose sugars) monosaccharides metabolize is the Propanediol pathway, where deoxyhexose sugars are being converted into propionate by *Salmonella* spp., *Roseburia inulinivorans* and *Ruminococcus obeum*. *Bacteroides* spp., *Phascolarctobacterium succinatutens*, *Dialister* spp. and *Veillonella* spp. are found to utilize the succinate pathway to produce propionate, while *Megasphaera elsdenii* and *Coprococcus catus* utilize acrylate pathway (Koh *et al.*, 2016).

Butyrate (C=4), is considered as an important SCFA due to its many beneficial effects on host health, can also be synthesized via two routes. One route is known as the classical pathway, which is catalyzed by phosphotransbutyrylase and butyrate kinase by condensing two acetyl-CoA molecules and reducing them to butyryl-CoA, subsequently converted into butyrate by bacteria such as *Coprococcus comes*, *Coprococcus euctactus*. Further, butyryl-CoA can be directly converted into butyrate along with an acetyl-CoA derived from an acetate molecule by the activity of butyryl-CoA:acetate-CoA transferase route by the cross-feeding activity of *Anaerostipes* spp., *C. catus*, *Eubacterium rectale*, *Eubacterium halii*, *Fecalibacterium prausnitzii* and *Roseburia* spp. (Fernández *et al.*, 2016). Apart from these two major routes, some bacteria are known to utilize lactate and acetate to synthesize butyrate via cross-feeding, which is known to stabilize colonic pH, for example by *C. catus*, *E. rectale*, *F. prausnitzii*, *Roseburia* spp.

using acetate and *Anaerostipes* spp. and *E. hali* using both lactate and acetate (Koh *et al.*, 2016). Among the butyrate producers, phylum Firmicutes consists of many different species belonging to several families such as *Lachnospiraceae* (*Roseburia* spp., *Eubacterium* spp.), and *Ruminococcaceae* (*F. prausnitzii*) (Fernández *et al.*, 2016). Apart from the phylum Firmicutes, certain microbial members of phyla Actinobacteria, Fusobacteria, Proteobacteria, Spirochaetes and Thermotogae are also identified to contain butyrate producers (Fernández *et al.*, 2016). Further, all these three SCFAs are found to be synthesized as minor by-products during amino acid fermentation (discussed in details in Chapter 3), where butyrate is found to be synthesized via lysine, glutarate and 4-aminobutyrate pathways (Fernández *et al.*, 2016; Koh *et al.*, 2016).

1.3.2. Importance of short chain fatty acids in physiology

Short chain fatty acids produced by dietary fiber breakdown by the gut microbiota are associated with many beneficial physiological outcomes. The relationship between dietary fiber and improved metabolism has been attributed to the SCFA mediated biochemical processes. Short chain fatty acid produced in the large intestine are absorbed into the circulation, thus along the length of the colon (cecum to distal colon) there is a SCFA concentration gradient. As butyrate is the preferred energy source by the colonocytes, butyrate is almost absorbed and utilized locally, while acetate and propionate are absorbed and drained into the portal vein via Na⁺-coupled monocarboxylate transporter SLC5A8 and H⁺-coupled low affinity monocarboxylate transporter SLC16A1 (Koh *et al.*, 2016). Upon absorption into the circulation, the first organ they reach is the liver and propionate is known to be mostly metabolized in the liver, while acetate is found to be transferred to many other organs, such as adipose tissue, lungs, pancreas, bone marrow and as far as the brain, thus the major SCFA found in the circulation is acetate (Koh *et al.*, 2016).

Apart from supplying the energy source, these SCFAs are known to mediate a plethora of functions via acting as signaling molecules or supplying ligands to mediate biochemical pathways, through which many

beneficial outcomes are acquired, such as the reduction of appetite via activated neurohumoral systems, prevention of neoplastic disease onset, amelioration or prevention of metabolic diseases, etc. For examples, mice fed butyrate enriched high fat diet exhibited increased energy expenditure and became resistant to obesity, while oral feeding of acetate to obese and diabetic rats showed reduced weight gain and improved glucose tolerance, further, propionate supplementation improved glucose homeostasis in rodents (Yamashita *et al.*, 2009; Koh *et al.*, 2016).

The most beneficial effects mediated via SCFAs are due to their ability to act as ligands for G-protein coupled receptors (GPRs) in the intestine and other organs. There are around 800 GPRs identified in the human genome and among them GPR40, 41, 42 and 43-a cluster of four GPRs, are known as free fatty acid receptors (FFARs) (Koh *et al.*, 2016). Propionate followed by butyrate are known as the preferred ligands for GPR41 (FFAR3), while acetate has a comparatively very low affinity. GPR41 expressed in colonic and intestinal epithelium and also co-expressed with glucagon-like peptide-1 (GLP-1) in enteroendocrine cells in crypts and lower part of the villi are known to mediate intestinal gluconeogenesis, while its expression in adipose tissue is found to mediate increased energy expenditure, oxygen consumption rate, leptin expression, reduced appetite, increased peptide-YY (PYY) expression (Koh *et al.*, 2016). Intestinal gluconeogenesis that occur via propionate and butyrate, is known to improve insulin sensitivity and glucose tolerance and further, gluconeogenesis via propionate in liver is known to improve satiety and reduce hepatic glucose synthesis. Apart from that, GPR41 expressed in colonic mast cells, lymph nodes, bone marrow are known to be involved in immune functions, such as hematopoiesis of dendritic cells from bone marrow, increasing regulatory T (Treg) cells and dendritic cell precursors for preventing asthma and improve protective immunity (Koh *et al.*, 2016).

GPR43 (FFAR2) couples with acetate and propionate in the mentioned affinity order and it is considered that in the gut these receptors are continuously saturated with the ligands. Among the locations where

GPR43 is expressed, colonic and small intestinal epithelium, enteroendocrine cell, colonic lamina propria cells (mast cells, neutrophils, eosinophils, colonic Tregs), small intestinal lamina propria (leukocytes) account for the most common locations. The colonic and intestinal GPR43 upon activation with ligand binding is known to secrete GLP-1 from enteroendocrine cells. Further, its expression in the white adipose tissue is known to secrete PYY and exert an anti-lipolytic effect, which is known to be mediated by acetate, which improves glucose and lipid metabolism that cannot be observed in the muscles or liver (Kimura *et al.*, 2013; Koh *et al.*, 2016). It has been previously observed that GPR43 knockout mice are obese compared to wild type, while over expression of GPR43 in adipose tissue correlated with leanness in mice (Koh *et al.*, 2016). Apart from the colon, small intestine and adipose tissue, GPR43 is known to be expressed in skeletal muscle, heart and spleen also. And this receptor has the reputation of mediating many important biochemical processes, such as increment of insulin sensitivity and energy expenditure, pre-adipocyte differentiation, appetite control, protection against cancer and inflammatory bowel disease mediating apoptosis in colon cancer lines and resolution of colitis, respectively, expansion and differentiation of Tregs to act against pathogenic bacteria, neutrophil chemotaxis, reduction of leukemia cell proliferation, among many others (Koh *et al.*, 2016).

Apart from GPR41 and 43, GPR109A is another receptor expressed in the apical membrane of the colon and small intestinal membrane, which is only activated by butyrate as a SCFA-based ligand (Koh *et al.*, 2016). These receptors expressed in the colonic and small intestinal epithelium are known to provide protection against cancer and inflammatory bowel disease. Butyrate is well-known for its effect on healthy proliferation of the colonic epithelium and prevention of neoplastic disease onset and development and this function is mediated mainly by its inhibitory effect on histone deacetylases.

Histone deacetylases have been used in cancer therapy widely due to their anti-inflammatory function. Function of butyrate as a histone deacetylase is found to protect against colorectal cancers and

inflammation, thus butyrate is considered as a modulator of neoplastic diseases and immune homeostasis. Butyrate is known to alter expression of many genes with diverse functions, such as cell proliferation, apoptosis and differentiation, apart from being a histone deacetylase in a neoplastic tissue. In contrast to a neoplastic tissue, butyrate does not function as a cell growth inhibitor in a healthy tissue (Butyrate Paradox), which could be explained by the preferred energy substrates of neoplastic cells and the normal healthy colonocytes, which are glucose and butyrate, respectively.

The anti-tumor function (histone deacetylation inhibition) of butyrate also mediate anti-inflammatory functions as it suppresses pro-inflammatory effector molecules in the lamina propria macrophages and differentiation of dendritic cells in the bone marrow (Koh *et al.*, 2016). Anti-inflammatory functions mediated by GPR109A include, protection against inflammatory bowel disease by making immune system hypoactive towards commensal bacteria, improved epithelial barrier function, increment of Treg and IL-10 producing T cells generation and reduction of pro-inflammatory Th17 cells in the colonic lamina propria (Koh *et al.*, 2016). Apart from anti-tumor and anti-inflammatory functions mediated via GPR109A, it is further known to mediate anti-lipolytic and triglyceride lowering functions also (Koh *et al.*, 2016).

1.3.3. Diversity and differential benefits of prebiotic fibers

As a broad class, dietary fiber consumption has been associated with beneficial effects on gut health and systemic health, for example, amelioration or prevention of colonic cancers, inflammatory diseases in gastrointestinal tract, diabetes, cardiovascular diseases, non-alcoholic fatty liver disease and chronic kidney disease (Kieffer *et al.*, 2016). The above mentioned physiological benefits are found to be mediated through the improved growth of selected groups of gut bacteria, their fermentative products and modified synthesis and secretion of hormones, cytokines like host factors regulating the physiology and biochemistry (Kieffer *et al.*, 2016). Being a versatile group in terms of structure as well as the functionality, beneficial health outcomes of the different classes of dietary fiber can be either specific or generalized.

Consumption of dietary fibers is considered as the best dietary intervention to maintain a healthy gut microbiota by provisioning nutrients required for their growth and development, attributed to their inherent physicochemical properties mediated substrate versatility. For example, RS, a more homogenous and simple chemical form is known to reduce the gut microbial diversity and in contrast, generic dietary fiber is known to improve the diversity due to the availability of a wide array of complex substrates, further known to broaden the metabolic capacity of the gut microbiome (Kieffer *et al.*, 2016). Microbial diversity has been observed to be recovered upon a high fiber diet feeding to mice after a short-term on a low fiber diet, yet it has been revealed that a long term exposure to low fiber diets can cause extinction of several microbial taxa from the gut microbiota (Kieffer *et al.*, 2016). For example, in human populations, where the diet is rich in indigestible carbohydrates, such as black African communities, Hadza hunter gatherers in Tanzania have exhibited higher gut microbial diversities over high-fat and high-sugar westernized diet consumers (Koh *et al.*, 2016).

Importance of a diverse gut microbiota has been proposed, as to the ability to successfully respond to environmental challenges such as pathogenic bacterial colonization, better adaptations against inflammatory diseases and stronger immune system. Being the largest immune organ in the body, the gut associated lymphoid tissue is the primary route of antigen introduction and the main system that maintains host-microbiota homeostasis in a healthy person. Several classes of dietary fiber, such as fructooligosaccharides, arabinoxylans and β -glucans in diet are found to possess immunomodulatory properties (Kieffer *et al.*, 2016). Ingestion of 0.06% shorter chain fructooligosaccharides was found to increase immunoglobulin A in the cecum, where immunoglobulin A is found to play an integral role in the barrier function by binding to microbes and preventing adhesion and translocation of bacteria across the mucus layer (Kieffer *et al.*, 2016).

Improvement of the gut barrier function has been well-characterized in relation to dietary fiber, where an increase in the mucin secretion and population of mucin secreting goblet cells have been observed (Kieffer *et al.*, 2016). Insufficient dietary fiber reaching the colon has been associated with a thin mucus layer and a higher breakdown of the barrier by the commensal bacteria themselves to obtain energy for their survival (Kieffer *et al.*, 2016). Feeding of 10% fructooligosaccharides was found to increase the tight junction protein expression and lowered plasma lipopolysaccharide content, which were attributed to the GLP-1 expression in plasma, and was similarly observed in rats fed 2.5% pectin diet (Kieffer *et al.*, 2016). Further, degraded gut permeability in total enteral and parenteral diets has been recovered with the incorporation of either fiber or SCFAs (Kieffer *et al.*, 2016). Lowered ammonia and ammonium hydroxide prevalence in the intestine caused by higher availability of dietary fiber in gut is associated with the reduced damage to tight junction proteins, thus improved gut barrier (Kieffer *et al.*, 2016).

Dietary fiber consumption is found to protect key organs such as liver, kidney and heart from adverse outcomes of metabolic impairments. Supplementation of hemodialysis patients with 15 g RS/day/6 weeks was associated with reduced cardiovascular diseases and all-cause mortality, which might have been due to the modified bacterial structure in the lower gut and reduced availability of potentially harmful metabolites, such as indole, *p*-cresol and indoxyl sulfate (Kieffer *et al.*, 2016). Further, supplementation of chronic kidney diseased rats with 59% RS for 3 weeks was found to improve kidney function and gut permeability indices (Kieffer *et al.*, 2016). Guar gum supplementation (50 g/day/4 weeks) in patients with chronic renal failure exhibited increased fecal nitrogen excretion and decrease level of serum urea, but interestingly not observed for pectin (Kieffer *et al.*, 2016).

Further, dietary fiber mediated intestinal gluconeogenesis is suggested to decrease hepatic glucose synthesis and improved satiety, which was observed in rats fed 10% fructooligosaccharides diet for 2 weeks by the increment of mRNA levels of intestinal gluconeogenic enzymes (Kieffer *et al.*, 2016).

Intestinal gluconeogenesis is found to play a key role in maintaining a proper glucose and insulin homeostasis, thus prevents adiposity and delays the disease progression of non-alcoholic disease and chronic kidney disease (Kieffer *et al.*, 2016).

As previously mentioned, mainly depending on the chemical structure, different fibers are found to be associated with different properties and outcomes. For examples, in the mice mucosal transcriptome, arabinoxylans increased tryptophan metabolism, fructooligosaccharides increased the unfolded protein response, inulin increased β -oxidation pathway and gaur gum increased cholesterol and arachidonic acid metabolism, while all these fibers were found to increase PPAR- γ gene expression associated with gut inflammation regulation (Kieffer *et al.*, 2016). Further, inulin supplemented rats (10% for 4 weeks) decreased liver triglycerides and expression of genes associated with lipid metabolism, fibrosis and inflammation (Kieffer *et al.*, 2016).

Resistant starch is known to significantly increase the pancreatic, hepatic and intestinal weights, intestinal length in rats, decrease postprandial glucose level and exert a laxative effect without gastrointestinal discomfort (Perera *et al.*, 2010). Feeding of adzuki and tebou starch have exhibited serum cholesterol lowering effect attributed to the enhanced level of hepatic scavenger receptor class B1 and cholesterol 7 α -hydroxylase mRNA expression (Sajilata *et al.*, 2006). Further, bean starch rich in RS was observed to reduce serum total cholesterol and low density lipoprotein cholesterol (VLDL, IDL and LDL) and improve fecal sterol excretion (Sajilata *et al.*, 2006). Further, a lower concentration of cholesterol in all lipoprotein fractions and lower triglyceride level in triglyceride rich lipoprotein fraction were observed upon RS feeding in rats (Sajilata *et al.*, 2006). And increased postprandial lipid oxidation observed upon RS consumption has been correlated with a lower fat accumulation in long term (Sajilata *et al.*, 2006). As previously mentioned, RS has the ability to reduce the calorific value of foods, as its rate of digestion is very low or negligible compared to rapidly digestible starch, which digests over a 5 to 7 h period (Sajilata

et al., 2006). Moreover, incorporation of RS in diet has been associated with improved absorption of calcium and iron from the intestine (Sajilatha *et al.*, 2006).

Further, different classes of RS also have exhibited substrates specific fermentative properties apart from their general contribution to the SCFA pool, which can be attributed to the underlying chemical and structural differences among the RS classes. High amylose corn starch, a well-known type 2 RS, is found to significantly increase the colonic acetate, propionate and butyrate production in rats, further exhibited amelioration of externally induced gene damage by increasing apoptosis (Perera *et al.*, 2010). Further, chemically modified starch (RS4), was found to reduce fecal bile acids and total neutral sterols, which have been correlated with the incidence of colon cancer, by increasing glutathione levels in mucosa (Perera *et al.*, 2010).

Resistant starch is known to increase the abundance of lactobacilli, bifidobacteria, staphylococci and streptococci, decrease enterobacteria and alter the microbial enzyme expression in rats (Perera *et al.*, 2010). In a previous study it was revealed that, RS2 enriched the abundance of *Ruminococcus bromii*, while RS3 improved *E. rectale* along with *R. bromii* (Martínez *et al.*, 2010). Consumption of RS4 by humans was found to significantly lower the abundance of fecal Firmicutes, increase Bacteroidetes and Actinobacteria at phylum level, while at genus level *Parabacteroides*, *Bifidobacterium* were found to be increased, while *Ruminococcus*, *Fecalibacterium* and *Dorea* were reduced (Martínez *et al.*, 2010). Further, enrichment of *Clostridium* cluster XIVa was observed upon RS4 supplementation, in contrast to the previously reported study, *R. bromii*, *E. rectale* or *D. formicigenerans* were not improved (Upadhyaya *et al.*, 2016). Additionally, new bacterial taxa belonging to *Christensenella minuta*, *Bacteroides ovatus*, *R. lactaris*, *E. oxidoreducens*, *B. xylanisolvens*, *B. acidifaciens* were enriched upon RS4 supplementation (Upadhyaya *et al.*, 2016).

1.4. Gut microbiota, dietary fiber and health impairments

1.4.1. Gut microbial diversity

Gut microbiota refers to the collection of a diverse set of microorganisms belonging to bacteria, methanogenic archaea, eukarya and viruses that inhabit the gastrointestinal tract, mainly the colon (Lozupone *et al.*, 2012). The bacteria inhabiting the colon ($10 \times$ somatic cell number) and their collective quantity of genetic material exceed the human cell number and the genetic material, respectively, thus the combination of the human host and the gut microbiota is known as the “super organism” (Conlon and Bird, 2015). Human gut microbiome is found to possess 150-fold more protein coding genes than the human genome, which are known to expand the metabolic capacity of the host (Kieffer *et al.*, 2016). In contrast to the largely fixed human genome, gut microbial genome is found to be plastic, ever-evolving depending on the intrinsic and extrinsic factors, thus phenotyping higher inter-individual variations among individuals (Kieffer *et al.*, 2016). Among the humans, three distinct enterotypes of gut microbiota have been identified, *Ruminococcus*, *Prevotella* and *Bacteroides* (Li *et al.*, 2017).

The abundance, the type and function of the microbial members vary along the length of the gastrointestinal tract, thus creating specific functional and ecological niches. Majority of the gastrointestinal tract microbiota are inhabitants of the colon, who are specialized in hydrolyzing the undigested carbohydrates. Gut microbiota mediate a wide array of functions within the colon itself, such as digestion of complex dietary nutrients and harvesting of energy, production of beneficial nutrient and vitamins, provision of protection against pathogenic microbial invasion and maintenance of adaptive immune system, etc. (Koh *et al.*, 2016). A balanced gut microbial composition is reported to be important in the maintenance of the general healthy status of the host, while a dysbiotic microbiota has been associated with health impairments such as metabolic disorders (obesity, type 2 diabetes), inflammatory diseases (ulcerative colitis, Crohn’s disease) and neoplastic diseases (cancers) (Koh *et al.*, 2016). The

ability of gut microbiota to produce either harmful metabolites or beneficial metabolites under prevailing circumstances, might be the underlying reason for the above observed paradox (Koh *et al.*, 2016).

The gut microbiota is typically dominated by the phylum Firmicutes who are active in carbohydrate metabolism and known as efficient energy harvesters from the indigested food materials reaching the colon, thus their impaired higher abundance is correlated with metabolic diseases such as obesity (Ottman *et al.*, 2012). Secondly, Bacteroidetes that composes more than 90% of the total gut microbiota together with Firmicutes, are known to express a wide array of functions such as energy production/conversion, amino acid transport/metabolism and carbohydrate metabolism (Ottman *et al.*, 2012). Apart from the phyla Firmicutes and Bacteroidetes, Actinobacteria, Verrucomicrobia and Proteobacteria are among the subsequent abundant phyla in the human gut microbiota (Ottman *et al.*, 2012). According to the metaproteomic studies, Actinobacteria are found to be responsible for active carbohydrate metabolism (particularly expressing sugar metabolizing proteins), similar to Firmicutes (Ottman *et al.*, 2012). Most commonly found genera that contribute to the core microbiota are *Bifidobacterium*, *Lactobacillus*, *Bacteroides*, *Clostridium*, *Escherichia*, *Streptococcus* and *Ruminococcus* (Conlon and Bird, 2015).

There are many theories that illustrate the gut microbial evolution within the human body and the currently accepted theory states that they co-evolve at birth (Ottman *et al.*, 2012). An infant born vaginally is known to be colonized by a microbiota similar to mother's vaginal and fecal microbiota mostly dominated by bifidobacteria, while an infant born via caesarean delivery is known to colonize a microbiota similar to mother's skin communities, which is substantially lower in bifidobacteria (Ottman *et al.*, 2012). Since the initial colonization, the gut microbiota is shaped up by the subsequent life events such as, type of infant feeding (breast-fed, dominated by bifidobacteria; formula-fed, rich in *E. coli*, *Clostridium difficile*, *Bacteroides fragilis* and lactobacilli), time of weaning, childhood diseases and hospitalization, antibiotic and other medication use, home and hospital condition, etc., thus the functional gene content and

expression are thus determined (Ottman *et al.*, 2012). Microbial gene expression of carbohydrate metabolism is considered to initiate at breast feeding due to the lactose in milk and further, human milk oligosaccharides are found to attract human milk oligosaccharide specific bifidobacteria (*Bifidobacterium longum* subsp. *infantis*) and mutualistic mucus adapted species (*Bacteroides thetaiotaomicron*), thus facilitate and prepare the infant for future solid food digestion (Ottman *et al.*, 2012).

The gut microbial composition varies at the inter-individual level depending on many environmental factors in later life such as, age, sex, diet, health status, living condition (individual housing, community housing), geographic location, etc. Since birth, the evolved gut microbiota is dynamically modified over the course of the life increasing the diversity and richness (alpha diversity) and during the later stages of life, the alpha diversity is again get reduced and it is characterized by higher Firmicutes to Bacteroidetes ratio, increased Proteobacteria abundance and a decrease in *Bifidobacterium* (Ottman *et al.*, 2012).

Apart from the health related perturbations, daily dietary pattern and diet composition are reported to significantly shape the evolving gut microbiota determining its functional capacities. The dietary pattern and diet composition can be significantly determined by the geographical location (Africa or Europe, landlocked or island, peninsula, sea-side or country-side), ethnic, religious and cultural signatures, socioeconomic status (purchasing power) and educational level of parents (awareness), etc. For example, the microbiota of European children consuming animal protein, sugar and fat rich diet, which is low in fiber, was enriched in Firmicutes and Proteobacteria, while the microbiota of African children consumed a predominantly vegetarian diet, rich in carbohydrate, fiber and plant proteins, was enriched in Actinobacteria and Bacteroidetes and further, *Xylanobacter* and *Prevotella* were only observed in African children's microbiota (Ottman *et al.*, 2012). Malnourished children from poor households exhibited a microbiota rich in Proteobacteria and lower Bacteroidetes compared to healthy children (Ottman *et al.*, 2012). And further, remarkable similarities were observed in the gut microbial composition and the

diversity, between a group of British people and African community adhering to a westernized diet, highlighting the significant effect of diet on the gut microbial shape, despite the differences in the geographical location and genetics (Ríos-Covián *et al.*, 2016).

1.4.2. Dysbiosis and health disorders

The gut microbiota that co-evolve at the birth is considered as an ever evolving eco-system depending on the environmental conditions (host and exogenous). Thus, perturbations such as poor health status, long term antibiotic and drug use, dietary habits and starvation, parenteral nutrition are known to significantly affect the diversity, composition and the richness with substantial shifts in abundances of the gut microbial species (Ottman *et al.*, 2012). Thus, an altered gut microbial phenotype, known as a “dysbiotic gut microbiota” is correlated with the incidence of many health disorders and impairments such as obesity, malnutrition, inflammatory bowel disease, neurological disorders and neoplastic diseases (Lozupone *et al.*, 2012).

Obesity and other co-morbidities of metabolic syndrome (hyperinsulinemia, hyperlipidemia, hypertriglyceridemia, cardiovascular diseases, etc.) have been linked with gut dysbiosis and subsequent changes in the microbial functions. One of the classical characteristics that is linked with obesity is the increased ratio of Firmicutes to Bacteroidetes, which could be due to the increased energy harvest by the microbial members belonging to phylum Firmicutes, who are known to be efficient energy harvesters. In support of this, several studies have reported that obesity is directly correlated with the gut microbiota, where the gut microbiota of an obese mice colonized in a germ free wild type mice exhibited a subsequent increase in fat mass (Ottman *et al.*, 2012). Development of obesity and metabolic syndrome has been linked to the evolution and the differentiation of the gut microbial composition during the early life stages. Excessive weight gain observed in infants during the first month after birth has been linked with lower levels of *Bifidobacterium* levels and higher abundance of *Staphylococcus* in their gut microbiota

(Rodríguez *et al.*, 2015). Further, the genetic predisposition for obesity passed down to infants, is suggested to be due to the lower abundance of *Bifidobacterium* in the milk microbiota of obese mothers (Rodríguez *et al.*, 2015). Further, the higher prevalence of *Bifidobacterium* is suggested to protect women from weight gain during and after pregnancy and infants of women with normal weight gain during pregnancy were found to harbor higher levels of bifidobacteria suggesting a protective role of bifidobacteria against weight gain (Rodríguez *et al.*, 2015). On the other hand, the gut microbiota of a severely malnourished person is characterized by a lower abundance of Bacteroidetes (specialized in carbohydrate hydrolysis) and rich in energy rich-western diet consumers (Ottman *et al.*, 2012).

One of the major disorders related to gut microbial dysbiosis is the inflammatory bowel disease, which is identified as an infuriating condition in the small intestine and the colon, which is characterized by an overly aggressive and inappropriate inflammatory response to enteric microbiota in genetically susceptible hosts (Eichele and Kharbanda, 2017). There are several hypotheses currently been proposed in relation to this disorder and most of them are linked to dysbiosis mediated increased intestinal permeability/loss of gut barrier function and subsequent dysregulation in intestinal immunity (Taghipour *et al.*, 2016). Metagenomic studies conducted in patients with inflammatory bowel disease have exhibited reduced abundance of several core microbial members of a healthy gut microbiota, such as *F. prausnitzii*, *Roseburia* spp. and *A. muciniphila* and interestingly a reduced expression was observed in the *Clostridium* cluster IV bacteria, who are well-known butyrate producers (Ottman *et al.*, 2012).

Apart from inflammatory bowel disease, there are several other common inflammatory diseases associated with a dysbiotic gut microbiota such as, allergic diseases, which are the inflammatory responses mediated against allergens that subsequently induce unfavorable immune responses initiating various symptoms in different organs (Rodríguez *et al.*, 2015). A reduced intensity and diversity of gut microbiota related abnormal immune maturation during the infancy has been linked with the incidence of allergic diseases

during infancy and later stages of life, for example, low abundance of bifidobacteria and lactobacilli and an early colonization of *C. difficile* (Rodríguez *et al.*, 2015). Further, lower total gut bacterial diversity, lower abundance in phylum Bacteroidetes and genus *Bacteroides* during the infancy have been observed in children who developed atopic eczema and also found to correlate with the higher risk of allergy development in babies born via caesarean surgeries (Rodríguez *et al.*, 2015).

Thus, the exposure to a diverse set of microbial antigens during the infancy is considered as a major driver of developing a strong and balanced adaptive and innate immune system, due to the exposure to diverse bacterial antigens (Rodríguez *et al.*, 2015). Limited microbial exposure is suggested to result in insufficient regulatory and Th1-like T cell introduction, which are well-known to be involved in counteracting allergy induced Th2 responses, is suggested to be the underlying mechanism (Rodríguez *et al.*, 2015). Further, the correlation between the abundance and diversity of phylum Bacteroidetes and the improvement of allergy conditions, is associated with the protective functions mediated by the increased SCFA circulation in the blood with anti-inflammatory functions against allergic inflammation, such as the production of Th1-associated chemokines (Rodríguez *et al.*, 2015).

1.5. Research statement and objectives

As discussed in details previously in this chapter, dietary fiber or more specifically prebiotic class of fibers, has an integral role in the salubrious status of health, attributed to their ability to be get selectively fermented, to alter the gut microbial structure and by extension the functionality and their fermentation products and mediate beneficial biochemical and physiological functions. The magnitude of the beneficial effects mediated is found to manly depend on the type/quantity of the prebiotic fiber reaching the colon and the availability of suitable specific gut bacteria to utilize them, thus the relationship among prebiotic fiber, gut bacteria and the beneficial effects is interdependent. With regard to these interdependencies, dietary interventions with well-characterized sources of dietary fiber/prebiotic fiber has a great advantage as it is considered as the most economic and successful means of maintaining a healthy gut microbiota, thus by extension improving health status.

It is clear that the most prebiotic fibers are plant-based and they have been identified, isolated and characterized from a wide variety of flora. Some of these identified prebiotic fiber sources can be agricultural products, which are consumed as whole foods or utilized as ingredients in food processing, while certain others have been identified in agricultural by-products, which are essentially waste products generated during the processing of agricultural products, thus require specialized techniques to isolate them. As discussed earlier, the nature of colonic fermentation and subsequent metabolic processes depend mainly on the functionality of the substrate, thus, an important question arises as to which type of plant indigestible materials are prebiotic or more beneficial or more affordable to a larger community. Thus, in the next few chapters I have examined an agricultural product (sorghum gains; *Sorghum bicolor* L. Moench) and an agricultural by-product (sugarcane bagasse; *Sacchurum officinarum* L.), for their potentials in colonic fermentation, under various conditions, with respect to many colonic fermentation parameters, in order to evaluate their suitability as prebiotic substrates.

CHAPTER 2

***In vitro* fermentation characteristics of sorghum (*Sorghum bicolor* L. Moench)**

enzyme resistant fraction (ERF)

2.1. Introduction

2.1.1. Structure and organization of the sorghum grain

Sorghum grains are generally round in shape, vary in the size from 1.0 to 3.0 g per 100 g kernels and the color contrasts from white to shades of yellow, red and brown (Wall and Blessin, 1969). Similar to most grains' physiology, sorghum seed also consists of three major anatomical sections: pericarp (bran), endosperm (storage organ) and the germ (reproductive organ). The pericarp/bran (8% of the grain) is a three-layered section: epicarp (outer layer), mesocarp (middle layer) and endocarp (innermost layer). The epicarp which acts as a protective layer usually has a thin waxy film and also may be pigmented (Wall and Blessin, 1969). The mesocarp of sorghum grain has a very distinctive anatomic feature that cannot be seen in any other cereal or food-grade crop. The sorghum mesocarp is found to store starch granules, where its thickness can range from very thin cellular remnants of small amount of starch granules to 3 to 4 layers containing a large amount of starch granules. The endocarp consists of layers of cross cells and tube cells (Wall and Blessin, 1969). Between the pericarp and the endosperm, there is a layer known as the "testa" and if present, it might be highly pigmented, as it is found to be absent in most sorghum varieties (Wall and Blessing, 1969).

The endosperm is the main storage organ (82% of the grain) consisting of aleurone layer, corneous and floury areas. The aleurone layer is rich in proteins (protein bodies, enzymes), ash (phytin bodies) and oil (spherosomes). Corneous (horny/vitreous) and floury endosperm areas are the major areas of starch granule storage. The starch granules in corneous and floury endosperms, along with protein bodies, are enclosed in a protein matrix. The germ (10% of the grain) that is placed near the base of the seed consists of embryonic axis, scutellum, plumule and a primary root and, the germ is known to contain high levels of lysine and tryptophan, which are excellent in quality (Wall and Blessing, 1969). As the germ/embryo

is deeply embedded in the sorghum kernel, it is comparatively difficult to remove the germ during dry-milling (Wall and Blessing, 1969).

Similar to most of the other cereal grains, the major constituent of sorghum grain is also carbohydrates, specifically starch, which is around 83% of the total endosperm (Wall and Blessing, 1969). Sorghum endosperm is known to consist of storage parenchyma cells filled with starch granules immersed in a protein matrix, which is clearly segregated into two distinct areas: a peripheral vitreous area and a central floury/opaque area (Wong *et al.*, 2009; Watterson and Shull, 1993). The vitreous endosperm area is characterized as dense and shiny, where the components are densely packed and a continuous protein matrix is clutching the starch granules and protein bodies (Watterson and Shull 1993). In contrast, the floury endosperm is identified as a soft and floury area with loosely packed protein bodies and a discontinuous protein matrix surrounding the starch granules (Watterson and Shull, 1993). Depending on the type of sorghum, either waxy (100% amylopectin) or non-waxy (25% amylose + 75% amylopectin), the endosperm characteristics varies (Rooney and Pflugfelder, 1986).

2.1.2. Starch digestibility

Digestibility of any starch depends on the starch granule structure and the organization, as it determines the rate or degree of hydrolytic enzyme accessibility to starch molecules, amylose and amylopectin that are stored in a highly ordered manner inside the granules. There are several levels of granule organization in relation to enzymatic hydrolysis: granular structure (shape, size, porosity), supramolecular structure (crystalline type, perfection of crystals, degree of crystallinity and organization of crystalline and amorphous material) and molecular structure (organization of amylose and amylopectin) (Buléon *et al.*, 1998).

Among the first set of hurdles against enzymatic digestion, shape and size determine the ease and available surface area for enzyme attachment, while porosity is the basis for enzymatic digestion in any type of starch granule, which facilitates the formation of channels for enzyme penetration into the central cavity of the starch granules, from where the starch digestion initiates (Benmoussa *et al.*, 2006). For example, in high digestible sorghum lines, the density of pores is higher compared to less digestible wild type lines and a mutant sorghum line with a starch granule shaped-like a “collapsed thallus”, provided rapid access to enzymes exhibiting a higher digestibility (Rooney and Pflugfelder, 1986).

Supramolecular structure of a starch granule reflects the structural integrity of the starch granule structure, thus, it determines the ease or hardness to breakdown the structural organization (crystalline and amorphous areas) of a starch granule, either by physical or chemical means (Buléon *et al.*, 1998). Molecular structure of amylose and amylopectin is generally universal for all starches, yet certain botanical-source specific characteristics might modify their fine structure and organization and ultimately the strength and the nature of the crystalline structure. For example, intermolecular cross-linking of amylopectin with phosphate groups in potato starch, determines the type of crystal units it forms (B-type) and subsequently the functional properties such as solubility, viscosity, thermal properties and digestibility, etc. (Pelpolage *et al.*, 2016).

Generally in cereals, the structure and composition of starch and their interactions with non-starch components (proteins, lipids, anti-nutritional factors, etc.) determine the digestibility of starch and subsequently the nutritive value of the source (Rooney and Pflugfelder, 1986). Starch in sorghum accounts for almost 70 to 80% of total dry weight and amylose and amylopectin fractions are reported to be 25 and 75% of total starch content, respectively (Lichtenwalner *et al.*, 1978; Wong *et al.*, 2009). Digestibility of any starch is considered to be inversely proportional to the amylose content due to its dense, crystalline nature (Rooney and Pflugfelder, 1986). Further, in sorghum the ratio between starch to protein (70 to

80%:10%) is found to affect the functionality of starch (digestibility and gelatinization) to a greater extent compared to other cereals (Wong *et al.*, 2009).

Corn and sorghum both share a very close phylogenetic relationship and starch granules are found to be similar in size, shape and composition, yet the digestibility of starch in corn is significantly higher than sorghum (Rooney and Pflugfelder, 1986; Emmambux and Taylor, 2009). The reduced digestibility of starch in sorghum is attributed to the structural and compositional differences between corn and sorghum endosperms. It has been observed that the digestibility of sorghum starch was substantially affected by the endosperm characteristics, where grains with floury endosperm characteristics exhibited better digestibility compared to corneous endosperm texture (Rooney and Pflugfelder, 1986; Wong *et al.*, 2009).

In comparison to the corn endosperm, sorghum is known to possess a considerably higher proportion of peripheral endosperm consisting of large, polygonal, tightly packed starch granules that are in a close association with small, spherical protein bodies and further immersed in a protein matrix (Wong *et al.*, 2009; Duodu *et al.*, 2003). In the peripherally located corneous endosperm, the protein matrix and the gluing protein bodies surrounding the starch granules, act as barriers to enzyme and moisture migration (due to the cross-links formed between matrix proteins and β - and γ -kafirins) into starch granules (Wong *et al.*, 2009; Rooney and Pflugfelder, 1986). This structure and organization make the peripheral endosperm extremely dense, hard and recalcitrant to enzymes and water, subsequently resulting a lower digestibility of starch (Rooney and Pflugfelder, 1986).

In comparison to the vitreous endosperm, floury endosperm reported significantly higher starch digestibility *in vitro* (Wong *et al.*, 2009). Albeit, the floury endosperm of sorghum is known to contain comparatively larger starch granules, fewer kafirin-rich protein bodies and a discontinuous protein matrix, which in compositional point of view very similar to the corn floury endosperm, the digestibility of sorghum starch in floury endosperm also ranks lower than that of corn. The difference in digestibility is

again attributed to the structural differences between the two endosperms, where the floury endosperm of sorghum is known to contain cross-linked kafirins, which decreases both starch and protein digestibility and further, starch granules and protein bodies are more tightly adhered on to each other compared to corn, which strengthens the starch-protein interaction reducing the digestibility (Rooney and Pflugfelder, 1986).

The recalcitrant behavior of protein in sorghum can be attributed to kafirins (major storage protein in sorghum), as zein (major storage protein in corn) in corn has not been reported to behave similarly (Rooney and Pflugfelder, 1986). *In vitro* digestibility studies coupled with microscopic examination have found that structural organization of sorghum kernel and endosperms have a significant influence on the degree of digestibility, where less digestible lines of sorghum were found to possess highly organized, tightly packed endosperms and a clear demarcation between floury and corneous endosperms (Wong *et al.*, 2009). Further, numerous and more tightly associated protein bodies were observed in less digestible sorghum lines (Wong *et al.*, 2009).

The significant effect of the protein matrix on the digestibility of starch had been studied previously under *in vitro* conditions and it was evident that starch digestibility is significantly improved in the absence of the protein matrix (due to the hydrolysis of protein by pronase enzyme) in sorghum, possibly due to the increased surface area of starch granules in contact with starch hydrolyzing enzymes (Rooney and Pflugfelder, 1986). Further, sequential digestion of sorghum with pepsin and human saliva α -amylase, respectively, was found to enhance *in vitro* starch digestibility of sorghum compared to sequential digestion in the converse order, suggesting the significant inhibiting effect of the protein-starch interactions on starch digestibility (Wong *et al.*, 2009). Thus, the unique structural organization of the protein matrix is found to determine the nutritional quality of sorghum that distinguishes it from other cereals (Wong *et al.*, 2009).

Other than protein, starch (amylose)-lipid complexes, enzyme inhibitors, phytates, lectins and tannins also are known to reduce the starch digestibility in different mechanisms. In sorghum, specifically brown color tannin-rich grains, protein-tannin complex formation not only diminishes the protein digestibility, but also reduces the starch digestibility by inhibiting certain enzyme systems (Rooney and Pflugfelder, 1986). Due to the compositional variations in non-starch components among the sorghum varieties as a consequence of the wide genetic diversity among them, digestibility and nutritional properties also vary significantly (Wall and Blessin, 1969). For example, brown tannin-rich varieties exhibit significantly lower digestibility and subsequently lower nutritional value, most probably due to the inactivation of amyloglucosidase by tannins (Rooney and Pflugfelder, 1986). Further, *in vitro* digestibility studies reported higher gas production values and dry matter disappearance rates for isolated starch over sorghum flour, suggesting the substantial effect of non-starch component interactions on starch digestibility (Rooney and Pflugfelder, 1986).

2.1.3. Factors affecting the resistant starch content in sorghum

As previously mentioned, the major compositional parameter in sorghum dry matter is starch, which accounts for 70 to 80% (Sang *et al.*, 2008). Similar to any starch, the physicochemical properties, thermal, rheological properties and digestibility of starch are directly dependent upon the ratio between amylose to amylopectin, amylopectin fine structure and chain length distribution (Pelpolage *et al.*, 2016; Seung *et al.*, 2008). Amylose content in any starch is known to strongly determine the gelatinization, digestibility by α -amylase, retrogradation and pasting properties, etc. (Seung *et al.*, 2008). Thus, in the point of view of the inherent resistant starch (RS) content in a botanical source, amylose content is a major influencer, whose content depends on the interaction effects between genetic and environmental factors (Pelpolage *et al.*, 2016).

In sorghum, amylose content in a specific grain is determined by the presence or absence or the dose of a recessive gene “*wx*”, where it is absent in normal sorghum (*WxWxWx*), present in heterowaxy (*WxWxwx* or *Wxwxwx*) and waxy sorghum (*wxwxwx*) in different doses, upon which their physicochemical properties are substantially different (Seung *et al.*, 2008). For example, the total starch content in normal, heterowaxy and waxy sorghum was reported to be 71.4, 71.2 and 68.4%, respectively, while amylose content was 23.7, 14.0 and 0%, respectively (Seung *et al.*, 2008).

In any type of starch, there are three major fractions, namely, rapidly digestible starch (RDS), slowly digestible starch (SDS) and RS and the proportions of these fractions in a starch determine its ileal digestibility (Perera *et al.*, 2010). Normal and heterowaxy sorghum starches exhibited significantly less RDS contents (12.0% dwb), while waxy starch contained almost two folds higher RDS content (21.5% dwb) (Seung *et al.*, 2008). Interestingly, the RS contents in heterowaxy starch topped with a 23.7% dwb followed by normal sorghum starch with 17.9% dwb, suggesting that the amylose content might not be the only determinant of the RS content in sorghum starch (Seung *et al.*, 2008).

Another important physicochemical factor that determines the degree of α -amylase digestibility is the amylopectin chain length distribution, where a higher proportion of short chain amylopectin (degree of polymerization < 15) is positively correlated with a higher RDS content and in heterowaxy sorghum the proportion of amylopectin chains with a degree of polymerization < 15 is significantly lower compared to normal sorghum starch (Seung *et al.*, 2008). Further, raw grain sorghum flour has exhibited significantly lower RDS and significantly higher RS contents in comparison to raw wheat flour (Poquette *et al.*, 2014). Moreover, unprocessed sorghum reported the highest RS content and lowest RDS content compared to barley, oat, maize and rice also (Giuberti *et al.*, 2013).

As previously discussed, albeit sorghum is comparable with corn in terms of composition and starch granule structure, it has always been distinguished from other cereals due to its unique functionality

involving the protein matrix, which is identified as the key player in sorghum starch digestibility (Poquette *et al.*, 2014). Thus, sorghum's prominent indigestible properties and high RS content are attributed to both compositional and structural features such as, starch structure, protein-starch interactions and amylose contents (Poquette *et al.*, 2014). Certain other studies have suggested that amylose content in sorghum does not necessarily indicate the digestibility rate or resistance to digestion, while starch granule characteristics such as channel density and sorghum protein matrix are suggested to influence digestibility and resistance (Benmoussa *et al.*, 2006). Due to the high genetic variation among the sorghum cultivars, the RS content reported by different studies vary substantially: 0.31 to 65.66% (Teixeira *et al.*, 2016), 3.4 and 4.3% (Saravanabavan *et al.*, 2013), 2.21 and 2.95% (Khan *et al.*, 2013), 1.77% (Ragaei *et al.*, 2006), 6.46% (Niba and Hoffman, 2003), which on average is considered to vary between 12 to 21% for most sorghum varieties (Zhu, 2014).

2.1.4. Fermentation potential of sorghum

As discussed in the Chapter 1, the components in diet that are insufficiently digested in the small intestine provide the carbon and energy substrate for large intestinal microbial population. In an *in vivo* study that used two breeds of swine reported that sorghum fed animals had a trend of higher amount of starch entering the large intestine suggesting the presence of higher amount of RS (Morales *et al.*, 2002). This could be due to the lower ileal breakdown of sorghum starch as previously mentioned in the section 2.1.2. Further, the same study showed that the microbial activity was higher in the sorghum fed animals compared to the corn based diet, based on the concentration of purine bases (Guanine and Adenine) in the colonic content and a higher amylopectinase activity also had been observed reflected by the purine base ratio (Guanine:Adenine) (Morales *et al.*, 2002). The above fact might suggest that, due to higher starch flow into the large intestine, the starch hydrolyzing microbial function might have been improved. And the propionate and acetate contents seemed to increase in the proximal and distal colons, while butyrate

was confounded by the breed of animals fed a sorghum diet (Morales *et al.*, 2002). Thus, this study sheds some light on the fact that sorghum might be a good candidate in obesity, overweight and diabetes management due to the exhibited lower ileal digestibility of starch (low glycemic index), improved colonic fermentation and higher short chain fatty acid (SCFA) contents.

Moreover, another study that used rats as the animal model reported that body weight and body fat weight was significantly reduced in overweight animals upon feeding a low fat sorghum based diet, while the above parameters were not reported to be improved in high fat sorghum based diet (Shen *et al.*, 2015). This observation could be bridged with the findings of the previously reported study, where it found a higher starch flow into the large intestine, which means a lower ileal digestibility and thus a lower calorie content. On the other hand, serum lipid profile was improved in sorghum fed overweight and obese animals compared to control diet despite the fat level in the diet, and serum adiponectin and leptin levels in sorghum fed groups were significantly higher and lower, respectively, than lean, overweight and obese controls (Shen *et al.*, 2015). Furthermore, in sorghum fed animals, *Lactobacillus* and *Bifidobacterium* counts were significantly higher and *Enterobacteriaceae* counts were significantly lower compared to control low/high fat diets fed animals (Shen *et al.*, 2015). Thus, Shen *et al.* (2015) suggested that lower body weight gain and fat weight gain in obese and overweight rats fed sorghum could be attributed to the functions of leptin and adiponectin mediated by microbial fermentation by-products. Further, *in vivo* studies involving animal and human subjects have reported promising evidence on reduced plasma glucose levels upon using whole grain sorghum (Emmambux and Taylor, 2009; Carciofi *et al.*, 2008; Wong *et al.*, 2009; Poquette *et al.*, 2014).

2.1.5. Research statement, objectives and hypothesis

Low *in vitro* flour digestibility of sorghum is considered as a potential trait for overweight and obesity management, is found to be associated with low digestibility of both starch and protein fractions, endosperm texture and structure, interactions between starch and non-starch components such as tannins, alcohol soluble proteins, as mentioned in section 2.1.2 (Souilah *et al.*, 2014; Axtell *et al.*, 1981). With the low digestibility of starch in sorghum, it becomes an assuring source of RS with an average between 12.0-21.5%, specifically RS type I, the physically inaccessible starch by the amyolytic enzymes and water (Zhu, 2014; Axtell *et al.*, 1981).

Resistant starch enriched food sources have earned the spotlight of many studies recently, aiming to mitigate the escalating increase of chronic metabolic diseases directly associated with the diet and life style (Duodu *et al.*, 2003). For instance, co-morbidities of metabolic syndrome, inflammatory bowel disease and colorectal cancers are found to be associated with dysbiosis or altered gut microbiota (Duodu *et al.*, 2003). And these diseases are predicted to be prevented or moderated by dietary changes, because diet can significantly affect the etiology of such diseases, as the composition of the diet may stimulate the growth of beneficial bacteria or inhibit unfavorable bacteria and the availability of fermentative by-products with beneficial biochemical and physiological effects (Valdes *et al.*, 2018; Birt *et al.*, 2013; Barczynska *et al.*, 2017; Fernández *et al.*, 2016; Yang *et al.*, 2017).

With the previously reported high amount of RS, which is in complement with the lower enzymatic digestibility of starch, sorghum is anticipated to be a promising prebiotic which has not yet been explored on its potential completely. Thus, the aim of this study was to determine the nature of the influence of sorghum flour enzyme resistant fraction on selected indicators of microbial function, such as microbiota composition, pH, toxic metabolite production and SCFAs fermentation using a mixed culture of swine fecal bacteria in a simulator laboratory scale fermenter.

Pig has been identified as a comparatively more suitable model for physiological studies related to many areas including intestinal microbiota studies, due to similar anatomical structure of the gastrointestinal tract, being an omnivorous mammalian with a similar gut microbial composition (Roura *et al.*, 2016). Thus, it was hypothesized that the use of swine fecal inoculum would represent the human fecal microbiota, by whom, the sorghum digestive enzyme resistant fraction would be utilized as a substrate for their metabolism and could bring about beneficial effects on the above mentioned indicators of microbial function and gut health.

2.2. Materials and Methods

2.2.1. Materials

Whole white sorghum (S-Wh) and refined white sorghum (S-Rf) flour (polished grain flour) were provided by Nakano Industry (Takamatsu, Japan) and cellulose (microcrystalline powder; 20 μm) was purchased from Sigma-Aldrich Co., (St.Louis, USA). All the chemicals used were of analytical grade.

2.2.2. Preparation of sorghum flour enzymes resistant fraction (ERF) by *in vitro* enzymatic digestion

Sorghum flour was subjected to *in vitro* enzymatic hydrolysis by a mixture of amyloglucosidase (4- α -D-glucan glucosidase from *Aspergillus niger*, ≥ 300 U/mL) and pancreatin (from porcine pancreas, 8 x USP specifications) purchased from Sigma-Aldrich Co. (St. Louis, USA). Four milliliters of amyloglucosidase solution and 3.0 g of pancreatin powder were dissolved in 400 mL of maleate buffer (0.1 M, pH 6.0) and centrifuged (H- 80R, Kokusan Co., Tokyo, Japan) at 3,000 rpm (4°C, 10 min) to collect the supernatant of the enzyme mixture. Twenty grams of each sorghum flour was homogenized with 100 mL of enzyme supernatant in a capped sealed 300 mL conical flask and incubated at 37°C in a water bath for 16 h with continuous agitation at 130 rpm.

After incubation, 100 mL ethanol (99.5% v/v) was mixed with the sample in a beaker and allowed to stand at room temperature for 3 h and centrifuged (3,000 rpm, 4°C, 10 min) in 50 mL capped plastic tubes to remove the supernatant. The pellet containing ERF was washed sequentially with ethanol and acetone to remove sugars as mentioned below. The pellet was re-suspended in 15 mL of 99.5% (v/v) ethanol by vortexing and the supernatant was discarded subsequently after centrifugation under the same conditions. Finally, the pellet was suspended in 15 mL of acetone and centrifuged to remove the supernatant. The pellet was dried on an Aluminum foil at room temperature overnight and later ground and sieved (180 μm aperture size), weighed and stored in clean airtight Zip-lock® bags at 4°C until further analysis.

2.2.3. Proximate composition analysis of the ERFs

a. Moisture content

The moisture content in ERFs was analyzed according to AOAC 930.15 method. One gram of ERF was measured into pre-weighed moisture cans and oven-dried at 135°C until a constant weight for around 2 h. The final weight was measured after cooling the capped moisture cans in a desiccator and moisture content was calculated gravimetrically in triplicates as follows;

$$\text{Moisture content (\%)} = \frac{(\text{Dry weight} - \text{Empty weight})}{\text{Sample wet weight}} * 100$$

b. Crude protein content

Crude protein content was analyzed by Kjeldahl method (AOAC 979.09) as mentioned below. Two grams of ERFs were measured into a filter paper and the folded filter paper was put into Kjeldahl tubes in triplicates (an empty filter paper as a control). A Kjeltab (contains Cu catalyst) and 20 mL concentrated H₂SO₄ were added into each Kjeldahl tube and kept overnight at room temperature. On the following day, the Kjeldahl tubes were heated on a heater at 420°C for 2 h until the color of the liquid in the Kjeldahl tubes changed from black to light blue. Distilled water was added to dilute H₂SO₄ and allowed to cool down. The cooled content in the Kjeldahl tubes were quantitatively transferred into 100 mL volumetric flasks and volumerized with distilled water. Later 10 mL of the volumerized sample with two drops of methyl red and four drops of mix indicator was distilled with 35% NaOH in the distillation unit, where the liberated ammonia was captured by 0.05 M H₂SO₄ in a conical flask at the receiving end, which was later titrated with 0.1 M NaOH. Crude protein content was calculated using a conversion factor of 6.25 for sorghum.

$$\text{Crude protein content (\%)} = \frac{[\text{NaOH volume (Control-Sample)} * 1.004 * 0.0014 * 10 * 6.25]}{\text{Sample dry weight}} * 100$$

c. Crude lipid content

Crude lipid content was analyzed according to AOAC 920.85 method. Three to five grams of the sample was measured into a filter paper, wrapped well, put into a thimble and the thimble was placed in the extraction tube. The extraction flask (pre-weighed) was filled with 250 mL of diethyl ether. The extraction process was conducted for 16 h on a water bath at 50°C followed by complete removal of diethyl ether by evaporation. The final weight of the extraction flask was measured and the crude lipid content was gravimetrically calculated as follows;

$$\text{Crude lipid content (\%)} = \frac{(\text{Final weight} - \text{Empty weight})}{\text{Sample dry weight}} * 100$$

d. Ash/mineral content

Ash content was determined by AOAC 923.03 method. Two grams of ERFs were measured into clean pre-weighed crucibles with caps and were charred on open Bunsen flame for 5 to 10 min. Then the crucibles were transferred into muffle furnace (FM-35, Yamato Scientific Co., Ltd., Japan), where they were digested at a temperature of 550° to 600°C for around 6 h. Ash content was measured and calculated gravimetrically in cooled samples later.

$$\text{Ash (mineral) content (\%)} = \frac{\text{Weight (Ash-Empty)}}{\text{Sample dry weight}} * 100$$

e. Carbohydrate content

Total carbohydrate content was calculated as follows;

$$\text{Carbohydrate content (\% w/w)} = [100\% - (\text{moisture\%} + \text{crude protein\%} + \text{crude lipid\%} + \text{ash\%})]$$

f. Resistant starch content

Resistant starch content in the sorghum ERFs was determined by Megazyme resistant starch assay procedure (K-RSTAR 08/11, Wicklow, Ireland) according to AOAC method 2002.02. ERF samples (100 ± 5 mg) in triplicate were incubated in a shaking water bath (37°C; 200 strokes/min), with 4.0 mL pancreatic α-amylase (10 mg/mL) containing amyloglucosidase (3 U/mL) for 16 h. Followed by the incubation, further reaction was terminated by 4.0 mL of 99.5% (v/v) ethanol and the RS pellets were obtained by centrifugation (3,000 rpm, 10 min). The RS pellet was further washed and cleaned with 50% (v/v) ethanol two times followed by centrifugation after each wash under the same conditions. Resistant starch pellet was dissolved in 2 M KOH, while vigorous stirring on an ice water bath for 20 min and then KOH was neutralized by 8 mL of sodium acetate buffer (1.2 M, pH 3.8). Resistant starch was quantitatively hydrolyzed by 0.1 mL of amyloglucosidase (3300 U/mL), while incubating on a water bath at 50°C. In order to quantify the amount of D-glucose, 3 mL of glucose oxidase/peroxidase (GOPOD) reagent was added into 0.1 mL aliquots of incubated samples followed by the color development in a water bath at 50°C for another 20 min (for samples <10% RS content). Absorbance of samples was measured at 510 nm against the reagent blank (0.1 mL of 100 mM sodium acetate buffer; pH 4.5 and 3.0 mL of GOPOD) and the D-glucose standard [0.1 mL of D-glucose standard (1 mg/mL) and 3.0 mL of GOPOD] incubated under the same conditions.

$$\text{RS content (\%)} = \text{Absorbance (sample-blank)} * F * \frac{10.3}{0.1} * \frac{1}{1000} * \frac{100}{\text{sample weight (dry)}} * \frac{162}{180}$$

F – (100 / absorbance of D-glucose standard); 10.3 / 0.1 – volume correction; 1 / 1000 – conversion factor for milligrams; 162 / 180 – conversion factor for free D-glucose into anhydrous D-glucose

The results of the proximate composition analysis is presented in Table 2.1.

2.2.4. *In vitro* intestinal fermentation model

a. Feces collection and fecal slurry preparation

Fresh feces from 4 to 5 mo old three male weaner pigs (breed-Berkshire) were collected from the herd that belonged to Hokkaido Obihiro Agricultural High School (Obihiro, Hokkaido, Japan). Feces were collected directly from the anus from each animal into separate aseptic plastic Zip-lock® bags and were sealed and stored in an ice box equipped with an Anaeropack-Anaero® sachet (Mitsubishi Gas Chemical, Tokyo, Japan) soon after collection. Collected feces were transported in the ice-box and soon after transportation they were stored in a designated refrigerator at 4°C. Two grams from each fecal sample was measured into separate Stomacher® extraction bags (Filtration Bag II TI7520, Eiken Chemical Co., Ltd., Tokyo, Japan) using separate heat sterilized spatula and 20 mL of sterilized (121°C; 20 min; SX-300 high pressure steam sterilizer, Tomy Seiko Co., Ltd., Tokyo, Japan) saline solution (0.85% v/v NaCl) was added into each bag using a sterile pipette. The three bags were homogenized in a homogenizer (Organo EXNIZER-400 bacteria test homogenizer, Misumi Co., Tokyo, Japan) for 5 min and the filtrate collected in each Stomacher® bag was conjugated in a sterile 50 mL plastic tube.

b. *In vitro* fermentation

In vitro fermentation of ERFs was conducted in separate laboratory scale fermenters (220 mL working volume, Able & Biot, Tokyo, Japan) with the ability to control temperature, pH and agitation speed and to maintain anaerobic conditions. Generally, the fermenter medium constitutes of 6.6 g of test sample with a fecal slurry of 2.0% (v/v), where a 3.0% (w/v) final carbohydrate content and a 0.8% (w/v) nitrogen content are maintained (Han *et al.*, 2014). After proximate composition analysis, the crude protein content was found to be 36.4% and 57.8% in whole sorghum flour ERF (ERF-Wh) and refined sorghum flour ERF (ERF-Rf), respectively, thus the final nitrogen content was adjusted to a maximum level of 1.73%

(w/v) in all three fermenter media with the basal nutrient broth (Difco, Sparks, MD, USA), similar to that of the ERF-Rf as shown in Table 2.2. Fermenter jars were sterilized (SX-300 high pressure steam sterilizer) with 170 mL distilled water and were allowed to cool down on an aseptic bench overnight. Initially 6.6 g from cellulose (CON), ERF-Wh and ERF-Rf and the required amounts of nutrient broth and cellulose powder to adjust carbohydrate and nitrogen levels were added into the three sterilized fermenter jars containing 170 mL sterilized distilled water, and finally 50 mL of fecal inoculum (2.0% v/v) was added into each jar and each jar was fixed on to the fermenter apparatus (Fig. 2.1).

Under normal conditions, the fermenter jars are allowed to pre-incubate overnight with the nutrient broth and fecal inoculum, before adding the test sample (Han *et al.*, 2014), but in this case the pre-incubation step was omitted as ERF-Rf containing medium was devoid of nutrient broth to avoid starvation of the microflora. Fermentation was conducted in quintuplets per each test sample under anaerobic conditions maintained by a continuous supply of CO₂ (0.4 Pa), at a minimum pH level of 5.5 (controlled by 2 M NaOH) and at a temperature of 37°C with an agitation speed of 100 rpm for 48 h. Samples (10 mL/sample/once) were collected at 0, 6, 12, 24 and 48 h into sterile 10 mL syringes, divided into 1.5 mL sterile Eppendorf® tubes and stored at -30°C until further analyses. At every sampling, pH and temperature were recorded.

2.2.5. Microbiological analyses

a. Viable plate count method

A serial dilution (10^1 to 10^7) was prepared from each sample (500 µL) in 4.5 mL of sterilized saline solution (0.85% NaCl). Respective diluted samples (100 µL) were cultured to enumerate specific bacterial species counts by viable plate count method with selective media. Coliform and lactic acid bacteria (LAB) were enumerated 24 h after culturing on eosin methylene blue (EMB) agar (Eiken chemical Co., Ltd.,

Tokyo, Japan) and de Man, Rogosa and Sharpe (MRS) agar (Oxoid, Hampshire, UK), respectively. Anaerobes and *Lactobacillus* were enumerated after 48 h of incubation on glucose blood liver (BL) agar (Eiken chemical Co., Ltd., Tokyo, Japan) and Rogosa agar (Oxoid, Hampshire, UK), respectively, while *Bifidobacterium* was enumerated from transgalactosylated oligosaccharide (TOS)-propionate agar (Yakult Pharmaceutical Industry, Tokyo, Japan) after 72 h of incubation. LAB was cultured using pour plate method, while the other four were cultured using spread plate method and all five were incubated at 37°C (TVN680DA Advantec® incubator, Toyo Seisakusho Kaisha Ltd., Tokyo, Japan). BL, Rogosa and TOS culture plates were stacked in 7 L anaerobic jars along with 3 Anaeropack-Anaero sachets (Mitsubishi Gas Chemical). Subsequently after the specific incubation periods, colonies were visually counted and were expressed as log₁₀ colony forming units per milliliter (CFU/mL) of the working volume.

b. 16S ribosomal RNA gene sequencing method

b (i). Extraction of genomic DNA

Extraction of bacterial DNA from the samples obtained at 48 h (stored at -30°C) was conducted by the modified phenol-free repeated beads beating plus column (RBB+C) method (Yu and Morrison, 2004) as mentioned below. Thawed cecal samples were centrifuged (16,000×g, 4°C, 5 min) and the supernatants were discarded. Three hundred microliter lysis buffer (500 mM NaCl, 50 mM Tris-HCl, 50 mM EDTA, 4% sodium dodecyl sulfate; pH 8.0) was added and the cecal content precipitate was conjugated well with the lysis buffer using pipette aspiration and the content was completely transferred into sterile screw-capped tubes (Watson® BioLab, Fukaekasei Co., Ltd., Kobe, Japan) containing 0.4 g beads (mixture of 0.3 g of 0.1 mm + 0.1 g of 0.5 mm). The screw-capped tubes were subjected to thorough mixing using the cell destroyer (4,260 rpm, 15 min, 3 cycles; PS1000, Prosense Inc., Tokyo, Japan) and later was incubated at 70°C for 15 min in a water bath. After incubation the tubes were centrifuged (16,000×g, 4°C, 5 min) and the supernatants were collected into new sterile 1.5 mL Eppendorf® tubes. The tubes contained cecal

precipitate were washed with another 300 μ L of lysis buffer and repeated the procedure once more. Two hundred and sixty microliter of ammonium acetate (10 mM) was added in to the conjugated supernatant and mixed well with pipette aspiration and kept for 5 min on ice and centrifuged (16,000 \times g, 4 $^{\circ}$ C, 10 min). The clear supernatants were transferred into new sterile 2 mL Eppendorf[®] tubes and a similar volume of isopropanol was added and mixed well with pipette aspirations. This was kept on ice for 30 min and later was centrifuged (16,000 \times g, 4 $^{\circ}$ C, 10 min). After centrifugation, the supernatant was removed carefully and the DNA pellet was re-suspended in 70 % (v/v) ethanol and again centrifuged (16,000 \times g, 4 $^{\circ}$ C, 10 min). The supernatant was completely removed and the tubes were allowed to dry under aseptic conditions for around 40 min. After the tubes were completely dried, the DNA pellet was dissolved well with 200 μ L of Tris-EDTA (TE) buffer (1 M Tris, 0.5 M EDTA; pH 8.0) and was stored at -30 $^{\circ}$ C until purification.

b (ii). Purification of genomic DNA

The DNA pellets dissolved in TE buffer were thawed and the extracted genomic DNA was purified (QIAamp DNA Stool Mini Kit, QIAGEN, Valencia, CA, United States) as follows. Two microliter of DNase-free RNase (10 mg/mL) was added into each sample and mixed with pipette aspiration followed by incubation in a 37 $^{\circ}$ C water bath for 15 min. Then 15 μ L of proteinase K was added into each sample, mixed with pipette aspirations and 200 μ L of AL buffer (same as lysis buffer) was added and similarly mixed by pipette aspirations and incubated at 70 $^{\circ}$ C for 10 min. Followed by the incubation, 200 μ L 99.5% (v/v) ethanol was added and mixed well with pipette aspiration and the content was quantitatively transferred into a column collection tube and centrifuged (16,000 \times g, 20 $^{\circ}$ C, 1 min). Five hundred microliter of AW1 buffer was added into the column tube fixed to a new collection tube and was centrifuged (16,000 \times g, 20 $^{\circ}$ C, 1 min). Then 500 μ L of AW2 buffer was added into the column tube fixed to a new collection tube and was centrifuged (16,000 \times g, 20 $^{\circ}$ C, 1 min) and again centrifuged under the same conditions with a new collection tube to dry. Finally 50 μ L of AE buffer (10 mM Tris-Cl, 0.5 mM EDTA,

pH 9.0) was added into the column tube fixed to a sterile 1.5 mL Eppendorf® tube, kept at room temperature for 2 min and was centrifuged (16,000×g, 20°C, 1 min). The quality and the concentration of extracted community DNA was measured (Nano Drop 2000c spectrophotometer, Thermo Fisher Scientific, Tokyo, Japan) and the genomic DNA concentration was adjusted to 5 ng/μL with Tris-EDTA buffer (10 mM Tris, 1 mM EDTA, pH 8.0). The concentration adjusted samples were stored at -30°C until further analysis.

b (iii). Quality control polymerase chain reaction and agarose gel electrophoresis

A Polymerase chain reaction (PCR) and an agarose gel electrophoresis was conducted further to assure the quality of extracted and purified genomic DNA. The employed PCR reaction mix is presented in Table 2.3. Twenty four microliters of the reaction mix (without DNA sample) and 1 μL of DNA sample (template DNA or sample DNA) were measured into each PCR tube. The PCR tubes were placed in the thermal cycler (2720, Applied Biosystems, CA, United States) and the employed PCR conditions for total bacteria are presented in Table 2.4.

Followed by PCR, agarose gel electrophoresis was conducted. The components and the required amount of agarose gel mixture are provided in Table 2.5. The prepared gel mixture was solidified using the appropriate gel solidifying well along with the plastic ladder to form wells for 20 min. After 20 min, the ladder was removed and the gel was transferred into the electrophoresis tank (Mupid®- 2 Plus, Mupid Co., Ltd., Tokyo, Japan), where the wells in the gel were aligned to the negative side of the electrophoresis tank. The gel was appropriately submerged in the electrophoresis tank with an adequate amount of 1X TAE buffer (40 mM Tris, 20 mM acetic acid, 1 mM EDTA, pH 8.0). DNA ladder (DM2100, ExcelBand™, 100 bp DNA ladder, SMOBIO Technology Inc., Hsinchu City, Taiwan) was added into the first well and then 4 μL of PCR samples were added into each well along with 1 μL of loading buffer. Finally, the electrophoresis tank was closed with the lid and electrophoresis was started (100 V; 30 to 40

min for 25 mL gel/15 min for 15 mL gel). When the diffusion reached the appropriate length, the electrophoresis was terminated and the gel was photographed to view the bands (Fig. 2.2).

B (iv). 16S metagenomics sequencing library preparation

Followed by the extraction, purification and quality testing, the 16S sequencing library was prepared. The preparation of 16S rRNA gene amplicon required for sequencing was done following the method described in the 16S Metagenomic Sequencing Library Preparation Guide (Illumina, 2013) as follows.

First stage PCR and PCR clean-up

During the first stage PCR, V3 and V4 variable regions of 16S rRNA gene were amplified using the following bacterial overhang adapters and universal primers; forward primer and the overhang adapter (5'-TCGTCGGCAGCGTCAGATGTGTATAAGAGACAGCCTACGGGNGGCWGCAG-3') and the reverse primer and the overhang adapter (5'-GTCTCGTGGGCTCGGAGATGTGTATAAGAGACAGGATTACHVGGGTATCTAATCC-3'). The first stage PCR reaction mix is presented in Table 2.6 and the PCR conditions for the first stage PCR are presented in Table 2.7.

Followed by the first stage PCR, a PCR clean-up was done to remove free primers and dimer species using AMPure XP® beads (Beckman Coulter Co., Tokyo, Japan). First stage PCR amplicon containing PCR plate was centrifuged (1,000×g, 20°C, 1 min) and 20 µL of AMPure XP® beads (homogenized for 30 s by vortexing before adding) per well using a multichannel pipette followed by mixing with pipette aspiration for 10 times. After incubating for 5 min at room temperature, the PCR plate was placed on a magnetic stand to obtain a clear supernatant and the supernatant was removed. The condensed amplicons were washed with 200 µL of 80% (v/v) ethanol for two times while standing on the magnetic stand, followed by discarding ethanol after each wash. The beads were allowed to air dry for 10 min and 52.5 µL of 10 mM Tris (pH 8.5) was added into each well after removing the PCR plate from the magnetic

stand and the beads were re-suspended well with pipette aspirations (10 times). Followed by standing at room temperature for 2 min, the plate was re-placed on the magnetic stand and allowed to stand until a clear supernatant was obtained. Fifty microliter from clear supernatants were obtained into a new 96-well PCR plate.

Second stage PCR and PCR clean-up

During the second stage PCR, Illumina sequencing adapters and dual index barcodes were multiplexed to the first stage PCR amplicons using Nextera® XT Index Kit (Illumina Inc., San Diego, CA, United States). The second stage PCR mix is presented in Table 2.8. Five microliter from previously obtained 50 µL amplicon samples was transferred into a new 96-well PCR plate. The index primer addition should be carefully conducted according to the set-up shown in the library preparation guide (Illumina, 2013). Following the addition of specific contents into each well, the contents were mixed by pipette aspirations 10 times and then the plate was sealed and centrifuged (1,000×g; 20°C; 1 min). The program for the second stage PCR is presented in Table 2.9. PCR clean-up followed by the second stage PCR was similar to the clean-up after the first stage PCR as mentioned in details earlier under the first stage PCR clean-up.

Library quantification, normalization and pooling

The concentration of the final amplicon library after second stage PCR was quantified (Quantus™ fluorometer, QuantiFluor® dsDNA System, Promega, Madison, WI, United States) and the concentration of the library components were diluted to 4 nM with 10 mM Tris (pH 8.5). Five microliter from each diluted DNA sample of the library were mixed together.

Library denaturing and MiSeq sample loading

Five microliter of pooled library (4 nM) was conjugated with 5 µL of 0.2 N NaOH, mixed on vortex briefly and centrifuged later (280×g; 20°C; 1 min). After centrifugation, it was kept at room temperature

for 5 min and 990 μL of pre-chilled hybridization buffer was added into 10 μL of denatured DNA library to bring the concentration to 20 pM. The denatured DNA library was diluted further with pre-chilled hybridization buffer to obtain a final concentration of 8 pM.

Each library should contain at least 5% PhiX as an independent internal control for low diversity libraries, which should be diluted to the same concentration as the original DNA library. Initially 2 μL of 10 nM PhiX library was combined with 3 μL of 10 nM Tris (pH 8.5) to dilute the concentration from 10 nM to 4 nM. Then it was further diluted to 2 nM with 0.2 N NaOH (5 μL from each). Followed by incubation at room temperature for 5 min, 990 μL of pre-chilled hybridization buffer was added to 10 μL of 2 nM PhiX library sample resulting a concentration of 20 pM. Similar to denatured DNA library dilution, Phix library was also diluted to 8 pM with pre-chilled hybridization buffer.

Thirty microliter from denatured and diluted PhiX library and 570 μL of denatured and diluted DNA library were combined together and the pooled library was denatured using a heat block (96°C, 2 min) immediately before loading it to MiSeq v3 reagent cartridge (Illumina Inc.). Followed by incubation, the contents were mixed by inverting the tubes 1 to 2 times and was placed in an ice-water bath (ice:water = 3:1) for 5 min. The heat de-generated DNA and PhiX combined library was loaded to MiSeq v3 cartridge, cartridge was loaded to MiSeq Illumina System (Illumina Inc.) and was subjected to paired-end sequencing by Illumina MiSeq System (Illumina Inc.).

b (v). 16S gene sequence analysis

The analysis of retrieved raw 16S rRNA gene sequences was conducted using Quantitative Insight Into Microbial Ecology (QIIME) software (version 1.9.1) (Lozupone and Knight, 2005). FASTQC reports were prepared for the raw sequences (R1, forward; R2, reverse) obtained from paired-end sequencing. The R1 and R2 reads were joined. The raw reads obtained from MiSeq platform are generally multiplexed

(attached with unique identifier indices), thus the raw sequences were demultiplexed to remove unique identifiers using QIIME. Then a split library was prepared which was used for further analysis. After preparing the split library, operational taxonomic units (OTUs) were assigned. Using the assigned OTUs, a BIOM table was prepared to be used in the downstream analysis. Next with reference to a reference database (Greengenes database version 13.8, at 97% similarity level), a program was run to align the sequences using open reference picking method. After picking the OTUs, the BIOM table was filtered for unidentified sequences and contamination samples from reagent and PCR negative control samples. The BIOM table was normalized using an equal subsampling size of 11,667 sequences. Alpha diversity parameters, Shannon's diversity index and observed species index were prepared using QIIME. Distances between bacterial communities in different samples were calculated by the weighted UniFrac distance metric and it was illustrated using a principal coordinate analysis (PCoA) plot, which was also prepared in QIIME. Calypso version 5.2 (Zakrzewski *et al.*, 2017) was used to generate hierarchical clustering, and microbial network maps.

2.2.6. Short chain fatty acid analysis in fermenter media

Samples obtained from fermenter media at 0, 6, 12, 24 and 48 h sampling points were centrifuged (3,000 rpm, 4°C, 15 min) and 450 µL was pipetted out from the supernatant into 2 mL Eppendorf® tubes and 1 mL of 0.5 N HClO₄ (60% v/v) was added into each tube. After leaving at room temperature for 5 min, the tubes were centrifuged under the same conditions for 10 min. Followed by centrifugation, 300 µL of the supernatant was filtered into new 1.5 mL Eppendorf® tubes using a 1 mL syringe and a micron membrane filter (0.45 µm; DISMIC-03CP, Advantec, Toyo Roshi Kaisha, Tokyo, Japan). The prepared samples were analyzed by High Performance Liquid Chromatography (HPLC, Shimadzu LC-10AD, Kyoto, Japan). Analytical specifications were as follows: column, RSpak KC-811 (8.0 mm x 300 mm, Shodex, Tokyo, Japan); eluent and flow rate, 2 mM HClO₄ at 1 mL/min; column temperature, 47°C;

reaction reagent and flow rate, ST3-R ($\times 10$ diluted, Cat. No. F56120000, Shodex) at 0.5 mL/min; UV-vis spectrophotometric detector (SPD-10A, Shimadzu) wavelength, 450 nm. SCFA concentration in samples were calculated as follows;

$$\text{SCFA concentration } (\mu\text{mol/mL}) = \frac{\text{Sample peak area}}{\text{Standard peak area}} * \frac{\text{Standard volume}}{\text{Sample volume}} * \frac{1.45}{0.45} * \frac{1000}{\text{molecular weight}}$$

(1.45 / 0.45)-dilution factor

2.2.7. Ammonia-nitrogen analysis

Ammonia-nitrogen content in the samples were analyzed using a commercially available kit (Wako Pure Chemical Industry Ltd., Tokyo, Japan). Samples obtained from fermenter media were mixed well on a vortex and centrifuged (3,000 rpm, 4°C, 15 min). The supernatant should be diluted according to the ammonia-nitrogen content in the samples, generally by 100 folds or 200 folds with phosphate buffer (0.1 M; pH 5.5). A standard series (0, 100, 200, 300, 400 $\mu\text{g/dL}$) should be prepared using the appropriate quantities of the standard solution and the diluent provided in the kit. Fifty microliter from samples and standards were conjugated with 400 μL of deproteinizing solution, mixed well on vortex and centrifuged (3,000 rpm, 4°C, 5 min). Two hundred microliter of the deproteinized samples and standards were pipetted out into new 1.5 mL Eppendorf® tubes and 200 μL of color reagent A was added and mixed well on vortex, followed by 100 μL of color reagent B and 200 μL color reagent C, followed by vortex mixing after adding each. Finally, the tubes were incubated in a 37°C water bath for 20 min for the color development. Soon after taking out from the water bath the tubes were cooled down in water to avoid further reaction until the measurement of absorbance. Absorbance was measured at 630 nm using UV-vis spectrophotometer (UV-1600, Shimadzu). Ammonia-nitrogen concentration in the samples were calculated as follows;

$$\text{Ammonia-nitrogen concentration (mg/mL)} = \frac{(\text{Sample absorbance} - \text{y intercept})}{\text{Gradient of line}} * \text{dilution} * \frac{1}{1000}$$

2.2.8. Statistical analysis

All data except microbial community DNA data were analyzed for their significance by analysis of variance (ANOVA) using SPSS statistical software version 17.0 (SPSS Inc., Chicago, IL, USA). When significant differences among the test groups were revealed, mean scores were compared by Tukey's test. Statistical significance of Shannon's diversity index was determined by ANOVA paired with Tukey's test (SPSS). Relative abundance and statistical significance of phyla, genera and species among the three samples were compared using Kruskal-Wallis H test in Calypso (version 5.2). A *p* value less than 0.05 was considered as statistically significant.

2.3. Results and Discussion

2.3.1. Proximate composition of ERFs and *in vitro* digestibility of sorghum flour

Proximate composition of the ERFs of sorghum are presented in Table 2.1. The two sorghum ERF samples were distinctively different in terms of the non-digested protein and carbohydrate contents, where ERF-Rf possessed significantly higher ($p < 0.05$) resistant protein content and ERF-Wh had significantly higher resistant carbohydrate and RS contents. Further, significantly and comparatively lower ash and fat contents in ERF-Rf, could be due to the removal of the bran and the germ during the milling and polishing processes. Thus, the ERFs were significantly different in terms of the availability of microbial accessible carbohydrates.

Most of the dietary proteins are considered to be highly hydrolysable with few exceptions, for example the subgroups of sorghum prolamins (specially β - and γ -kafirin) are found to be resistant to enzymatic hydrolysis and known to form an enzymatic resistant layer of disulfide bonds that restricts protease diffusion, which subsequently maintain the integrity of the protein bodies attached to the surface of the starch granules (Chibber, Mertz, and Axtell, 1980). In sorghum flour as previously discussed, the *in vitro* starch digestibility was found to be inhibited due to the restricted accessibility of amylolytic enzymes through the protein matrix and the protein bodies that encapsulate the starch granules (Axtell *et al.*, 1981). The above mentioned structural barrier function of proteins could be the reason behind the very high protein content observed in ERF-Rf/Wh as presented in Table 2.1. Additionally, the channels, the main enzyme penetration routes towards the center of the starch granules, are found to be lined by the prolamins (Rooney *et al.*, 1986). Thus, both the external protein barrier and the internal protein barrier within starch granules might have interfered migration of amylolytic enzymes (towards the starch granule and inward within the starch granule) and subsequently the starch digestion (Axtell *et al.*, 1981).

2.3.2. Microbiota composition in the fermenter media during the fermentation period

Viable plate count method

The levels of anaerobes, coliform, LAB, *Lactobacillus* and *Bifidobacterium* in the fermenter media during the total incubation period are presented in Fig. 2.3. Anaerobic microbial count was significantly higher ($p < 0.05$) in ERF-Rf and ERF-Wh between 6 to 24 h period compared to the CON group, where the anaerobic counts were similar between the two ERFs between the said period. Coliform level of ERF-Wh was significantly lower than CON and ERF-Rf between 6 to 24 h, while ERF-Rf expressed coliform counts similar to CON throughout the incubation period except at 24 h, where the count was significantly lower than CON, yet higher than ERF-Wh. *Lactobacillus* and *Bifidobacterium* counts were significantly higher in both sorghum ERFs compared to the CON group between 6 to 48 h incubation period. A clear trend could not be observed in the LAB count among the three substrates, yet in ERF-Rf, there was an increased LAB count until 6 h sampling point and remained constant since then. LAB counts in ERF-Wh and CON groups fluctuated between 6 to 48 h period, and all three substrates leveled at 48 h with similar LAB counts.

The two sorghum ERFs reported similar counts for anaerobes, *Lactobacillus* and *Bifidobacterium* between 6 to 48 h incubation period, which suggested a similar influence on the carbohydrate fermenting microbiota by the two substrates, further supported by the fact that especially bifidobacteria number is known to be influenced by the presence of readily fermentable substrates such as RS (Zhang *et al.*, 2006). The above mentioned observation suggested that, either the availability or accessibility to the microbial accessible substrates in the two sorghum ERFs might have been similar irrespective of the significant differences in their resistant carbohydrate and RS contents (Table 2.1). Interestingly, with the constant bacterial counts for anaerobes, *Lactobacillus* and *Bifidobacterium* from 6 h onwards suggested that the microbial growth might have reached the stationary phase, where either there had been no net growth

further or a minimal growth. Among the reasons for a batch culture to reach the stationary phase, complete exhaustion of carbon and energy source and inhibition of cell growth due to the toxicity developed by the waste products, could have played significant roles in the above mentioned scenario, owing to the fact that we could observe a higher ammonia-nitrogen production (section 2.3.5), which is known to cause cytotoxicity (Lichtenwalner *et al.*, 1978; Aarthi *et al.*, 2003).

16S rRNA gene sequencing technique

Generally, high-throughput DNA sequencing methods such as 16S rRNA next generation sequencing methods, yield a large amount of data on gut microbiota, thus enable us to derive important features of the bacterial communities, utilizing the tools in microbial ecology and other quantification tools recently developed. One of the main features of a bacterial community is its diversity, which is defined as the variability among the living organisms from ecological niches of which the organisms are a part of. Biological diversity (not only microbial diversity) can be illustrated using two main parameters, species richness and relative species abundance/evenness (Kim *et al.*, 2017). Evenness compares the uniformity of the population size of each of the species present in the community. Species richness presents the numerical value of the different kinds of organisms present in the particular community, a measurement based on the OTUs defined at a preferred level of taxonomic resolution (Kim *et al.*, 2017). When these two parameters are higher in a given niche, biological diversity is considered to be higher, which can be mathematically quantified using ecological tools such as Shannon-Weaver, Rarefaction, Simpson and Chao1 indices (Kim *et al.*, 2017).

Shannon's diversity index (synonyms: Shannon-Weaver index, Shannon-Wiener index, Shannon entropy, etc.) is an estimate of both species richness and species evenness, which focuses more on species richness and calculated as follows;

$$\text{Shannon's index} = - \sum_{i=1}^s (p_i \ln p_i)$$

s - number of OTUs

p_i - proportion of the community represented by OUT “ i ”

The value of Shannon’s index is found to be higher when both the species richness and the distribution of individual organisms among the observed species become even (Kim *et al.*, 2017). In this study, both the Shannon’s index (Fig. 2.4.a) and observed species index (Fig. 2.4.b) were significantly higher ($p < 0.05$) in the CON group compared to the two sorghum groups, where the two sorghum groups exhibited similar microbial diversities. Similar diversities observed in the two sorghum ERFs might also further strengthen the fact that despite the significant differences in the proximate compositions between them (Table 2.1), the microbial available substrates might have been similar in quality and quantity. The higher Shannon’s index observed in the CON group might have been due to both higher evenness and richness of the microbial community, which might be unusual for a substrate like cellulose which is known as a negligibly fermented carbohydrate. But it could be due to the certain members in pig fecal microbiota that was utilized as the inoculum in this study, who are able to ferment cellulose, a distinct difference between human and swine fecal gut microbial functions (Han *et al.*, 2014).

When the microbial community structure among the three samples (β -diversity) was compared using the principle component analysis (PCoA) plot, there was a clear separation between cellulose medium (CON) and the two sorghum ERF media (Fig. 2.4.c). Further, the two sorghum ERF media clustered together, suggesting that the microbial community structure (synonymously the microbial composition) between ERF-Wh and ERF-Rf was similar, which again provided evidence to the fact that the available quality and quantity of the microbial accessible substrates might have been similar in the two sorghum ERFs. Yet,

one of the samples obtained at 48 h from each of the three substrates showed a substantial variation in the microbial structure as evident on PC1 and PC2 axes. This could be due to the inter-sample variations in fecal inoculum mainly as the gut microbiota is known to respond to even slightest changes in the environment, management practices, growth stage, etc. albeit, they were controlled as constant as possible.

At the highest level of taxonomy, all three samples showed a very high abundance of phylum Firmicutes, while other dominant phyla included were Spirochaetes, Proteobacteria and Fusobacteria (Fig. 2.5.a). Firmicutes abundance was similar between the two sorghum ERFs, while both ERFs had a significantly higher abundance compared to CON. Other important phyla such as Bacteroidetes, Actinobacteria and Verrucomicrobia abundance was not significantly different. Fig. 2.5. b to d, shows the changes in the microbial composition in the three fermenter media at different levels of taxonomy in the descending order. Least discriminant effect size plot (LEfSe) plot (Fig. 2.5.e) presents the characteristic microbial genera for each fermenter medium, who had been responsible for the observed biochemical differences discussed later. LDA score represents the magnitude of the contribution of each genera to the observed variability. CON group showed a higher diversity of the characteristic microbial genera similar to the α -diversity (Shannon's and observed species indices) observed previously (Fig. 2.4.a, b). In contrast, the two sorghum ERFs possessed a very few characteristic microbial genera, where genus *Slackia* dominated ERF-Wh and genera *Lactobacillus* and *Streptococcus* represented ERF-Rf. Members of genus *Slackia* are known for their roles in lipid, xenobiotic and isoflavone metabolism (Cho *et al.*, 2016; Rafii, 2015).

2.3.3. pH in the fermenter media

As shown in Fig. 2.6, pH in the CON fermenter medium constantly increased throughout the incubation period. The two sorghum ERFs exhibited similar variations in the pH between 0 to 24 h period. Between 0 to 6 h period, there was a reduction of pH in the sorghum ERFs media compared to CON medium, subsequently between 6 to 24 h period, pH gradually increased in the two sorghum ERF media, yet was

significantly lower than CON. Fermenter medium pH in ERF-Wh stabilized at 24 h and remained constant for the next 24 h period, but pH in ERF-Rf medium continued to increase reaching a value significantly higher than ERF-Wh and similar to that of CON at the end of the incubation period of 48 h.

Generally, a lower pH in the gut is considered to be healthy and beneficial as it suppresses growth and proliferation of pathogenic microorganisms (Seung *et al.*, 2008). In this study, albeit the pH of the sorghum ERFs were significantly lower compared to that of CON between 6 to 24 h period, pH continuously increased as described previously. Increase in pH can be a result of progressive depletion of fermentable carbohydrate substrate and concomitant increase in protein fermentation and alkaline substance production such as ammonia (Seung *et al.*, 2008).

2.3.4. Short chain fatty acid production

Fig. 2.7 shows the changes in SCFA production during the incubation period. Acetate, propionate and butyrate are the major individual SCFAs (collectively accounts for >90% of total SCFAs), which are generally found in a molar ratio of 3:1:1 (Upadhyaya *et al.*, 2016). The concentrations of the three major SCFAs were statistically similar among the three substrates between 0 to 12 h period.

Acetate is the major and one of the initial organic acids produced along with pyruvate and lactate as a result of the fermentation of readily available fermentable carbohydrates (hexoses and pentoses) by probiotic bacteria (Fernández *et al.*, 2016). In this study also it was the major fermentation by-product with the highest proportion in all three substrates at the end of the incubation period. Acetate content reached 70% of total SCFAs production in CON medium, while it was only 58 and 53% in ERF-Wh and ERF-Rf, respectively, which were in contrast to the findings reported by Giuberti *et al.* (2013). Albeit, acetate production in the two ERFs media was comparatively higher, its concentration was not significantly different among the substrates throughout the whole incubation period at each sampling point.

The similar acetate concentrations at the sampling points could be due to its utilization in the butyrate biosynthetic pathway by cross-feeding microbiota (Fernández *et al.*, 2016). Previously, it has been reported that the butyrate production and acetate disappearance were significantly correlated (Birt *et al.*, 2013). One other possible reason for the similar levels of acetate in the three substrates could be the low availability or accessibility to microbial accessible substrates in the two sorghum ERFs due to the resistant protein matrix (Axtell *et al.*, 1981; Upadhyaya *et al.*, 2016).

Acetate production is mainly attributed to genera *Bifidobacterium* and *Lactobacillus* who belong to the functional group of LAB (Fernández *et al.*, 2016). Albeit, the sorghum ERFs possessed significantly higher counts for *Bifidobacterium* and *Lactobacillus* between 6 to 48 h incubation period (Fig. 2.3) according to the results obtained by viable plate count method, acetate production was not significantly different among the three substrates during the mentioned incubation period. According to previous reports, increased counts of bifidobacteria are related to the greater production of acetate (Zhang *et al.*, 2014). Higher variability observed for the LAB counts during the incubation period might have conferred an effect on the acetate production. Additionally, as previously mentioned, bacterial growth reached their stationary phase at 6 h, thus minimal metabolic activity of the microbiota in the medium might have been another possible reason for the similar concentrations of acetate among the three substrates during 6 to 48 h period. On the other hand according to community DNA data obtained by 16S rRNA sequencing at 48 h, *Bifidobacterium* abundance was not significantly different among the substrates, yet the abundance was comparatively higher in the two sorghum ERF media compared to CON medium (Fig. 2.5.f). Thus, results obtained from both microbial evaluation methods exhibited similar trends for *Bifidobacterium* abundance, yet DNA sequencing methods are identified as high precision tools over traditional plate count method. Moreover, the *Bifidobacterium* abundance obtained from DNA sequencing technique and acetate production at 48 h can be clearly related. Further, *Lactobacillus* and *Streptococcus* abundance was

significantly higher in the two sorghum ERFs (Fig. 2.5.f) which could have been the reason behind the increased rate of acetate production between 12 to 24 h period.

Similar to acetate, propionate production also exhibited a sharp increase in production at 24 h for the two sorghum ERFs and the concentrations were significantly higher ($p < 0.05$) at 24 and 48 h compared to CON. But there was no significant difference in the concentration between ERF-Wh and ERF-Rf. A lag phase (very low production period) in propionate and butyrate production was observed from 0 to 6 h and 0 to 12 h periods, respectively. As the pre-incubation step was omitted in this experiment, the long lag phase might represent the time required for the physiological adaptation of the bacterial cells to the culture conditions. Further, the lag phase observed in butyrate production could also be attributed to the lower production and availability of acetate in the media, which is a precursor for butyrate synthesis (Fernández *et al.*, 2016).

Butyrate production also exhibited the similar sharp increase in production at 24 h. At 24 h butyrate production was significantly ($p < 0.05$) higher in both sorghum ERFs compared to CON, but similar between ERF-Wh and ERF-Rf. At 48 h, butyrate concentration exhibited a dramatic increase in ERF-Rf, which was significantly higher compared to the CON and ERF-Wh. Thus, ERF-Rf can be speculated as a butyrogenic substrate, as it fermented almost two folds higher butyrate content than the CON medium, which is an insoluble dietary fiber source (Seung *et al.*, 2008). Butyrate concentration of ERF-Wh remained almost similar at 24 and 48 h, for which the exact underlying reason is unclear, yet it could be due to substrate preferences, substrate availability to microbiota and competitive abilities exist in the fermenter environment, which might have affected the proliferation of butyrate producing bacteria (Martínez *et al.*, 2010; Han *et al.*, 2005).

Total SCFAs production remained similar among the fermentation substrates from 0 to 12 h period in this study, despite the anaerobe counts being significantly ($p < 0.05$) higher in the sorghum ERFs than CON,

where SCFAs production in the gut is considered to be reflective of the anaerobic microbial count (Upadhyaya *et al.*, 2016). This could reflect a potential deficiency in fermentative substrates in the media, further supported by the acquisition of stationary phase from 6 h onwards by the anaerobes (Lichtenwalner *et al.*, 1978). At the end of the incubation period, total SCFAs content was significantly higher in ERF-Wh and ERF-Rf, where ERF-Rf had the significantly highest amount of total SCFAs concentration, which might have resulted due to the higher butyrate production observed at 48 h and accumulation over the time (Han *et al.*, 2014). Individual SCFAs and total SCFAs concentrations in the CON sample were observed to be similar to that of the sorghum ERFs between 0-12 h, which might be due to the ability of pig fecal microbiota to ferment cellulose like dietary fiber, which is highly unlikely to be fermented by the human gut/fecal microbiota (Roura *et al.*, 2016).

The fermentation rates were not significantly different among the three substrates between 0 to 12 h (except for propionate), except at 48 h sampling point (Fig. 2.8). All three individual SCFAs exhibited a distinct increase in the rate of production between 12 to 48 h period, compared to 0 to 12 h period. Observed higher rate of production in the two sorghum ERFs between 12 to 48 h period, could be attributed to either an increment in the population of certain microbial members or structural changes to the fermentable substrates (Han *et al.*, 2005). The fermentative substrate may be subjected to structural changes due to hydrolysis by microbial enzymes, such as weakening or formation of entry routes through protein barriers, formation of pores on the surface of starch granules increasing surface area, etc. which can improve the accessibility (Blazek and Gilbert, 2010; Müntz, 1996).

Molar ratios of individual SCFA were not significantly different among the samples between 6 to 24 h period (Fig. 2.9). At 48 h sampling point, molar ratio of acetate in the CON sample was significantly ($p < 0.05$) higher compared to the sorghum ERFs, where the two ERFs had a similar ratio, which might reflect the utilization of acetate in the sorghum media. Significantly higher propionate production rate observed

in the two sorghum ERFs can be further strengthened by the higher rate of production observed at 24 h sampling point. Propionate molar ratio was similar between the sorghum ERFs, yet comparatively and significantly higher than CON at 24 h and 48 h sampling points, respectively. Butyrate exhibited an increasing trend in the molar ratio towards the end of the incubation period, which was significantly higher in ERF-Rf and CON compared to ERF-Wh. Lower molar ratio of acetate and higher molar ratio of butyrate observed in the sorghum ERFs, reflected the ability of sorghum ERFs to influence the growth and proliferation of bacteria who were able to cross feed on acetate and produce butyrate (Thursby and Juge, 2017).

2.3.5. Ammonia-nitrogen content

Ammonia-nitrogen content in all three substrates gradually increased up to 12 h sampling point (Fig. 2.10). At 6 h sampling point, CON sample had significantly higher ($p < 0.05$) ammonia-nitrogen content compared to the sorghum ERFs and in comparison to 0 h sampling point, the ammonia-nitrogen content in the sorghum ERFs at 6 h point also clearly increased in different rates. Up until 12 h and 24 h, ammonia-nitrogen content in ERF-Rf was either significantly or comparatively lower than that of the ERF-Wh and CON, respectively. After 12 h, ammonia-nitrogen content in ERF-Wh got stabilized, while CON and ERF-Rf continued to rise. At 12 h, ammonia-nitrogen content in ERF-Rf exhibited a sharp increase compared to 6 h sampling point. At 24 h, ammonia-nitrogen content in ERF-Rf was significantly lower compared to CON. At 48 h, ERF-Rf exhibited the highest ammonia-nitrogen content, along with the highest total SCFA content.

The significantly higher ammonia-nitrogen content observed in ERF-Rf at 48 h could have been due to the accumulation of ammonia-nitrogen in the fermenters during the incubation period (Han *et al.*, 2014). Generally, a lower pH in the fermentation medium is attributed to higher SCFAs production, yet a rise in pH could be observed in ERFs even with higher SCFAs concentration during 24 to 48 h period, which

might be due to the basifying effect of ammonia released into the medium (Taciak *et al.*, 2015; Guergoletto *et al.*, 2016).

The higher ammonia-nitrogen production observed towards the end of the incubation period, could be due to the initiation of amino acid fermentation (Taciak *et al.*, 2015; Guergoletto *et al.*, 2016; Han *et al.*, 2014). When energy supply for the growth and development of the microbiota from carbohydrate fermentation becomes deficient, deamination of amino acid initiates to meet the energy demand (Guergoletto *et al.*, 2016; Han *et al.*, 2014). The higher and increasing ammonia-nitrogen content in ERF-Rf could be attributed to the lower availability or accessibility of fermentable carbohydrates (Giuberti *et al.*, 2013).

Prior to microbial fermentation, the complex carbohydrates are hydrolyzed by the bacterial glycoside hydrolases or polysaccharide lyases into simple molecules (hexoses, pentoses, fucose, rhamnose, etc.) and the rate of complex carbohydrate depolymerization directly affects the rate of availability of microbial accessible carbohydrate substrates (Giuberti *et al.*, 2013; Taciak *et al.*, 2015). These depolymerization reactions also occur via hydrolyzing enzymes generated from either microbiota or host, thus genetic expression of host and composition of gut microbiota might significantly affect the initiation of the previously mentioned depolymerization reactions, thus limiting the availability of fermentative carbohydrate substrates.

Additionally, the amount of protein escaping into the colon and the ratio between fermentative carbohydrates:proteins and protein type affect the extent of microbial fermentation of protein in the colon (Taciak *et al.*, 2015). Further, according to Taciak *et al.* (2015), protein fermentation progresses when the said ratio decreases, which suggests the fact that the low availability of fermentative carbohydrates at the time. As presented in Table 2.1, the resistant carbohydrate and the resistant protein contents in the two sorghum ERFs were significantly different and the ratio of the carbohydrates (fermentative carbohydrates=RS):protein (without nutrient broth protein) in ERF-Rf is lower compared to ERF-Wh

(ERF-Rf:0.25; ERF-Wh:0.43) at the beginning of the incubation, which might have further decreased later. This fact highlighted the potentially lower availability of energy from RS fermentation in ERF-Rf, which might be the reason for continuously increasing ammonia production in ERF-Rf since its sharp increase at 12 h.

2.4. Implications and Conclusions to Chapter 2

Both sorghum ERFs demonstrated their prebiotic nature as they influenced the growth and proliferation of beneficial gut microbial species such as *Lactobacillus*. The two ERF fractions exhibited a slow initial fermentation of SCFAs, which drastically increased after 12 h of incubation. Albeit, the acetate concentrations of ERFs were similar to that of the CON medium, both ERFs yielded significantly higher propionate, butyrate and total SCFAs between 24 to 48 h period than CON. Butyrogenic nature of ERF-Rf was manifested by its significantly higher butyrate molar ratio (24 to 48 h) and production rate (12 to 48 h). Thus as hypothesized, sorghum ERFs exhibited potential prebiotic characteristics, as they induced the growth and proliferation of beneficial bacteria and subsequent production of important individual SCFAs.

Both ERF fractions caused a progressive fermentation of protein as reflected by the continuously increased ammonia-nitrogen content in the media. Albeit, the pH in the sorghum ERF media was significantly lower than that of the CON, the pH increased successively between 6 to 24 h and 6 to 48 h periods in ERF-Wh and ERF-Rf, respectively. Thus, the lack of microbial fermentable carbohydrates available for microbial metabolism in the fermentation medium as the carbon and energy source, might have shifted to utilize proteins in ERF-Rf.

Inherent deficiency of fermentative substrates can be eliminated as the sorghum ERFs reported significantly higher amounts of RS contents (Table 2.1). Thus, less availability of fermentable carbohydrate substrates due to either lower depolymerization or barred accessibility to available fermentative substrates could have consequently deprived the availability of energy for microbiota. Thus, it might have been the driving factor for the higher ammonia production as a repercussion of deamination of amino acids for energy harvesting. Further, the higher ratio between protein and carbohydrate in the

two sorghum ERFs might have also influenced the amino acid fermentation as previously mentioned (section 2.3.5).

Accordingly, these observations implicated that, albeit sorghum is reported to possess the highest RS content available among the cereals, and predicted to be an assuring source of fermentative carbohydrates, protein fermentation seemed more prominent. Though the sorghum ERFs had beneficial influence on gut microbiota and SCFAs production, they can infer negative effects on host health because of the higher ammonia-nitrogen content and high pH, especially by ERF-Rf despite its butyrogenic nature. Higher protein fermentation in sorghum ERFs indicated a low availability of fermentative carbohydrates regardless of the higher RS contents observed, which might be due to the dietary resistant protein matrix and protein bodies surrounding the starch granules in sorghum. Thus, it is important to observe and confirm these observations using a suitable *in vivo* animal model.

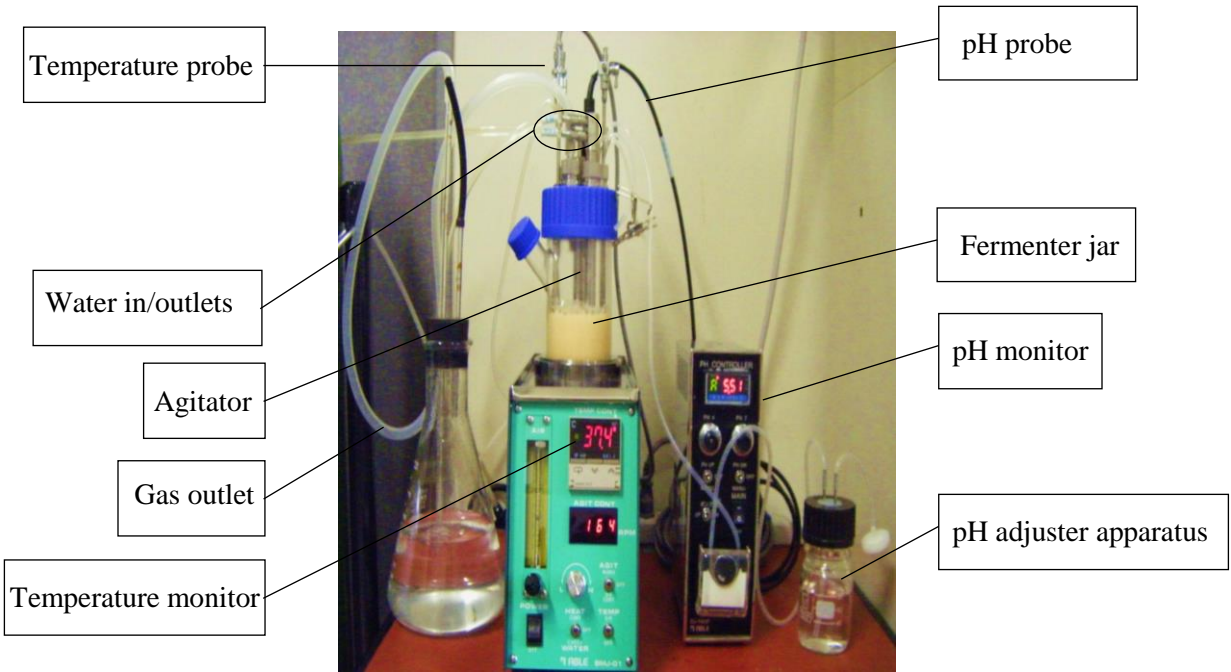


Fig. 2.1. *In vitro* simulator fermenter apparatus

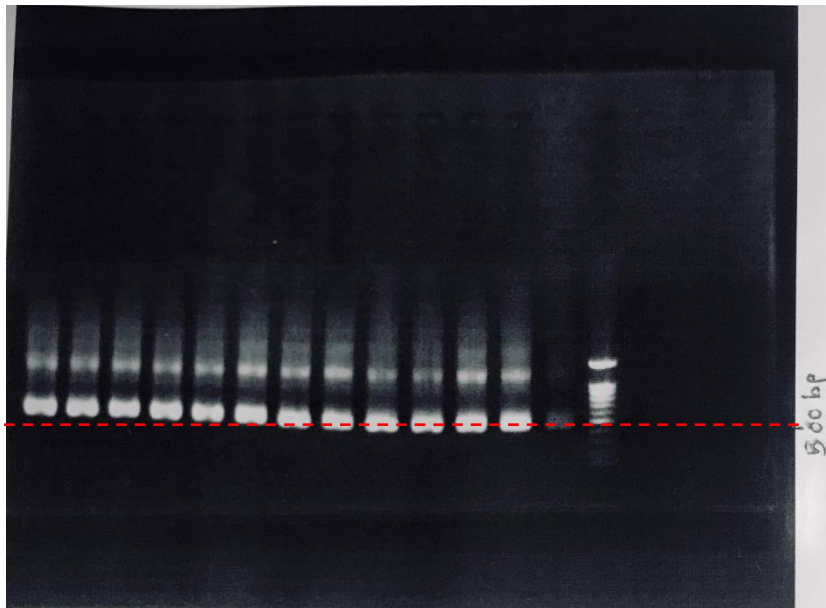


Fig. 2.2. Gel electrophoresis bands for quality assurance PCR samples

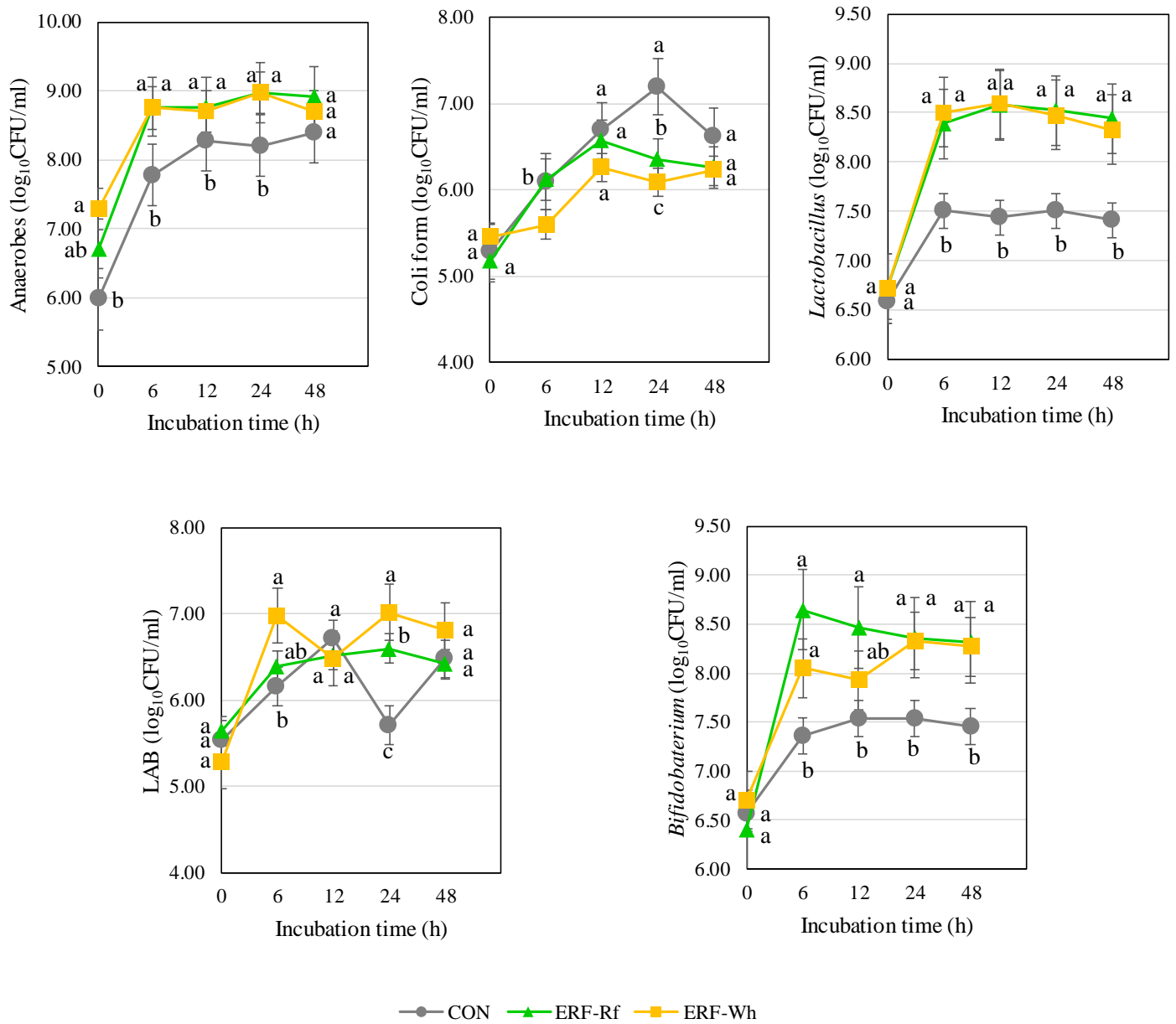


Fig. 2.3. Selected microbial population counts in the fermenter media during the 48 h fermentation period.

Data presented are mean \pm SE (n=5). Different letters at each sampling point represent significant differences among the substrates at ($p < 0.05$).

(CON, Cellulose; ERF-Wh, enzyme resistant fraction of whole white sorghum flour; ERF-Rf, enzyme resistant fraction of refined white sorghum flour)

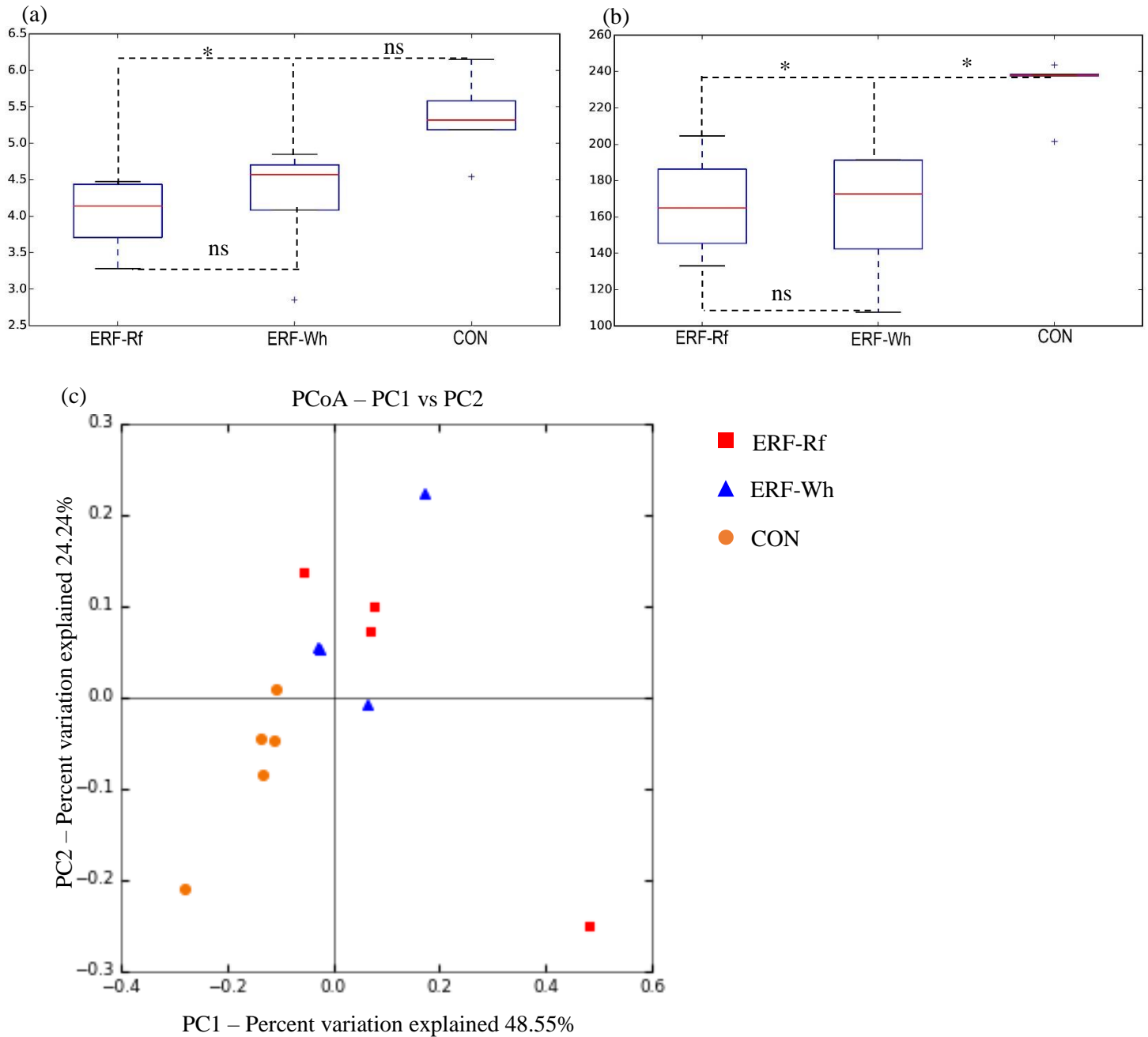
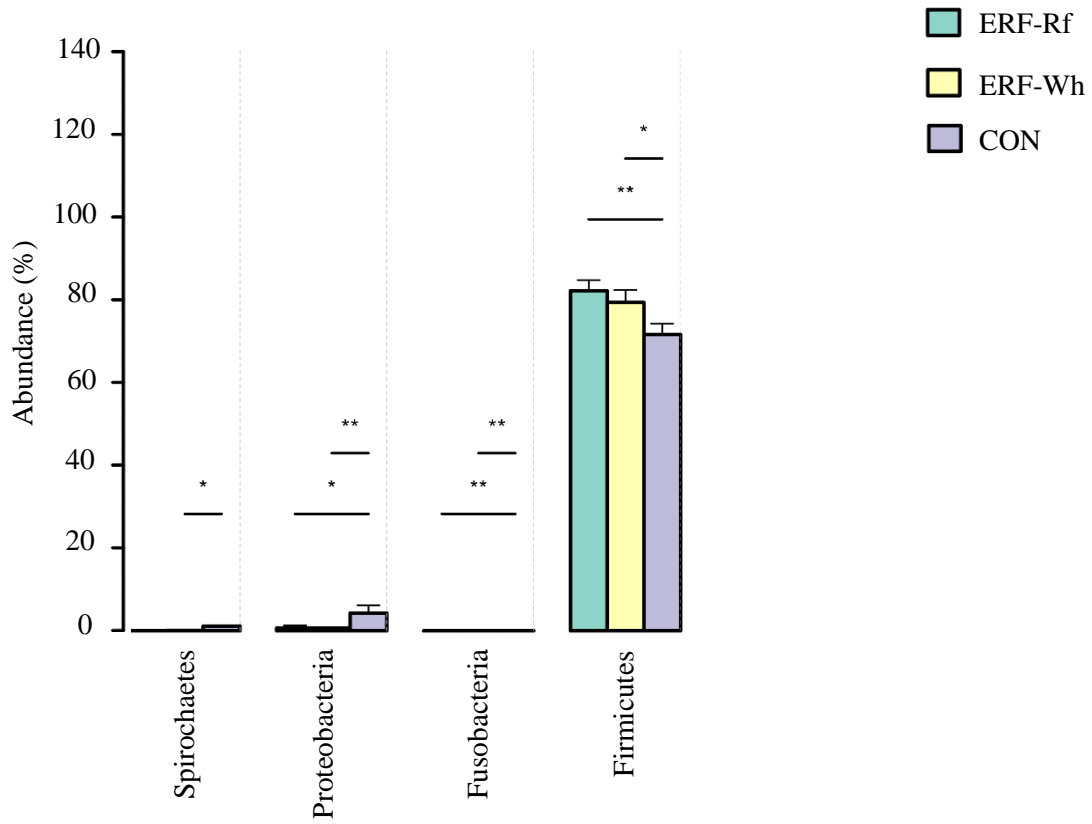


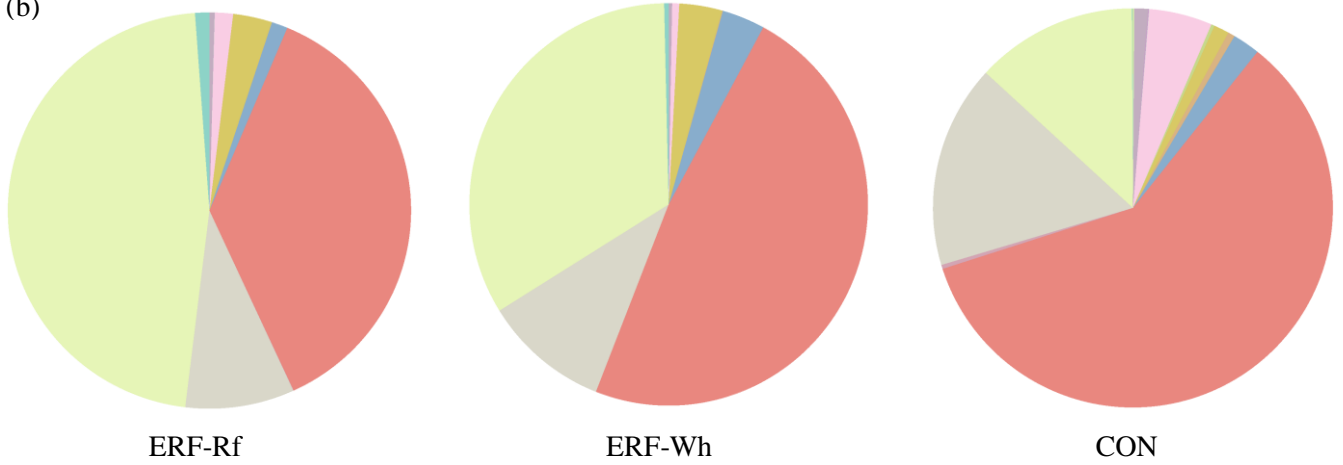
Fig. 2.4. Box and whisker plots of (a) Shannon's diversity index and (b) Observed species index (c) PCoA plot for the β -diversity of the microbial community data. (CON, Cellulose; ERF-Wh, enzyme resistant fraction of whole white sorghum flour; ERF-Rf, enzyme resistant fraction of refined white sorghum flour)

The red line in each box depicts the average value of Shannon's and observed species indices in (a) and (b). Statistical significance was determined by ANOVA (post hoc Tukey's test); ($*p < 0.05$). β -diversity was determined by the weighted UniFrac distance metric in QIIME.

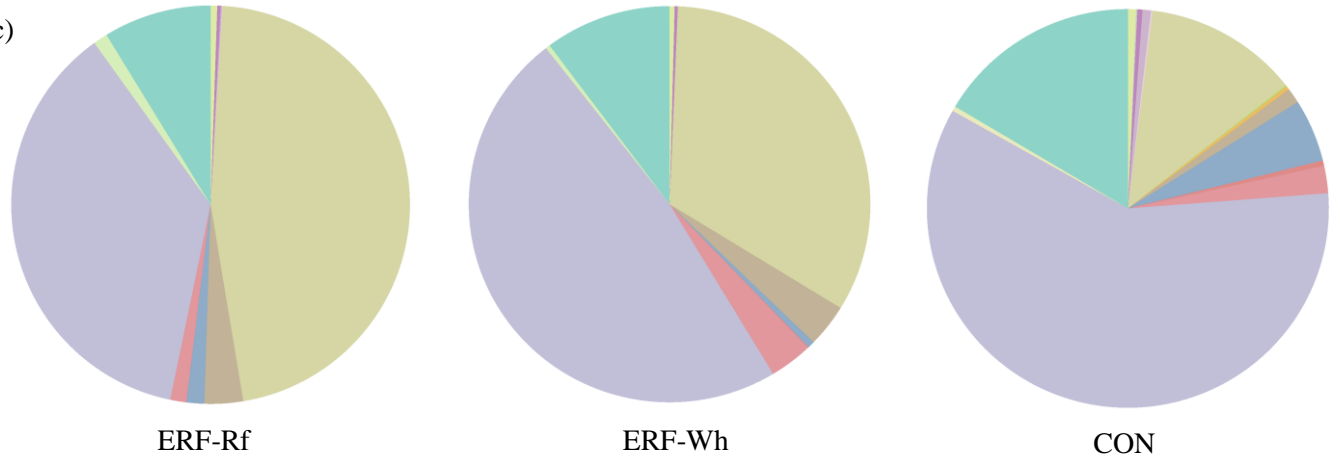
(a)



(b)

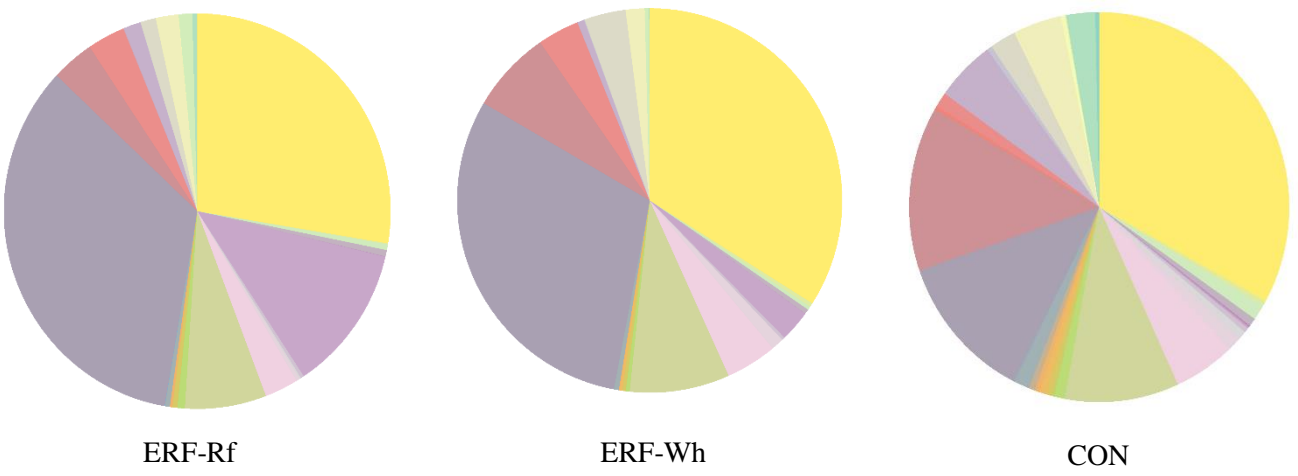


(c)



- Bacteroidales
- Bifidobacteriales
- Burkholderiales
- Clostridiales
- Coriobacteriales
- Desulfovibrionales
- Enterobacteriales
- Erysipelotrichales
- Fusobacteriales
- GMD14H09
- Lactobacillales
- Methanobacteriales
- Pirelluales
- Sphaerochaetales
- Synergistales
- Turicibacteriales
- WCHI141

(d)



- Alcaligenaceae
- Bacteroidaceae
- Bifidobacteriaceae
- Christensenellaceae
- Clostridiaceae
- Coriobacteriaceae
- Desulfovibrionaceae
- Enterobacteriaceae
- Erysipelotrichaceae
- Fusobacteriaceae
- Lachnospiraceae
- Lactobacillaceae
- Methanobacteriaceae
- p253418B5
- Paraprevotellaceae
- Peptostreptococcaceae
- Prellulaceae
- Porphyromonadaceae
- Prevotellaceae
- Remaining
- RF16
- RFPI2
- Ruminococcaceae
- S247
- Sphaerochaetaceae
- Spirochaetaceae
- Streptococcaceae
- Synergistaceae
- Tissierellaceae
- Turicibacteraceae
- Unclassified
- Unclassified Bacteroidales
- Unclassified Clostridiales
- Unclassified GMD14H09
- Veillonellaceae

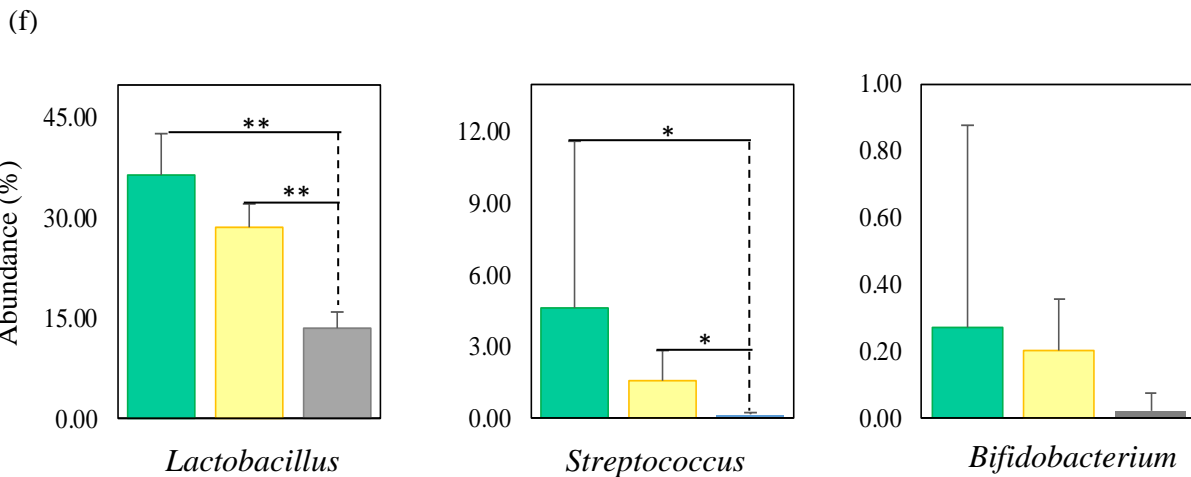
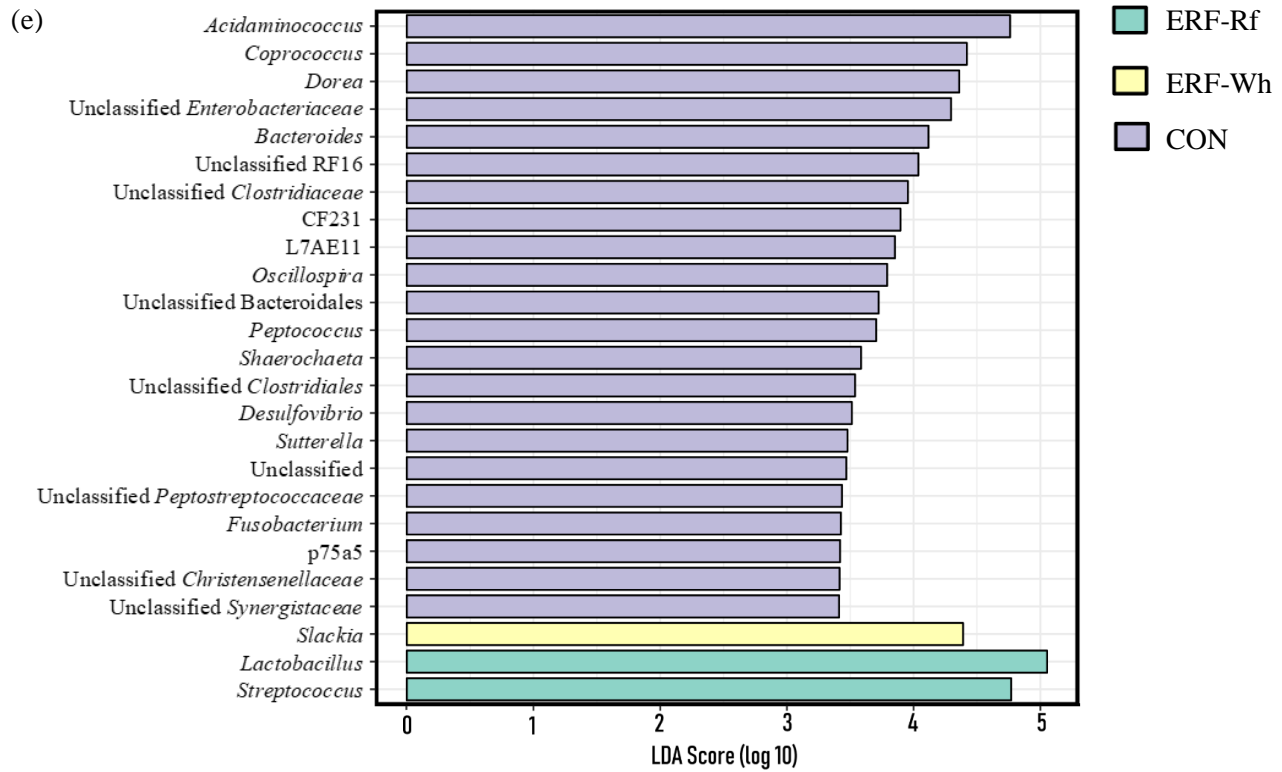


Fig. 2.5. (a) Rank test bar chart for relative abundance (median \pm SE) of microbial taxa at phylum level. Pie charts for microbial composition at (b) order (c) class (d) family levels, respectively (e) Linear discriminant analysis (LDA) effect size (LEfSe) plot at genus level (f) Rank test plots for selected microbial genera. Statistical significance was determined by Kruskal-Wallis H test in Calypso (version 8.72) (* $p < 0.05$; ** $p < 0.01$).

(CON, Cellulose; ERF-Wh, enzyme resistant fraction of whole white sorghum flour; ERF-Rf, enzyme resistant fraction of refined white sorghum flour)

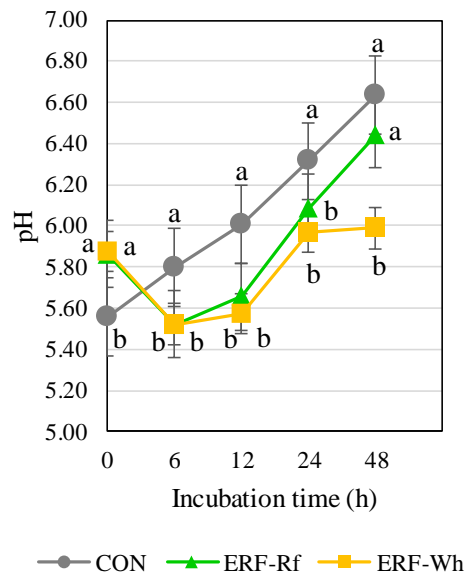


Fig. 2.6. Variation in the pH in fermenter media during the 48 h fermentation period.

Values presented are mean \pm SE (n=5). Different letters at each sampling point represent significant differences among the substrates at ($p < 0.05$).

(CON, Cellulose; ERF-Wh, enzyme resistant fraction of whole white sorghum flour; ERF-Rf, enzyme resistant fraction of refined white sorghum flour)

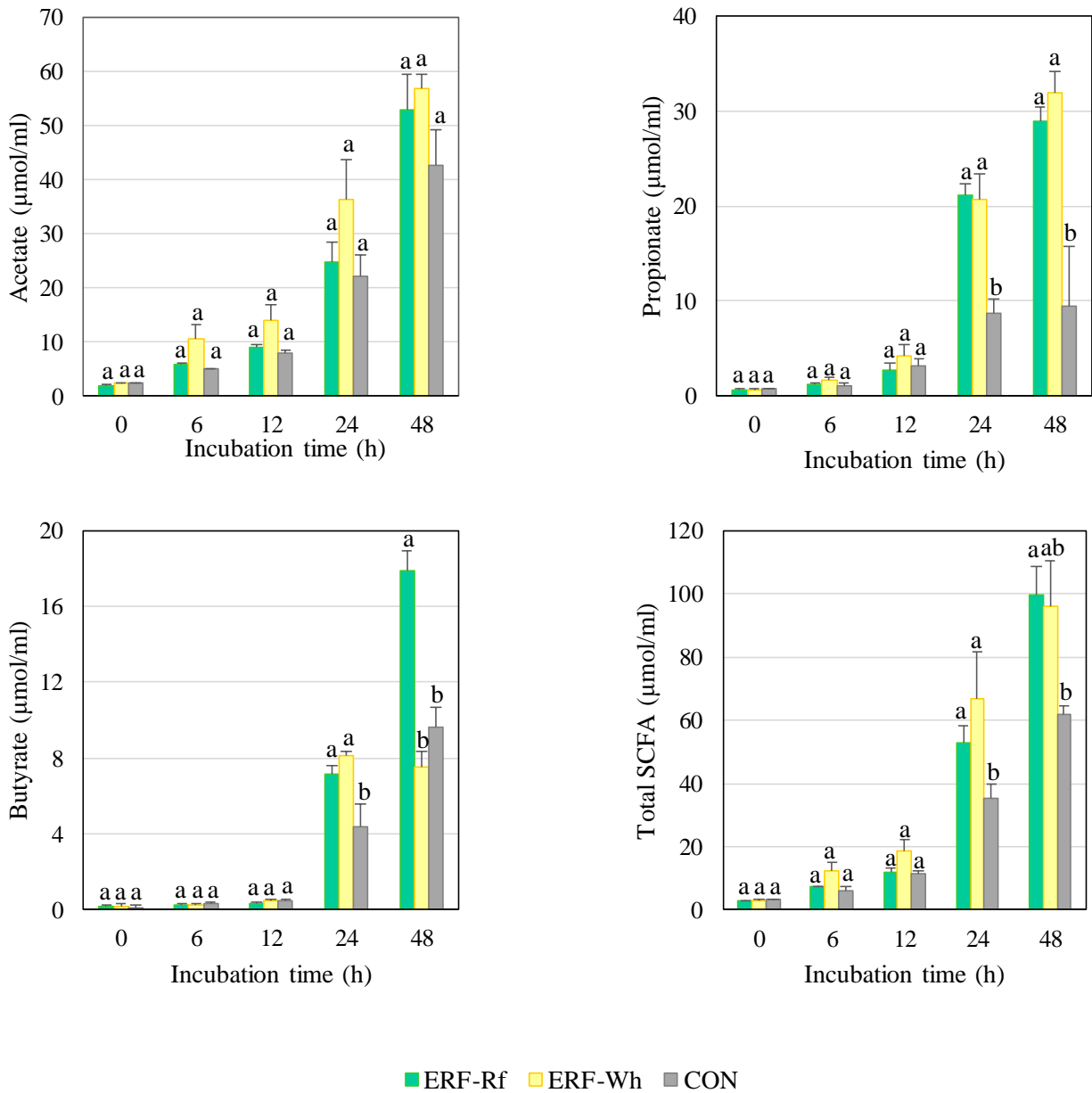


Fig. 2.7. Variation in the SCFA concentrations in fermenter media during the 48 h fermentation period.

Values presented are mean \pm SE (n=5). Different letters at each sampling point represent significant differences among the substrates at ($p < 0.05$).

(CON, Cellulose; ERF-Wh, enzyme resistant fraction of whole white sorghum flour; ERF-Rf, enzyme resistant fraction of refined white sorghum flour)

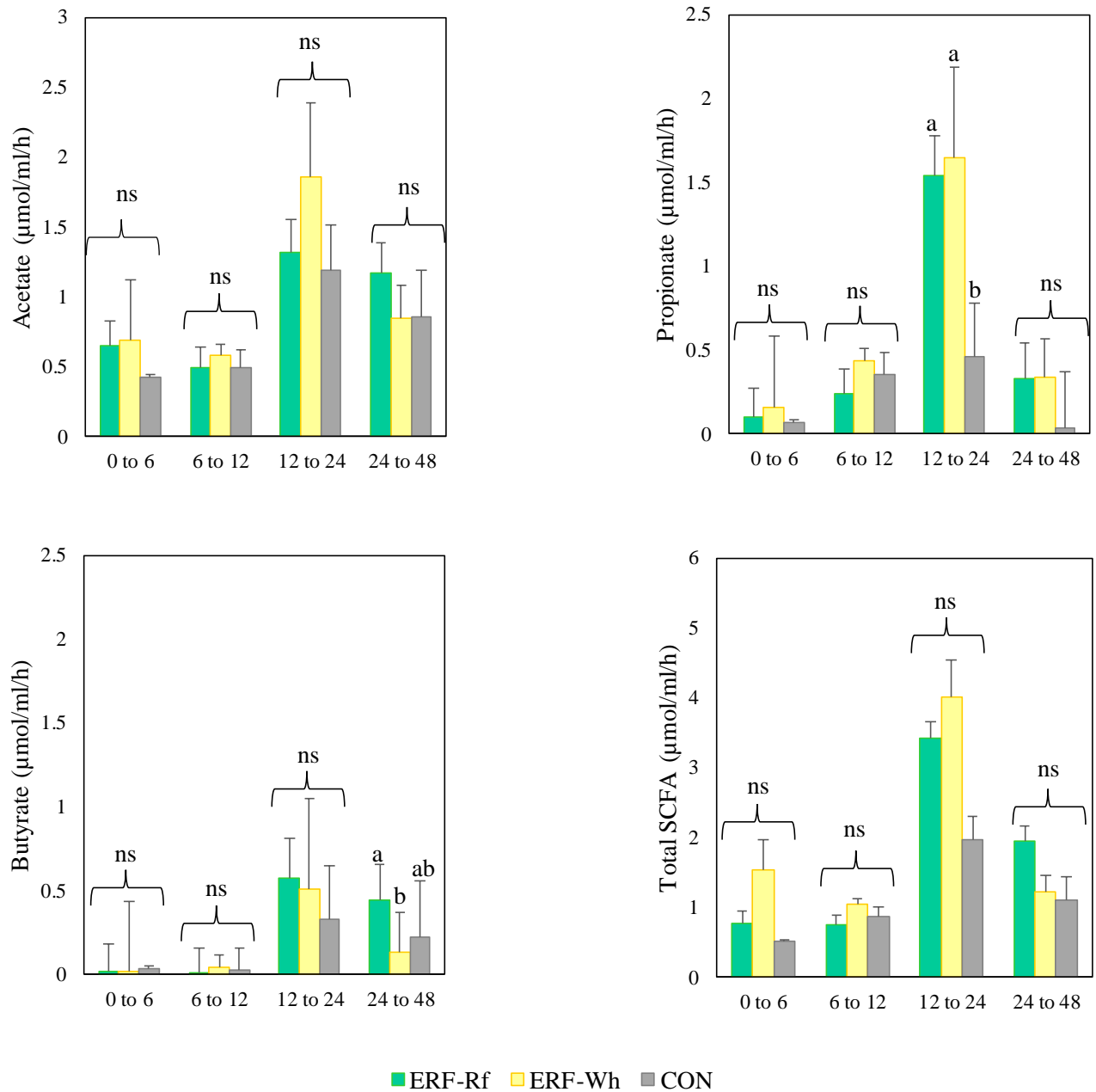


Fig. 2.8. Variation in the SCFA production rate in fermenter media during the 48 h fermentation period.

Values presented are mean \pm SE (n=5). Different letters at each period of sampling represent significant differences among the substrates at ($p < 0.05$).

(CON, Cellulose; ERF-Wh, enzyme resistant fraction of whole white sorghum flour; ERF-Rf, enzyme resistant fraction of refined white sorghum flour)

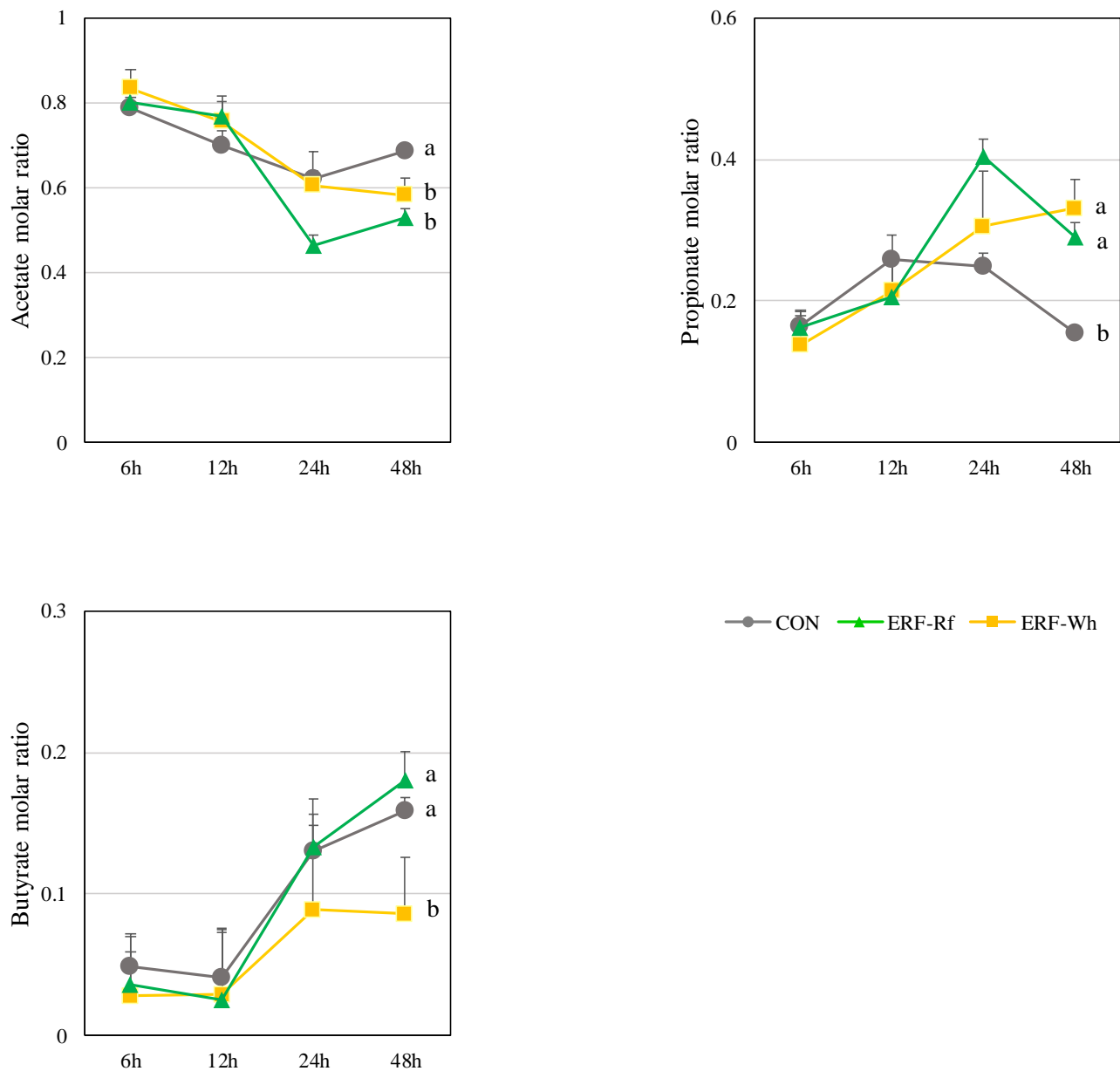


Fig. 2.9. Variation in the SCFA molar ratio at 6, 12, 24 and 48 h sampling points in the fermenter media during the 48 h fermentation period.

Values presented are mean \pm SE (n=5). Different letters at each sampling point represent significant differences among the substrates at ($p < 0.05$).

(CON, Cellulose; ERF-Wh, enzyme resistant fraction of whole white sorghum flour; ERF-Rf, enzyme resistant fraction of refined white sorghum flour)

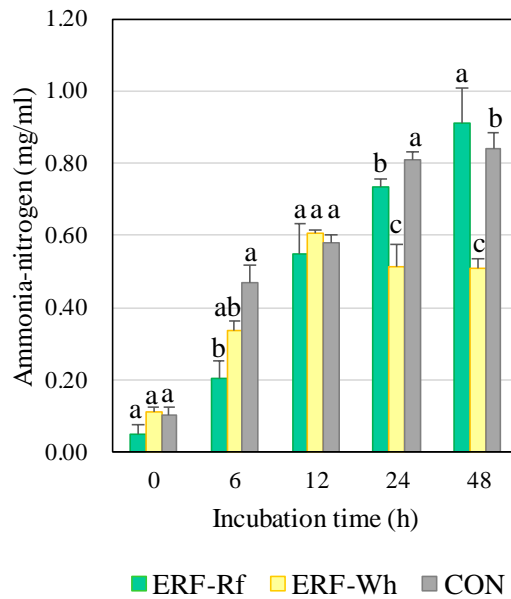


Fig. 2.10. Variation in the ammonia-nitrogen production in the fermenter media during the 48 h fermentation period.

Values presented are mean \pm SE (n=5). Different letters at each sampling point represent significant differences among the substrates at ($p < 0.05$).

(CON, Cellulose; ERF-Wh, enzyme resistant fraction of whole white sorghum flour; ERF-Rf, enzyme resistant fraction of refined white sorghum flour)

Table 2.1. Proximate composition of the enzyme resistant fractions (ERFs) of the two sorghum flours.

Sample	Moisture content (%)	Ash content (% dwb)	Protein content (% dwb)	Fat content (% dwb)	Carbohydrate content (% dwb)	Resistant starch content (% dwb)
ERF-Rf	12.41 ± 0.39	8.85 ± 0.49 ^b	57.76 ± 1.12 ^a	0.75 ± 0.17	20.21 ± 0.52 ^b	14.4 ± 0.1 ^b
ERF-Wh	12.61 ± 0.47	10.51 ± 0.13 ^a	36.39 ± 0.64 ^b	1.14 ± 0.20	39.34 ± 0.50 ^a	15.9 ± 0.1 ^a

Different superscript letters represent significant differences at $p < 0.05$. (ERF-Rf, refined white sorghum; ERF-Wh, whole white sorghum)

Table 2.2. The nutrient composition of the fermenter media of control (CON) and the enzyme resistant fraction (ERF) of whole white sorghum (ERF-Wh) and refined white sorghum (ERF-Rf).

Test sample	Sample weight	Sample carbohydrate	Sample nitrogen	Nutrient broth	Cellulose powder	Final carbohydrate	Final nitrogen	Fecal inoculum (2 % v/v)	Sterilized distilled water	Final volume
ERF-Rf	6.6 g	1.33 g	3.18 g	-	5.27 g	3%	1.73%	50 ml	170 ml	220 ml
ERF-Wh	6.6 g	2.59 g	2.40 g	0.78 g	4.01 g	3%	1.73%	50 ml	170 ml	220 ml
CON	6.6 g	6.60 g	-	3.81 g	-	3%	1.73%	50 ml	170 ml	220 ml

(ERF-Rf, refined white sorghum; ERF-Wh, whole white sorghum; CON, cellulose)

Table 2.3. Polymerase chain reaction (PCR) mix composition for quality assurance PCR.

Component	Volume per sample (μL)
Distilled water	13.875
5X buffer	5.0
25 mM MgCl_2	1.75
dNTP	0.75
Fw primer (10 mM)	1.25
Rv primer (10 mM)	1.25
Polymerase	0.125
Template DNA/sample DNA	1.0
Total volume	25

Table 2.4. PCR conditions for total bacteria.

Step 1		Step 2		Step 3	
Initial denaturation	Denaturation	Annealing	Extension	Final extension	Store
94°C	94°C	55°C	72°C	72°C	4°C
2 min	15 s	15 s	30 s	7 min	∞
1 cycle		35 cycles		1 cycle	

Table 2.5. The composition of agarose gel mixture.

Component	(v/v%) of gel mixture	15 mL gel	25 mL gel
Agarose	1%	0.15 g	0.25 g
10X TAE buffer	10%	1.5 mL	2.5 mL
Distilled water	Balance up to final volume	13.5 mL	22.5 mL
Fluorescent agent	0.005%	0.75 μ L	1.25 μ L
DNA loading buffer		1 μ L	1 μ L

Table 2.6. PCR reaction mix for first stage PCR during 16S sequencing library preparation.

Component	Quantity per sample
Microbial Genomic DNA (5 ng/ μ L in 10 mM Tris pH 8.5)	2.5 μ L
Amplicon PCR Reverse Primer (1 μ M)	5 μ L
Amplicon PCR Forward Primer (1 μ M)	5 μ L
2x KAPA HiFi HotStart ReadyMix	12.5 μ L
Total volume	25 μ L

Table 2.7. PCR conditions for first stage PCR during 16S sequencing library preparation.

Step 1		Step 2		Step 3	
Initial denaturation	Denaturation	Annealing	Extension	Final extension	Store
95°C	95°C	55°C	72°C	72°C	4°C
3 min	30 s	30 s	30 s	5 min	∞
1 cycle		25 cycles		1 cycle	

Table 2.8. PCR reaction mix for second stage PCR during 16S sequencing library preparation.

Component	Quantity per sample
First stage PCR amplicon (in 10 mM Tris pH 8.5)	5 μ L
Nextera XT Index Primer 1 (N7xx)	5 μ L
Nextera XT Index Primer 2 (S5xx)	5 μ L
2x KAPA HiFi HotStart ReadyMix	25 μ L
PCR Grade water	10 μ L
Total volume	50 μ L

Table 2.9. PCR conditions for second stage PCR during 16S sequencing library preparation.

Step 1		Step 2		Step 3	
Initial denaturation	Denaturation	Annealing	Extension	Final extension	Store
95°C	95°C	55°C	72°C	72°C	4°C
3 min	30 s	30 s	30 s	5 min	∞
1 cycle		25 cycles		1 cycle	

CHAPTER 3

Colonic fermentation characteristics of raw sorghum flour in murine models

3.1. Introduction

In the previous study reported in Chapter 2, a prominent ammonia-nitrogen production was observed in the two sorghum samples under *in vitro* conditions, which possibly might have been due to the amino acid fermentation by the swine fecal microbiota. As previously mentioned in Chapter 2 (section 2.1), the starch digestibility in sorghum is significantly controlled by the protein fraction (Wong *et al.*, 2009). Further, after *in vitro* digestion (section 2.2.2), in the sorghum residue (ERF) the undigested protein proportion was very high (Table 2.1), suggesting a lower *in vitro* digestibility of protein also. Albeit, there was a considerable proportion of undigested carbohydrates including resistant starch (RS) in both sorghum residues, only a moderate level of short chain fatty acid (SCFA) production was observed compared to cellulose containing CON medium.

The proximate composition of ERFs implicated that, apart from the undigested carbohydrates, a considerably very high amount of undigested proteins also might reach the colon when sorghum is fed to animals. Thus, it is important to identify the factors behind the lower protein digestibility in sorghum (discussed in details in section 3.1.1). Further, the fate of undigested proteins that reach the colon must be clearly reviewed in order to understand and interpret the outcomes under a dynamic setting such as an *in vivo* experiment, thus, current knowledge on protein metabolism in the colon (with special emphasis on fermentation of amino acids by gut microbiota) is discussed in section 3.1.2. And the confounding effects of macro and micromolecules in a substrate on any biochemical, physical process such as digestibility or processing, is common when a non-refined substrate like whole grain flour is used. Thus, such confounding effects are reviewed with respect to the colonic fermentation in the section 3.1.3.

3.1.1. Sorghum protein digestibility

Sorghum is known to contain 6 to 18% protein content averaging around 11% (de Mesa-Stonestreet *et al.*, 2010). In sorghum, the major class of protein is alcohol soluble prolamin-kafirin, with a lesser proportion of water and salt-soluble proteins (non-prolamin proteins) (Wall *et al.*, 1969; Shewry and Tatham, 1990). Kafirin constitutes of 77 to 82% of the total proteins in the endosperm, while the non-prolamin proteins (albumins, globulins, and glutelins) account for 30% (Belton *et al.*, 2006).

Kafirin, the major storage protein, contains high levels of proline and glutamine as the name suggests itself 'prolamin' (Shewry and Tatham, 1990). Based on the molecular weight, structure and solubility, kafirins are classified into several classes, namely, α , β , γ and δ (Shull *et al.*, 1991). In sorghum endosperm, the relative compositions of the different fractions of kafirins are as follows: 66 to 84% α -kafirin (vitreous endosperm, 80 to 84%; flouy endosperm, 66 to 67%), 8 to 13% β -kafirin (vitreous endosperm, 7 to 8%; flouy endosperm, 10 to 13%) and 9 to 21% γ -kafirin (vitreous endosperm, 9 to 12%; flouy endosperm, 19 to 21%) and low levels of δ -kafirins (Watterson *et al.*, 1993; Belton *et al.*, 2006). Some characteristics of different kafirin fractions of sorghum are presented in Table 3.1.

In nutritional point of view a constraint of sorghum as a staple food is, its poor quality of proteins (deficient in essential amino acid lysine) and lower protein digestibility (Duodu *et al.*, 2003). *In vitro* digestibility studies involving pepsin reflects the *in vivo* digestibility, thus poor *in vitro* protein digestibility in wet milled/boiled sorghum suggests a lower availability of protein as a nutrient for physiological processes (Duodu *et al.*, 2003). Previous research have reported that specifically protein in porridge and bread made from tannin-free sorghum is poorly digested (Oria *et al.*, 1995).

Further, it has been previously reported that in sorghum kafirins are the last to be digested among its other components, which is attributed to the organization of the endosperm, localization of protein within the endosperm and the structure of protein bodies. Sorghum kafirins are known to contain a higher fraction

of cross-linked proteins, which is suggested to be the reason for their hydrophobicity due to cross-linked protein aggregate (polymeric form) formation (Wong *et al.*, 2009).

The manner in which the sub-classes of kafirin located within the protein body is found to affect the protein digestibility and subsequently the starch digestibility. In the endosperm, kafirins are mainly found in spherical protein bodies found glued onto the starch granules that are embedded in the protein matrix made of glutelin according to evidence from scanning and transmission and confocal laser scanning microscopic studies (Elkalifa *et al.*, 2005; Seung *et al.*, 2008). Generally, α -kafirin is identified as a highly digestible class of kafirin, while β - and γ -kafirins are found to be resistant to digestion, attributed to their disulfide cross-link formation ability (higher in sulfur-containing amino acid cysteine) in both raw and cooked states (Hamaker *et al.*, 1995; Belton *et al.*, 2006; Seung *et al.*, 2008; Wong *et al.*, 2009; de Mesa-Stonestreet *et al.*, 2010). Further, proteins are found to line the channels running towards the center of the starch granules that act as enzyme penetrating routes, thus the proteins lining the channels may also interfere with enzyme access (Han *et al.*, 2005). And the glutelin protein matrix that glues starch granules and protein bodies also reduces the protein digestibility due to the restricted access of protein hydrolyzing enzymes (Wong *et al.*, 2009).

Apart from the above mentioned factors affecting protein digestibility, localization of sorghum proteins within the sorghum grain also plays a significant role in digestibility, thus depending on the area of concern (whole grain, endosperm, etc.) the digestibility was found to vary significantly (Duodu *et al.*, 2003). Thus, another important factor that determines the sorghum protein digestibility is the physical nature of sorghum source, such as grains, flour or meal etc., because different physical forms and proportions (flour, starch, germ, etc.) of sorghum grain contain different amounts and types of protein that differ structurally too.

Sorghum protein digestibility is found to depend on its interactions with non-protein components (starch, lipids, polyphenols, phytates, and cell wall components) other than protein-protein interactions (Duodu *et al.*, 2003). Sorghum tannins are known to bind and precipitate protein ($\times 12$ as tannin weight), which involves hydrogen bonding and non-polar hydrophobic associations with γ -kafirins (Duodu *et al.*, 2003; Taylor *et al.*, 2007). Tannin not only forms bonds with kafirins, but also known to have interactions with albumin and globulin, thus tannin-protein interactions are capable of making sorghum proteins insoluble and less digestible (Duodu *et al.*, 2003). Phytic acid (in germ and pericarp in sorghum), found in high abundance as potassium, magnesium and calcium salts in cereals is a highly charged molecule with six phosphate groups with good chelation ability, thus forms insoluble complexes with cationic minerals and proteins (Duodu *et al.*, 2003). Interactions between starch component and protein are discussed in details in Chapter 2 (section 2.1).

3.1.2. Protein metabolism in the colon

Importance of gut microbiota, their functions and the functions mediated by the by-products of carbohydrate fermentation have been reviewed extensively in relation to host health. Another less focused area related to gut microbial metabolism is their ability to alter the distribution of free amino acids in the gastrointestinal tract. Amino acid profiles in germ-free mice and conventional mice have exhibited significant differences suggesting that gut microbiota might be able to affect the bioavailability of amino acids (Neis *et al.*, 2015). Interestingly enough it has been postulated that certain amino acids are able to serve as precursors for the SCFA production by gut microbiota (Neis *et al.*, 2015).

Amino acids or peptides resulted from the hydrolysis of endogenous and alimentary (exogenous) proteins via host and bacteria derived proteases and peptidases either get absorbed into the portal blood stream (less absorption via colonic mucosa) or utilized by the gut microbiota (Dai *et al.*, 2011; Neis *et al.*, 2015). Amino acids absorbed by the gut microbiota have two distinct fates, either incorporated into microbial

cells as a building material or become catabolized, and it was found that some amino acids such as lysine and methionine in piglets being catabolized by intestinal bacteria than being absorbed by the host tissues (Neis *et al.*, 2015).

The most abundant amino acid fermenting bacteria are found to be mainly belonging to the phylum Firmicutes, belonging to *Clostridium* clusters (*Clostridium* spp., *Fusobacterium* spp., *Peptostreptococcus* spp., *Veillonella* spp., *Megasphaera elsdenii*, *Acidaminococcus fermentans*, *Selenomonas ruminantium*), *Bacillus*, *Lactobacillus*, *Streptococcus* groups and *Proteobacteria* (*Klebsiella* spp., *Escherichia coli*), while in humans, *Clostridia* and *Peptostreptococci* are identified as the most prevalent amino acid fermenters (Dai *et al.*, 2011; Neis *et al.*, 2015).

Their functions in amino acid fermentation is further backed up by the highly active peptidases found to be expressed by these bacteria, for example lactic acid bacteria are known to possess a strong protease-peptidase proteolytic enzyme system involved in protein and peptide breakdown in the colon (Neis *et al.*, 2015). Further, *Prevotella ruminicola*, *Butyrivibrio fibrisolvens*, *M. elsdenii*, *Mitsuokella multiacidus*, *S. ruminantium* and *Streptococcus bovis* are known to possess highly active dipeptidyl peptidases and dipeptidases, where *P. ruminicola* is found to utilize peptides as the only preferred nitrogen source (Dai *et al.*, 2011). These members of gut bacteria are found to utilize several metabolic pathways to ferment amino acids, such as deamination, decarboxylation and Stickland reaction specifically by *Clostridia* (Dai *et al.*, 2011).

Bacterial amino acid fermentation is positively correlated with high colonic pH and low availability of carbohydrate substrates for microbial utilization (Neis *et al.*, 2015). It was revealed that at higher ranges of pH and under deficiency of fermentable carbohydrates, amino acid fermentation was found to improve by 60% and this process is found to be compartmental-specific, where it is increased towards the distal colon (Rowland *et al.*, 2018). Among the amino acids, glutamine/glutamate, lysine, asparagine/aspartate,

arginine, serine, glycine, threonine, histidine, leucine, valine and isoleucine are found to be the most favored sources by the amino acid fermenting gut microbial members (Dai *et al.*, 2011; Neis *et al.*, 2015).

Among the products of microbial amino acid fermentation, gases (ammonia, H₂, CO₂, H₂S, CH₄), SCFAs, branched-chain fatty acids (isobutyrate, isovalerate), phenolic and indolic compounds, other organic acids (lactate, formate, succinate, oxaloacetate) and bio-active amines (cadavarine, agmatine, putrescine, histamine) are the main effector molecules identified to modulate gut epithelial physiology and gut bacterial gene expression, which are known to further upregulate amino acid metabolizing enzymes (Macfarlane *et al.*, 1986; Dai *et al.*, 2011; Neis *et al.*, 2015). Further, aromatic amino acids (phenylalanine, tyrosine, and tryptophan) are found to be fermented into phenyl propanoid metabolites, phenylacetic acid and 4-hydroxyphenyl-acetic acid, which are the same breakdown products of plant polyphenols by microbiota (Rowland *et al.*, 2018).

Generally, SCFAs are known as the products of microbial fermentation of indigestible carbohydrates, yet certain amino acids also can act as precursors for SCFA production (Neis *et al.*, 2015). For example, acetate is known to be produced by metabolizing glycine, threonine, glutamate, lysine, ornithine and aspartate, propionate by threonine and butyrate by threonine, glutamate and lysine (Davila *et al.*, 2013; Neis *et al.*, 2015). Branched-chain amino acids do not serve as precursors for SCFA production, instead they promote branched-chain fatty acid (BCFA) production, which is considered to be dependent upon the intrabacterial amino acid composition, which varies across different bacterial strains, yet the major proportion is branched-chain amino acids implicating their favor in synthesizing branched-chain amino acids upon fermentation (Neis *et al.*, 2015).

3.1.3. Confounding effects between carbohydrate and protein in a substrate on colonic fermentation

A high protein diet has been associated with increased risk of health impairments, especially colorectal cancers, while a diet rich in indigestible carbohydrates (fruits, vegetables, and cereals) is identified to reduce colonic and systemic physiological impairments. As previously reviewed, the adverse effects of a high protein diet is directly associated with the bacterial metabolism of protein in the colon (Toden *et al.*, 2007). Yet, in ancient times, the diets were mostly meat-based, yet high prevalence of health impairments that can be seen today (colorectal cancers, obesity, diabetes, etc.) were not reported. Thus, solely protein richness in a diet might not implicate today's challenges faced in health. An important characteristic of the ancient diets based in animal protein was the inclusion of a variety of fruits, bee honey and sometimes leaves and tree barks, thus the secret of healthiness was due to a "balanced diet".

It has been previously reported that, the extend of protein fermentation in colon by bacteria depends on the amount of protein and carbohydrate reaching the colon, the type/structure and chemical properties of the proteins and carbohydrates and the ratio between carbohydrate and nitrogen in the colon (Williams *et al.*, 2001; Taciak *et al.*, 2015). The nature of carbohydrates reaching the colon, especially their composition and functionality significantly determine the pattern of colonic fermentation (Taciak *et al.*, 2015). For examples, pectin is a highly soluble form, which gets rapidly fermented, while cellulose is an insoluble form, which exhibits a negligible fermentation (Taciak *et al.*, 2015). Further, depending on the rate of fermentation of a fermentative carbohydrate substrate along the colon, the carbohydrate:nitrogen ratio changes and a rapidly fermentable substrate might influence a lower ratio, thus a higher amino acid fermentation (Kaur *et al.*, 2018). In contrast, a slow releasing fermentative substrate facilitates a considerable carbohydrate fermentation throughout the colon, thus reducing the risk of adverse effects (Kaur *et al.*, 2018).

Protein type, protein level are reported to interact with the carbohydrate level and type, which result in a high complexity of the microbiological processes in the colon (Taciak *et al.*, 2015). Interactions among the mentioned parameters have been found to affect SCFA production, ammonia production, morphological and histological changes in organs and bacterial composition also. Further, depending on the expressed metabolic functions of the gut microbiota, by-products, location and extent of protein fermentation can be differed. Thus, in an unrefined substrate, isolating the specific effects of each component might be challenging and the phenotype might exhibit the interaction and confounding effects of all the factors.

3.1.4. Research statement, objectives and hypothesis

Low *in vitro* flour digestibility of sorghum (*Sorghum bicolor* L.), is considered as a potential trait for overweight and obesity management, and is found to be associated with low digestibility of both starch and protein fractions (Zhu, 2014). With the low digestibility of starch, it becomes an assuring source of RS with an average between 12.0-21.5%, presenting potentials as a prebiotic substrate (Zhu, 2014). Inclusion of RS in diet not only influences the gut microbiome, but also dilutes the caloric value of diet, reducing energy intake (Goldsmith *et al.*, 2017). Thus, RS enriched food sources have earned the spotlight of many studies recently, which can be a healthy and an economic means of mitigating the chronic metabolic diseases directly associated with diet, for instance co-morbidities that encompasses metabolic syndrome (Kaur, 2014).

In Chapter 2, it was found that sorghum ileal enzyme resistant fractions (ERFs) possessed a higher starch content suggesting a higher inflow of starch to the colon favoring gut microbial fermentation. Under *in vitro* conditions with a swine fecal inoculum, a significantly lower pH between 0 to 24 h period, significantly higher propionate, butyrate and total SCFA production between 24 to 48 h period and a higher abundance of beneficial microbial classes such as *Bifidobacterium* (viable plate count method), *Lactococcus* and *Streptococcus* (16S community DNA data), indicated promising potentials as a prebiotic candidate.

On the other hand, observed higher ammonia-nitrogen production can be a negative trait considering its negative impact on health. Similar to resistant carbohydrates, amino acids produced from resistant proteins/peptides are also reported to be fermented by the gut microbiota, when the fermentable carbohydrates are depleted (Neis *et al.*, 2015). The higher undigested protein content observed in ERFs might further strengthen this fact. Further, confounding and interactive effects among macro and

micromolecules in unrefined substrates such as whole grain flour, are found to affect the availability, accessibility and priority of the substrates being utilized by the gut microbiota.

As *in vitro* and *in vivo* systems derive important information under static and dynamic conditions, respectively, thus conducting an *in vivo* experiment to confirm the observations obtained under an *in vitro* experiment is important. It is important to investigate the magnitude of these biochemical reactions in a dynamic state using a suitable animal model and the potential biological and physiological effects, which are not plausible through *in vitro* experimental conditions. So it was aimed to evaluate the biochemical, biological and physiological effects of colonic fermentation of sorghum flour (a heterogeneous substrate) in comparison to a well-characterized RS source using an *in vivo* model.

3.2. Materials and Methods

3.2.1. Preparation of experimental diets

Two types of sorghum flour, whole white sorghum (S-Wh) and refined white sorghum (S-Rf) flour were provided by Nakano Industry Co. (Takamatsu, Japan) and the experimental diets were prepared according to AIN-93G diet guidelines by Oriental Yeast Co., Ltd., (Tokyo, Japan). The proximate composition of the sorghum flour samples is presented in Table 3.2. The compositions of experimental diets (CON, α -corn starch; HAS, High amylose starch (35% RS; HS-7, J-OIL Mills Co., Ltd., Tokyo, Japan); S-Wh, whole white sorghum flour; S-Rf, refined white sorghum flour) for animals are presented in Table 3.3.

3.2.2. Animal experimental design, maintenance and post-mortem excision of organs

The animal experiment was conducted according to the guidelines of “Guide for the Care and Use of Laboratory Animals” and all the procedures were approved by the Animal Care and Experiment Committee of Obihiro University of Agriculture and Veterinary Medicine (License no: 29-94). The schematic representation of the animal experimental design is presented in Fig. 3.1. Twenty five Fischer 344 male rats (7 weeks old; average body weight 130-160 g) were purchased from Charles River Laboratories Japan Inc., (Yokohama, Japan). The animals were given cage tags from 1 to 25 and they were acclimatized on a commercial rodent diet (Standard powder diet for mouse, rat, hamster, Oriental Yeast Co.,) for one week with *ad libitum* access to water. At the end of the acclimatization period, the body weight was measured and the animals were grouped into similar body weight groups (6 animals/group) as presented in Table 3.4.

Followed by grouping, each group was assigned a group name (G1, CON; G2, HAS; G3, S-Rf; G4, S-Wh) and animals in each group were given a sub-group number (CON; CON-1, CON-2.....CON-6, etc.). Each animal was housed in cages individually with free access to test diets (\approx 25g/day) and water

(≈ 150 mL). Feeder and drinker placement in individual cages were prepared as shown in Fig. 3.2. Feeders were individually labeled on the bottom to avoid the damage by the animals as shown in Fig. 3.3. Feed and water were replenished every day at 8.00 a.m. The incubator was maintained at $23 \pm 1^\circ\text{C}$ temperature and $60 \pm 5\%$ relative humidity under a 12 h light/dark cycle.

During the experimental period, body weight and feed intake were measured weekly and daily, respectively. Following a 12 h fasting period, blood (≈ 1 mL) was collected from the jugular vein of each animal weekly and the serum was separated by centrifugation (8,000 rpm, 15 min, 2 times; CFA-12, Iwaki Glass Co., Ltd., Tokyo, Japan) and stored at -80°C until serum biochemical analysis. Feces were collected during the last four days of the experimental period into clean, labelled plastic bags that can be sealed and were stored at -30°C until further analysis.

On the day of the sacrifice, the final body weight was measured and the animals were injected with the narcotic (sodium pentobarbital, 40 mg/kg body weight, Abbott Laboratories, Chicago, IL, United States) intraperitoneally. Following the sacrifice, the body cavity was cut opened and blood, cecum, liver, epididymal and perirenal adipose tissues were excised and weighed. Liver was separated into its three lobes and they were frozen in liquid nitrogen and stored at -80°C . Followed by total cecum weight measurement, cecum was cut opened and the cecal content was removed into sterile tubes. The cecal tissue was washed in sterilized saline (0.85% v/v), blotted to dry and the weight was measured.

Part of the cecal content (≈ 1 g) was measured into 15 mL sterile plastic tubes and was diluted ($\times 5$ folds) with sterile distilled water. Cecal pH was measured in the diluted cecal samples using a bench-type pH meter (Metler Toledo, Columbus, OH, United States). Followed by pH measurement, the diluted cecal solutions were divided into aliquots (≈ 1 mL) in 1.5 mL Eppendorf® tubes and were stored at -30°C until further analyses. Rest of the cecal content was stored at -30°C .

3.2.3. Rat cecal bacterial DNA extraction, sequencing and analysis of 16S rRNA sequences

Extraction of bacterial DNA from the cecal digesta, purification, the 16S genome library preparation and sequencing were conducted according to the methods described in Chapter 2 (section 2.2.5). The generated biome table was normalized using an equal subsampling size of 11,667 sequences. Analysis of retrieved 16S rRNA sequences was conducted according to the method described in Chapter 2 (section 2.2.5.b.v). Distances between bacterial communities in different samples were calculated by the weighted UniFrac distance metric in QIIME and the Principle Coordinate Analysis (PCoA) plot was also generated in QIIME (Lozupone and Knight, 2005). Calypso version 8.72 was used to generate hierarchical cluster illustrations (Zakrzewski *et al.*, 2017).

3.2.4. Rat cecal short chain and branched-chain fatty acid analysis

Short chain fatty acid and BCFA contents in diluted cecal samples of rats were analyzed by high performance liquid chromatography (Shimadzu LC-10AD, Kyoto, Japan). Samples were prepared according to the method described in Chapter 2 (section 2.2.6) and analytical specifications were as follows; column, RSpak KC-811 (8.0 mm x 300 mm, Shodex, Tokyo, Japan); eluent and flow rate, 2 mM HClO₄ at 1 mL/min; column temperature, 47°C; reaction reagent and flow rate, ST3-R (×10 diluted) at 0.5 mL/min; UV-vis spectrophotometric detector (SPD-10A, Shimadzu) wavelength, 450 nm. Quantification of SCFA and BCFA content was same as Chapter 2.

3.2.5. Ammonia-nitrogen analysis in cecal samples

The thawed diluted cecal samples were mixed well on vortex and centrifuged to obtain (3,000 rpm, 4°C, 15 min) the supernatant. Ammonia-nitrogen content was analyzed and quantified in the supernatant of the samples according the method described in Chapter 2 (section 2.2.7) using the ammonia-nitrogen analysis kit (Wako Pure Chemical Industry Ltd., Tokyo, Japan).

3.2.6. Immunoglobulin A (IgA) in cecal samples

Immunoglobulin A in the diluted cecal samples were analyzed by a sandwich based enzyme linked immunosorbent assay (ELISA) kit by Bethyl Laboratories Inc. (Montgomery, TX, United States). In order to capture rat IgA present in the samples, anti-Rat IgA antibody (affinity purified goat anti-Rat IgA coating antibody, 1 mg/mL) was pre-absorbed to the surface of the microwells. First, coating antibody solution was prepared with 0.05 M coating buffer (carbonate-bicarbonate buffer, pH 9.6), in the ratio of sample (to be tested):antibody:buffer = 1 μ L:1 μ L:100 μ L. The buffer mixture with coating antibody was pipetted into the required number of wells (100 μ L/well) using a multichannel pipette and was allowed to stand at room temperature for 1 h. After 1 h, the contents in the microwell plate was discarded and it was washed with an automatic wash system (Microplate washer, Thermo Fischer Scientific Oy, Vantaa, Finland) under the following specifications; 350 μ L wash buffer (0.05 M Tris, 0.14 M NaCl, 0.05% Tween20, pH 8.0)/well; wash, 5 times/well; well depth, 4.5 mm. After washing was completed, the plate was dried by tapping the plate on an absorbent paper and 200 μ L of block solution (50 mM Tris, 0.14 M NaCl, 1% bovine serum albumin powder, pH 8.0) was added into the wells, kept at room temperature for 30 min and later stored at 4°C overnight.

On the following day or after 30 min at room temperature, the block solution was discarded and the wells were washed similarly. Diluted cecal samples were thawed, mixed well on a vortex and were centrifuged (3,000 rpm, 4°C, 15 min) to obtain the supernatant for IgA analysis. The samples (Table 3.5) and the standards (Table 3.6) were prepared accordingly. Diluent (conjugated diluent) for samples and standards was prepared by mixing 1 mL of 10% Tween20 in 200 mL of block solution. Followed by the preparation of the samples and the standards, 100 μ L from each sample and standard was pipetted into designated wells in duplicates and the plate was allowed to stand at room temperature for 1 h. After 1 h, unbound proteins and molecules were washed off similarly as mentioned above.

Hundred microliter of a biotinylated detection antibody (streptavidin-conjugated horseradish peroxidase (HRP) conjugated Goat anti-Rat IgA detection antibody; 1 mg/mL) was added into each well prepared in the ratio of 1:75000 with conjugated diluent as shown in Fig. 3.4. After adding HRP conjugated antibody, the wells were allowed stand at room temperature for 1 h and the contents were discarded later and washed as mentioned above. Followed by washing and drying the plate as previously mentioned, 100 μ L of 3,3',5,5'-tetramethylbenzidine (TMB) was added into the wells and allowed to stand for 20 min under dark condition to facilitate the colorimetric reaction. Soon after 20 min, a blue color product was observed, upon addition of stop solution (0.18 M H₂SO₄) it was turned into a bright yellow color. The absorbance of the yellow product was measured at 450 nm using a microwell plate reader (Multiskan™ FC, Thermo Fisher Scientific). After the measurement of absorbance, a standard curve was created and IgA content in the cecal samples were calculated as follows;

$$\text{IgA concentration (mg/mL)} = \frac{(\text{Sample absorbance} - \text{y intercept})}{\text{Gradient of line}} * \text{dilution factor}/(10^6)$$

3.2.7. Mucin analysis in cecal samples

Diluted cecal suspensions (\approx 1 mL) were used to fractionate mucin by the method of Bovee-Oudenhoven *et al.* (1997) and quantified the liberated mucin content according the method by Crowther and Wetmore (1987) as follows. Diluted cecal samples were mixed on vortex and incubated (95°C, 10 min) to inactivate bacterial glucosidase. After the initial incubation, the samples were again incubated (37°C, 90 min) to solubilize mucin. After the second incubation, the samples were mixed well on vortex and centrifuged (20,000 \times g, 4°C, 15 min). Hundred microliter from the supernatant was transferred into a 1.5 mL Eppendorf® tube and 0.4 M acetate buffer (pH 4.75) was added and mixed well. The buffered supernatants were conjugated with 10.4 μ L of amyloglucosidase (300 U/mL) and mixed with pipette aspiration. The samples were incubated at 50°C for 20 min to facilitate the enzyme reaction. Followed by incubation, 310

μL of cold 99.5% (v/v) ethanol was added, mixed well on vortex and was stored at -30°C overnight. The thawed samples were mixed well on vortex and centrifuged ($20,000\times g$, 4°C , 10 min). The supernatant was removed carefully by suction and the precipitate was solubilized in 1.5 mL PBS buffer (1.9 mM NaH_2PO_4 , 8.1 mM Na_2HPO_4 , 0.154 M NaCl , 0.05% NaN_3 , pH 7.2). Standard series of N-acetylgalactosamine was prepared accordingly (Table 3.7).

Three hundred microliters of the solubilized samples and standards were pipetted into test tubes and 360 μL of 0.6 M cyanoacetamide diluted in NaOH (cyanoacetamide:NaOH = 1:5 v/v) was added and mixed well on vortex. The samples were incubated (100°C , 30 min) using a glass ball as a cap and the tubes were cooled down in water immediately after incubation. Soon after cooling down, 3 mL of 0.6 M borate buffer (pH 8.0) was added, mixed well on vortex and the fluorescence was measured using a fluorescence spectrophotometer (FP-6200, Jasco International Co., Ltd., Tokyo, Japan) at an excitation wavelength of 336 nm and a measurement wavelength of 383 nm. A standard curve was prepared and the mucin content was calculated as follows;

$$\text{Mucin content } (\mu\text{mol/mL}) = \frac{(\text{Sample absorbance} - y \text{ intercept})}{\text{Gradient of line}} * (\text{dilution factor} * 1000) / 221$$

3.2.8. Serum biochemical analysis

Serum biochemical profile was analyzed using Toshiba TBA-120FR autoanalyzer (Toshiba Medical Systems Co., Tochigi, Japan) according to manufacturer's instructions.

3.2.9. Statistical analysis

All data (except community DNA data) were analyzed for their significance by analysis of variance (ANOVA) using SPSS statistical software version 17.0 (SPSS Inc., Chicago, IL, USA) coupled with Tukey's test. Correlations among the parameters were obtained by Pearson's correlation analysis tool in

SPSS. Statistical significance of alpha diversity indices (Shannon's and observed species indices) was determined by ANOVA paired with Tukey's test (SPSS). Relative abundance and statistical significance of phyla, genera and species among the four diet groups were compared using Kruskal-Wallis H test in Calypso (version 8.72). A p value less than 0.05 was considered as statistically significant.

3.3. Results and Discussion

3.3.1. Zoometric parameters, feed intake and organ weights

Zoometric parameters, feed intake and organ weights are presented in Table 3.8. At the end of the experimental period of one month, final body weight of the rats was significantly ($p < 0.05$) lower in the HAS group compared to S-Wh group, where CON and S-Rf fed rats showed comparatively lower final body weight compared to S-Wh fed rats. On the other hand, total body weight gain in CON, S-Wh and S-Rf groups was significantly higher than that of the HAS group. Interestingly, cumulative feed intake and final body weight had a similar trend, which might suggest a direct relationship between the quantity of feed consumed and final body weight. Liver weight was significantly lower in the S-Rf group compared to the CON group, while it was comparatively lower in S-Wh and HAS compared to CON. Perirenal and epididymal adipose tissue weights were significantly lower in the HAS group in comparison to the two sorghum groups and CON group. Cecal parameters were significantly higher in the HAS group, while other three groups reported significantly lower values.

Final body weight and body weight gain at the end of the experimental period in S-Wh, S-Rf and CON groups, seemed to be significantly contributed by the liver weight ($r=0.599^{**}$, 0.474^* , respectively; $*p < 0.05$, $**p < 0.01$), perirenal ($r=0.614$, 0.645 , respectively; $p < 0.01$) and epididymal ($r=0.671$, 0.693 , respectively; $p < 0.01$) adipose tissue weights, clearly evinced by the positive correlation coefficients. Further, significantly positively correlated feed intake with final body weight ($r=0.869$; $p < 0.01$), body weight gain ($r=0.552$; $p < 0.01$), liver ($r=0.543$; $p < 0.01$) and total adipose tissue weights ($r=0.749$; $p < 0.01$) suggested a significant impact of calorie intake. The positive correlation with the total adipose tissue weight clearly suggested an effect of adiposity on the final body weight and body weight gain. On the other hand, the significant negative correlations of final body weight and body weight gain with cecal parameters suggested that cecal fermentation might have negatively affected final body weight and body

weight gain; cecal weight ($r=-0.546$, -0.607 , respectively; $p < 0.01$), cecal tissue weight ($r=-0.488^*$, -0.691^{**} , respectively; $*p < 0.05$, $**p < 0.01$) and cecal content weight ($r=-0.542$, 0.583 , respectively; $p < 0.01$), an observation clearly apparent in the HAS group (Goldsmith *et al.*, 2017).

3.3.2. Microbial community DNA data

Both alpha diversity parameters, Shannon's diversity index and observed species index were significantly higher ($p < 0.05$) in S-Rf and CON groups compared to HAS and S-Wh groups, suggesting a higher diversity and evenness in the two former groups (Fig. 3.5. a,b). Generally, the alpha diversity (richness and evenness) depends on the available microbial accessible substrates for metabolism. A higher number of species (higher richness; higher diversity) in a sample indicates several implications about the substrates, such as availability of diverse substrates to cater metabolically diverse microbial species or availability of a wide array of species with similar or adaptable metabolic requirements or availability of microbial species with cross-feeding ability.

A higher evenness (how equally abundant the species in a niche are) is also positively correlated with higher alpha diversity, which suggests that the specific substrate might have provided favorable conditions for the growth of a wide array of microbial species. On the other hand, a higher abundance (how common or rare a species is in a community) suggests that the niche environmental conditions might be favorable for the specific microbial growth and proliferation, while a rare species might also implicate either the substrate does not meet its metabolic necessities or the current substrate provides at least the minimal conditions for its growth in comparison to another substrate, where the rare species is not found. Thus, the manner in which the alpha diversity information statistics are discussed is subjective and it largely varies depending on the specific objectives of a study. Shannon's diversity index and the observed species index are known to be influenced by the presence of rare operational taxonomic units (OTUs).

Beta diversity (beta diversity = {total species diversity in all communities / sample's alpha diversity}), represents the OTU diversity between two or among more than two substrates and it can be either a non-phylogenetic tree based analysis (Jaccard, Bray-Curtis, etc.) or a phylogenetic tree based assessment (Unweighted/weighted UniFrac, Comdist, etc.) of differences, within an overall bacterial community composition. For example, the UniFrac distances used to measure the beta diversity (how close or far on the phylogenetic tree) in this study, are based on the fraction of branch length shared between two communities within a phylogenetic tree constructed from the 16S rRNA sequences from all the communities being compared.

In weighted UniFrac distances, branch lengths are weighted based on the relative abundance of the lineages within communities. Depending on the weighted distances between the samples, in terms of their locations on the phylogenetic tree, they can be ordinated on a principal component plot (principal coordinate analysis plot), which indicates the variability among the samples along the x and y-axes (Lozupone and Knight, 2005). As seen in Fig. 3.5.c., three distinct clusters can be observed: HAS, S-Wh and CON/S-Rf, suggesting that HAS and other three groups might be located on distinct branches in the phylogenetic tree and S-Rf and CON might be located on nearby sub-branches, while S-Wh might be located on a distant sub-branch to CON and S-Rf groups, suggesting that the phylogenetic variation between HAS and other three groups might be higher than the variation between S-Wh and S-Rf/CON, which is clearly illustrated in Fig. 3.5.d (this figure is only for observing the group cluster formation).

When the microbial diversity was visualized at the phylum level (Fig. 3.6.a), it was observed that phylum Firmicutes was the highest abundant group in all four groups, where its abundance was significantly lower in HAS compared to the other three groups. Further, Verrucomicrobia and Actinobacteria abundance was also observed to be significantly higher in the HAS group. Albeit, quantitatively Firmicutes abundance

was higher, this phylum comprises a group of beneficial bacteria, such as butyrate producing clusters and lactic acid bacteria, thus it is important to further fine tune this phylum at lower taxonomic levels.

The LEfSe plot (Fig. 3.6.b) filters out the most important microbial genera with respect to the specific substrate and in this scenario by the relative abundance most probably, as biochemical data were not compared alongside. As seen here, genera *Bifidobacterium*, *Ruminococcus*, *Akkermansia*, *Bacteroides* and *Parabacteroides* were seen to be the characteristic genera for HAS group. Higher RS content in HAS (35% w/w dry weight basis) might have been a good fermentative substrates for these key bacterial species who are known for their complex carbohydrate degrading ability in the colon (Liu *et al.*, 2008). On the other hand in S-Wh, S-Rf, and CON, *Lactococcus*, *Lactobacillus* and *Blautia*, respectively, were seen to be dominating.

At species level, *Bifidobacterium pseudolongum* was seen to be only predominantly found in the HAS group, attributed to its renowned RS utilizing ability (Fig. 3.7). Lower *B. pseudolongum* abundance in the two sorghum groups might indicate that the substrates favorable for its growth and proliferation might have been deficient. In contrast, *Lactococcus gravieae*, *Ruminococcus gnavus* and *Blautia producta* abundance was observed to be significantly higher in sorghum groups, specifically in S-Rf. Genus *Lactococcus* belongs to the functional group of lactic acid bacteria (*Lactobacilli*, *Lactococci*, *Enterococci*, *Streptococci*, *Leuconostoc*, and *Pediococci*), which is identified as a probiotic class, thus its higher abundance is favorable (Pessione, 2012).

3.3.3. Cecal short chain fatty acid content and pH

Cecal SCFA contents are presented in Fig. 3.8. Acetate was the most abundant form of SCFA in the cecal digesta of all feed groups followed by propionate and butyrate. Acetate content was significantly ($p < 0.05$) higher in the HAS fed group compared to S-Rf fed rats, while CON and S-Wh exhibited

comparatively higher acetate contents compared to S-Rf. Propionate content was not statistically significant among the four experimental groups, yet its content was clearly higher in the CON fed group followed by HAS, S-Rf and S-Wh. But lack of a significant correlation between observed species index and cecal propionate content ($r=-0.067$) also might suggest the lack of species expressing propionic acid producing enzymes, which was elucidated by the raw data itself too (Fig. 3.8). Butyrate content was significantly and distinctively very high in the HAS fed rats compared to the other three diets fed rats, further showing the butyrogenic nature of HAS. Total SCFA content was reflective of acetate content in the cecal content, where HAS exhibited significantly higher content compared to the other three groups.

Similar acetate levels observed in CON and S-Wh groups can be attributed to their higher relative abundance of genus *Blautia*, identified as an acetogenic microorganism closely associated with mucus layer possessing the ability to utilize mucus degradation products for fermentation, even though the CON diet was deficient in fermentable carbohydrates (Liu *et al.*, 2008). Further, negative correlations of alpha diversity indices with cecal parameters and SCFA might suggest the negligible contribution to cecal fermentation by the bacterial OTUs observed in higher abundance in the CON and S-Rf groups, which might explain the observed lower SCFA contents in the mentioned groups. Cecal pH was significantly lower in the HAS group compared to other three groups as shown in Fig. 3.9. CON, S-Wh and S-Rf groups had statistically similar cecal pH values.

Neither cecal weight parameters (Table 3.8) nor SCFA contents in the cecal content exhibited evidence of beneficial effects of cecal fermentation. But Pearson's correlation analysis provided unseen evidences of colonic fermentation driven biological and physiological effects. For examples, negative correlation values with final body weight ($r=-0.445^*$, -0.686^{**} , -0.494^* for acetate, butyrate and total SCFA content, respectively; $*p < 0.05$, $**p < 0.01$), body weight gain ($r=-0.561$ for butyrate; $p < 0.01$), perirenal ($r=-0.500$ for butyrate; $p < 0.05$) and epididymal ($r=-0.630$ for butyrate; $p < 0.01$) adipose tissue weights and

cumulative feed intake ($r=-0.566$ for propionate; $p < 0.01$) similar to the observations reported by Goldsmith *et al.* (2017). The negative correlation effects suggested that cecal SCFA contents, especially propionate content ($r=-0.508$; $p < 0.05$) significantly reduced the cumulative feed intake, which might be due to its pronounced satiety inducing effect specifically in the HAS group (Carlson *et al.*, 2017). Further, butyrate and total SCFA contents seemed to negatively affect the cumulative feed intake ($r=-0.566^{**}$, -0.463^* , respectively; $*p < 0.05$, $**p < 0.01$), which is suggested to lower the final body weight and body weight gain. The above effect could be related to reduced adiposity as apparently seen in HAS, and it was further evinced by the negative correlations between butyric content and adipose tissue weights ($r=-0.596$; $p < 0.01$).

3.3.4. Ammonia-nitrogen content and branched-chain fatty acid content in the cecal content

Ammonia-nitrogen content in the HAS fed group was significantly ($p < 0.05$) lower compared to the other three groups (Fig. 3.10). Among CON, S-Wh and S-Rf, the two sorghum groups exhibited comparatively higher ammonia-nitrogen contents. As previously mentioned, ammonia-nitrogen content and cecal pH are positively correlated and a similar trend can be observed in this study also ($r=-0.588$; $p < 0.01$) (Taciak *et al.*, 2015).

Origin of cecal ammonia can be either urea hydrolysis or amino acid fermentation (Vince *et al.*, 1973). According to the positive correlations observed between ammonia content and cecal weight ($r=0.614$; $p < 0.01$) and cecal content weight ($r=0.649$; $p < 0.01$), it is obvious that the origin might have been amino acid fermentation by microbiota. Further, the relationships between ammonia and cecal acetate, butyrate and total SCFA contents ($r=0.537$, 0.542 , 0.564 , respectively; $p < 0.01$) also might suggest that amino acid fermentation in the cecum might have contributed to the cecal acetate, butyrate and total SCFA pools in S-Wh, S-Rf and CON groups (Neis *et al.*, 2015).

Significantly higher crude protein content in S-Wh and S-Rf groups and lack of fermentable carbohydrate substrates in the CON group might have caused amino acid fermentation and higher cecal ammonia content (Neis *et al.*, 2015). Ammonia is considered as a cytotoxic substance and its higher concentrations are known to cause stress in animals hindering their growth, as manifested by the negative correlations between ammonia and final body weight ($r=-0.499$; $p < 0.05$), which might be apparent in the CON and S-Rf groups.

In line with the significant correlations among ammonia-nitrogen, SCFA and pH, it was postulated that cecal fermentation of amino acid might have taken place and the potential bacteria who might have involved in this could be lactic acid bacteria. In both sorghum groups, members of lactic acid bacteria were present, for example *Lactococcus* in S-Rf and *Lactobacillus* in S-Wh (Fig. 3.6.b). Albeit, the functional group of lactic acid bacteria is well-known for its beneficial conversion of lactose into lactic acid, members of this group are known to possess other adjunct metabolic pathways, such as Arginine deimination, acid and amino acid decarboxylation, which are known to be used under nutritionally poor niche conditions (Pessione, 2012). Both arginine deimination and amino acid decarboxylation are found to give rise to ammonia, undesirable (histamine, tyramine) and desirable (γ -amino butyrate, β -phenylalanine) bioactive amines (Pessione, 2012). Further, ammonia production via these metabolic processes are known to confer a basifying effect, which also can be related to the pH of CON, S-Rf and S-Wh groups (Pessione, 2012). Moreover, lactic acid bacteria are known to possess a proteolytic enzyme system consisting of proteolytic and peptidolytic enzymes in order to acquire nitrogen source or use substrates for energy metabolism under higher amino acid availability, which also can be related to this study, where the two sorghum groups exhibited higher protein contents (Table 3.2) (Pessione, 2012). Lactic acid bacterial proteolytic enzyme system is known to be involved in digesting incompletely hydrolyzed proteins into smaller peptides/amino acids (Pessione, 2012).

Branched-chain fatty acid contents observed in the cecal content are presented in Fig. 3.11. In the HAS group, none of the BCFA were detected, which might have been due to the abundantly available fermentable substrate for the microbiota in this group. As mentioned in the section 3.1.2, bacteria switch to amino acid fermentation only when the fermentable carbohydrate substrate becomes deficient. In the two sorghum groups both individual BCFA were detected similar to the level of CON group, thus it might suggest the fact that the two sorghum diets might not have possessed adequate amount of fermentable carbohydrate substrates or the accessibility to the fermentable carbohydrate substrates might have been hindered.

Clostridium, *Lactococcus*, *Enterococcus* and *Lactobacillus* observed in the two sorghum groups might have been involved in amino acid fermentation (Fig. 3.6.b). Significantly higher pH observed in CON, S-Wh and S-Rf could also be due to the BCFA production, which is further strengthened by the significant positive correlations between cecal pH and BCFA ($r=0.607^{**}$, 0.471^* , 0.666^{**} , isobutyrate, isovalerate and total BCFA, respectively; $*p < 0.05$, $**p < 0.01$). Further, it has been reported that the BCFA impose negative impacts on metabolic disorders such as obesity and overweight, and this trend also was observed in this study between BCFA and body weight gain ($r=0.510^*$, 0.540^{**} , 0.654^{**} , isobutyrate, isovalerate and total BCFA; $*p < 0.05$, $**p < 0.01$) and final body weight ($r=0.436$ with total BCFA; $p < 0.05$).

3.3.5. Immunoglobulin A (IgA) content in cecal content

Immunoglobulin A content in the cecal content among the samples was not statistically different, yet HAS group clearly exhibited a higher content followed by S-Wh, S-Rf and lowest by CON (Fig. 3.12). Immunoglobulin A is a biomarker of immunomodulation as it involves in secretion and induction of anti-inflammatory compounds, such as antibodies, cytokines and anti-microbial compounds by the host (O'Flaherty *et al.*, 2010). Thus, immunomodulatory bacteria are known to influence the mucosal immunity

or gut barrier function by multi-faceted mechanisms, such as modulating mucus production, reducing bacterial adhesion, inducing IgA production and enhancing tight junctions (O'Flaherty *et al.*, 2010).

Immunoglobulin A or otherwise known as secretory IgA, is the most abundant class of antibody found in the intestinal colon and considered as the first line of defense against pathogens and toxins to protect the intestinal epithelium (Mantis *et al.*, 2011). Further, prebiotic supplementation is reported to increase the fecal secretory IgA, possibly via modifying the composition of gut microbiota, such as increased abundance of immunomodulatory bacteria such as *Bifidobacterium* and *Akkermansia* as seen in this study in the HAS group (O'Flaherty *et al.*, 2010). *Bifidobacterium* is known to reduce ileal and colonic permeability, thus improve gut barrier function (O'Flaherty *et al.*, 2010).

Further, microbial fermentation by-products, SCFA are found to exhibit anti-inflammatory properties (O'Flaherty *et al.*, 2010). The positive correlation observed between IgA and cecal parameters, might explain the significant effect of colonic fermentation of RS in the HAS group, on the improvement of gut secretory immunity ($r=0.622, 0.635$, cecal weight, cecal content weight, respectively; $p < 0.01$). Lack of fermentable carbohydrate substrate for fermentation, minimal cecal fermentation, lower SCFA production, higher cecal ammonia-nitrogen content and higher cecal pH might have been the reasons behind the lower IgA contents in sorghum and CON groups. Yet, comparatively higher IgA contents in the two sorghum groups compared to CON, can be attributed to the higher abundance of lactic acid bacteria as they are known to improve adaptive immunity via various mechanisms, such as secretion of exopolysaccharide and production of bioactive peptides with anti-microbial functions due to their proteolytic ability (Pessione, 2012).

3.3.6. Mucin content in cecal content

Cecal mucin content was significantly ($p < 0.05$) higher in S-Rf followed by HAS and CON, while the lowest content was observed in S-Wh (Fig. 3.13). Mucus layers found in different locations of body have differentiated functions other than the common function, which is the protection of the internal environment (i.e. epithelium and underlying tissue) from external harsh environmental conditions or internal risk factors.

The mucus layer in the colon, which consists of two distinct layers is known to be critical in the maintenance of gut homeostasis (Tailford *et al.*, 2015). Outer mucosal layer in the colon is a nutrient-rich niche for a specific group of microbiota, who are able to utilize glycan bound to proline-threonine-serine domain, which accounts for 80% of total mucin mass (Tailford *et al.*, 2015). Between the two major groups of mucins (membrane bound or secreted), secreted mucins which forms the major component of mucus gel layer, is known to act as a selective niche for microbial colonization, where microbial community composition is known to be selected depending on the type and degree of glycosylation of mucins, thus secretory mucin is known to possess immunomodulatory functions (Tailford *et al.*, 2015).

Mucus layer is frequently renewed due to the activity of associated microbiota and the daily load that passes through the gastrointestinal tract, thus renewal of mucus layer is important to maintain the integrity of the outer mucus layer to maintain the gut homeostasis. Having mentioned that, one of the main reasons for increased secretion of mucins, is the activity of mucin degrading microbiota, belonging to several phyla. Among the various mucin degraders, *Akkermansia muciniphila* is identified as the key mucin degrader, thus higher abundance of *A. muciniphila* in the HAS group might be a main reason for the higher mucin content observed in HAS (Tailford *et al.*, 2015). Albeit, reports have not shown the mucin degrading ability of *B. pseudolongum*, *B. longum* and *B. breve* have reported to possess mucin degrading enzymes, thus this ability is highly species and strain dependent (Tailford *et al.*, 2015). The significantly

highest mucin content observed in S-Rf group can be attributed to the presence of *R. gnavus* and *A. muciniphila* in this group, where *R. gnavus* is identified as a mucosa associated immunomodulatory bacteria (Croft *et al.*, 2013).

3.3.7. Serum biochemical data

Serum biochemical data after one month of experimental period are presented in Table 3.9. Serum lipid profile (total cholesterol, HDL-C, non-HDL-C, triglycerides, free fatty acids) were observed to be significantly ($p < 0.05$) lower in the HAS fed group. S-Wh fed rats exhibited significantly highest values for the serum lipid profile parameters. On the other hand S-Rf fed rat serum had comparatively lower concentrations of lipid parameters. Serum glucose also followed the same trend as the lipid parameters among the experimental groups. Total protein, albumin, glutamic oxaloacetic transaminase (GOT) and creatine levels were not significant among the diet groups. Glutamic pyruvic transaminase (GPT) level was significantly higher in the HAS group, while the two sorghum groups reported significantly lower values. Alkaline phosphatase level was significantly and comparatively lower in the two sorghum groups compared to CON and HAS groups, respectively.

Total cholesterol, HDL-C, non-HDL-C, triglycerides in the final week's fasting blood serum were significantly positively correlated with feed intake ($r=0.620, 0.600, 0.530, 0.518$, respectively; $p < 0.01$), final body weight ($r=0.584^{**}, 0.422^*, 0.544^{**}, 0.503^*$, respectively; $*p < 0.05$, $**p < 0.01$), body weight gain ($r=0.563$, ns, $0.569, 0.650$, respectively; $p < 0.01$), liver weight ($r=0.573^{**}$, ns, $0.636^{**}, 415^*$, respectively; $*p < 0.05$, $**p < 0.01$) and total adipose tissue weights ($r=0.702, 0.527, 0.648, 0.743$, respectively; $p < 0.01$). Considering the correlations among body weight and organ weight parameters with the serum lipid profile, significantly higher feed intake could be suggested as the culprit for the higher final body weight, body weight gain, adipose tissue weights and liver weights along with higher serum total cholesterol, HDL-C and non-HDL-C levels in the S-Wh group. Thus, the similar trends in

correlations observed for serum non-HDL-C and triglycerides with feed intake and liver weight could be either due to higher dietary fat intake (due to higher feed intake, otherwise all four diets possessed similar levels of fat content) and/or higher hepatic lipogenesis (Cox, 1990). According to the magnitude of the correlations among the serum lipid parameters, the elevated serum total cholesterol levels in CON and S-Wh groups might have been due to elevated non-HDL-C levels. The contribution to serum total cholesterol from non-HDL-C ($r=0.968$; $p < 0.01$) seemed to be more prominent over HDL-C, ($r=0.608$; $p < 0.01$) as evident from Pearson's coefficients among the above parameters.

Further, free fatty acid content in the serum was positively correlated with liver weight ($r=0.451$; $p < 0.05$) and epididymal adipose tissue weight ($r=0.432$; $p < 0.05$). Serum free fatty acid content is determined by the balance among lipolysis in adipose tissues and *de novo* lipogenesis in liver and fatty acid oxidation in muscles and liver, where a higher free fatty acid content in the serum might suggest an abnormal lipolysis in adipose tissues or impaired ability of liver to export lipogenesis products or utilize free fatty acid (den Besten *et al.*, 2013; Frohnert *et al.*, 2013). Relationships between serum free fatty acid and epididymal adipose tissue weights and liver weight might suggest an increased lipolysis in epididymal adipose tissue depot and higher free fatty acid uptake and utilization by liver, respectively, as evident in the CON group.

Serum glucose content was also in a significant positive correlation with the total adipose tissue weight ($r=0.531$; $p < 0.01$) and body weight gain ($r=0.483$; $p < 0.05$). Higher serum glucose levels and their correlations with feed intake and adipose tissue weights in CON and S-Wh groups might reveal the contributing counterparts, while epididymal adipose tissue weight showed a higher contribution, suggesting an impaired adipocyte functions (Frohnert *et al.*, 2013).

As a whole, the serum lipid profile and glucose level along with zoometric and organ weight parameters, might suggest the fact that, sorghum fed rats might have developed certain abnormal metabolic functions in the adipose tissue, which subsequently might have affected the liver metabolic functions, leading to

unfavorable physiological conditions such as increased adiposity and higher body weight gain due to higher feed intake, lower cecal fermentation and fermentative by-products compared to the HAS group. Higher availability of BCFA in the sorghum groups compared to HAS, might have played a key role in this phenotype, where they are linked with increased risks of obesity, insulin resistance and type 2 diabetes (Neis *et al.*, 2015). Moreover, the prevalence of certain bacterial members, such as *Clostridium* (Fig. 3.6.b), has been correlated with the onset of type 2 diabetes and obesity (Neis *et al.*, 2015).

3.4. Implications and Conclusions to Chapter 3

HAS group showed significantly lower feed intake, final body weight, favorable serum lipid profile with significantly higher cecal parameters and SCFA contents exhibiting its prominent cecal fermentation ability and beneficial physiological effects as a well-known RS substrate. On the other hand, cecal fermentation was not seemed to be prominent in the CON, S-Wh and S-Rf groups with respect to lower cecal parameters and SCFA contents. Similarly, the zoometric parameters and organ weights also were not improved in the sorghum fed groups compared to the HAS group. The cecal microbial compositions in HAS, S-Wh and CON/S-Rf exhibited three distinct clusters suggesting a significant effect of the cecal microbial composition on cecal parameters, SCFA contents and physiological parameters.

Similar to the *in vitro* study reported in Chapter 2, a higher ammonia-nitrogen content was observed in the two sorghum groups, further suggesting a higher colonic amino acid fermentation. This was further strengthened by the higher BCFA contents observed in sorghum fed groups compared to HAS. The main reason for the observed higher cecal pH could be amino acid fermentation as ammonia (a by-product of amino acid fermentation) is known to possess basifying effects. Further, the higher abundance of members belonging to lactic acid bacteria, such as *Lactococcus*, *Lactobacillus* in the sorghum fed groups strengthened the amino acid fermentation scenario, as they are identified to possess alternative metabolic pathways that utilize peptides/amino acids as substrates, especially when the fermentable carbohydrate substrates are low. As previously mentioned in Chapter 2 (section 2.4), the higher protein content reaching the colon due to lower protein digestibility, which is prominently known for sorghum, might have been a major factor that mediated amino acid fermentation, due to the lower ratio between carbohydrates:protein in the colon. Lower abundance of genus *Parabacteroides* in sorghum groups compared to HAS, might suggest healthy colonic conditions, despite the higher ammonia-nitrogen and BCFA, as under impaired

metabolic conditions, members of genus *Parabacteroides* are known to induce gut or systemic inflammation.

Albeit, a moderate cecal fermentative ability was observed for sorghum under *in vitro* conditions in Chapter 2, *in vivo* study in rats did not exhibit a considerable fermentative potential for raw sorghum, except the underlying beneficial correlations observed among the biochemical and physiological parameters, whose effects were not prominent in the raw data. As revealed by the zoometric, organ weight and serum biochemical data, raw sorghum flour fed rats exhibited an undesirable physiological status compared to HAS fed rats. Thus, the observations in the *in vitro* study were further confirmed by the *in vivo* study and the potential physiological effects of those observations could be clearly identified. Thus, it was clear that the higher resistant protein fraction in sorghum flour might have played a key role in the lower cecal fermentability of the carbohydrate fraction, thus identifying methods to improve the accessibility/availability of RS in sorghum is important in order to be able utilized as a prebiotic substrate, and such methods were examined in the next study.

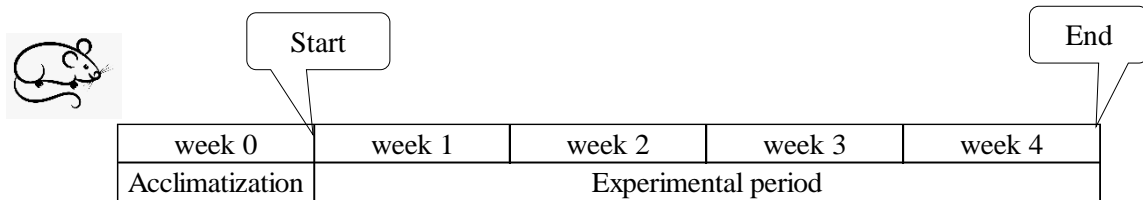


Fig. 3.1. Schematic representation of the animal experimental design.

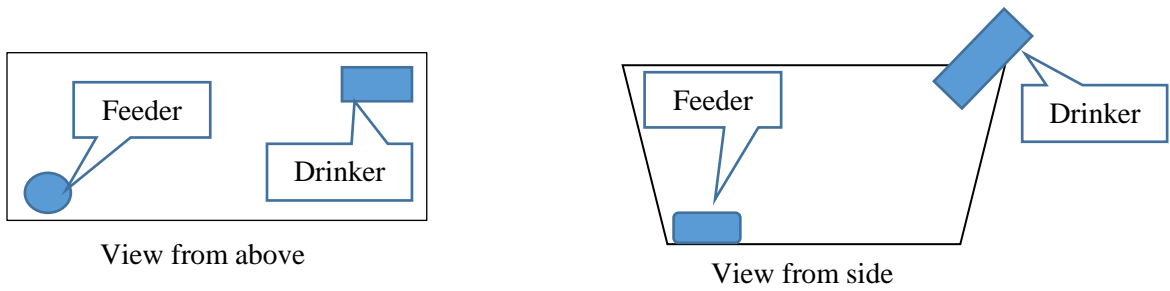


Fig. 3.2. Placement of feeder, drinker in the animal cage.

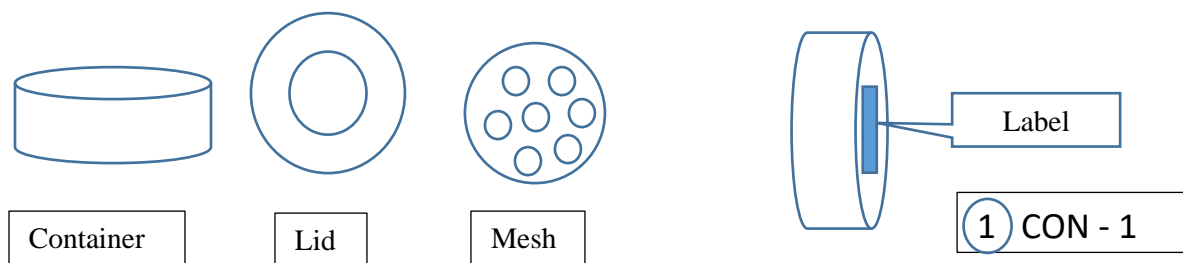


Fig. 3.3. Preparation of feeder for individual animals during the experimental period.

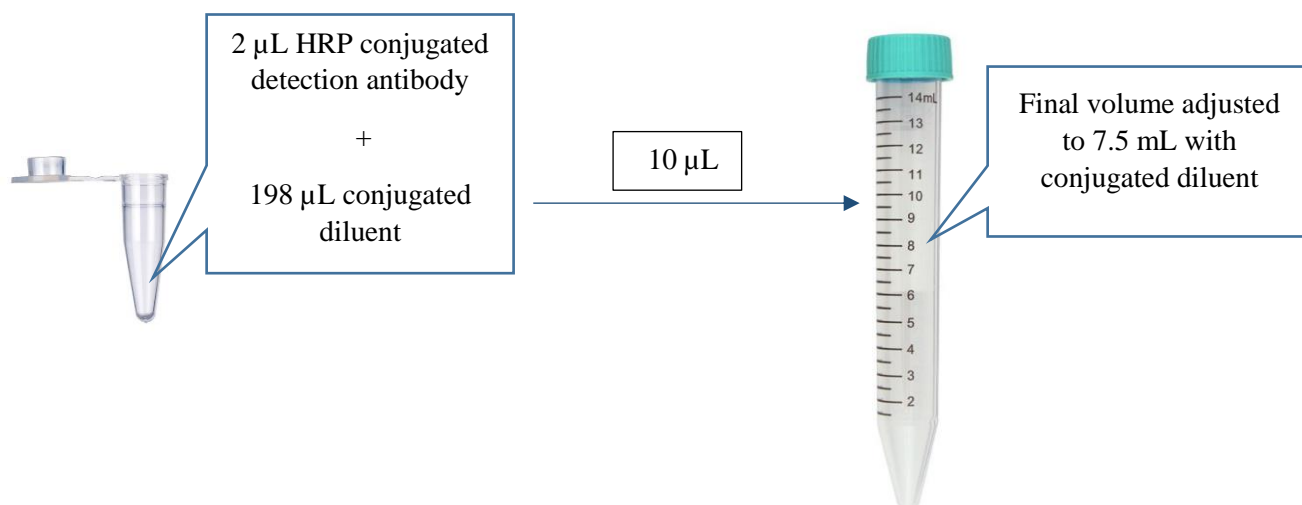


Fig. 3.4. Preparation of biotinylated detection antibody (streptavidin-conjugated horseradish peroxidase (HRP) conjugated Goat anti-Rat IgA detection antibody; 1 mg/mL) in the ratio of 1:75000.

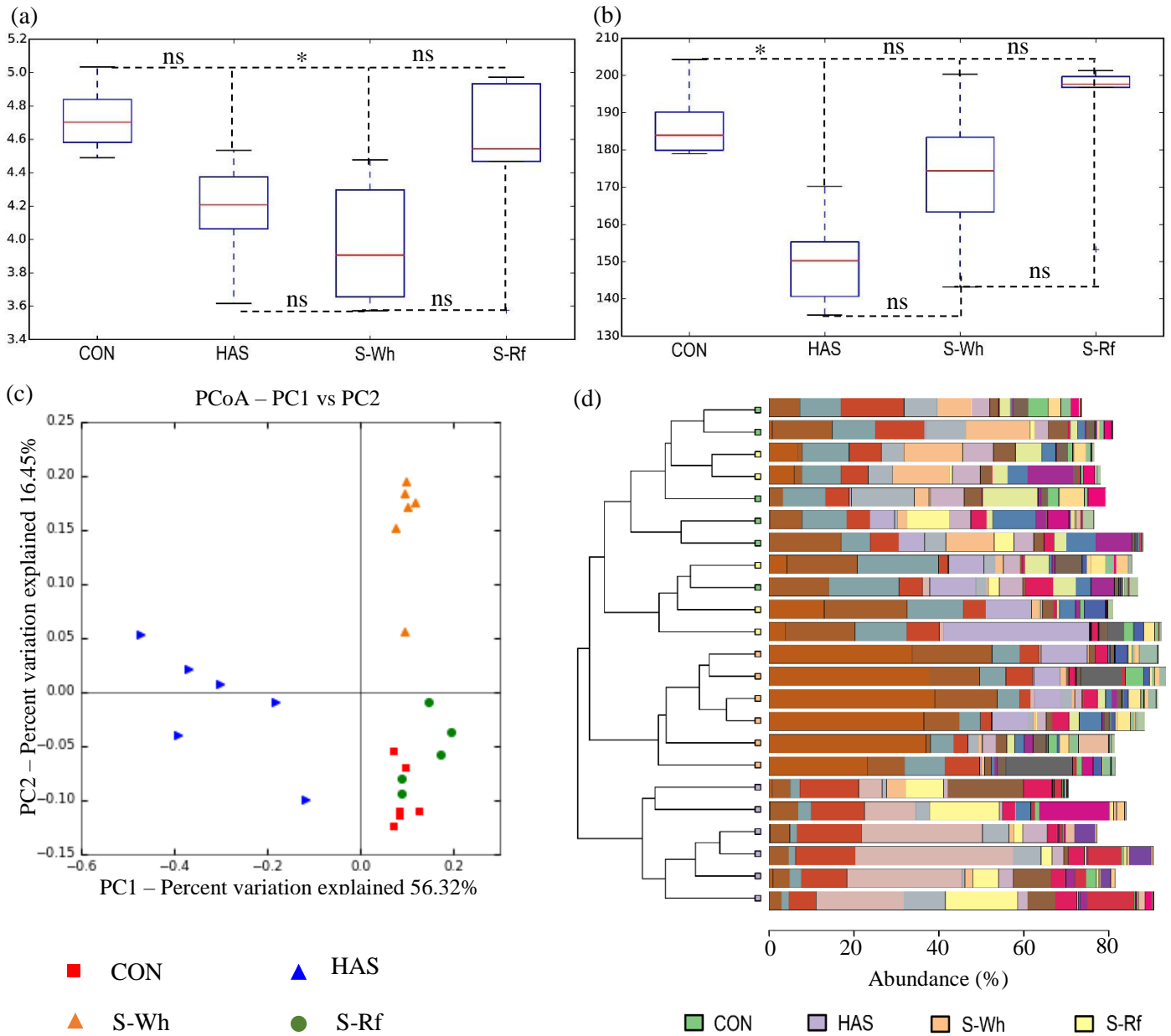
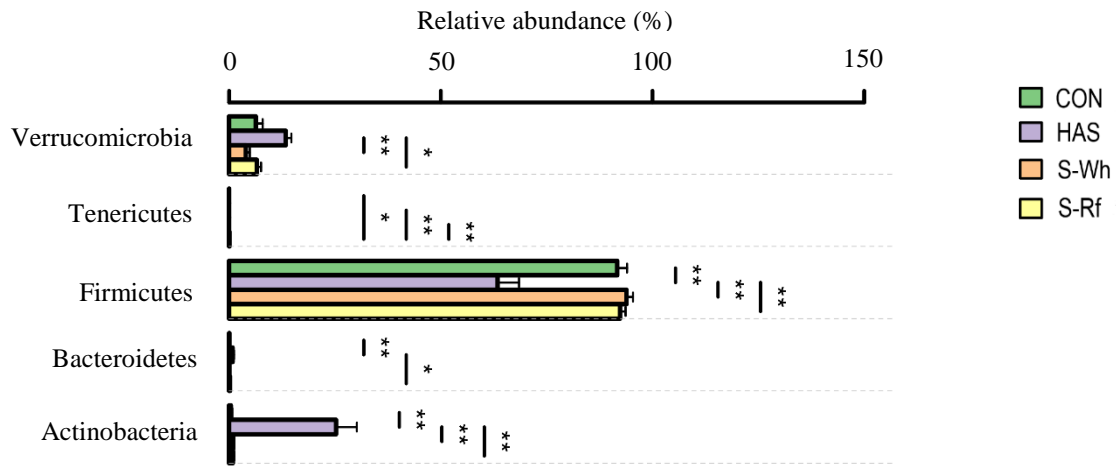


Fig. 3.5. Box and whisker plots of (a) Shannon's diversity index and (b) Observed species index (c) Weighted UniFrac PCoA plot for the β -diversity (d) Clustered bar chart at OUT level for the microbial community data.

(CON, α -corn starch; HAS, High amylose starch; S-Wh, whole white sorghum flour; S-Rf, refined white sorghum flour)

The red line in each box depicts the average value of Shannon's and observed species indices in (a) and (b). Statistical significance was determined by ANOVA (post hoc Tukey's test); (* $p < 0.05$). β -diversity was determined by the weighted UniFrac distance metric in QIIME. Clustered bar chart was prepared in Calypso version (8.72).

(a)



(b)

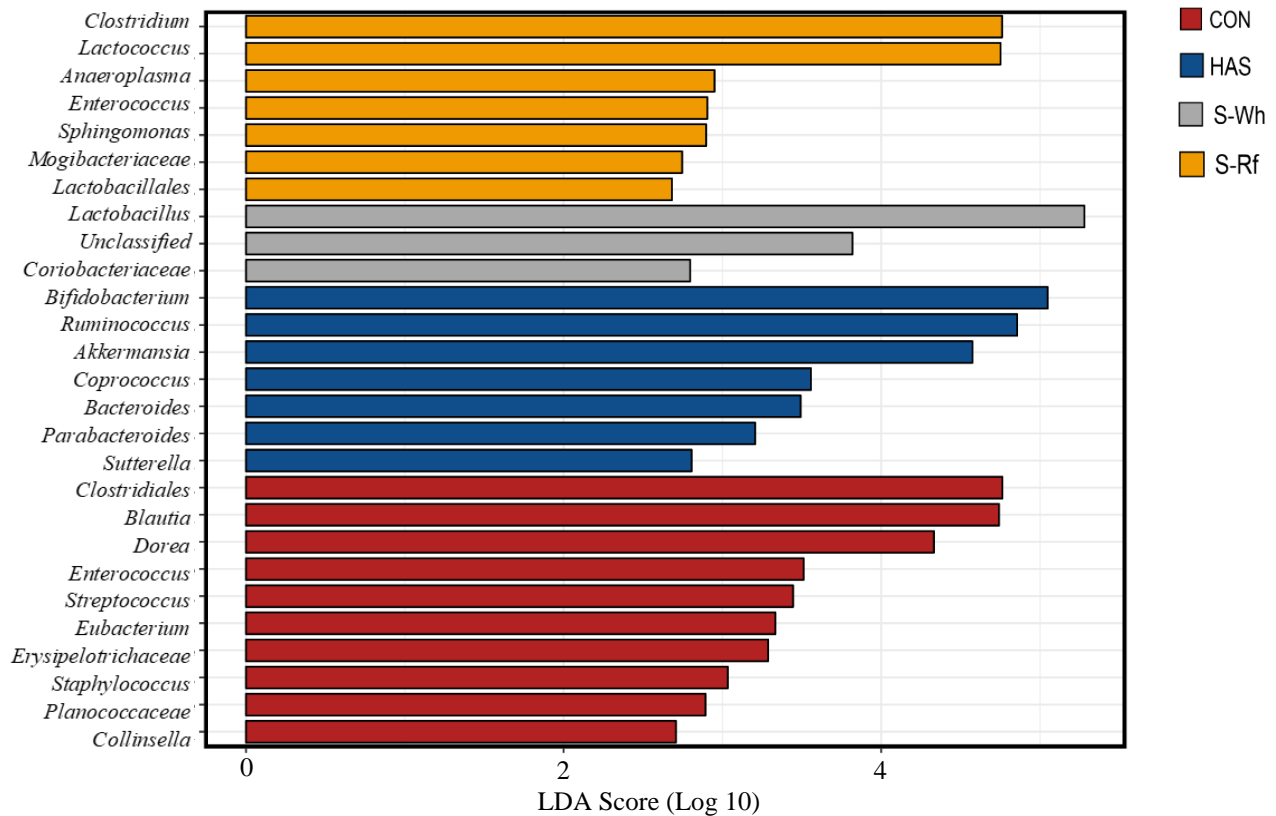


Fig. 3. 6. (a) Rank test bar charts for the relative abundance (median \pm SE) of dominant microbial phyla in the rat cecal digesta and (b) Linear discriminant analysis (LDA) effect size (LEfSe) plot at genus level. (CON, α -corn starch; HAS, High amylose starch; S-Wh, whole white sorghum flour; S-Rf, refined white sorghum flour)

Statistical significance was determined by Kruskal-Wallis H test in Calypso (version 8.72) (* $p < 0.05$; ** $p < 0.01$).

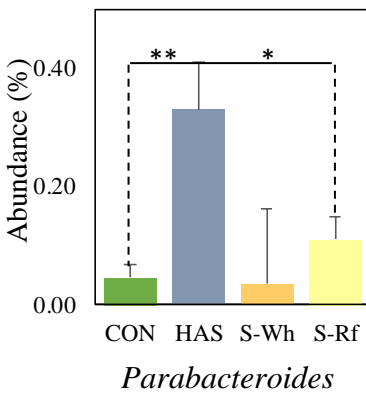
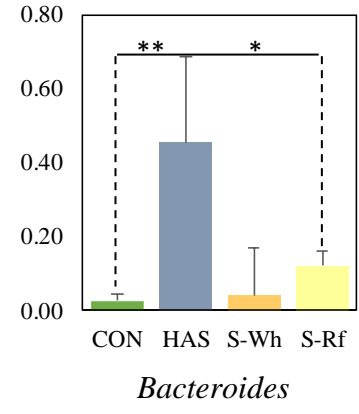
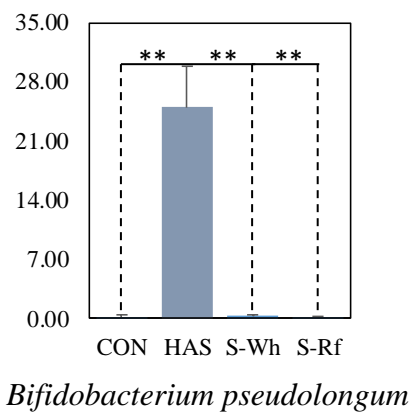
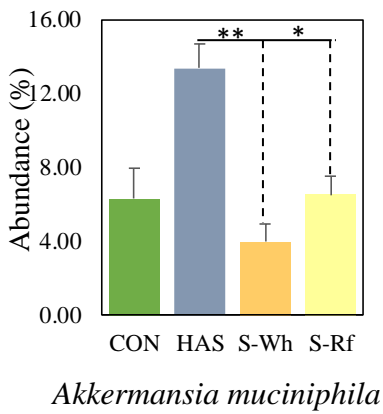
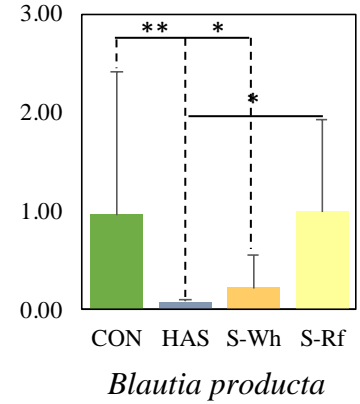
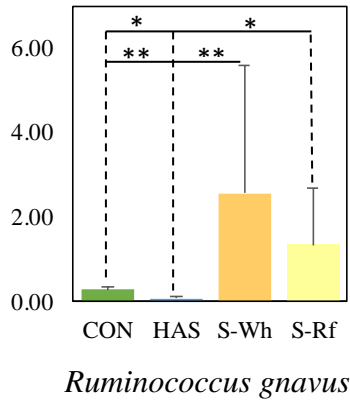
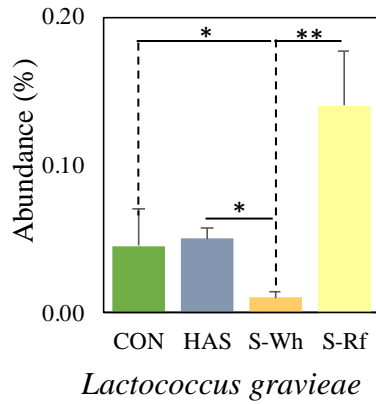


Fig. 3.7. Rank test bar charts for the relative abundance of selected microbial species in the rat cecal digesta. Data presented are median \pm SE (n=6, CON, HAS, S-Wh; n=5, S-Rf). Statistical significance was determined by Kruskal-Wallis H test in Calypso (version 8.72) (* $p < 0.05$; ** $p < 0.01$). (CON, α -corn starch; HAS, High amylose starch; S-Wh, whole white sorghum flour; S-Rf, refined white sorghum flour).

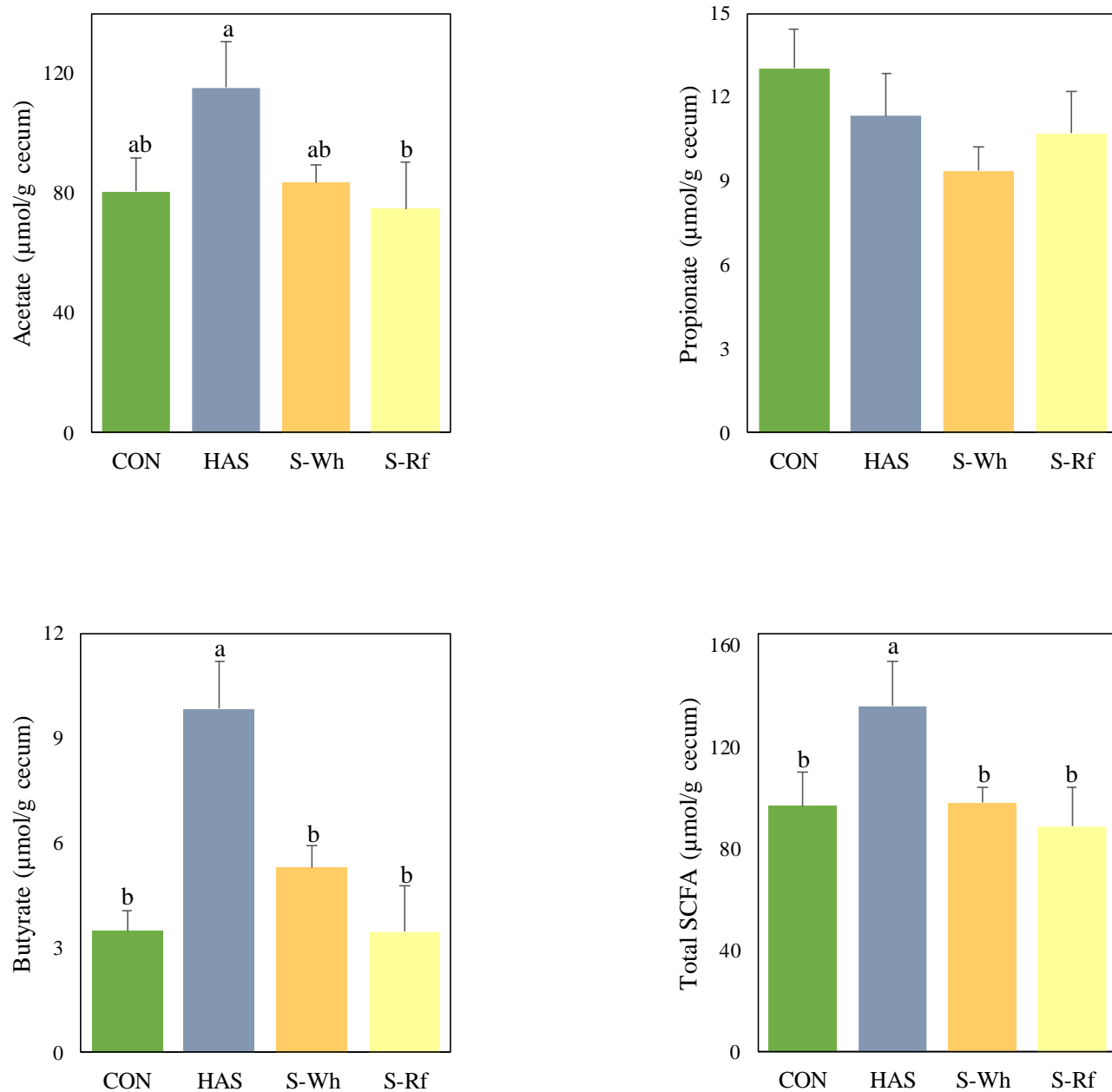


Fig. 3.8. Short chain fatty acid concentrations in the cecal content of rats.

Data presented are mean \pm SE (n=6). Different letters represent significant differences among the samples at ($p < 0.05$). (CON, α -corn starch; HAS, High amylose starch; S-Wh, whole white sorghum flour; S-Rf, refined white sorghum flour)

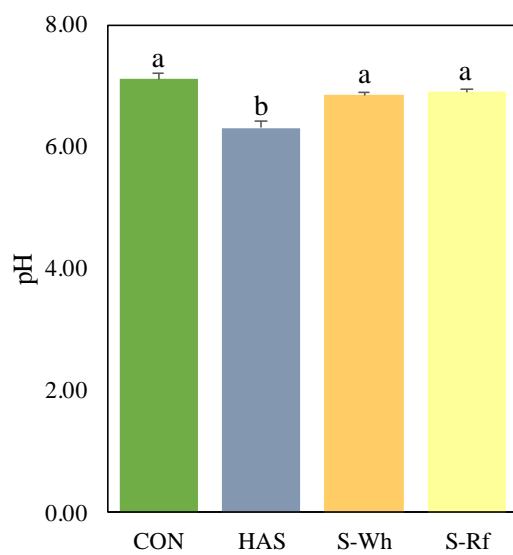


Fig. 3.9. pH in the cecal content of rats.

Data presented are mean \pm SE (n=6). Different letters represent significant differences among the samples at ($p < 0.05$). (CON, α -corn starch; HAS, High amylose starch; S-Wh, whole white sorghum flour; S-Rf, refined white sorghum flour)

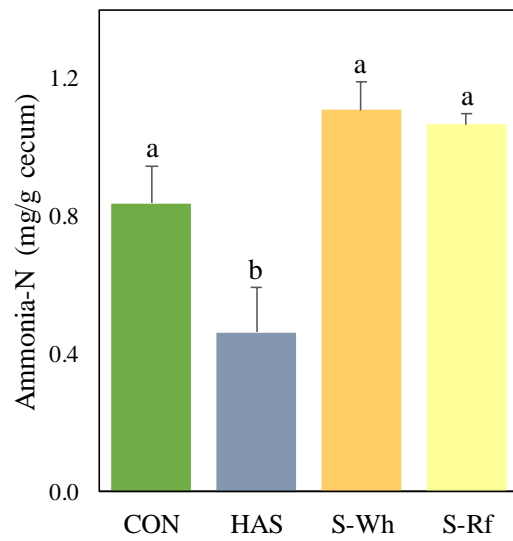


Fig. 3.10. Cecal ammonia-nitrogen content of rats.

Data presented are mean \pm SE (n=6). Different letters represent significant differences among the samples at ($p < 0.05$). (CON, α -corn starch; HAS, High amylose starch; S-Wh, whole white sorghum flour; S-Rf, refined white sorghum flour)

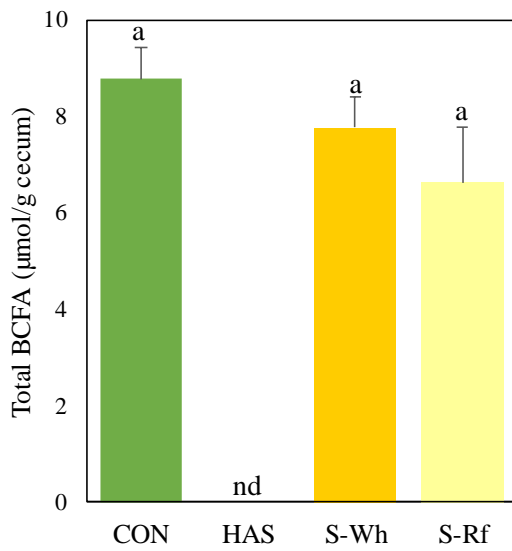
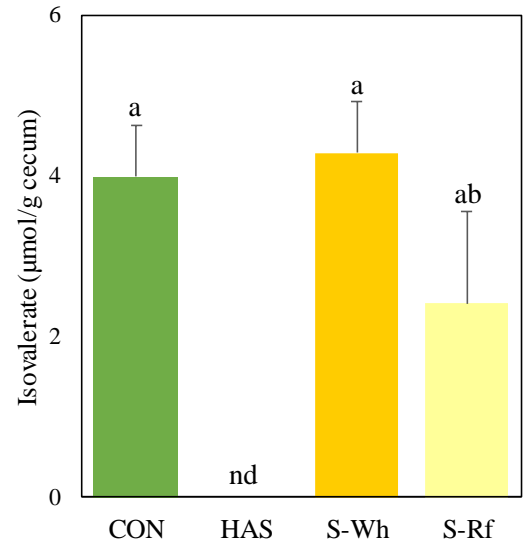
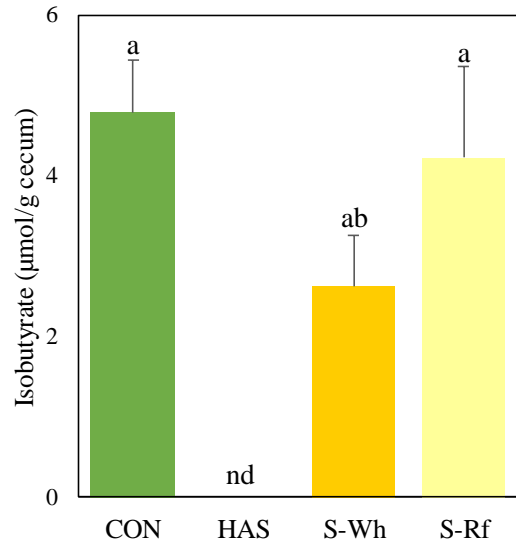


Fig. 3.11. Cecal branched-chain fatty acid contents in rats.

Values presented are mean \pm SE (n=6). Different letters represent significant differences among the samples at ($p < 0.05$). (CON, α -corn starch; HAS, High amylose starch; S-Wh, whole white sorghum flour; S-Rf, refined white sorghum flour; nd, not detected)

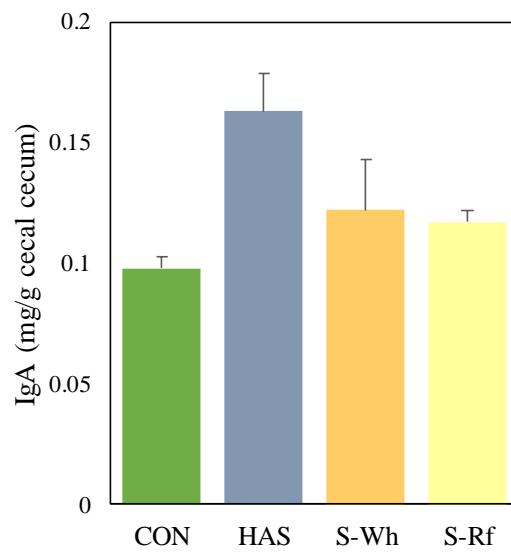


Fig. 3.12. Cecal immunoglobulin A (IgA) content of rats.

Data presented are mean \pm SE (n=6). Different letters represent significant differences among the samples at ($p < 0.05$). (CON, α -corn starch; HAS, High amylose starch; S-Wh, whole white sorghum flour; S-Rf, refined white sorghum flour)

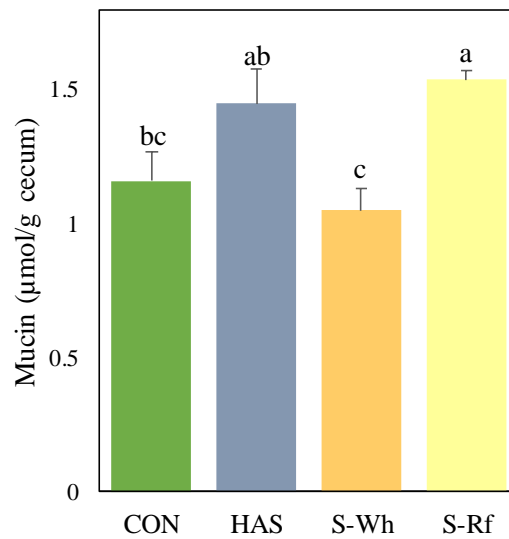


Fig. 3.13. Cecal mucin content in rats.

Data presented are mean \pm SE (n=6). Different letters represent significant differences among the samples at ($p < 0.05$). (CON, α -corn starch; HAS, High amylose starch; S-Wh, whole white sorghum flour; S-Rf, refined white sorghum flour)

Table 3.1. Different fractions of sorghum prolamin and their characteristics.

Kafirin fraction	Molecular weight classes	Characteristic amino acids	Remarks
α -kafirin	23 kDa and 25 kDa	Non polar amino acids (proline, leucine, alanine)	Found as monomers or oligomers/ do not extensively crosslink/ mainly form intramolecular disulfide bonds
β -kafirin	\approx 18 kDa	Methionine, cysteine	Found as monomers or polymers/ highly cross-linked/ form inter- /intramolecular disulfide bonds
γ -kafirin	\approx 28 kDa	Proline, cysteine, histidine	Found as oligomers and polymers/ highly cross-linked/ form inter- /intramolecular disulfide bonds
δ -kafirins	\approx 13 kDa	Methionine	Poorly characterized

(Source: Belton *et al.*, 2006; Shull *et al.*, 1991)

Table 3.2. Proximate composition of sorghum flour.

Sample	Energy (kcal)	Moisture (g/100g)	Protein (g/100g)	Lipid (g/100g)	Carbohydrate (g/100g)	Dietary fiber (g/100g)	Ash (g/100g)
S-Wh	348	12.8	9.1	3.7	72.9	3.9	1.5
S-Rf	354	13.1	5.8	1.8	78.7	1.5	0.6

(S-Wh, whole white sorghum flour; S-Rf, refined white sorghum flour)

Table 3.3. Experimental diet composition.

Ingredients (g/kg diet)	Dietary group			
	CON	HAS	S-Wh	S-Rf
Casein	200.0	200.0	172.7	182.6
L-Cystine	3	3	3	3
Sucrose	200	200	200	200
Soybean oil	70.0	70.0	58.9	64.6
<i>t</i> -Butylhydroquinone	0.014	0.014	0.014	0.014
Cellulose	50	50	38.3	45.5
Mineral Mix (AIN-93G-MX)	35	35	35	35
Vitamin Mix (AIN-93G-VX)	10	10	10	10
Choline bitartrate	2.5	2.5	2.5	2.5
HAS (HS-7)	0	300	0	0
Refined white sorghum	0	0	0	300
Whole white sorghum	0	0	300	0
α -Cornstarch	429.486	129.486	179.586	156.786
Sum	1000	1000	1000	1000

(CON, α -corn starch; HAS, high amylose starch; S-Wh, whole white sorghum; S-Rf, refined white sorghum)

Table 3.4. Random groups of similar body weight at the end of the acclimatization period.

Groups	G1	G2	G3	G4
	162.6	165.0	165.1	169.2
	176.6	170.3	170.7	171.8
	172.6	172.6	172.8	174.0
	174.6	174.6	175.1	170.3
	178.6	180.1	181.6	181.6
	182.5	183.6	184.5	186.8
Mean	174.6	174.4	175.0	175.6
SD	6.8	6.7	7.2	7.0

Table 3.5. Cecal supernatant dilution for IgA analysis.

Sample dilution	Sample volume	Diluent volume	Final volume
× 100	10 μ L	990 μ L	1 mL
× 200	500 μ L from × 100 dilution	500 μ L	1 mL

Table 3.6. Standard preparation for IgA analysis.

Standard	Standard concentration (ng/mL)	Rat reference serum (0.2 mg/mL IgA)	Diluent
1	1000	5 μ L	1 mL
2	500	500 μ L from previous standard	500 μ L
3	250	500 μ L from previous standard	500 μ L
4	125	500 μ L from previous standard	500 μ L
5	62.5	500 μ L from previous standard	500 μ L
6	31.25	500 μ L from previous standard	500 μ L
7	15.6	500 μ L from previous standard	500 μ L
8	0	-	500 μ L

Table 3.7. Standard series preparation for mucin analysis.

Standard	Standard concentration (mg/mL)	N-acetylgalactosamine	Distilled water
1	1	1 mg	1 mL
2	0.5	500 μ L from previous standard	500 μ L
3	0.25	500 μ L from previous standard	500 μ L
4	0.125	500 μ L from previous standard	500 μ L
5	0.0625	500 μ L from previous standard	500 μ L
6	0	-	500 μ L

Table 3.8. Zoometric parameters, feed intake and organ weights of rats.

Parameter	Feed groups							
	CON		HAS		S-Wh		S-Rf	
Final body weight (g)	243 ± 3	ab	232 ± 3	b	246 ± 3	a	244 ± 3	ab
Body weight gain (g)	69 ± 2	a	57 ± 2	b	71 ± 3	a	68 ± 1	a
Feed intake (g)	380 ± 5	ab	365 ± 5	b	393 ± 5	a	381 ± 5	ab
Liver weight (g)	9.43 ± 0.16	a	8.32 ± 0.12	bc	9.00 ± 0.16	ab	8.26 ± 0.24	c
Fat tissue weight (g)								
Perirenal fat	4.53 ± 0.12	ab	3.75 ± 0.25	b	4.86 ± 0.30	a	4.76 ± 0.16	a
Epididymal fat	5.29 ± 0.16	a	4.09 ± 0.19	b	5.41 ± 0.38	a	5.23 ± 0.17	a
Cecum								
Ceacal weight (g)	2.53 ± 0.28	b	5.82 ± 0.71	a	2.18 ± 0.09	b	1.96 ± 0.21	b
Tissue weight (g)	0.55 ± 0.03	b	0.99 ± 0.06	a	0.50 ± 0.02	b	0.51 ± 0.02	b
Content weight (g)	1.98 ± 0.29	b	4.83 ± 0.68	a	1.68 ± 0.08	b	1.46 ± 0.22	b

Abbreviations: CON, α -corn starch; HAS, High amylose starch; S-Wh, whole white sorghum flour; S-Rf, refined white sorghum flour. Mean values \pm SE are provided in the table.

Different letters in each row represent significant differences at ($p < 0.05$).

Table 3.9. Serum biochemical parameters of rats.

Parameter	Feed groups							
	CON		HAS		S-Wh		S-Rf	
Total cholesterol (mmol/L)	1.91 ± 0.06	a	1.55 ± 0.04	b	1.92 ± 0.08	a	1.77 ± 0.10	ab
HDL-C (mmol/L)	0.42 ± 0.01	b	0.45 ± 0.01	b	0.54 ± 0.02	a	0.48 ± 0.03	ab
Non-HDL-C (mmol/L)	1.49 ± 0.05	a	1.10 ± 0.03	b	1.38 ± 0.06	a	1.29 ± 0.08	ab
Triglycerides (mmol/L)	1.17 ± 0.10	ab	0.78 ± 0.06	b	1.33 ± 0.14	a	1.19 ± 0.11	ab
Free Fatty Acids (mmol/L)	1.35 ± 0.09	a	0.93 ± 0.05	b	1.11 ± 0.07	ab	1.07 ± 0.05	ab
Glucose (mmol/L)	6.74 ± 0.39	a	5.61 ± 0.14	b	6.12 ± 0.31	a	5.99 ± 0.19	ab
Total protein (g/L)	76.15 ± 0.67	ns	74.45 ± 0.82	ns	75.37 ± 0.67	ns	74.47 ± 0.56	ns
Albumin (g/L)	48.10 ± 0.34	ns	48.30 ± 0.34	ns	48.30 ± 0.30	ns	47.77 ± 0.55	ns
Alkaline phosphatase (U/L)	910.83 ± 26.74	a	737.50 ± 15.54	ab	681.83 ± 18.92	b	716.83 ± 29.68	b
GOT (U/L)	147.17 ± 6.73	ns	135.33 ± 5.08	ns	134.83 ± 3.42	ns	144.33 ± 13.53	ns
GPT (U/L)	33.83 ± 0.70	ab	38.67 ± 1.02	a	32.50 ± 0.67	b	32.50 ± 0.92	b
Creatine (mg/L)	2.78 ± 0.07	ns	2.62 ± 0.08	ns	2.60 ± 0.10	ns	2.65 ± 0.14	ns
Phospholipids (mmol/L)	1.26 ± 0.04	b	1.22 ± 0.02	b	1.51 ± 0.06	a	1.38 ± 0.07	ab

Abbreviations: CON, α -corn starch; HAS, High amylose starch; S-Wh, whole white sorghum flour; S-Rf, refined white sorghum flour; HDL-C, high density lipoprotein cholesterol; GOT, Glutamic oxaloacetic transaminase; GPT, Glutamic pyruvic transaminase. Mean values \pm SE are provided in the table. Different letters in each row represent significant differences at ($p < 0.05$).

CHAPTER 4

Effect of cooking on the colonic fermentation potential of sorghum and potential physiological benefits

4.1. Introduction

Starch is the most abundant form of edible carbohydrate cultivated and consumed globally. Generally, starch stored in plants are of three fractions depending on the degree of digestibility in the small intestine; rapidly digestible starch (RDS), which digests completely within 20 min reaching the small intestine and causes an abrupt increase in blood glucose level, slowly digestible starch (SDS), which digests between 20 to 120 min completely, but slowly, maintaining a lower glycemic response and finally resistant starch (RS), which skips small intestinal digestion and reaches the colon to be fermented by the gut microbiota (Haralampu, 2000; Chung *et al.*, 2009). Thus, the starch fraction compositions determine the extent of the digestibility of a particular starch.

Depending on the botanical source of starch and the environmental factors prevailed during cultivation are known to affect the digestibility, as they are found to play key roles during starch biosynthesis, causing structural and physicochemical alterations in the starch molecules and their organization within the granules (Pelpolage *et al.*, 2016). Apart from that, the RDS, SDS and RS fractions are largely affected by the interactions between starch and other macromolecules, such as protein and lipid also (Chung *et al.*, 2009).

Effect of different cooking methods have been reviewed in the point of view of many sensitive food components, such as vitamins and minerals and also macromolecules such as carbohydrates, proteins and fat, yet the knowledge, interest and importance of the cooking effect on RS surfaced later, along with its popularity as a prebiotic substrate. In different food cultures, there is a wide array of different cooking methods, such as boiling, pressure cooking, baking, steaming, roasting, grilling, frying (stir and deep), etc., where some methods involve addition of external water and some methods involve reaction with inherent water in the food material. Thus, the nature of the reactions taking place within the substrate, their end products and final sensory/nutritional effects are multifarious. Yet, there is one thing that might

be common under most cooking conditions, which is cooking of starch or more technically, “starch gelatinization”. Starch gelatinization is the process that determines the physicochemical, sensory and nutritional properties of the starchy food after cooking, thus it is important to know the underlying mechanisms taking place during gelatinization, in order to understand its effect on RS and to design thermal methods to improve RS contents in starchy foods.

4.1.1. Scientific background of cooking of starch

Under conventional cooking conditions, gelatinization occurs when starch is heated in excess amount of water (>1:2), above a certain temperature (gelatinization temperature), where the starch granules absorb water and swell, swollen granules further absorb water until the internal molecular organization is disrupted by melting the internal crystalline structure and finally rupture (Liu *et al.*, 2002). According to the nature of the packing of the amylopectin double helices in the crystalline lamellae, different crystal structures are formed in native starches, for example A-type (dense packing) in cereals, B-type (loose packing) in tubers (Waterschoot *et al.*, 2015). The knowledge of the internal organization of starch granules is very important in understanding the gelatinization processes, as the internal structure significantly changes the way the starches get gelatinized or simply cooked.

Naturally, starch granules are not water soluble, but during the gelatinization process these granules become water soluble increasing their solubilization. Generally, during the gelatinization of starch, the processes that take place within the starch granule in simple are, absorption of water, swelling of granules and solubilization of granules making a gel structure with water by intermolecular H-bonding (Liu *et al.*, 2002). Normally, the internal organization of the granule (reflected by the maltose cross under the refraction mode of the light microscope) is maintained by the intra-molecular H-bonding and hydrophobic bonds, where during gelatinization these intra-molecular bonds are disrupted, so that the internal molecular organization is distorted (fading and disappearance of maltose cross), while the starch granules

make intermolecular bonds with exogenous water. Thus, gelatinization is a process where, the intramolecular bonds are exchanged or converted into intermolecular bonds, which is influenced by the starch-water interactions. This disruption of molecular order of granules and melting of the crystallites during gelatinization depends substantially on the moisture content and heat energy, for example when starch is heated at a low moisture content (<1:2 = starch: water), gelatinization (disruption and melting of granule order) partly postpones to a higher temperature (onset temperature) (Waterschoot *et al.*, 2015).

4.1.2. Effect of thermal processing on the native resistant starch contents and functionality

Extrinsic factors involved in food production can significantly alter the starch digestibility, for instance, processing conditions such as physical methods (hydro-thermal treatments, annealing), chemical methods (acid hydrolysis, oxidation, cross-linking), and other methods (steeping, pre-germination) etc. (Liu *et al.*, 2002). For examples, both warm-water treatments (high moisture/low temperature) and heat-moisture treatments (low moisture; <30g moisture/100 kg starch/high temperature) are known to modify starch with minimal starch gelatinization (Vu *et al.*, 2017). Depending on the inherent physicochemical factors and the strength of the heat moisture treatments, the degree of starch gelatinization varies and thus, modifies the proportions of RDS, SDS and RS in starch sources. Since starch digestibility is an important determinant of glycemic index and treatment of non-insulin dependent diabetes, methods involved in the alteration of starch digestibility are of significant importance.

Heat-moisture treatment of starch is known to modify physicochemical characteristics of starch, for example, starch crystallinity, starch molecule interactions, granule swelling and solubility, rheological and pasting characteristics, thermal properties and thus the *in vitro* digestibility (Chen *et al.*, 2015; Xiao *et al.*, 2018). Either an increment or a decrease in the *in vitro* digestibility of starch can be observed, depending on the biological origin of the starches (cereal or tuber or root starch), which highlights the important effect of starch granule organization (crystallinity) and morphology in each source (Vu *et al.*, 2017). Yet,

heat moisture treatments employing <30 g/100 kg moisture content and 80 to 140°C temperature has been shown to improve the SDS and RS contents of starches from a wide array of origins (Vu *et al.*, 2017). Further, autoclaving coupled with retrogradation has reported to increase the RS content in rice starch in a previous study (Ashwar *et al.*, 2016).

Most native RS (i.e. RS1; raw banana, potato) are known to lose their resistant potential due to complete gelatinization of the previously inaccessible starch granules, a process which cannot be avoided during conventional cooking. Thus, most native RS sources become completely digestible in the small intestine upon hydrothermal treatments, and fail to extend the beneficial effects expected by the colonic fermentation (Haralampu, 2000). On the other hand, RS3 which is known to form in cooked starch due to the retrogradation, is known to be highly resistant to thermal and enzymatic degradation due to the highly ordered re-crystallized amylose (Haralampu, 2000). The re-crystallized linear amylose chains, which form tightly packed double helices stabilized by inter chain H-bonds hinder the accessibility of enzymes to starch chains, and thus, are resistant to degradation by thermal and chemical means (Haralampu, 2000; Liu *et al.*, 2015; Ashwar *et al.*, 2016)

Digestibility of starch is determined by a complex set of interactions among starch inherent physicochemical properties as previously mentioned, and among them, solubility and swelling ability of starch granules determine the degree of enzyme exposure into granules, thus directly affect the digestibility. In autoclaved-retrograded starch, the solubility and swelling indices were observed to be significantly reduced, which is attributed to the increased crystallite perfection, additional interactions between leached amylose-amylose and amylose-amylopectin chains and strengthening of amylose-lipid complexes, which subsequently reduced the digestibility due to the improved recalcitrance (Ashwar *et al.*, 2016).

4.1.3. Effect of thermal processing on sorghum digestibility

As we have already discussed in the previous chapters, sorghum generally has reported a strikingly less digestibility in comparison to its closest relative corn, which echoes both in the starch and protein fractions of sorghum due to their very close co-existence. As discussed in details in Chapters 2 and 3, sorghum inherits native RS and also presents a unique structural advantage for the improvement of RS further (Vu *et al.*, 2017). Unlike other native RS sources such as raw banana or potato, which become completely gelatinized and digestible upon cooking, sorghum has reported further low digestibility upon cooking, mostly attributed to the substantially diminished digestibility of the protein fraction upon cooking.

Protein matrix and the protein bodies around the starch granules, resist the access to water and water uptake, swelling of granules and gelatinization, which subsequently reduce the susceptibility to enzymatic digestion, attributed to the hydrophobic characteristics of kafirins even at the raw state (Aarthi *et al.*, 2003; Belton *et al.*, 2006). Upon cooking, the kafirins are known to increase their hydrophobicity, which is attributed to the extensive disulfide bonding, polymerization of kafirin monomers and change in the β -sheets alignment, which subsequently strengthen the native protein barrier and diminish the moisture absorption capacity (de Mesa-Stonestreet *et al.*, 2010). Due to the diminished ability to absorb moisture, susceptibility of protein digestibility is also substantially reduced (Emmambux and Taylor, 2009). For example, pepsin hydrolysable protein content in sorghum cooked at a high moisture ratio was found to be increased by almost two folds (Hamaker *et al.*, 1987). Further, cooked sorghum exhibited reduced availability of albumin and globulin, along with the subsequent increment of cross-linked glutelin and non-extractable proteins (Hamaker *et al.*, 1987).

In the raw state, sorghum protein digestibility is found to be around 60%, yet this value was found to downturn during wet cooking or conventional cooking, which compromises the nutritional value of the grain (Emmambux and Taylor, 2009). Protein cross-linking during wet cooking, which involves cysteine

rich γ - and β -kafirins and increase of β -sheet structure of protein that occur simultaneously especially in the vitreous endosperm, diminishes the access of moisture and amylolytic enzymes (Ezeogu *et al.*, 2005). Thus, it has been suggested that wet cooking of sorghum might increase the RS content further, without gelatinizing starch granules, and which might resist ileal digestion due to the protein barrier and finally facilitating the passing of a higher starch content into the large intestine (Vu *et al.*, 2017).

The effect of proteins in the digestibility modification of starch is well illustrated by Vu *et al.* (2017), where a clear void formation in the hilum area in the isolated starches upon heat treatment was observed compared to the isolated starch from heat-moisture treated flour, suggesting the initiation of starch hydrolysis in the former. And further, the maltose cross was almost faded when the isolated starch was heat-moisture treated compared to the isolated starch from heat-moisture treated flour was examined, suggesting a higher degree of gelatinization in the former. When proteins were viewed under fluorescence, the protein channels in starch granules towards the hilum were only observed in the isolated starch from heat-moisture treated flour, which might have been due to the lower extractability of proteins after heat-moisture treatment as previously reported (Vu *et al.*, 2017). Thus, it explains the lower digestibility of starch upon heat-moisture treatment of sorghum flour, which might be partially due to the restricted access to starch hydrolyzing enzymes through the protein channels, attributed to the modified channel proteins by heat-moisture treatment.

Further, the theory of less digestibility of cooked sorghum attributing to the polymerization via disulfide bonding was supported by the increased proportions of kafirin dimers, oligomers and polymers and an increased concentration of monomers when cooked in the presence of a reducing agent (Emmambux and Taylor, 2009). Further, it was revealed that kafirin polymerization depends on the cooking condition, where boiling might cause a higher proportion of kafirins to be polymerized by forming disulfide bonds

compared to pressure cooking, as the digestibility of kafirins were found to increase under pressure cooking (Emmambux and Taylor, 2009).

A heat-moisture study conducted by Vu *et al.* (2017) has observed higher RS contents (221 g/kg, 187 g/kg and 245 g/kg) compared to sorghum raw flour (56 g/kg), subjected to the following moisture/temperature combinations; (200 g/kg moisture/100°C/4 h), (200 g/kg moisture/120°C/4 h) and (125 g/kg moisture/140°C/4 h), respectively. Further, the same authors have examined the effect of heat-moisture treatment on isolated sorghum starch and found out that isolated starch does not increase the RS content significantly compared to the raw starch, thus it was suggested that the substantial increment of RS in the heat-moisture treated sorghum flour might be due to the changes occur in the protein fraction of sorghum flour, where the latter affects the digestibility of sorghum starch in flour (Vu *et al.*, 2017). Non-protein components forming complexes with kafirins or starch were found to diminish digestibility further upon cooking, due to the enhanced interactions among them (Duodu *et al.*, 2003). For example, the amylose lipid-complex in sorghum flour was found to be strengthened and become resistant during high moisture/high temperature heat treatment due to a phase change in amylose-lipid complex (amorphous to Vh-type) (Vu *et al.*, 2017).

Thus, most types of cooking involving high temperatures and high moisture contents are found to improve RS content in sorghum flour, due to the modifications to the protein structure and functionality and amylose-lipid complex structure, which are found to render moisture and enzyme access to starch fraction, diminishing gelatinization (cooking ability) and digestion, respectively. It has been reported that the increment of RS in starches from other botanical sources had not been effective with a heat-moisture treatment alone, without a correction for pH, enzymatic treatment or other chemical method, in contrast to sorghum (Vu *et al.*, 2017).

4.1.4. Research statement, objectives and hypothesis

In Chapter 1, we have reviewed the beneficial effects on colonic and systemic health by the fermentative end products of RS, which are directly and indirectly imposed via end product-mediated biochemical processes. For example, the beneficial biochemical reactions in adipose tissue, liver, brain axis and the intestine itself are known to exert beneficial health effects on host, such as anti-carcinogenic effects, homeostasis of lipid and glucose metabolism (reduce postprandial blood glucose and insulin levels), prevention of fat accumulation and decreasing the incidences of overweight, obesity, diabetes and colorectal cancers (Chung *et al.*, 2009; Tsuiki *et al.*, 2016; Vu *et al.*, 2017).

Thus, improving the RS contents in the starch sources has become the novel prospectus of most food processing industries and many chemical and thermal methods have been experimented for their effectiveness and safety as food-grade methods currently. Among such methods, thermal treatments that involve reactions with heat and moisture are very important as they can be easily and economically employed, even at domestic level in an environmental friendly manner compared to chemical methods. Further, during everyday food preparations at domestic level, thermal treatments are very common and used in almost all the food cultures, thus it is very important for the people to know how the cooking methods employed in their households might affect the functional value of their food.

Different RS types (RS1, 2, 3 and 4) are known for different colonic fermentation trends and characteristics, as their physicochemical structure and compositions are different. While RS1 is observed to lose recalcitrance upon cooking, RS3 and RS4 are known to form recalcitrance upon respective processing reactions. In RS3, resistance is built up due to thermal processing of starch (gelatinization) coupled with retrogradation, attributed to the formation of heat and enzyme stable amylose crystals during retrogradation (Haralampu, 2000).

Under conventional human food preparation that involves reactions with heat and moisture renders the digestibility in cooked sorghum and makes it unfavourable in the nutritional point of view (Emmambux and Taylor, 2009). In the contrary to nutritional value, in the point of view as a functional substrate, cooked sorghum might be a good source for transporting starch substrates for colonic microbiota, improving colonic fermentation of starch. A handful of parallel studies to this study have also examined the effect of cooking of sorghum flour under different conditions on its potential to improve physiological conditions. But the effect of cooked sorghum has not been studied well for its capabilities in terms of colonic fermentation. In this study we hypothesized that cooking of sorghum similar to conventional cooking conditions might improve the RS content, which then would influence the colonic fermentation and mediate subsequent biological and physiological benefits. Thus, we aimed to examine the colonic fermentation characteristics and physiological modifications in rats fed a cooked sorghum diet.

4.2. Materials and Methods

4.2.1. Preparation of experimental diets

The aim of this study was to determine the effect of cooking of sorghum on intestinal fermentation characteristics. Whole grain white sorghum and refined grain white sorghum were provided by the Nakano Industry Co. (Takamastu, Japan). In order to determine the most suitable cooking condition to enhance cecal fermentation by improving RS content, several cooking conditions were tested as shown in Table 4.1. Initially to determine the suitable cooking condition, RS content of all samples were determined by Megazyme resistant starch assay procedure (K-RSTAR 08/11, Wicklow, Ireland) according to AOAC method 2002.02 (Chapter 2; section 2.2.3.f). The RS contents for cooked sorghum under different cooking conditions are presented in Table 4.1.

Upon comparison of the RS contents, the grains cooked under autoclaving conditions (120°C; 20 min) in a grains:water ratio of 1:2 was selected as the test cooking condition. The required amount of grains were cooked by autoclaving (121°C; 20 min; SX-300 high pressure steam sterilizer, Tomy Seiko Co., Ltd., Tokyo, Japan), cooked grains were stored overnight at -30°C before they were freeze-dried (-80°C, Eyela FDU-2100, Tokyo Rikkai Co., Ltd., Japan). Freeze-dried cooked grains were milled (mill aperture size; 1mm, MRK-RETSCH, Cross Beater Mill, Giesbeek, Netherlands) and the flour was stored at -30°C until further analyses.

The moisture content (AOAC 930.15), protein (AOAC 979.09) with a conversion factor of 6.25, lipid (AOAC 920.85) and ash (AOAC 923.03) were analyzed for the two freeze-dried samples as mentioned in Chapter 2 (section 2.2.3). Amylose, amylopectin and total starch contents were determined by Megazyme amylose/amylopectin assay (K-AMYL 07/11) according to the method by Yun and Matheson (1990). Dietary fiber in the two samples were measured according to AOAC 2011.25 method. All the chemicals used were of analytical grade. Proximate composition of the two sorghum samples, whole white cooked

sorghum (S-Wh) and refined white cooked sorghum (S-Rf) are presented in Table 4.2. Four experimental diets, α -corn starch (CON), High amylose starch (HAS; 30% w/w; HS-7, J-OIL Mills Co., Ltd., Tokyo, Japan; RS, 35%), whole sorghum (S-Wh; 30% w/w), refined sorghum (S-Rf; 30% w/w) were prepared according to the AIN-93G diet guidelines by Oriental Yeast Co., Ltd., (Tokyo, Japan). Experimental diet compositions are presented in Table 4.3.

4.2.2. Animal experimental design, care for laboratory animals and post-mortem excision of organs

The animal experiment was conducted according to the guidelines of “Guide for the Care and Use of Laboratory Animals” and all the procedures were approved by the Animal Care and Experiment Committee of Obihiro University of Agriculture and Veterinary Medicine (License no: 18-86) and detailed procedure for this section is presented in Chapter 3 (section 3.2.2).

Twenty five Fischer 344 male rats (7 weeks old; average body weight 135-165 g) were purchased from Charles River Laboratories Japan Inc., (Yokohama, Japan). The rats were acclimatized for one week prior to the experiment on a commercial diet (Standard powder diet for mouse, rat, hamster, Oriental Yeast Co.) and were grouped into four similar body weight groups (\approx 187 g) at the end of the acclimatizing period as shown in Table 4.4. Followed by grouping, rats were fed with experimental diets (G1, CON; G2, HAS; G3, S-Wh; G4, S-Rf) with free access to *ad libitum* water.

Each rat was housed individually, a feeder (\approx 25g) and a drinker (\approx 150 ml) were allocated to each animal, which were replenished every morning at 8 o’ clock. The cages were maintained at $23 \pm 1^\circ\text{C}$ temperature and $60 \pm 5\%$ relative humidity under a 12 h light/dark cycle. Body weight and feed intake were measured once a week and daily, respectively. Following a 12 h fasting period, blood (\approx 1ml) was collected from the jugular vein weekly and the separated serum via centrifugation (8,000 rpm, 15 min, 2 times; CFA-12, Iwaki Glass Co., Ltd., Tokyo, Japan) and was stored at -80°C until biochemical analysis. Feces were

collected during the last four days of the experimental period for fecal lipid analysis. Fresh feces were collected directly from the anus for fecal moisture analysis.

After the experimental period of four weeks, the final body weight was measured and the animals were sacrificed (sodium pentobarbital, 40 mg/kg body weight, Abbott Laboratories, Chicago, IL, United States). Following the sacrifice, cecum, liver, epididymal and perirenal adipose tissue masses were excised and weighed. Cecal weight, cecal content weight and cecal tissue weight were measured and a part of the cecal content (≈ 1 g) was diluted ($\times 5$) in sterilized distilled water for pH measurement (Chapter 3; section 3.2.2) and other analyses, while the rest was stored at -80°C . Liver was frozen in liquid nitrogen and stored at -80°C for liver lipid analysis. Mesenteric adipose tissue was fixed in freshly prepared 10% neutral buffered formalin and was stored at 4°C until staining.

4.2.3. Rat cecal bacterial DNA extraction, sequencing and analysis of 16S rRNA sequences

Extraction of bacterial DNA from the cecal digesta, purification, the 16S genome library preparation and sequencing were conducted according to the methods described in Chapter 2 (section 2.2.5). The generated biome table was normalized using an equal subsampling size of 6,232 sequences. Analysis of retrieved 16S rRNA sequences was conducted according to the method described in Chapter 2 (section 2.2.5.b.v). Calculation of the distances between the bacterial communities in different samples by the weighted UniFrac distance metric and the preparation of Principle Coordinate Analysis (PCoA) plots were conducted in QIIME (Lozupone and Knight, 2005). Calypso version 8.72 was used to generate the hierarchical cluster illustrations (Zakrzewski *et al.*, 2017).

4.2.4. Rat cecal short chain and branched-chain fatty acid analysis

Short chain and branched-chain fatty acid (BCFA) content in the cecal digesta of rats were analyzed by high performance liquid chromatography (HPLC, Shimadzu LC-10AD, Kyoto, Japan). Samples for HPLC

were prepared according to the method described in Chapter 2 (section 2.2.6) and the analytical specifications were as follows; column, RSpak KC-811 (8.0 mm x 300 mm, Shodex, Tokyo, Japan); eluent and flow rate, 2 mM HClO₄ at 1 mL/min; column temperature, 47 °C; reaction reagent and flow rate, ST3-R (×10 diluted, Cat. No. F56120000, Shodex) at 0.5 mL/min; UV-visible spectrophotometric detector (SPD-10A, Shimadzu) wavelength, 450 nm. Quantification of fatty acid concentrations was performed same as Chapter 2.

4.2.5. Determination of cecal ammonia-nitrogen content

Ammonia-nitrogen content in the diluted samples of cecal content was analyzed using a commercially available kit (Wako Pure Chemical Industry Ltd., Tokyo, Japan) as described in details in Chapter 2 (section 2.2.7) with slight modifications. Fifty microliter from samples and standards were conjugated with 200 µL of deproteinizing solution, mixed well on vortex and centrifuged (3,000 rpm, 4°C, 5 min). Hundred microliter of the deproteinized samples and standards were pipetted out into a microwell plate in duplicates and 100 µL of color reagent A was added and mixed well on vortex, followed by 50 µL of color reagent B and 100 µL color reagent C followed by vortex mixing after adding each. Finally, the microwell plate was incubated at 37°C (Isotemp* hybridization Incubator, Thermo Fischer Scientific) for 20 min for the color development. Followed by incubation, absorbance was measured at 630 nm using a microwell plate reader (MultiskanTM FC, Thermo Fisher Scientific). Quantification of ammonia-nitrogen content was similar to Chapter 2.

4.2.6. Analysis of mucin content in rat cecal digesta

Mucin in the rat cecal digesta was fractionated according to the method by Bovee-Oudenhoven *et al.* (1997) as described in Chapter 3 (section 3.2.7) with slight modifications; 5 µL from 5,000 U/mL amyloglucosidase was used for the hydrolysis instead of 10.4 µL of 300 U/mL amyloglucosidase. The

standard curve was prepared according to the following standard concentration series; 0, 0.78, 1.56, 3.125, 6.25 and 12.5 $\mu\text{g/mL}$ of N-acetylgalactosamine. Fractionated mucin was analyzed by the fluorometric assay procedure described by Crowther and Wetmore (1987) presented in details in Chapter 3 (section 3.2.7). Mucin content was calculated as follows;

$$\text{Mucin content } (\mu\text{mol/mL}) = \frac{(\text{Sample absorbance} - \text{y intercept})}{\text{Gradient of line}} * \text{dilution factor}/221$$

4.2.7. Analysis of cecal Immunoglobulin A (IgA) content

Immunoglobulin A content was analyzed by ELISA quantitative kit for Rat IgA provided by Bethyl Laboratories Inc. (Montgomery, TX, United States) as per the method described in Chapter 3 (section 3.2.6). IgA content was calculated similar to Chapter 3.

4.2.8. Fecal and liver lipid profile analysis

(a) Fecal and liver total lipid content

Total lipid fractions in feces (0.5 g of freeze-dried cumulative feces of four days; Eyela FDU-2100; at -80°C and milled) and liver (1 g) were extracted with chloroform-methanol (2:1 v/v) and chloroform-methanol-water (1:1:0.9 v/v) solvents, respectively, according to the method by Folch *et al.* (1957). Lipid fraction was collected by sequential extractions with either chloroform/methanol (feces) or chloroform/methanol/water (liver) solvents three times and 1.5 mL 1% BaCl₂ was added and centrifuged (2,000 rpm, 10 min, 20°C). After removing the upper layer containing contaminants, the lipid containing lower layer was completely evaporated to dryness on a rotavapor (Büchi rotavapor, R-114, Büchi, Tokyo, Japan). The fecal/liver total lipid contents were gravimetrically measured as follows;

$$\text{Total fecal lipid content (mg/day)} = \frac{\text{Tube weight (Final-Empty)}}{\text{Fecal sample dry weight}} * \text{total dry feces weight} * 1/4$$

(b) Liver cholesterol and triglyceride contents

The hepatic triglyceride and cholesterol levels were measured in the total lipid fraction dissolved in isopropyl alcohol using commercially available kits (Wako Pure Chemical Industries, Ltd., Osaka, Japan) according to the manufacturer's instructions.

$$\text{Liver cholesterol/triglycerides (mg/liver)} = \frac{(\text{Sample absorbance} - \text{y intercept})}{\text{Gradient of line}} * 1/100 * \text{liver weight}$$

(c) Fecal neutral and acidic sterol contents

Fecal neutral (cholesterol and coprostanol) and acidic (bile acids) sterol contents were measured by Gas Liquid Chromatography (GC-2014, Shimadzu Co., Ltd., Kyoto, Japan) following the methods of Matsubara *et al.* (1990) and Grundy *et al.* (1965), respectively. For the neutral sterol analysis, first the cholesterol in the total lipid fraction (dissolved in 5% HCl in methanol) was methylated using a methanol:water (10:9) solvent mixture three times. Upon centrifugation (2,000 rpm, 10 min) and removal of the upper layer, the lower layer was evaporated (Büchi rotavapor) until complete dryness. Dried methylated sample was dissolved in 0.1 mL of chloroform:methanol (2:1) solvent and 50 µL of the dissolved sample was applied on to a thin-layer chromatographic (TLC) plate and allowed to develop in a closed chamber. Later, the separated methylated cholesterol containing area was scraped off and was homogenized in 3 mL of chloroform:methanol (2:1) solvent and centrifuged (2,000 rpm, 10 min) to separate the supernatant. The supernatant was further purified using a column of three layers of sea sand (3 mm) and two layers of beads (5 mm) placed alternatively in a pasture pipette and the process was repeated once more for the filtrate.

The collected sample from the bottom of the pasture pipette was completely dried (Büchi rotavapor) and acetylated as follows; 100 µL of pyridine:anhydrous acetic acid (1:1) was added and allowed to stand in a dark place for 16 h after filling with N₂ and sealing with paraffin. Later 1 mL chloroform and 1.9 mL of

methanol:water (10:9) were added and vortexed followed by centrifugation (2,000 rpm, 10 min). After discarding the upper layer, the previous step was repeated two more times and the final lower layers were evaporated (Büchi rotavapor) to complete dryness. The dried sample was dissolved in 100 µL of acetone and stored at -30°C.

One microliter of the sample was injected to gas chromatograph and the analytical conditions for neutral sterol were as follows; column, BD17 capillary column (0.25 mm × 30 m; J & W Scientific, Folsom, CA, United State); carrier gas, N₂ (1.41 mL/min); inlet pressure, 187 kPa; temperature of column, injection port, detector, 260°C, 300°C, 300°C, respectively; detector, flame ionization detector (FID-2014, Shimadzu); retention time of coprostanol and cholesterol, 19 min and 23 min, respectively. One microliter from a 1,000 ppm standard mixture of acetylated cholesterol and coprostanol was used as the standard.

Analytical conditions for fecal acidic sterols were as follows: column, BD17 capillary column (0.25 mm × 30 m; J & W Scientific); carrier gas, N₂ (1.38 mL/min); inlet pressure, 187.5 kPa; temperature of column, injection port, detector, 270°C, 300°C, 300°C, respectively; detector, flame ionization detector (FID-2014, Shimadzu); retention time of cholic, chenodeoxycholic, lithocholic and deoxycholic acids, 51 min, 38 min, 23 min and 34 min, respectively. One microliter from a 1,000 ppm standard mixture of cholic acid, chenodeoxycholic acid, lithocholic acid and deoxycholic acid was used as the standard.

The concentration of neutral and acidic sterols was calculated as follows;

$$\text{Neutral/acidic sterol (mg/day)} = \frac{\text{Sample peak area}}{\text{Standard peak area}} * \frac{1}{(10 * \text{molecular weight})} * \frac{\text{Feces dry weight/ day}}{\text{Sample dry weight}}$$

4.2.9. Histological procedure for mesenteric adipocyte staining

Removal of trapped water

The mesenteric adipocyte tissue samples preserved in 10% buffered formalin were placed in the middle of the labelled cassettes. In order to extract the moisture trapped within the sample, the cassettes were homogenized on a multi-shaker (120 rpm) under the fume hood, in a series of ethanol solutions (450 to 500 mL) as follows; 70% (v/v), 12 h; 80% (v/v), 12 h; 90% (v/v), 12 h; 95% (v/v), 12 h and 100%, 12 h. Followed by the 12 h period in absolute ethanol (100%), the cassettes were homogenized in \approx 200 mL (just enough to cover the cassettes) of 100% ethanol on the multi-shaker for 1 h, followed by discarding the ethanol and this was repeated two more times. After the final wash with 100% ethanol, \approx 200 mL of xylene was added into the beaker containing cassettes, homogenized on shaker for 30 min, later xylene was discarded and this was also repeated two more times.

Preparation of paraffin blocks

Required amount of paraffin pellets were measured into a metal jar and placed in a 60°C oven to get dissolved. Then the cassettes were placed in paraffin at 60°C for 1.5 h and then the cassettes were moved into a new paraffin jar at 60°C for another 1.5 h. After 1.5 h in the second paraffin, the paraffin container was placed on a heater under the fume hood and the metal blocks used for making paraffin blocks were also warmed on the heater. After the blocks were warmed up sufficiently, paraffin was poured into the metal block and the tissue in each cassette was taken out and put into the center of the metal block followed by placing the bottom part (that contains the sample label) of the cassette on top using a pair of twisters. The blocks were kept on levelled ice to solidify and after proper solidification the paraffin blocks were separated from the metal block.

Cutting the paraffin block

The paraffin block was trimmed to remove excess paraffin around the trapped tissue and fixed on to the cutter (microtome replacement blade S35, KN3321485) tightly. The block was cut several times until a suitable cross section of the tissue is obtained. When an appropriate cross section was obtained, the cut surface was cooled and levelled using an ice block and a 4 µm thick tissue cross section was cut. Immediately after cutting the tissue section, it was put into distilled water using a painting brush. Two more 4 µm cuts were obtained followed by the levelling with ice after each cut. For each sample, all three cuts were next transferred into a 40°C water bath using a glass slide and each cut was pasted on to the middle of a labelled glass slide. The excess water on the glass slide was removed by blotting and the slides were kept on a heating surface to be dried and the slides were incubated in an oven (40°C) overnight and stored at room temperature until staining.

Staining the tissue cross sections

The slides were placed in a slide rack as the labelled side orienting up. The slides were immersed in a series of xylene solutions and ethanol solutions for 1 min in each in the following order; xylene I, xylene II, xylene III, AbAl I, AbAl II, 100% ethanol, 95%, 90%, 80% and 70%. Followed by 1 min in 70% ethanol, the slide rack was immersed in a container filled with running tap water for 15 min and then moved into a container filled with distilled water for about 1 min and then moved into another container filled with distilled water for another 1 min and repeated the previous step one more time.

Next the slide rack was immersed in a container filled with Hematoxylin solution for 3 min and later the slides were washed in running tap water placed within a container for 5 min followed by washing with distilled water three time as previously described. Then the slide rack was immersed in 70% ethanol for 1 to 2 s, taken out immediately after and this was repeated three more times. Followed by washing with 70%

ethanol the slide rack was washed with running tap water and distilled water (three times) as previously described. After washing with water, the slides were immersed in 1% Eosin for 4 min and washed in distilled water once.

Finally, the slides were immersed in the previous series of xylene and ethanol solutions 1 min in each solution, in the divergent order starting from 70% ethanol. After the slide rack was taken out from the xylene I solution, slides were taken out one at a time, followed by blotting the bottom of the slide to remove excess xylene. One drop of MGK-S was put on the tissue cross section and a cover slide was placed on it parallelly, to avoid entrapping of air bubbles in between the slide and the cover slide and they were allowed to dry.

Obtaining photographs and calculating the area of adipocytes

The slides were mounted on the stage of the microscope (BA210E, Shimadzu), the magnification was set to $\times 10$. On the digital screen the tissue cross section was observed and a photo was taken in an area which seemed to contain approximately 100 adipocytes and three photos were taken per each sample. Using the Fuji Image J software (ImageJ bundled with 64-bit Java 1.8.0_112), the adipocyte areas were obtained with reference to a reference scale bar. The specifications for the Fuji Image J software were as follows; distance pixels, 180.0; known distance, 100.0, pixel aspect ratio, 1.0; unit of length, μm ; scale, 1.80 pixels/ μm . Adipocyte area was calculated as the average area of adipocytes obtained from three photographs per each sample.

4.2.10. Serum biochemical analysis

Serum biochemical profile was analyzed using Toshiba TBA-120FR autoanalyzer (Toshiba Medical Systems Corp., Tochigi, Japan) according to manufacturer's instructions.

4.2.11. Statistical analysis

All data except the microbial community data were analyzed for their significance by analysis of variance (ANOVA) using SPSS statistical software version 17.0 (SPSS Inc., Chicago, IL, USA). When significant differences among the test groups were revealed, mean scores were compared by Tukey's test. Pearson's correlation analysis was conducted using SPSS. Statistical significance of alpha diversity indices was determined by ANOVA paired with Tukey's post hoc test (SPSS). Relative abundance and the statistical significance of phyla, genera and species among the four diet groups were compared using Kruskal-Wallis H test in Calypso (version 8.72). A *p* value less than 0.05 was considered as statistically significant.

4.3. Results and Discussion

4.3.1. Zoometric parameters, feed intake and organ weights

Zoometric and organ weight data are presented in Table 4.5. At the end of the experimental period, final body weight was significantly ($p < 0.05$) lower in the HAS group compared to CON group, while both sorghum groups gained comparatively lower final body weight compared to CON. Both total body weight gain and body weight gain per day also followed the same trend as final body weight. Total feed intake and daily feed intake were significantly lower in HAS, S-Wh and S-Rf compared to the CON group. HAS group reported the lowest perirenal and epididymal adipose tissue weights (per 100 g body weight) and total visceral adipose tissue weight (per 100 g body weight) compared to CON and the two sorghum groups. The two sorghum fed groups had significantly lower epididymal, perirenal and total visceral adipose tissue weights (per 100 g body weight) compared to CON group. Adipocyte size was also comparatively lower in the two sorghum groups compared to CON group (Fig. 4.1). Cecal parameters (cecal weight, cecal content weight and cecal tissue weight) were significantly higher in the HAS group while the other three groups reported significantly lower and similar values among each other (Table 4.5).

Excess fat accumulation in adipose tissue, skeletal muscle and liver are considered as phenotypes of obesity and can be implicated by the increased body weight, where the two sorghum groups might suggest a low predisposition for obesity development, implicated by lower body weight and visceral fat accumulation (Yamashita *et al.*, 2009). Lower calorie intake due to lower feed intake might have been a reason behind the comparatively lower body weight gain in the sorghum groups compared to CON (Lu *et al.*, 2016), which was further strengthened by the positive correlations between body weight parameters and feed intake parameters (final body weight, body weight gain and body weight gain/day; $r=0.650$, 0.530 , respectively; $p < 0.01$). Further, lower calorie intake could also have been a reason behind the lower visceral fat accumulation in rats, as suggested by the positive correlation between total feed intake and the

visceral adipose tissue mass (perirenal, epididymal, total visceral adipose tissue weights/100g body weight; $r=0.411, 0.533, 0.488$, respectively; $p < 0.05$). As suggested by the comparatively lower adipocyte size of the two sorghum groups, the adipose tissue in the two sorghum groups was suggested to be properly functioning compared to CON fed animals (Bjørndal *et al.*, 2011). Lower visceral adipose tissue mass suggested the presence of properly functioning adipose tissue depots in the HAS, S-Wh and S-Rf compared to CON (Bjørndal *et al.*, 2011). Higher cecal parameters indicated the prominent fermentation that took place in HAS fed animals (Montagne *et al.*, 2003).

4.3.2. Microbial community DNA data

Metagenomics analysis of microbial DNA revealed significantly ($p < 0.05$) higher alpha diversity (Shannon's diversity index and observed species index) in the two sorghum samples compared to the positive control HAS (Fig. 4.2.a, b), which suggested the presence of a more diverse microbial community and an evenly distributed abundance of the observed species (evenness). Thus, a higher alpha diversity in the two sorghum groups might suggest the positive impact of the cooked sorghum diets on maintaining a diverse microbiota, possibly due to the availability of suitable substrates to feed a wide variety of microbiota. Principle component analysis (PCoA) plot (beta diversity) exhibited evidence for distinct microbial compositions among the diet groups by clear cluster formation (Fig. 4.2.c). The two cooked sorghum groups clustered together, while CON and HAS groups clustered separately from sorghum groups and each other. PCoA plot suggested that the different diets had significant effects in shaping the microbial composition, yet whole or refined nature of sorghum seemed not have had any significant influence on determining the microbial composition in the sorghum fed groups.

The above fact was further proved by the clustered bar chart obtained at genus level (Fig. 4.3), where the groups were similarly clustered as seen in Fig. 4.2.c. As presented in Fig. 4.3, the two sorghum groups could be characterized by a higher abundance of genus *Ruminococcus*, while HAS group was

characterized by genus *Bifidobacterium*. The characteristic microbial genera in sorghum and HAS might indicate the potential major substrates available for microbial utilization in each group, which might have been the main reason for influencing the conventional dietary fiber fermenters and RS fermenters in sorghum groups and HAS group, respectively. This fact could be further strengthened by the higher availability of dietary fiber in the sorghum groups and the higher RS content in the HAS group (Table 4.2).

At species level, *R. flavefaciens*, *R. gnavus*, unclassified *Ruminococcus* abundances were significantly higher in the two sorghum groups (Fig.4.4). In contrast, in raw sorghum fed rats, the key microbial genera observed were potential protein fermenters (Chapter 3; section 3.3.2). Further, in the HAS group, *B. pseudolongum*, unclassified *Blautia* and in the CON group, *Akkermansia muciniphila*, *Lactococcus gravieae*, *Blautia producta*, Unclassified *Clostridiales* and Unclassified *Lactococcus* were found in higher abundance (Fig. 4.4). Importance of these microbial taxa are discussed in details where applicable in relation to biochemical data later.

4.3.3. Cecal short chain fatty acid content and pH

Acetate content in the cecum was significantly ($p < 0.05$) higher in the HAS group compared to CON and S-Wh groups, while S-Rf had comparatively higher acetate content than CON and S-Wh (Fig. 4.5). Albeit, the propionate content (per cecum) was not significant among the four groups, propionate content was comparatively higher in S-Rf compared to the CON and S-Wh fed groups. Butyrate content was highest in the HAS group, where S-Rf had comparatively higher butyrate content compared to CON and S-Wh, which was statistically similar to HAS. Total short chain fatty acid (SCFA) content was significantly higher in the HAS group similar to the individual SCFA reported for the group, while S-Rf group exhibited comparatively higher SCFA content compared to CON and S-Wh groups.

Cecal pH was significantly lower in the HAS group, while both CON and S-Wh had significantly higher values, yet S-Rf exhibited comparatively lower cecal pH compared to CON and S-Wh groups (Fig.4.6). Negative correlation coefficients observed for cecal weight, cecal content weight and cecal tissue weight with cecal pH ($r=-0.716$, -0.676 , -0.708 , respectively; $p < 0.01$) suggested a significant link among SCFA production, pH and cecal parameters, where SCFA production might have caused the reduction of cecal pH and cecal hypertrophy (Montagne *et al.*, 2003; Vazquez-Gutierrez *et al.*, 2016).

Moreover, cecal fermentation also might have had a significant effect on the reduced visceral fat accumulation as suggested by the negative correlation between acetate content and visceral adipose tissue mass (perirenal, epididymal, total visceral adipose tissue mass/100 g body weight; $r=-0.553^{**}$, -0.505^* , -0.547^{**} , respectively; $*p < 0.05$, $**p < 0.01$, respectively). Short chain fatty acids are known to act as signaling molecules in diverse carbohydrate and lipid metabolic pathways, where acetate, propionate and butyrate are known to be involved in lipid biosynthesis (Ríos-Covián *et al.*, 2016; Li *et al.*, 2017). Profound anti-obesity and anti-diabetic effects of acetate had been previously reported (Yamashita *et al.*, 2009).

Acetate is found to impart an effect on the body weight control and fat accumulation via regulation of energy intake and energy expenditure (González Hernández *et al.*, 2019). One of the mechanisms of appetite regulation mediated by acetate is known to be coordinated through the central nervous system, where acetate crosses the blood-brain barrier and increase hypothalamic acetyl-CoA carboxylase activity, which in turn increases malonyl-CoA, thereby causes a reduction in feed intake through the expression of orexigenic and anorexigenic neuropeptides in the hypothalamus (González Hernández *et al.*, 2019).

Another mechanism where acetate is involved in reduced feed intake is via activation of gut derived satiety hormones, such as GLP-1 and PYY secreted from enteroendocrine cells, where the said hormones are known to be secreted by the activation of G-protein coupled receptor (GPR) 41 and 43, respectively, by

acetate (González Hernández et al., 2019). Furthermore, acetate is known to induce the secretion of leptin from adipose tissue, which is well-known for its activity in satiety improvement (Li *et al.*, 2017; González Hernández *et al.*, 2019). Acetate is known to affect the adipose tissue morphology by influencing the proliferation and differentiation of adipocytes (inhibit hypertrophy), where it is involved in re-structuring the adipose tissue morphology and improving adipose tissue function by its anti-lipolytic effects and further improving energy metabolism and overall metabolic health (Yamashita *et al.*, 2009; González Hernández *et al.*, 2019). Further, acetate mediated activation of GPR 43 in adipocytes had been found to inhibit lipolytic response (González Hernández *et al.*, 2019).

On the other hand, propionate content was significantly negatively correlated with the component and total visceral fat mass (perirenal, epididymal, total visceral adipose tissue mass/100 g body weight; $r = -0.458, -0.430, -0.460$, respectively; $p < 0.05$). Propionate produced during fermentation of fibers are known to lower cholesterol by suppressing cholesterol synthesis in the hepatocytes by its inhibiting activity on lipolytic enzymes (Hara, 2002; Huazano-García *et al.*, 2017).

4.3.4. Liver lipid profile and fecal moisture and dry matter contents, lipid and bile acid profiles

Liver weight, liver total lipids and triglycerides contents were similar among the four groups, yet the liver cholesterol content was significantly ($p < 0.05$) lower in the HAS group, while CON and S-Wh groups had comparatively lower content compared to S-Rf group (Table 4.6). Liver is considered as the first organ to receive microbial-derived acetate and considered as a key player of acetate metabolism, where acetate is found to be a carbon donor of hepatic cholesterol biosynthesis and several other biosynthetic pathways in liver (González Hernández *et al.*, 2019).

Higher acetate content in liver is found to decrease hepatic lipid accumulation, improve hepatic function and improve mitochondrial efficiency (González Hernández *et al.*, 2019). On the other hand propionate

in the liver is known to inhibit the activity of lipolytic enzymes and inhibit hepatic lipogenesis and improve gluconeogenesis (Chung *et al.*, 2009; Li *et al.*, 2017; González Hernández *et al.*, 2019). Yet, there have been many inconsistencies regarding acetic and propionic acid mediated hepatic lipogenesis, similarly this study also found a positive correlation between liver cholesterol concentration and propionate content ($r=0.479$; $p < 0.05$) (González Hernández *et al.*, 2019).

Fecal dry matter content was significantly higher in the HAS group, while it was significantly lower in the two sorghum groups, but there was no significant difference in the fecal moisture content (Table 4.6). On the other hand fecal lipid profile was similar among the four diet groups, despite the higher fecal dry weight in the HAS group. But there was clearly a higher total lipid content excreted in the HAS group followed by S-Wh group compared to CON and S-Rf groups. Further, comparatively higher cholesterol contents were also found excreted via feces in S-Rf group followed by HAS group compared to CON and S-Wh groups.

Fecal total bile excretion was significantly higher in S-Wh group, while it was comparatively lower in the HAS and S-Rf groups compared to S-Wh (Table 4.7). There were no significant differences in the individual (Cholic acid and chenodeoxycholic acid) and total primary bile acid contents, yet they were comparatively higher in the HAS and S-Rf groups compared to CON. On the other hand, individual and total secondary bile acid contents were significantly different among the groups (Table 4.7). Deoxycholic acid content was significantly higher in the S-Wh group, while it was comparatively higher in the S-Rf group compared to CON and HAS. Lithocholic acid content was significantly higher in the S-Rf group, while it was comparatively higher in the S-Wh group compared to CON and HAS. Total secondary bile acid content was significantly higher in the two sorghum fed groups compared to CON and HAS.

Fecal bile excretion is known to play a role in lowering blood cholesterol levels, and dietary soluble fibers are known to improve bile excretion by binding with bile acids and reducing their re-absorption at ileum

(Hara, 2002; Ghaffarzadegan *et al.*, 2018). Similar primary bile acid contents among the test groups could have been due to the similar dietary fat content, because secreted amount of primary bile acid depends on the dietary fat content and also there is a possibility of more primary bile acids being converted into secondary bile acids in the two sorghum fed groups as reflected by the significantly higher secondary bile acid content (Ghaffarzadegan *et al.*, 2018).

Negative correlation between total primary bile acid excretion per day and epididymal adipose tissue weight (per 100g body weight) suggested a relationship between higher lipid excretion (via hepatic cholesterol conversion into bile acids) and lower accumulation ($r=-0.417$; $p < 0.05$). Further, Cholic acid was significantly negatively associated with the visceral fat accumulation (perirenal, epididymal, total visceral adipose tissue weight/100g body weight; $r=-0.435$, -0.430 , -0.428 , respectively; $p < 0.05$). Moreover, bile excretion via feces could also have been a reason for lower body weight gain ($r=-0.412$; $p < 0.05$), which might have been due to lower visceral fat accumulation as suggested by the negative correlation between adipocyte size and total primary bile excretion ($r=-0.447$; $p < 0.05$). Further, higher bile excretion observed in S-Wh group might have been another reason for the higher hepatic cholesterol content in S-Wh group, as hepatic cholesterol synthesis is regulated via a feed-forward mechanism according to the amount of bile acids re-absorbed at ileum (Qi *et al.*, 2015).

Higher secondary bile acid content observed in the two sorghum fed groups might suggest that a higher proportion of primary bile acids bound to fiber at the ileum might have been liberated upon fiber fermentation in the colon and dehydroxylated and transformed into secondary bile acids by the activity of microbial 7 α -dehydroxylase (Ghaffarzadegan *et al.*, 2018). Further, significant positive correlation between total bile excretion and total SCFA content ($r=0.505$; $p < 0.05$), might also suggest the above fact. Moreover, a higher colonic pH is known to influence the activity of 7 α -dehydroxylase, thus influencing the conversion of primary bile acids to secondary bile acids, which might have been a possibility in S-Wh

group due to its significantly higher pH (Ghaffarzadegan *et al.*, 2018). The secondary bile acid formation is known to be significantly dependent upon the gut microbial composition, colonic pH and consequently the type of dietary fiber source (Ghaffarzadegan *et al.*, 2018). Positive correlation between total secondary bile excretion and Shannon's diversity index and observed species index also might suggest a significant effect of the microbial function on the secondary bile acid content excreted via feces ($r=0.620$, 0.664 , respectively; $p < 0.01$). Members of *Clostridium* cluster XVIa have been identified as potential secondary bile acid producers, for examples, *Blautia* and *Ruminococcus* spp., thus the observations for bile acids in sorghum groups can be attributed to the higher abundance of *Ruminococcus* spp. (Ridlon *et al.*, 2014). Further, these bacteria are suggested to impose anti-microbial effects reducing the abundance of gram negative bacteria that produce potent lipopolysaccharides and pathogenic classes such as *Enterobacteriaceae* (Ridlon *et al.*, 2014).

Recently, several findings have reported that the secondary bile acids to act as ligands for TGR5 (another GPR), which was found to stimulate the secretion of Incretin hormone and GLP-1, which were subsequently found to regulate host energy metabolism (Li *et al.*, 2017; Hegyi *et al.*, 2018). Albeit, there is a suggestion on an association between fecal secondary bile acid content and onset of colon cancer, there has been a discussion that dietary fiber from plant materials might reduce the risk of colorectal cancers by extracting more secondary bile acids such as lithocholic acid into feces (Ajouz *et al.*, 2014; Ghaffarzadegan *et al.*, 2018).

4.3.5. Ammonia-nitrogen content and branched-chain fatty acid content in the cecal content

Cecal ammonia content was similar among the four groups as shown in Fig. 4.7. Yet the ammonia-nitrogen content was not statistically different, both sorghum groups exhibited comparatively higher contents compared to HAS group. This could be due to the higher protein content that passes down to the colon escaping ileal digestion, as sorghum prolamins are well-known for their less digestibility. As previously

discussed (Chapter 3), initiation of amino acid fermentation depends on many factors such as deficiency in fermentable carbohydrates, higher protein/peptide/amino acid content reaching the large intestine, lower carbohydrate:protein ratio in the colon, etc. Similar ammonia-nitrogen contents among the groups might suggest an improvement of the fermentative substrates in sorghum upon cooking, with respect to fermentation.

Cecal BCFA are one of the major metabolites of colonic amino acid fermentation by microbiota and their contents were not significantly different among the groups (Table 4.8). Thus, these results also were in complement with the ammonia-nitrogen content. Further, in the two sorghum groups, potential amino acid fermenting microbial species were not found in higher abundance, despite certain such species were observed in CON group as characteristic microbial genera; *Lactococcus*, *Streptococcus*, etc. Thus, upon cooking of sorghum, amino acid availability for fermentation might have been reduced. Moreover, as reflected by the improved SCFA production (Fig. 4.5) and higher abundance of dietary fiber fermenting *Ruminococcus* spp., (Fig. 4.3), amino acid fermentation might have been inhibited by the higher availability of fermentable carbohydrates in cooked sorghum.

4.3.6. Immunoglobulin A (IgA) content in cecal content

Immunoglobulin A content was significantly ($p < 0.05$) higher in CON and the two sorghum groups compared to HAS group (Fig. 4.8). A higher IgA content reflects a well-functioning secretory immune system specialized in maintaining colonic mucosal homeostasis. Consumption of prebiotics are well-known to improve the IgA content via several mechanisms. Among the immunomodulatory mechanisms mediated by IgA, maintenance of non-invasive commensals and neutralization of invasive pathogens are among the integral hurdles.

Anti-inflammatory effects related to prebiotics are likely derived by the action of SCFA, where they are attributed to mediate beneficial effects on gut health, for example decrease in SCFA and healthy microbial members have been observed in inflammatory bowel disease patients (Vieira *et al.*, 2013). The main SCFA associated with anti-inflammatory effects is butyrate, where it is known to reduce DNA damage, improve regulatory T cells, activate anti-inflammatory receptors and downregulate pro-inflammatory pathways (Vieira *et al.*, 2013). Further, via activation of GPR 43, mainly by acetate followed by propionate, is known to maintain both gut and systemic anti-inflammatory effects (Vieira *et al.*, 2013).

In this study, higher *A. muciniphila* abundance in the CON group could have been the reason behind the higher IgA content reported in this group, as *Akkermansia* is well-known to influence secretory immunity (Belzer and Vos, 2012). On the other hand, in the two sorghum groups, apart from *A. muciniphila*, higher abundance of *R. gnavus* also might have played a role in higher IgA production. *R. gnavus* is not only known for its salicylic acid degradation ability (mucin degradation ability), it has been identified as an immunomodulatory bacteria at the mucosal surface improving the immunity of the hosts (Crost *et al.*, 2016).

Apart from facilitating SCFA production, improving the abundance of immunomodulatory bacteria in gut and enhancing the synthesis and secretion of IgA, prebiotics are known to mediate other protective mechanisms, such as inhibiting adherence of pathogenic bacteria to gut epithelium by improved and regular bowel movements.

4.3.7. Mucin content in cecal content

Cecal mucin content was significantly ($p < 0.05$) higher in the S-Wh compared to HAS, S-Rf and CON groups (Fig. 4.9). Interestingly, secondary bile acids such as lithocholic acid, are found to influence secretion of mucin, which was proposed to minimize bacterial translocation into the underlying epithelium

(Barcelo *et al.*, 2001; Hegyi *et al.*, 2018). Further, primary bile acids being failed to induce mucus secretion, mucus secretion improvement by secondary bile acids is also considered as a beneficial effect of gut microbial function (Barcelo *et al.*, 2001). Moreover, the positive correlation between mucin and bile acid excretion ($r=0.510$; $p < 0.05$) in this study might partly explain the higher mucin content observed in the S-Wh group.

R. gnavus had been identified as a mucin utilizer similar to *A. muciniphila* and both bacteria are found to improve mucin synthesis as a consequence of their utilization at the intestinal mucosa (Crosthair *et al.*, 2013; Tailford *et al.*, 2015). Thus, the higher mucin content in the S-Wh group could be attributed to the higher abundance of both bacteria. Further, insoluble dietary fiber is also known to improve mucin secretion due to their mechanical scraping effect on the outer mucus layer, when they pass through the intestine (Montagne *et al.*, 2003). On the other hand, less abundance of previously mentioned microbial members in the S-Rf group might reflect the lower mucin content. Similarly, lower abundance of immunomodulatory microbial abundance such as *A. muciniphila* could have been the reason for significantly lower mucin content in HAS, despite the higher abundance of *B. pseudolongum* and lower cecal pH, which are also known to improve mucin production (Vazquez-Gutierrez *et al.*, 2016).

4.3.8. Serum biochemical data

Serum lipid profiles of the four groups were well within the reference values of F344 rats at fasted state at the end of the experiment as shown in Table 4.9. Serum triglycerides, free fatty acids, total cholesterol, high density lipoprotein-cholesterol and non-HDL-cholesterol (non-HDL-C=Total cholesterol-HDL-cholesterol) were comparatively lower in the two sorghum fed groups compared to the CON fed rats between weeks 0 to 3 (data not shown). Yet, serum total cholesterol, phospholipids, non-HDL-cholesterol were significantly ($p < 0.05$) higher in CON, S-Wh and S-Rf groups compared to HAS group at the end of the experimental period. Serum triglyceride content, free fatty acid content were comparatively lower

in S-Rf compared to CON and S-Wh groups at the end, while HDL-cholesterol content was similar among the four groups.

In previous studies increased levels of plasma triglyceride, free fatty acid, HDL-cholesterol and total cholesterol had been observed after a 16 h fasting period compared to a 4 h of fasting period, regardless of the rat strain or diet, where the higher plasma triglyceride level had been attributed to the decreased very low density lipoprotein clearance during fasting (LeBoeuf *et al.*, 1994). Moreover, it has been reported that during fasting conditions, higher rates of adipose tissue triglyceride hydrolysis is observed, which might improve circulatory free fatty acids (Pantaleão *et al.*, 2017). Further, reported anti-lipolytic functions of propionate had been inconsistent over the time similar to this study, where a positive relationship was observed between cecal propionate and serum triglyceride and total cholesterol concentrations (González Hernández *et al.*, 2019). Apart from the serum lipid profile, most other serum biochemical parameters were similar among the diet groups. Especially, similar liver enzyme levels might suggest proper liver function despite the higher liver cholesterol content in the sorghum groups.

4.4. Implications and Conclusions to Chapter 4

The present study exhibited beneficial potentials of cooked sorghum in energy metabolism, where cooked sorghum influenced lower feed intake, lower body weight gain and lower visceral fat accumulation. Further, improved SCFA profiles compared to raw sorghum, thus indicated better colonic fermentation ability of cooked sorghum in comparison to *in vitro* study (Chapter 2) and *in vivo* study (Chapter 3), which was further significantly negatively correlated with feed intake, body weight gain and visceral fat accumulation. In contrast to the Chapter 3, where raw sorghum was fed to rats (same breed, similar age, same sex), in this study, individual and total SCFA contents were quantitatively increased, especially in S-Rf fed rat cecal content.

Higher abundance of members of genus *Ruminococcus* in the sorghum groups, further suggested the availability of preferable substrates for microbial fermentation, such as dietary fiber and RS in cooked sorghum, in contrast to the higher abundance of amino acid fermenters in the raw sorghum fed rats as reported in Chapter 3. Higher abundance of *R. gnavus* in sorghum groups partly explained the higher mucin and IgA contents observed in the sorghum groups (especially in S-Wh). Interestingly, the higher secondary bile excretion via feces was also found to influence lipid metabolism and further was correlated with higher mucin production. Thus, cooking of sorghum improved colonic fermentation potential and beneficial physiological characteristics compared to raw sorghum in our previous study, suggesting that simply cooking of the grain might have improved indigestible substrate flow into colon, thus improving colonic microbial fermentation and production of beneficial effector molecules, through which beneficial biological (higher mucin and IgA) and physiological (lower body weight, feed intake, visceral fat accumulation) processes might have been mediated.

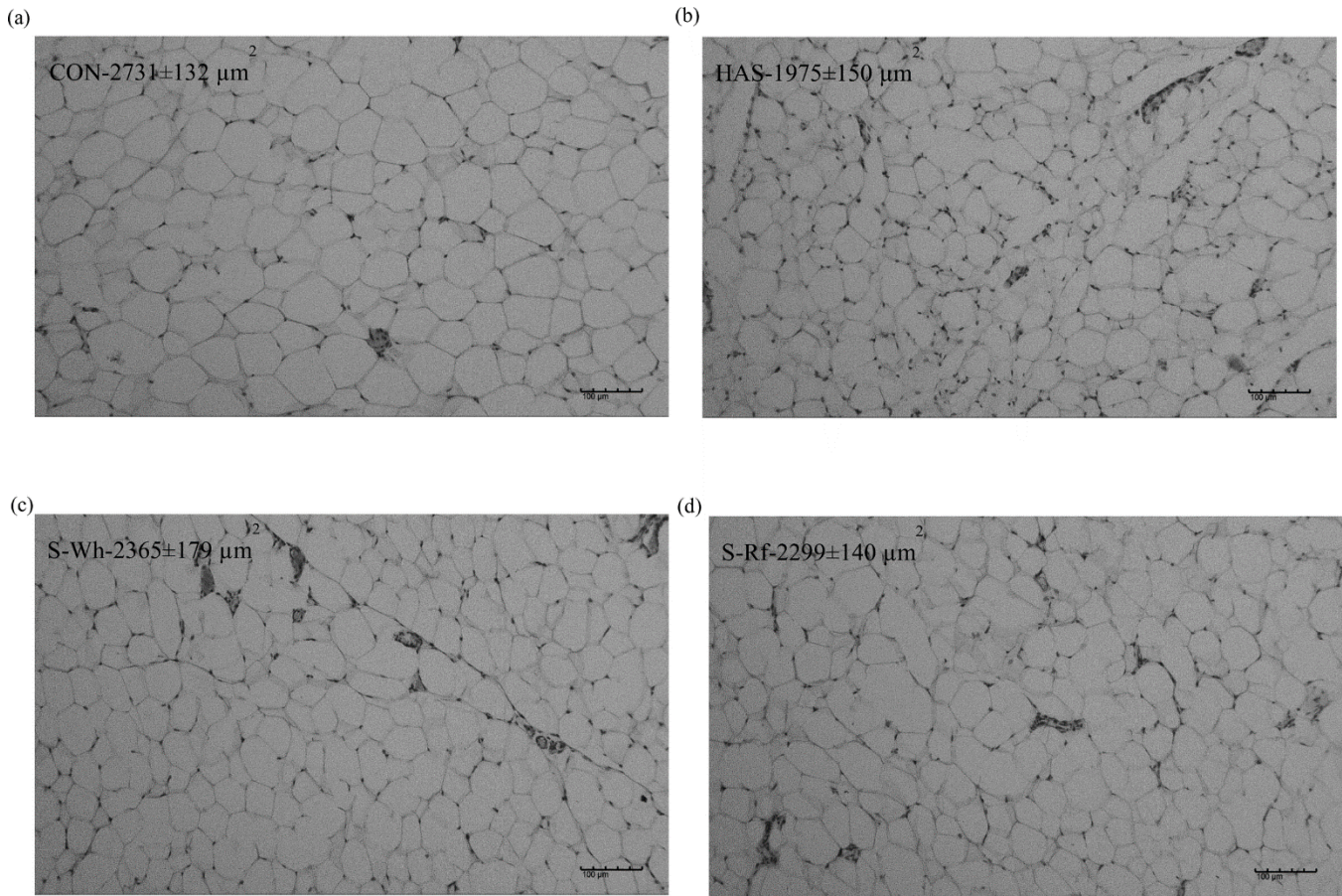


Fig. 4.1. Microscopic view of the mesenteric adipocyte area of rats. Data presented are mean \pm SE (n=6) and statistical significance was determined by ANOVA paired with Tukey's test ($p < 0.05$). (CON, α -corn starch; HAS, high amylose starch; S-Wh, whole white cooked sorghum; S-Rf, refined white cooked sorghum).

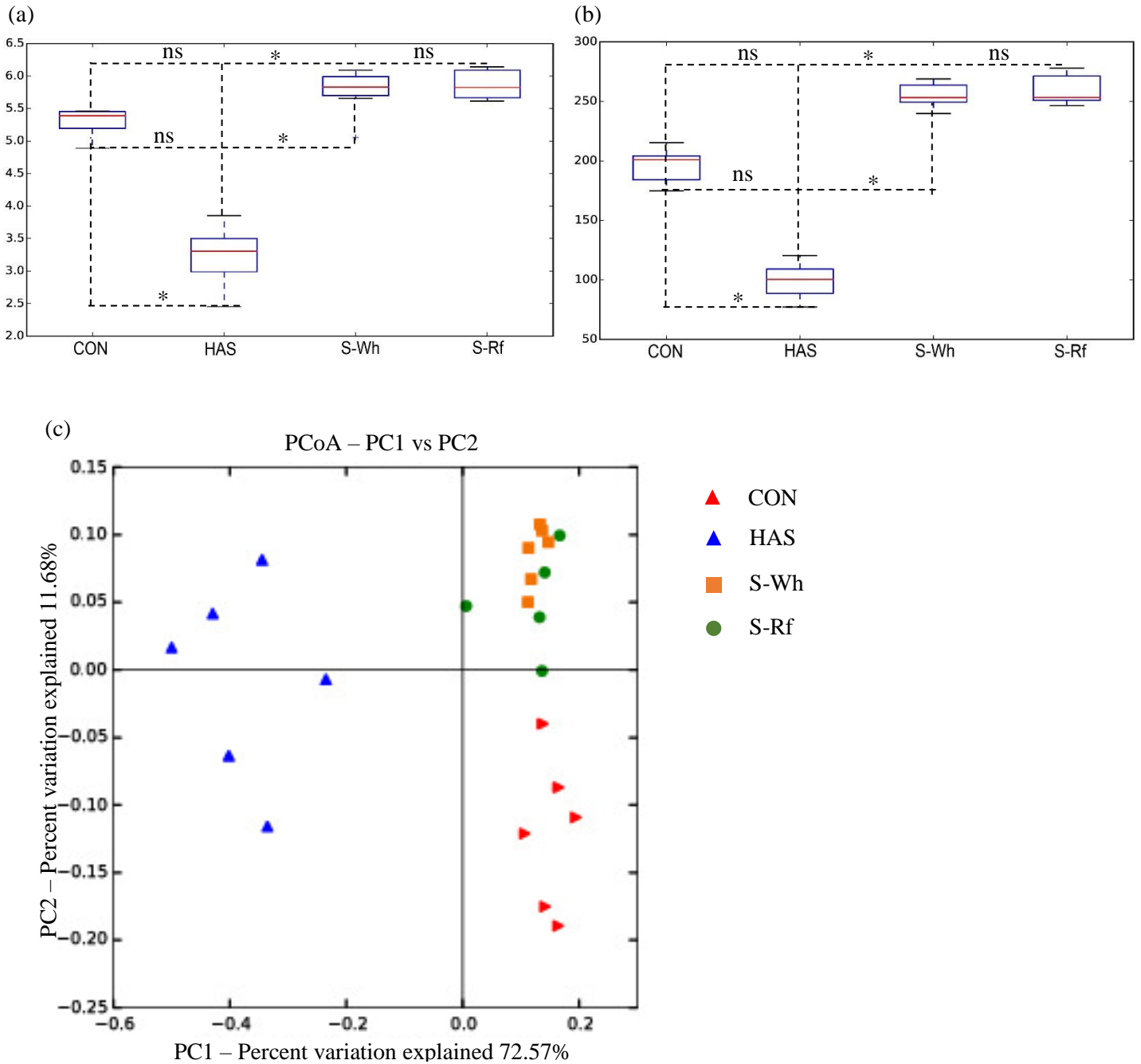


Fig. 4.2. Box and whisker plots of (a) Shannon's diversity index and (b) Observed species index (c) Weighted UniFrac PCoA plot for the β -diversity.

For (a) and (b), data presented are mean \pm SE (n=6) and statistical significance was determined by ANOVA (post hoc Tukey's test); ($p < 0.05$). β -diversity was determined by the weighted UniFrac distance metric in QIIME. (CON, α -corn starch; HAS, high amylose starch; S-Wh, whole white cooked sorghum; S-Rf, refined white cooked sorghum).

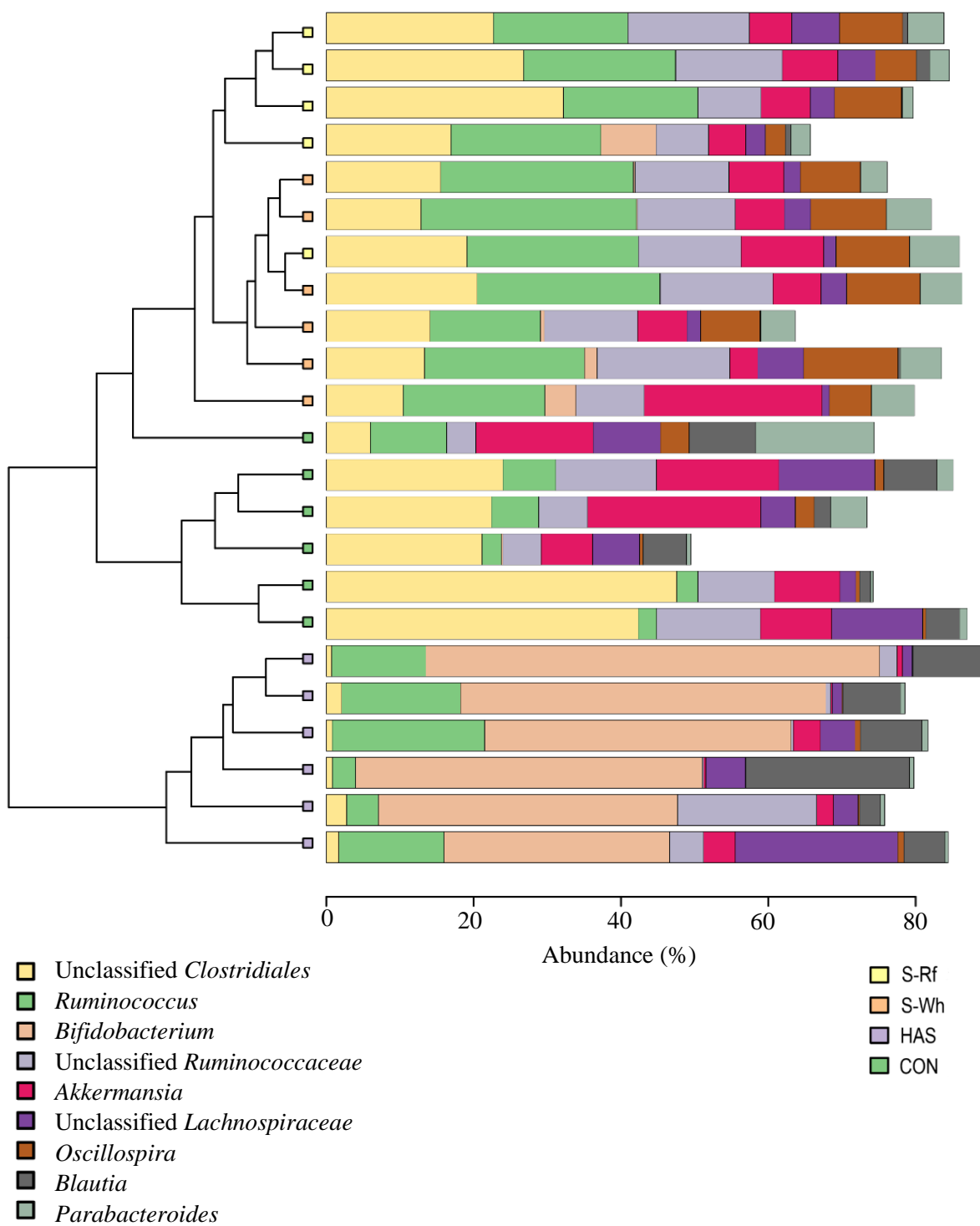


Fig. 4.3. Clustered bar chart at genus level for cecal microbiota.

(CON, α -corn starch; HAS, high amylose starch; S-Wh, whole white cooked sorghum; S-Rf, refined white cooked sorghum).

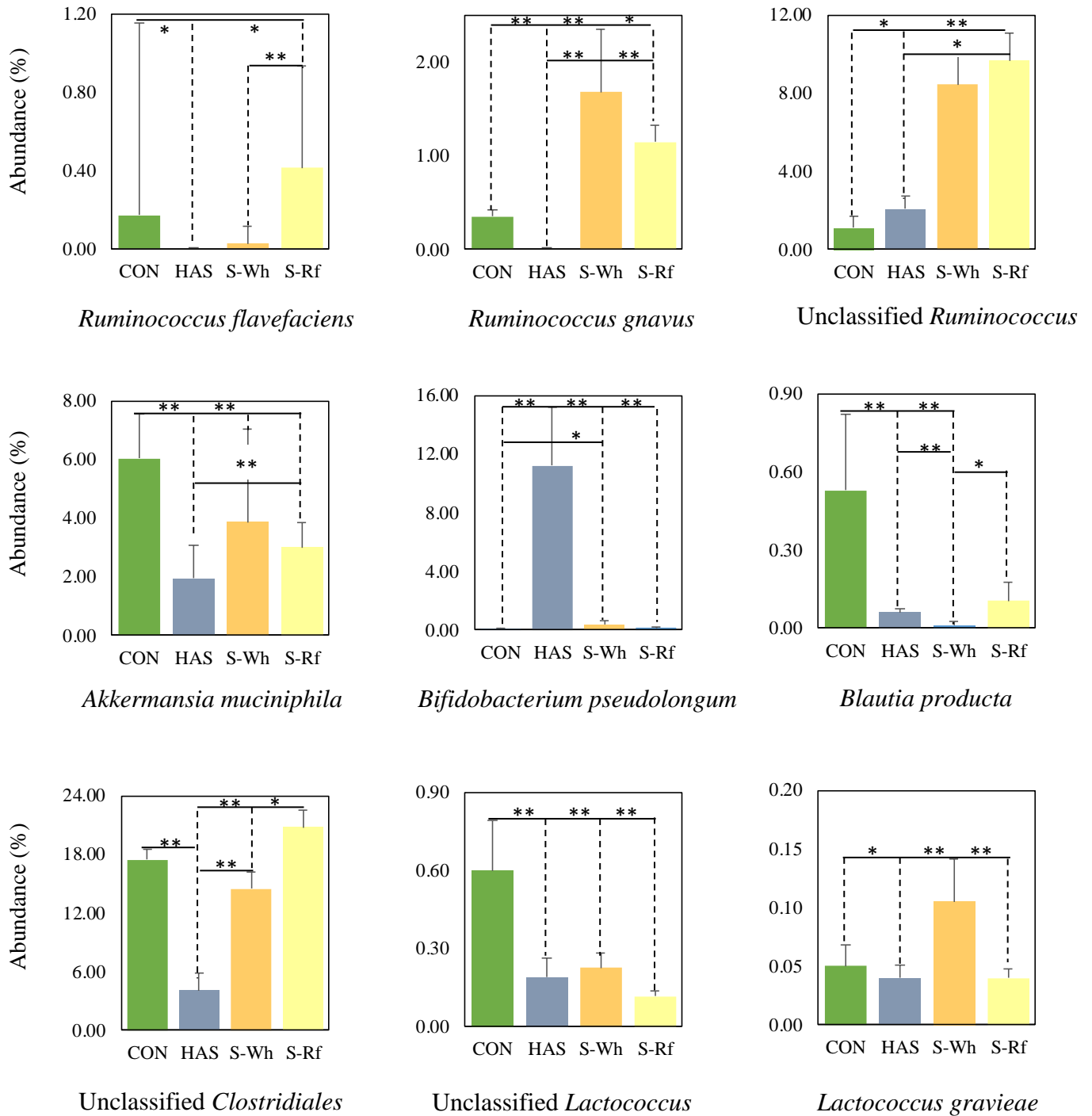


Fig. 4.4. Rank test bar charts for the relative abundance of selected microbial species in the rat cecal digesta.

Data presented are median \pm SE (n=6). Statistical significance was determined by Kruskal-Wallis H test in Calypso (version 8.72) (* $p < 0.05$; ** $p < 0.01$). (CON, α -corn starch; HAS, high amylose starch; S-Wh, whole white cooked sorghum; S-Rf, refined white cooked sorghum).

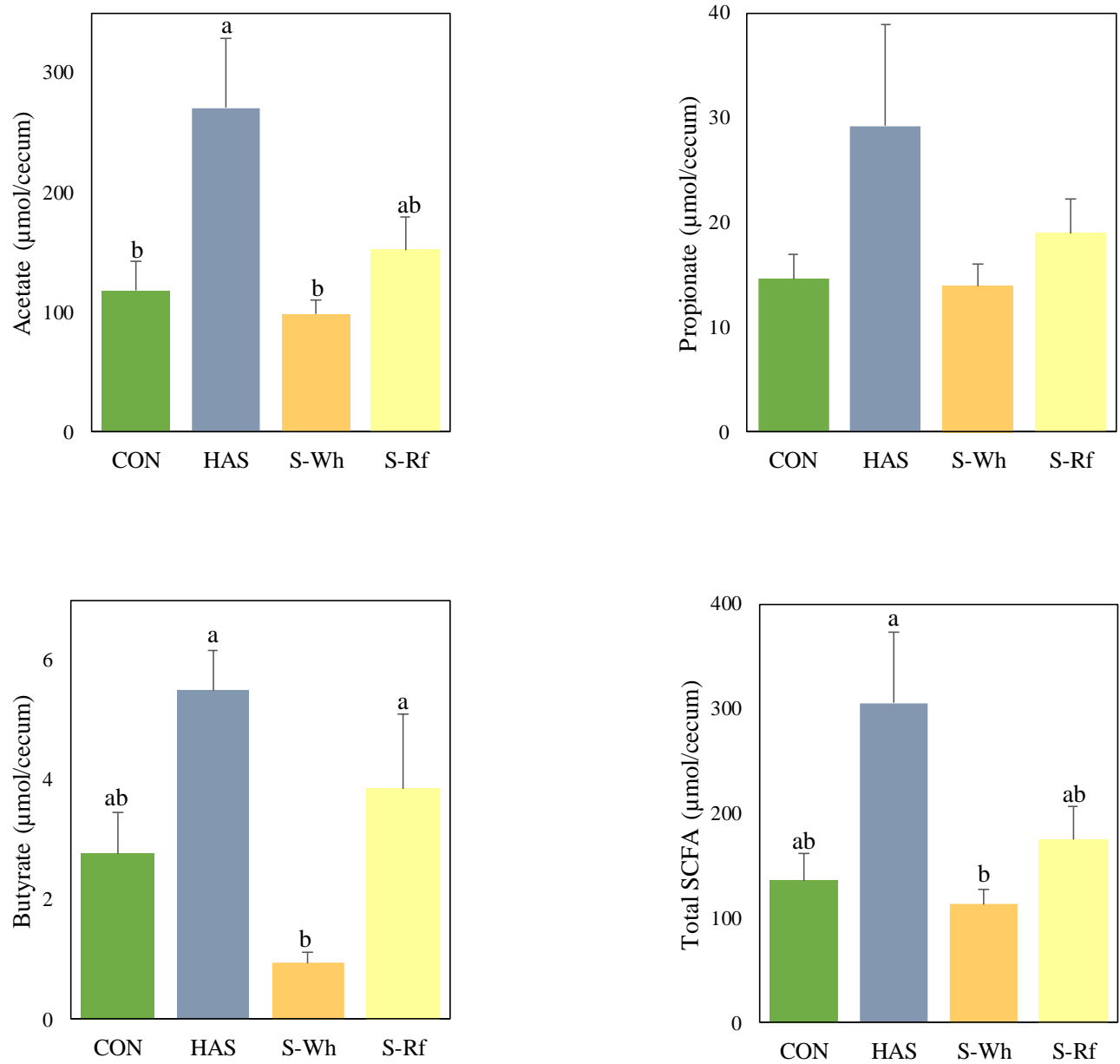


Fig. 4.5. Short chain fatty acid concentrations in the cecal content of rats.

Data presented are mean \pm SE (n=6) and different letters represent significant differences among the diet groups at $p < 0.05$. (CON, α -corn starch; HAS, high amylose starch; S-Wh, whole white cooked sorghum; S-Rf, refined white cooked sorghum).

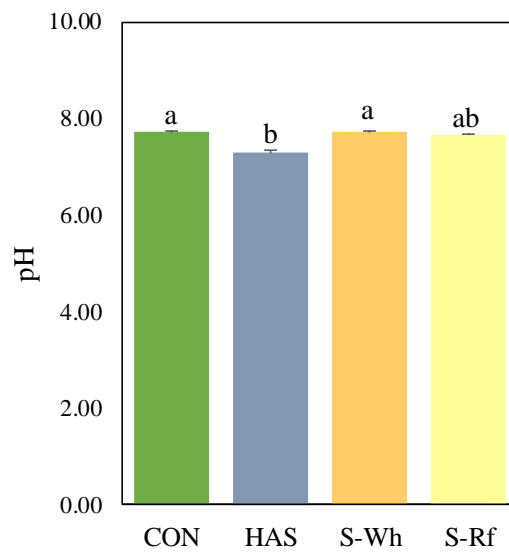


Fig. 4.6. Cecal pH of rats.

Data presented are mean \pm SE (n=6) and different letters represent significant differences among the diet groups at $p < 0.05$. (CON, α -corn starch; HAS, high amylose starch; S-Wh, whole white cooked sorghum; S-Rf, refined white cooked sorghum).

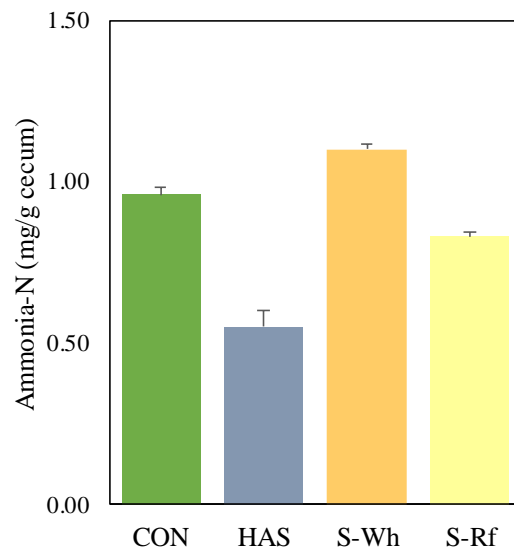


Fig. 4.7. Cecal ammonia-nitrogen content of rats.

Data presented are mean \pm SE (n=6) and different letters represent significant differences among the diet groups at $p < 0.05$. (CON, α -corn starch; HAS, high amylose starch; S-Wh, whole white cooked sorghum; S-Rf, refined white cooked sorghum).

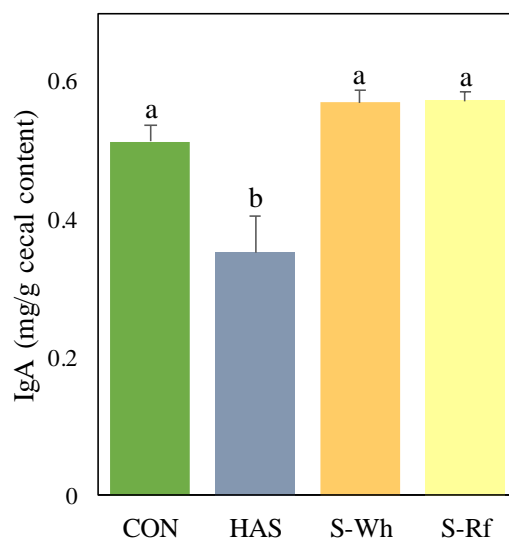


Fig. 4.8. Cecal immunoglobulin A (IgA) content of rats.

Data presented are mean \pm SE (n=6) and different letters represent significant differences among the diet groups at $p < 0.05$. (CON, α -corn starch; HAS, high amylose starch; S-Wh, whole white cooked sorghum; S-Rf, refined white cooked sorghum).

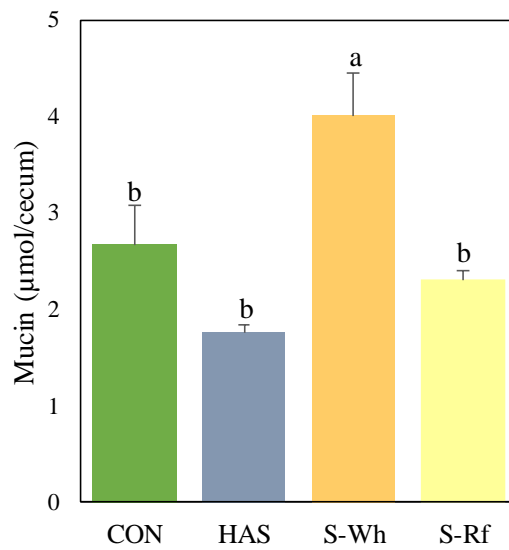


Fig. 4.9. Cecal mucin content of rats.

Data presented are mean \pm SE (n=6) and different letters represent significant differences among the diet groups at $p < 0.05$. (CON, α -corn starch; HAS, high amylose starch; S-Wh, whole white cooked sorghum; S-Rf, refined white cooked sorghum).

Table 4.1. Different cooking conditions for sorghum grains and resistant starch contents.

Sample	Sample : water ratio	Cooking condition	RS content (%)	
			S-Wh	S-Rf
Raw grains	-	-	2.67	1.40
Grains	1 : 1	120°C; 20 min	3.29	3.44
	1 : 2		3.95	3.55
	30 g/100 g grains	110°C; 4 h	1.80	2.82

(Values presented are mean of three replicates per each sample; S-Wh, whole white sorghum; S-Rf, refined white sorghum)

Table 4.2. Proximate composition analysis of cooked sorghum flour.

Sample	Moisture (% dwb)	Ash (% dwb)	Fat (% dwb)	Protein (% dwb)	Carbohydrate (% dwb)	Total starch (% dwb)	RS (% dwb)	Amylose (% dwb)	Dietary fiber (%)
S-Wh	3.7 ± 0.2	1.6 ± 0.0	2.6 ± 0.2	9.5 ± 0.0	82.6 ± 0.5	72.1 ± 1.9	3.5 ± 0.1	29.1 ± 0.5	12.3
S-Rf	4.7 ± 0.1	0.6 ± 0.3	0.9 ± 0.0	8.4 ± 0.3	85.4 ± 0.7	80.2 ± 2.9	4.3 ± 0.2	27.5 ± 1.7	6.4

(S-Wh, whole white cooked sorghum; S-Rf, refined white cooked sorghum; RS, resistant starch)

Table 4.3. Experimental diet compositions.

Ingredients (g/kg diet)	Dietary group			
	CON	HAS	S-Wh	S-Rf
Casein	200.0	200.0	171.4	174.9
L-Cystine	3	3	3	3
Sucrose	200	200	200	200
Soybean oil	70.0	70.0	62.1	67.3
<i>t</i> -Butylhydroquinone	0.014	0.014	0.014	0.014
Cellulose	50	50	13.1	30.8
Mineral Mix (AIN-93G-MX)	35	35	35	35
Vitamin Mix (AIN-93G-VX)	10	10	10	10
Choline bitartrate	2.5	2.5	2.5	2.5
HAS (HS-7)	0	300	0	0
Refined white sorghum	0	0	0	300
Whole white sorghum	0	0	300	0
α -Cornstarch	429.486	129.486	202.896	176.496
Sum	1000	1000	1000	1000

(CON, α -corn starch; HAS, high amylose starch; S-Wh, whole white sorghum; S-Rf, refined white cooked sorghum)

Table 4.4. Similar body weight groups prepared after acclimatization period.

Groups	G1	G2	G3	G4
	197.0	195.9	195.3	195.0
	191.7	192.7	194.1	194.2
	188.7	188.4	188.2	188.0
	186.2	186.5	185.5	187.9
	182.4	181.7	181.4	181.1
	179.3	179.8	179.9	178.8
Mean	187.6	187.5	187.4	187.5
SD	6.4	6.2	6.4	6.6

Table 4.5. Zoometric parameters, feed intake and organ parameters of rats.

Parameter	CON	HAS	S-Wh	S-Rf
Final body weight (g)	249.6 ± 4.8 a	228.3 ± 4.7 b	241.4 ± 5.1 ab	241.3 ± 3.3 ab
Body weight gain (g)	62.0 ± 3.9 a	40.8 ± 4.4 b	54.0 ± 2.7 ab	53.8 ± 2.8 ab
Body weight gain per day (g)	2.1 ± 0.1 a	1.4 ± 0.1 b	1.8 ± 0.1 ab	1.8 ± 0.1 ab
Feed intake (g)	384.3 ± 6.4 a	357.3 ± 6.4 b	348.6 ± 6.5 b	341.3 ± 6.7 b
Feed intake per day (g)	12.8 ± 0.2 a	11.9 ± 0.2 b	11.6 ± 0.2 b	11.4 ± 0.2 b
Ep-AT (g/100 g BW)	2.57 ± 0.14 a	1.71 ± 0.06 c	2.17 ± 0.10 b	2.12 ± 0.05 b
Pe-AT (g/100 g BW)	2.29 ± 0.07 a	1.46 ± 0.09 c	2.00 ± 0.12 b	1.94 ± 0.10 b
Tv-AT (g/100 g BW)	4.86 ± 0.20 a	3.17 ± 0.13 c	4.17 ± 0.22 b	4.06 ± 0.12 b
Cecal weight (g)	2.32 ± 0.22 b	5.80 ± 1.37 a	1.99 ± 0.08 b	2.14 ± 0.13 b
Cecal tissue weight (g)	0.67 ± 0.02 b	1.27 ± 0.09 a	0.67 ± 0.05 b	0.65 ± 0.02 b
Cecal content (g)	1.65 ± 0.21 b	4.52 ± 1.28 a	1.31 ± 0.10 b	1.48 ± 0.12 b

Abbreviations: CON, α -corn starch; HAS, high amylose starch; S-Wh, whole white cooked sorghum; S-Rf, refined white cooked sorghum; Ep-AT, epididymal adipose tissue; Pe-AT, perirenal adipose tissue; Tv-AT, total visceral adipose tissue.

Values presented are mean ± SE (n=6); values followed by different lowercase letters are significantly ($p < 0.05$) different.

Table 4.6. Liver lipid content and fecal moisture content and lipid content of rats.

Parameter	CON	HAS	S-Wh	S-Rf
Liver weight (g)	5.9 ± 0.1 ns	5.8 ± 0.2 ns	5.8 ± 0.1 ns	5.8 ± 0.1 ns
Liver total lipids (mg/liver)	305.1 ± 32.4 ns	324.3 ± 25.7 ns	430.8 ± 48.8 ns	304.8 ± 39.5 ns
Liver cholesterol (mg/liver)	21.7 ± 1.3 ab	19.3 ± 0.7 b	20.9 ± 0.9 ab	23.9 ± 0.9 a
Liver TG (mg/liver)	56.2 ± 3.9 ns	46.9 ± 3.3 ns	56.2 ± 3.3 ns	55.3 ± 3.4 ns
Fecal DW (g)	0.91 ± 0.03 ab	1.16 ± 0.18 a	0.77 ± 0.02 b	0.76 ± 0.03 b
Fecal MC (%)	54.7 ± 3.5 ns	63.3 ± 4.6 ns	59.6 ± 2.9 ns	51.9 ± 2.3 ns
Fecal total lipids (mg/day)	29.8 ± 4.8 ns	58.6 ± 12.0 ns	38.1 ± 8.8 ns	27.7 ± 7.1 ns
Fecal cholesterol (mg/day)	4.9 ± 0.7 ns	5.2 ± 1.1 ns	4.0 ± 0.5 ns	5.4 ± 0.5 ns

Abbreviations: CON, α -corn starch; HAS, high amylose starch; S-Wh, whole white cooked sorghum; S-Rf, refined white cooked sorghumns, ns, not significant.

Values presented are mean ± SE (n=6); values followed by different lowercase letters are significantly ($p < 0.05$) different.

Table 4.7. Fecal bile excretion in rats.

Parameter	CON	HAS	S-Wh	S-Rf
Primary bile acids (mg/ day)				
Cholic acid	0.38 ± 0.07 ns	0.93 ± 0.23 ns	0.85 ± 0.20 ns	0.57 ± 0.13 ns
Chenodeoxycholic acid	0.00 ± 0.00 ns	0.07 ± 0.04 ns	0.01 ± 0.00 ns	0.00 ± 0.00 ns
Total	0.46 ± 0.11 ns	1.19 ± 0.30 ns	1.04 ± 0.14 ns	0.69 ± 0.19 ns
Secondary bile acids (mg/day)				
Deoxycholic acid	0.46 ± 0.06 b	0.34 ± 0.07 b	0.79 ± 0.09 a	0.56 ± 0.06 ab
Lithocholic acid	0.61 ± 0.13 b	0.41 ± 0.10 b	0.92 ± 0.11 ab	1.21 ± 0.34 a
Total	1.15 ± 0.21 ab	0.81 ± 0.15 b	1.85 ± 0.20 a	1.88 ± 0.29 a
Total bile acid excretion	1.61 ± 0.29 b	2.01 ± 0.40 ab	2.89 ± 0.32 a	2.57 ± 0.31 ab

Abbreviations: CON, α -corn starch; HAS, high amylose starch; S-Wh, whole white cooked sorghum; S-Rf, refined white cooked sorghum.

Values presented are mean ± SE (n=6); values followed by different lowercase letters are significantly ($p < 0.05$) different; ns, not significant.

Table 4.8. Cecal branched-chain fatty acid content in rats.

Parameter	CON	HAS	S-Wh	S-Rf
Isobutyrate ($\mu\text{mol/ g cecum}$)	1.10 \pm 0.07 ns	0.99 \pm 0.22 ns	1.23 \pm 0.11 ns	1.64 \pm 0.22 ns
Isovalerate ($\mu\text{mol/ g cecum}$)	1.13 \pm 0.12 ns	1.53 \pm 0.35 ns	1.03 \pm 0.14 ns	1.78 \pm 1.78 ns
Total BCFA ($\mu\text{mol/ g cecum}$)	2.23 \pm 0.29 ns	2.53 \pm 0.47 ns	2.27 \pm 0.25 ns	3.43 \pm 3.43 ns

Abbreviations: CON, α -corn starch; HAS, high amylose starch; S-Wh, whole white cooked sorghum; S-Rf, refined white cooked sorghumns, ns, not significant.

Values presented are mean \pm SE (n=6); values followed by different lowercase letters are significantly ($p < 0.05$) different.

Table 4.9. Serum biochemical parameters at the end of the experimental period in rats.

Parameter	Feed groups							
	CON		HAS		S-Wh		S-Rf	
Total cholesterol (mmol/L)	1.39 ± 0.06	a	1.15 ± 0.03	b	1.48 ± 0.03	a	1.47 ± 0.04	a
HDL-C (mmol/L)	0.34 ± 0.01	ns	0.32 ± 0.01	ns	0.37 ± 0.00	ns	0.36 ± 0.01	ns
Non-HDL-C (mmol/L)	1.05 ± 0.05	a	0.82 ± 0.03	b	1.11 ± 0.02	a	1.10 ± 0.03	a
Triglycerides (mmol/L)	0.53 ± 0.02	a	0.24 ± 0.05	b	0.54 ± 0.07	a	0.50 ± 0.09	ab
Free Fatty Acids (mmol/L)	0.80 ± 0.02	a	0.57 ± 0.03	b	0.74 ± 0.04	a	0.71 ± 0.05	ab
Glucose (mmol/L)	6.7 ± 0.3	ns	6.6 ± 0.3	ns	7.0 ± 0.3	ns	7.4 ± 0.3	ns
Total protein (g/L)	65.3 ± 1.1	ns	65.6 ± 0.8	ns	64.6 ± 0.5	ns	64.2 ± 1.3	ns
Albumin (g/L)	40.7 ± 0.6	ns	41.3 ± 0.6	ns	40.9 ± 0.4	ns	40.4 ± 0.7	ns
Alkaline phosphatase (U/L)	526.5 ± 13.4	ns	546.8 ± 25.8	ns	542.5 ± 17.5	ns	533.3 ± 22.3	ns
GOT (U/L)	131.2 ± 7.9	ns	146.8 ± 14.3	ns	152.3 ± 9.1	ns	147.3 ± 10.8	ns
GPT (U/L)	32.8 ± 3.4	ns	41.8 ± 3.7	ns	31.2 ± 1.4	ns	39.8 ± 4.8	ns
Creatine (mg/L)	2.91 ± 0.06	ns	2.87 ± 0.25	ns	2.90 ± 0.08	ns	2.95 ± 0.15	ns
Phospholipids (mmol/L)	1.05 ± 0.03	a	0.88 ± 0.03	b	1.18 ± 0.02	a	1.12 ± 0.04	a

Abbreviations: CON, α -corn starch; HAS, high amylose starch; S-Wh, whole white cooked sorghum; S-Rf, refined white cooked sorghum; HDL-C, high density lipoprotein cholesterol; GOT, Glutamic oxaloacetic transaminase; GPT, Glutamic pyruvic transaminase; ns, not significant. Mean values \pm SE are provided in the table. Different letters in each row represent significant differences at ($p < 0.05$).

CHAPTER 5

Colonic fermentation characteristics of soluble fiber fraction of sugarcane

(Saccharum officinarum L.) bagasse

5.1. Introduction – sugarcane bagasse and bagasse xylan

Sugarcane (*Saccharum officinarum* L.) is a C4 perennial grass that stores sucrose (Brienzo *et al.*, 2016). It has been originated in Asian continent and thus being cultivated in tropical and sub-tropical countries, where the largest producer of sugarcane is currently Brazil (721 million ton), followed by India (347 million ton), China (123 million ton) and Thailand (96 million ton) (Brienzo *et al.*, 2016). The major product processed from sugarcane is granulated sugar and in this process sugarcane stems are crushed and the sugar sap is extracted and the fibrous material remaining is discarded largely.

The fibrous waste material that is discarded is known as “sugarcane bagasse” and it is considered as the most important lignocellulosic waste material in the world currently (135 kg of dried bagasse/ton of crushed cane) in terms of the magnitude of generation and its component versatility (Brienzo *et al.*, 2016; Carvalho *et al.*, 2013). Currently discarded bagasse is being utilized as a fuel source for sugar mills for burning boilers and producing steam, heating the sugar sap to concentrate and sometimes to produce electricity (Carvalho *et al.*, 2013).

Sugarcane bagasse consists of cellulose, hemicellulose and lignin similar to any other lignocellulosic waste product, which accounts for 15% of the sugarcane stems in dry basis (Brienzo *et al.*, 2016). Cellulose in sugarcane bagasse (35 to 50% dwb of bagasse) consists of mainly two types of fibers, cellulose fibers in parenchyma cells of rind and sclerenchyma cells of pith area of the sugarcane culm, which are resistant to degradation via biochemical or biotechnological conversions (Brienzo *et al.*, 2016). Cellulose is found to form microfibrils forming a network structure with hemicellulose, which is further covered by lignin (Brienzo *et al.*, 2016). This structural organization of the cell walls found in the lignocellulosic materials makes it resistant to degradation. Generally, cellulose is a linear homopolysaccharide made of β -D-anhydro-glucopyranose units linked by β -(1,4)-glycosidic linkages

(Brienzo *et al.*, 2016). In all plants cellulose functions as a structural polysaccharide providing strength, integrity, shape and resistance to plant cells.

Lignin (14 to 30%) acts as a cementing agent of cellulose fibers-hemicellulose network, further strengthening the cell wall. This function of lignin further inhibit chemical or physical extraction, microbial attack to the cell wall, thus making it difficult to isolate important biomolecules such as hemicellulose (Brienzo *et al.*, 2016). Lignin is known for its recalcitrant nature due to its chemical structure, albeit it is an amorphous molecule which can be extracted with hot water, weak acids or chelating agents (Brienzo *et al.*, 2016; Ebringerova *et al.*, 2005). Lignin is made from *p*-hydroxy-phenylpropane, syringil and guaiacyl monolignol units as a result of enzyme-mediated radical coupling, making a three-dimensional polymer and the ratio among the monolignol units are found to be related to the degree of recalcitrance (Brienzo *et al.*, 2016).

Hemicelluloses account for the second largest non-starch polysaccharide in sugarcane bagasse averaging between 22 to 36% (Brienzo *et al.*, 2016). In contrast to cellulose, hemicellulose comprises of short, branched heteropolysaccharide chains of hexoses and pentoses (Brienzo *et al.*, 2016). The major constituent sugars reported are D-xylose, L-arabinose as pentoses and D-glucose, D-galactose, D-mannose as hexoses, yet D-mannose, L-rhamnose and D-galactose are found in very small quantities (Brienzo *et al.*, 2016). Sugarcane bagasse hemicellulose fraction is identified as a xylose-based structure, where it is defined as L-arabino-(4-O-methyl-D-glucurono)-D-xylan (Brienzo *et al.*, 2016). Xylose content in sugarcane bagasse is reported to be between 8.8 to 20.4%, where xylose is found to make 80% of the molecule's backbone (Brienzo *et al.*, 2016). Similar to cellulose content, hemicellulose content also varies depending on the sugarcane variety and anatomical location.

As briefly discussed previously, the major hemicellulose type in sugarcane bagasse is xylan (L-arabino-(4-O-methyl-D-glucurono)-D-xylan), due to its higher content ranging between 43 to 93% (Brienzo *et al.*,

2016). L-arabino-(4-O-methyl-D-glucurono)-D-xylan is generally known as arabinoglucuronoxylan and it has a single 4-O-methyl- α -D-glucopyranosyluronic acid residue and α -L-arabinofuranose residues attached to positions 2 and 3, respectively to the β -(1 \rightarrow 4)-D-xylopyranose backbone with a slight acetylation (Ebringerova *et al.*, 2005; Brienzo *et al.*, 2016).

This type of xylans are reported to be the dominant type of hemicelluloses in the cell walls of the lignified supporting tissues of plant species belonging to Family *Poaceae* (grasses and cereals) (Ebringerova *et al.*, 2005). Arabinose is found to be in a higher quantity as a branched group to the xylan backbone by either α -1,2 or α -1,3 linkages, while galactose is also found linked by β -1,5 linkages (Brienzo *et al.*, 2016). Further, there can be other minor links with aromatic feruloyl, *p*-coumaroyl attached to arabinose residues at O-5 position (Saulnier *et al.*, 1995).

Attributed to the diversity of the branched residues linked to the xylan backbone of sugarcane bagasse, the hemicellulose biomass in sugarcane bagasse is a heteropolysaccharide and further different fractions isolated from different anatomical areas of the sugarcane culm, amount of xylan and the composition of the component sugars may be subjected to change (Brienzo *et al.*, 2016). Native or extracted xylan might contain different numbers of xylose units, thus different degrees of freedom (DP). Generally, a native xylan is considered to be made of up to 200 xylose residue bound with β -1,4 linkages, while the extracted xylans are known to have less DP due to the cleavages that occur during the extraction process (Brienzo *et al.*, 2016). Further due to the same reasons, the molecular mass of sugarcane bagasse xylan has reported a wide range of values between 6500 to 86000 g/mol (Brienzo *et al.*, 2016).

Apart from the three major cell wall components described previously, there is a fraction of extractable compounds, which are not chemically linked to the cellulose-hemicellulose-lignin network (Brienzo *et al.*, 2016). These compounds are easily extractable with ethanol, hexane and water like solvents, which comprises of 3 to 14% of sugarcane bagasse, yet this amount varies according to the variety, agronomical

practices, growth stage, etc. (Brienzo *et al.*, 2016). For example, phenolics, fats, fatty acids, resin, waxes and lignans are the major types of extractable compounds found in sugarcane bagasse (Brienzo *et al.*, 2016).

5.1.1. Beneficial effects of xylooligosaccharides

Xylooligosaccharides are also classified into non-digestible oligosaccharides similar to fructooligosaccharides, mannanoligosaccharides and galactooligosaccharides, attributed to the absence of suitable enzymes to hydrolyze the β -1,4 linkage in them within the human hydrolytic enzyme repertoire and thus, they reach the large intestine and provide substrates for gut microbiota, promoting colonic and systemic health, similar to inulin and fructooligosaccharides (Carvalho *et al.*, 2013; Brienzo *et al.*, 2016). Xylooligosaccharides are xylose sugar oligomers with a DP varying from 2 to 10 (sometimes up to 20) resulted from xylan (DP up to 200) hydrolysis via chemical, enzymatic, combined methods or auto-hydrolysis under high temperature and pressure (Samanta *et al.*, 2015; Brienzo *et al.*, 2016).

Xylooligosaccharides are a group of emerging dietary resistant oligosaccharides, yet they have shown some promising beneficial effects upon well-established oligosaccharides, such as fructooligosaccharides and inulin, for examples, resistance to a broad range of pH (2.5 to 8.0) and stability above 100°C, etc. (Brienzo *et al.*, 2016). They have reported several beneficial physiological effects such as, prevention of tooth decay and as a dietary component in diabetic diet, when sucrose is substituted by xylitol, preventing cardiovascular diseases, beneficial effects on skin and blood, anti-inflammatory, anti-allergic, anti-oxidant and anti-cariogenic activities (Grootaert *et al.*, 2007; Aachary and Prapulla, 2011; Flávia *et al.*, 2013; Brienzo *et al.*, 2016).

Further, feeding of a mixture of xylooligosaccharides and fructooligosaccharides to pregnant rats has shown beneficial effects, such as protection of the fetus, development of brain and protection against

oxidative stress and maintenance of enzymatic antioxidant and mitochondrial functions (Brienzo *et al.*, 2016). Replacement of dietary starch and sucrose by xylooligosaccharides is found to improve hepatic lipid profile, alleviate diabetic, cancerous and stress symptoms (Gobinath *et al.*, 2010; Samanta *et al.*, 2015).

Daily consumption of xylooligosaccharides has been reported to regulate many biological processes, such as insulin secretion from the pancreas, increment of mineral absorption from the large intestine, enrichment of fecal moisture content, regulation of bowel function and maintenance of stool frequency in the normal range, amelioration of constipation in pregnant women, lowering of fecal pH, strengthening the immune system and improvement of abdominal conditions without side effects such as diarrhea and flatulence as in the case of inulin (Aachary and Prapulla, 2011; Samanta *et al.*, 2015).

The beneficial physiological effects of xylooligosaccharide intake are considered to be linked to the prebiotic potential of xylooligosaccharides, such as increasing cecal weight, improving *Bifidobacterium* and *Lactobacillus* abundance, modifying short chain fatty acid (SCFA) composition, stimulating immune responses, decreasing colonic pH, suppressing nitrogenous substrate and pro-carcinogenic enzymes synthesis (Aachary and Prapulla, 2011; Samanta *et al.*, 2015; Brienzo *et al.*, 2016).

5.1.2. Colonic fermentation potential of xylooligosaccharides

Xylooligosaccharides are considered as an emerging class of prebiotics, which have exhibited assuring traits in colonic fermentation, such as stimulating bifidobacterial growth to a greater extent than fructooligosaccharides or any other oligosaccharide (Carvalho *et al.*, 2013). Further, reported to cause beneficial changes in the gut microbial diversity, where an inhibited growth of pathogenic genera related to intestinal disorders and toxin production have been observed, for example, *Escherichia*, *Salmonella*, *Enterobacteriaceae* and *Streptococcus* (Brienzo *et al.*, 2016).

Addition of xylooligosaccharides into chicken ration has shown positive effects similar to antibiotics without building up bacterial resistance as in the case of generic antibiotics, further reducing the risk of residual antibiotics in meat (Carvalho *et al.*, 2013; Brienzo *et al.*, 2016). Studies conducted under *in vitro* conditions on ruminant intestine have exhibited stimulated growth of probiotic bacterial strains (Samanta *et al.*, 2012; Brienzo *et al.*, 2016). These oligosaccharides are reported to selectively stimulate the growth of *Bifidobacterium* and *Lactobacillus*, thus considered as prebiotic substrates (Brienzo *et al.*, 2016).

A 1% crude xylooligosaccharides containing growing media has shown a significantly higher growth compared to the control and 1% glucose growth media for major probiotic strains of bacteria, such as *Enterococcus faecium* TCD3, *Lactobacillus maltromicus* MTCC108 and *Lactobacillus viridiscens* NCIM2167 (Carvalho *et al.*, 2013). Further, *in vitro* studies using corn cob xylooligosaccharides have shown its improvement on the *Lactobacillus plantarum* S2 and the combination of xylooligosaccharides and *Lactobacillus plantarum* S2 have exhibited symbiotic effects (Brienzo *et al.*, 2016). Another study reported that several species of *Bifidobacterium*, *Lactobacillus brevis* and some *Bacteroides* were able to grow in a media that only contained xylooligosaccharides of DP 2 to 5 as the sole carbon source (Crittenden *et al.*, 2002; Brienzo *et al.*, 2016). Studies conducted on commercialized xylooligosaccharides have also shown to improve the growth of *Bifidobacterium* and *Lactobacillus* (Wako chemicals), *Bifidobacterium adolescentis*, *Bifidobacterium catenulatum* (xylooligosaccharides produced from *Miscanthus giganteus*) and *Bifidobacterium adolescentis* and *Bifidobacterium longum* (Xylooligo 95P; 83% xylobiose and xylotriose; Suntory, Japan) (Chen *et al.*, 2013; Brienzo *et al.*, 2016).

A previous study, where a 6% (w/w) xylooligosaccharides containing diet fed rats showed a significant increase in cecal and fecal bifidobacteria, which evinced the bifidogenic nature of xylooligosaccharides (Carvalho *et al.*, 2013). Further, oral administration of xylooligosaccharides (DP 2 to 3), five grams per day for three weeks have shown to improve the growth of genus *Bifidobacterium*, especially

Bifidobacterium adolescentis and even a low dose of xylooligosaccharides has shown the capability to inhibit the growth of *Clostridium* and *E. coli* (Brienzo *et al.*, 2016). In another study, where 65 year old test subjects were given xylooligosaccharides, four grams per day for three weeks, exhibited improvements in the gut microbial composition (Carvalho *et al.*, 2013). Maximum tolerant dose of xylooligosaccharides consumption for humans has been determined to be 12 g per day (Brienzo *et al.*, 2016).

Further, it has been reported that xylooligosaccharides obtained via xylan hydrolysis from alkali pre-treated sugarcane bagasse, are prebiotic (Samanta *et al.*, 2015; Brienzo *et al.*, 2016). And many beneficial biological effects of xylooligosaccharides and their derivatives related to gastrointestinal health such as anti-inflammatory and anti-tumor effects, are mainly hailed for acidic oligosaccharides containing uronic acid substitutions as in sugarcane bagasse (Aachary and Prapulla, 2011). On the other hand, the biological activity of xylooligosaccharides is considered to depend on the molecular weight or DP, where $DP < 4$ are reported to possess important prebiotic effects (promote proliferation of bifidobacteria), while long chain xylooligosaccharides have not shown considerable biological activity (Carvalho *et al.*, 2013; Brienzo *et al.*, 2016).

5.1.3. Research statement, objectives and hypothesis

Bagasse is the fiber residue of the industrial juice extraction process from sugarcane (*Saccharum officinarum* L.), mainly comprising of cellulose and hemicellulose that are embedded in a lignin matrix as previously mentioned. Sugarcane bagasse is identified as a rich source of xylan and due to the structural versatility of xylan, it is considered as a promising resource for commercial xylooligosaccharides production (Brienzo *et al.*, 2016). It has been reported that xylooligosaccharides obtained via xylan hydrolysis from alkali pre-treated sugarcane bagasse, are prebiotic (Samanta *et al.*, 2015; Brienzo *et al.*, 2016). Further, many beneficial biological effects related to gastrointestinal health such as anti-inflammatory, anti-tumor, anti-cancer, anti-microbial effects, have been reported for acidic xylooligosaccharides and derivatives containing uronic acid substitutions as in sugarcane bagasse (Aachary and Prapulla, 2011).

Despite the reported beneficial biological and physiological effects, incorporation of xylooligosaccharides in human diet is limited, mostly due to the less production and availability (Brienzo *et al.*, 2016). As previously mentioned sugarcane bagasse is a promising resource for xylooligosaccharides production, which might yield xylooligosaccharides of versatile characteristics and benefits, depending on the production methods and processing conditions (Brienzo *et al.*, 2016). In agreement with its higher xylooligosaccharides content (Table 5.1), we hypothesized that the water soluble fiber fraction obtained from hydrothermal decomposition of sugarcane bagasse could be a promising substrate for gut microbial fermentation, which might improve colonic health by selective stimulation of beneficial bacteria and beneficial metabolite production. Thus, in this study we aimed to characterize the biochemical and physiological effects of colonic fermentation of bagasse water soluble fraction in rats.

5.2. Materials and Methods

5.2.1. Preparation of experimental diets

Bagasse was hydrothermally decomposed (200°C, 1.8 MPa) to obtain the water soluble fiber fraction, which was subjected to membrane ultrafiltration (2500 g/mol) to concentrate (×5 folds). The concentrated water soluble fraction of bagasse was provided by Mitsui Sugar Co. Ltd., (Tokyo, Japan). The proximate composition of bagasse water soluble fraction is presented in Table 5.1.

The intestinal fermentation characteristics of bagasse water soluble fiber fraction was tested against a commercially available xylooligosaccharide (Xylo-oligo 95P; DP: 2-3; 95% purity; B Food Science Co. Ltd., Aichi, Japan) as the positive control and α -corn starch as the negative control. All three experimental diets, α -corn starch (CON), commercial xylooligosaccharide (XYO) and bagasse water soluble fiber fraction (BGS) were prepared according to the AIN-93G diet guidelines (Oriental Yeast Co., Ltd., Tokyo, Japan). Experimental diet compositions are presented in Table 5.2.

5.2.2. Animal experimental design, care for laboratory animals and post-mortem excision of organs

The animal experiment was conducted according to the guidelines of “Guide for the Care and Use of Laboratory Animals” and detailed experimental procedure is presented in Chapter 3 (section 3.2.2.). All the procedures were approved by the Animal Care and Experiment Committee of Obihiro University of Agriculture and Veterinary Medicine (License no: 29-94).

Nineteen Fischer 344 male rats (7 weeks old; average body weight 125-155 g) were purchased from Charles River Laboratories Japan Inc., (Yokohama, Japan). Prior to the experiment, the rats were acclimatized for one week on a commercial diet (Standard powder diet for mouse, rat, hamster, Oriental Yeast Co.,). The acclimatized rats were grouped (6 rats/group) into three similar body weight groups (\approx 170 g) as shown in Table 5.3. During the experimental period, rats were fed with experimental diets with

free access to *ad libitum* water. Each rat was housed individually, a feeder (≈ 25 g) and a drinker (≈ 150 mL) were allocated to each animal, which were replenished after the measurement of feed intake every day at 8 o' clock in the morning. The cages were maintained at $23 \pm 1^\circ\text{C}$ temperature and $60 \pm 5\%$ relative humidity under a 12 h light/dark cycle. Body weight was measured once a week and blood was collected from the jugular vein every week followed by a 12 h fasting period and serum was separated by centrifugation (8,000 rpm, 15 min, 2 times; CFA-12, Iwaki Glass Co., Ltd., Tokyo, Japan) and stored at -80°C until biochemical analysis.

At the end of the experimental period of 4 weeks, the final body weight was measured, fresh feces from the anus was collected and the animals were sacrificed by an intraperitoneal injection of the narcotic (sodium pentobarbital, 40 mg/kg body weight, Abbott Laboratories, Chicago, IL, United States) under minimal suffering. After the sacrifice, cecum, liver, perirenal and epididymal adipose tissues were excised and weighed. Cecal weight, cecal content weight and cecal tissue weight were measured. A portion of the cecal content ($\approx 1\text{g}$) was diluted ($\times 5$) in sterilized distilled water for biochemical analysis and pH measurement, while the rest was stored at -80°C .

5.2.3. Rat cecal bacterial population analyses

a. Viable plate count method for anaerobes and coliform

Five hundred microliter (from 1 mL samples stored at -30°C) from diluted cecal samples was cultured to enumerate Coliform and anaerobic counts by viable plate count method with selective media according to the method described in Chapter 2 (section 2.2.5.a). After the specific incubation periods, colonies were visually counted and were expressed in \log_{10} colony forming units per milliliter (CFU/mL) of the working volume.

b. Cecal bacterial DNA extraction, sequencing and analysis of 16S rRNA sequences

Extraction of bacterial DNA from the cecal digesta, purification, the 16S genome library preparation and sequencing were conducted according to the methods described in Chapter 2 (section 2.2.5). The generated biome table was normalized using an equal subsampling size of 13,674 sequences. Analysis of retrieved 16S rRNA sequences was conducted according to the method described in Chapter 2 (section 2.2.5.b.v). Calculation of the distances between bacterial communities in different samples by the weighted UniFrac distance metric and the generation of the Principle Coordinate Analysis (PCoA) plots were conducted in QIIME (Lozupone and Knight, 2005). Calypso version 8.72 was used to generate hierarchical cluster illustrations (Zakrzewski *et al.*, 2017).

5.2.4. Rat cecal short chain fatty acid analysis

Short chain fatty acid contents in the cecal digesta of rats were analyzed by High Performance Liquid Chromatography (HPLC, Shimadzu LC-10AD, Kyoto, Japan). Samples for HPLC were prepared according to the method described in Chapter 2 (section 2.2.6) and analytical specifications were as follows; column, RSpak KC-811 (8.0 mm x 300 mm, Shodex, Tokyo, Japan); eluent and flow rate, 2 mM HClO₄ at 1 mL/min; column temperature, 47 °C; reaction reagent and flow rate, ST3-R (×10 diluted) at 0.5 mL/min; UV-vis spectrophotometric detector (SPD-10A, Shimadzu) wavelength, 450 nm. Short chain fatty acid content was calculated same as Chapter 2.

5.2.5. Ammonia-nitrogen analysis in cecal suspension

Ammonia-nitrogen content in the diluted samples of cecal content was analyzed using a commercially available kit (Wako Pure Chemical Industry Ltd., Tokyo, Japan) according to method described in Chapter 2 (section 2.2.7) and the ammonia-nitrogen content was calculated similar to Chapter 2.

5.2.6. Analysis of mucin content in rat cecal digesta

Mucin was fractionated according to the method by Bovee-Oudenhoven *et al.* (1997) from diluted cecal digesta samples stored at -30°C. Mucin contents in the cecal digesta were analyzed by the fluorometric assay procedure described by Crowther and Wetmore (1987) as described in Chapter 3 (section 3.2.7) and mucin content was calculated similarly.

5.2.7. Analysis of Immunoglobulin A (IgA) content in cecal content

Immunoglobulin A content was analyzed by ELISA quantitative kit for Rat IgA provided by Bethyl Laboratories Inc. (Montgomery, TX, United States) according to the method described in Chapter 3 (section 3.2.6) and Immunoglobulin A content was calculated same as Chapter 3.

5.2.8. Serum biochemical analysis

Serum biochemical profile was analyzed using Toshiba TBA-120FR autoanalyzer (Toshiba Medical Systems Corp., Tochigi, Japan) according to manufacturer's instructions.

5.2.9. Fecal total lipid analysis

Total lipid content in freeze-dried feces was analyzed gravimetrically and calculated according to the method described in details in Chapter 4 (section 4.2.8.a).

5.2.10. Statistical analysis

All data except the microbial community data were analyzed for their significance by analysis of variance (ANOVA) using SPSS statistical software version 17.0 (SPSS Inc., Chicago, IL, USA). When significant differences among the test groups were revealed, mean scores were compared by Tukey's test. Statistical significance of alpha diversity indices (Shannon's and observed species indices) was determined by ANOVA paired with Tukey's test (SPSS). Relative abundance of genera among the three diet groups were

compared using Kruskal-Wallis H test and statistical significance was determined using Calypso (version 8.72). A p value less than 0.05 was considered as statistically significant.

5.3. Results and Discussion

5.3.1. Feed intake, zoometric parameters and organ parameters

As presented in Table 5.4, feed intake at the end of the experimental period was significantly different ($p < 0.05$) among the three diet groups, where CON and XYO reported the highest and lowest intakes, respectively. Final body weight and body weight gain were not significantly different among the diet groups. Trends similar to that of the body weight gain and final body weight have been reported previously (Hsu *et al.*, 2004).

Both cecal weight and cecal tissue weight were significantly higher in the XYO group, followed by BGS and CON groups, which reported similar values (Table 5.4). Albeit, the cecal content weight was not statistically significant, it was clearly higher in the XYO and BGS groups compared to the CON group. Higher cecal parameters observed in the XYO and BGS groups can be attributed to the prominent cecal fermentation that took place (Montagne *et al.*, 2003). Increment of cecal weight and cecal tissue weight are attributed to the trophic effect exerted by the cecal fermentation products, mainly SCFA (Hsu *et al.*, 2004). Initially, butyric acid and subsequently acetic acid are known to influence the healthy epithelial cell proliferation (Montagne *et al.*, 2003; Hsu *et al.*, 2004; Calabrò *et al.*, 2012).

Increased total weight of cecum had been previously observed upon XOS intake, followed by the increased abundance of beneficial gut microbiota and acidification of colonic environment (Samanta *et al.*, 2015). Cecal pH also was significantly lower in the XYO and BGS groups compared to that of the CON group (Table 5.4). Lower cecal pH observed in the former two groups further strengthened the evidence on cecal fermentation (Hsu *et al.*, 2004; Achary and Prapulla, 2011; Fukuda *et al.*, 2011).

5.3.2. Short chain fatty acids in cecal digesta

Cecal SCFA contents are presented in Fig. 5.1. Acetate was the major SCFA produced in all three diet groups similar to previous studies. Interestingly, BGS group exhibited significantly higher ($p < 0.05$) acetate content, which was more than 1.5 folds higher than the XYO group. A previous study also has revealed that xylooligosaccharides are capable of producing higher acetate contents upon fermentation, even than that of inulin and β -glucan (Aachary and Prapulla, 2011; Carlson *et al.*, 2017).

In contrast to the acetate content, propionate content in the XYO group was statistically similar to that of the BGS group, while it was significantly higher compared to the CON group. Further, propionate content was 6 and 12 folds less compared to the specific acetate contents in the XYO and BGS groups, respectively. Similarly, propionate production by xylooligosaccharides has been reported to be significantly lower compared to the other well-established prebiotic substrates, such as inulin and β -glucan, upon fermentation similar to the present study (Carlson *et al.*, 2017). Previous similar studies reported that the main products of linear and branched xylooligosaccharides fermentation to be acetic and lactic acids (Aachary and Prapulla, 2011; Abbeele *et al.*, 2011). Propionate is known for its ability to improve satiety, and thus the significantly lower feed intake in the XYO group can be attributed to the highest propionate content, while the propionate content and feed intake in the BGS and CON groups were also in complement with each other (Carlson, *et al.*, 2017; Ottman, *et al.*, 2017).

Butyrate content was significantly higher in the XYO and BGS groups compared to the CON group. It was statistically similar between XYO and BGS groups, with a marginally higher content observed in the BGS group. Compared to the butyrate content in the CON group, the XYO and BGS groups exhibited almost three folds higher butyrate contents, which showed their butyrogenic nature (Giuberti *et al.*, 2013; O'Callaghan and van Sinderen, 2016).

Total SCFA content was significantly higher in the BGS group over the XYO group, attributing to the significantly higher content of acetate observed in the former group. CON group reported significantly lower total SCFA content compared to both XYO and BGS groups. The observed higher total SCFA contents in XYO and BGS groups are in complement with a similar previous study, where the highest total SCFA production was obtained for xylooligosaccharides among a variable array of other well-established oligosaccharides, such as fructooligosaccharides (Aachary & Prapulla, 2011). Further, significantly lower cecal pH observed in XYO and BGS groups were also due to the significantly higher SCFA contents compared to the CON group (Fukuda *et al.*, 2011; Vazquez-Gutierrez *et al.*, 2016).

The significantly higher yield of total SCFA content reflected the presence of a favorable and abundant source of fermentable substrate in the BGS group. In the BGS diet, soluble fraction obtained by bagasse hydrothermal decomposition was incorporated in a rate of 5% w/w, which contained 51% oligosaccharides (dry weight basis) in the carbohydrate fraction (Table 5.1). Generally, the hydrothermal treatments of lignocellulosic material are known to yield mainly soluble oligosaccharides, which might explain the higher oligosaccharide fraction in the soluble fraction obtained from bagasse (Aachary and Prapulla, 2011). Similarly, XYO diet contained a 5% w/w commercial xylooligosaccharide (95% purity) mixture, which is composed of xylobiose and xylotriose.

Samanta *et al.* (2015) has reported that β -(1,4)-xylosidic bonds present in xylooligosaccharides cannot be hydrolyzed by the native digestive enzymes secreted by the vertebrates, thus they reach the colon without any compromise in the structural integrity and the resident gut microbiota selectively utilize these xylooligosaccharides for their metabolism forming SCFA as end products. Thus, both XYO and BGS diets might have provided favorable substrates for cecal microbial fermentation (Hsu *et al.*, 2004; Aachary and Prapulla, 2011; Brienzo *et al.*, 2016).

5.3.3. Cecal microbial community data

Viable plate counts for anaerobes in XYO and BGS groups exhibited their ability to enhance the growth and proliferation of anaerobes significantly ($p < 0.05$) in the cecum compared to the CON group (Fig. 5.2.a). Further, BGS had a significantly lower coliform count compared to XYO group (Fig. 5.2.b). Mammalian colon is considered to be an anaerobic environment, and the microbial community reside in the colon is considered to be predominantly anaerobic with a smaller percentage of facultative anaerobes (Thursby & Juge, 2017). XYO and BGS groups found to facilitate the growth and proliferation of anaerobes in the cecal digesta, exhibiting their ability to feed and maintain the gut microbial community (Vieira *et al.*, 2013).

One of the beneficial health effects of xylooligosaccharide intake is considered to be the restrained growth and multiplication of pathogenic and putrefactive microflora, which is attributed to the lowering of pH due to higher SCFA content (Fukuda *et al.*, 2011; Samanta *et al.*, 2015; Vazquez-Gutierrez *et al.*, 2016). Due to established correlations between colonic pH and the abundance of pathogenic and beneficial bacteria, cecal pH reduction in XYO and BGS groups can be used as a marker of prebiotic effects of xylooligosaccharides fermentation (Madhukumar and Muralikrishna, 2012).

Despite the significantly lower cecal pH observed in XYO group in the present study, coliform count was significantly higher. In contrast, the coliform count in the BGS group was significantly lower complementing well with the substantially higher total SCFA content and significantly lower cecal pH. The higher coliform abundance could be attributed to the fact that possession of enzymes that are capable of degrading xylooligosaccharides derived from xylan by *Escherichia coli* (Aachary and Prapulla, 2011). Having mentioned that, the higher coliform abundance in XYO fed rat cecal content, might have been due to the availability of degradable xylooligosaccharides by coliform (Aachary and Prapulla, 2011). Interestingly, a previous study had found that, *E. coli* was not affected by the low pH and high organic

acid concentrations produced by bifidobacteria strains in *in vitro* co-cultures (Vazquez-Gutierrez *et al.*, 2016). In contrast, it has been previously reported that the acidic environment in the colon due to SCFA formation was associated with the inhibition of several pathogenic microbial members, such as *Salmonella* and *Clostridium* species in mice, which was similar to the observations for *Clostridium* in this study, in XYO and BGS diet fed groups (Montagne *et al.*, 2003).

Cecal bacterial community data obtained from 16S rRNA sequencing, highlighted distinct differences in the microbial diversity among the test groups. As presented in Fig. 5.3.a, CON group possessed a significantly higher diversity or species richness, which was followed by the BGS group and lastly the XYO group. Observed species index (Fig. 5.3.b) also followed the same trend as the Shannon's diversity index indicating a higher alpha diversity (diversity within samples) in the CON and BGS groups. As previously mentioned in Chapter 4 (section 4.3.2), the discussion of the microbial diversity statistics are subjective and depends strictly on the objectives of the study.

Thus, the significantly lower alpha diversity observed in the XYO group indicated a less microbial richness and evenness, yet in the point of view of cecal fermentation, it might also have indicated the fermentative capability of xylobiose and xylotriose. Thus, it might suggest that, only the microbiota that were able to utilize the said substrates had been influenced and favored. On the other hand, higher alpha diversity in BGS compared to XYO, might indicate its substrate versatility to influence a wide array of microbiota to improve richness and evenness. The alpha diversity statistics in the CON group stands for the general microbial composition in rats under a conventional balanced diet. Thus, the differences observed in the alpha diversity statistics, further highlighted the modifications occurred in the conventional gut microbial structure due to the dietary interventions by the XYO and BGS diets (Vieira *et al.*, 2013). Linear and pure xylooligosaccharides in the XYO diet and branched derivatives of

xylooligosaccharides in the BGS diet might have selectively influenced the members of colonic microbiota in different degrees (Aachary & Prapulla, 2011).

Beta diversity plot (Fig. 5.3.c) of microbial community data clearly indicated the presence of significantly distinct microbial community structures among the test groups. According to the nature of the cluster formation along the x-axis, it is clear that CON group and the other two groups are placed on two distinct branches on the phylogenetic tree, while XYO and BGS groups might be located on a common branch, yet significantly apart from each other. These observations further indicated the difference in fermentable substrate diversity in these two xylooligosaccharides substrates. Finally, the close clustering observed among the individual animals within each group exhibited the similarity in the gut microbial community structures within each group.

At phylum level, Firmicutes was the most abundant microbial phylum, across all diet groups. Firmicutes abundance was significantly higher in the CON group, followed by BGS and XYO groups (Fig. 5.4.a). Apart from Firmicutes, Actinobacteria, Proteobacteria and Verrucomicrobia were also found in a lesser abundance. Verrucomicrobia and Actinobacteria abundance was significantly higher in the XYO group followed by the BGS group, while BGS group exhibited significantly higher abundances of mentioned phyla over the CON fed group. Bacteroidetes was not significantly different among the diet groups.

At genus level, more distinct differences among the diet groups were observed as shown in Fig. 5.4.b. The LDA scores highlighted the degree of significance of the microbial genera with respect to each diet. In BGS group, *Blautia* and *Roseburia* were among the characteristic genera, while *Bifidobacterium* and *Akkermansia* constituted the XYO group. The number of signature genera identified among the most abundant 300 genera reflects a similar scenario as observed in alpha diversity indices.

In this study, two bifidobacterial strains were clearly characterized along with an unclassified *Bifidobacterium* fraction; *B. pseudolongum* (23%, 6%, 0.2%; XYO, BGS and CON, respectively) and *B. adolescentis* (0.1%, 0.05%, 0.001%; XYO, BGS and CON, respectively) (Fig. 5.5). *B. pseudolongum* is identified as one of the dominant gut microbial species in animals known to be able to metabolize the xylan backbone of arabinoxylooligosaccharides (AXOS) up until the xylo-tetraose moiety (O'Callaghan & van Sinderen, 2016). But its ability to utilize substitutions on xylan backbone is considered to be limited (O'Callaghan & van Sinderen, 2016). In contrast, certain strains of *B. adolescentis* abundantly found in the human gut are considered to be able to utilize neither the substitutions nor the xylan backbone of AXOS, but able to utilize only the monomeric xylose and arabinose, while some other strains are known to have similar capabilities similar to that of *B. pseudolongum* (O'Callaghan & van Sinderen, 2016). Thus, xylooligosaccharides (DP 2 to 3) being the exclusive digestible substrate in XYO diet group, the lower abundance of *B. adolescentis* indicated less favorable niche conditions prevailed for its growth/proliferation in XYO diet fed rat cecum. Thus, as reflected by the higher abundance, it was suggested that *B. pseudolongum* might have been the key utilizer in the XYO group.

In the BGS group also, the key bifidobacterial strain was *B. pseudolongum* as per Fig. 5.5. The significantly lower abundance compared to the XYO group could be attributed to its limited capacity to utilize substitutions on xylan backbone as previously mentioned, as xylooligosaccharides found in BGS diet should be branched as bagasse contains a branched xylan as the main hemicellulose (O'Callaghan & van Sinderen, 2016). Furthermore, all currently characterized bifidobacterial arabinoxyylan degrading enzymes are predicted to be intracellular, suggesting that the bifidobacterial strains have to rely on the other microbial members encoded for extracellular hydrolytic enzymes for fermentative substrates (O'Callaghan and van Sinderen, 2016). Thus, deficient availability of xylooligosaccharides substrates due

to restrictions in the physical structure of the substrate in BGS diet could be another reason behind the lower abundance of bifidobacteria in BGS fed animals over XYO fed animals.

Bifidobacterium is considered to exert beneficial effects on host health, such as regulation of gut microbial composition, prevention of infection and regulation of immunity (Vazquez-Gutierrez *et al.*, 2016). Further, the abundance of bifidobacteria in the gastrointestinal tract is positively correlated with decreased blood lipopolysaccharides and inflammatory reagents and negatively correlated with obesity and weight gain, suggesting its importance as a marker of healthy gut (Carlson *et al.*, 2017). In the gut microbiota, bifidobacterial strains are identified to possess a strong affinity towards fermenting oligosaccharides and known to be the most efficient xylose based oligo and polysaccharide fermenters (Madhukumar and Muralikrishna, 2012; Carlson *et al.*, 2017). Further, various *in vivo* and *in vitro* studies have exhibited evidences for the bifidogenic nature of xylooligosaccharides and its derivatives (Gobinath *et al.*, 2010; O'Callaghan and van Sinderen, 2016). Observations in this study also further strengthened the above fact.

Akkermansia muciniphila is a well-known specialist mucin degrader in the gut and known to infer important benefits on the host physiology and microbial structure (Ottman *et al.*, 2017). Its abundance in this study was significantly higher in the XYO group compared to CON, while the abundance in the BGS group was comparatively lower than the XYO group (Fig. 5.5). *A. muciniphila* is considered as a marker of the host health status, as its abundance is found to negatively correlate with the incidence of inflammatory bowel disease, appendicitis, obesity, autism, atopy and diabetes (Belzer & De Vos, 2012). This bacteria uses mucin as the only carbon and nitrogen substrate for its metabolism, thus it gains a competitive niche advantage in the gut, even at distressed times, such as fasting, malnutrition or total parenteral nutrition (Belzer and De Vos, 2012). Upon utilization of mucin, *A. muciniphila* is known to produce oligosaccharides and SCFA, specifically, acetate and propionate within the mucus layer that is readily available for the uptake by the host cells (Belzer and De Vos, 2012). Significantly very high acetate

contents in the BGS and XYO might have also been contributed by *A. muciniphila* via mucin degradation (Belzer & De Vos, 2012).

Genus *Blautia* is another characteristic microbial group identified in XYO fed group, while it was significantly abundant in the BGS fed animals also (Fig. 5.5). Genus *Blautia* that belongs to the family *Lachnospiraceae* is a major gut bacterial group, whose members are capable of degrading complex polysaccharides and produce SCFA (Eren *et al.*, 2015). These bacteria are placed within the *Clostridium coccoides* group, which is also infamously known as the “*Clostridium* cluster XIVa”, a butyrate producing cluster (Bajaj *et al.*, 2012). Ironically, there are no reports on the butyrate production ability of *Blautia*, which is apparent in the present study also with observed similar butyrate contents in XYO and BGS groups despite the higher abundance of *B. producta* in BGS group (Eren *et al.*, 2015). Members of genus *Blautia* are found to produce acetate, lactate and succinate, apart from hydrogen and ethanol upon carbohydrate catabolism and thus, known to be acetogenic bacteria (Liu *et al.*, 2008). The significantly very high abundance of *Blautia* and the highest acetic acid content in the BGS group could be correlated.

Genus *Roseburia* is another member of the “*Clostridium* cluster XIVa”, and its members are well-known butyrate producers in the colon (Louis and Flint, 2009). Members of this genus utilize non-digestible carbohydrates such as RS and oligosaccharides, for examples, inulin type fructans, xylans, arabinoxylans and fucose (Louis & Flint, 2009). *R. faecis* found in higher abundance in the BGS group (Fig. 5.5), is known to predominantly yield butyrate upon carbohydrate metabolism (Hatzioanou *et al.*, 2013). Thus, significantly higher abundance of *R. faecis* in BGS fed rats suggested that bagasse soluble fraction might have contained favorable butyrogenic substrates in comparison to the CON and XYO groups. A previous study has reported that *R. faecis* is specialized in type 1 arabinogalactan utilization (Sheridan *et al.*, 2016). Thus, the higher abundance of *R. faecis* in the BGS fed group could be due to its ability to utilize plant cell wall materials such as arabinoxylans, further backed up the previous finding. Reasons for the similar

butyric acid contents in the XYO and BGS groups, despite the significantly higher abundance of *R. faecis* in the BGS group, could be due to the fact that the members of genus *Roseburia* are known to colonize the mucus layer and govern mucosal butyric acid production, which might have increased the bioavailability of butyric acid in the mucosal layers to be up taken by the colonocytes (Abbeele *et al.*, 2011; Rivière *et al.*, 2016).

5.3.4. Cecal ammonia-nitrogen content

Ammonia-nitrogen content in CON and BGS groups were significantly lower, while XYO group exhibited a significantly higher ($p < 0.05$) content (Fig. 5.6). Ammonia-nitrogen can be produced either by the hydrolysis of urea by ureases produced by the gut microbiota and mucosa or by the deamination of amino acids and other nitrogenous substances by the gut microbiota in the large intestine (Vince *et al.*, 1973). Gut microbial members belonging to *Bacteroides*, *Bifidobacterium*, *Clostridia*, *Proteus* and *Klebsiella* are known to express ureases and another dominant pathogenic member, *E. coli* is identified as one of the most active ammonia producers in the gut via deamination of substances other than urea (Vince *et al.*, 1973).

Suppressant effect of lower colonic pH mediated through dietary fiber fermentation on ammonia production is found to depend on the existing dominant origin of ammonia in the gut, where a prodigious effect was found to be on the urea hydrolysis (Vince *et al.*, 1973). Thus, in XYO diet fed rats, the main source of ammonia-nitrogen might have been the deamination of proteinous substances, with complement to its higher ammonia-nitrogen content, higher coliform abundance and lower cecal pH. In contrast, it has been previously reported that the ammonia production in the colon was suppressed by xylooligosaccharides inclusion, inhibiting enteric colonization of ammonia producing anaerobes such as *Bacteroides*, whose abundance was not significantly different among the three diet groups in the present

study, which further backed up the fact that the dominant origin of ammonia-nitrogen in XYO group might have been deamination (Aachary and Prapulla, 2011).

Moreover, xylooligosaccharides consumption is reported to reduce the concentration of putrefactive substances as a consequence of the bifidogenic activity, which again was in contrast to the observations in the XYO group, where the ammonia-nitrogen content and the abundance of bifidobacteria were both significantly higher (Samanta *et al.*, 2015). As previously mentioned in section 5.3.1, the higher ammonia-nitrogen content in XYO group, despite the lower pH and higher bifidobacteria abundance, might have been due to the fact that coliform is not affected by the incubation at low pH, with high organic acid concentrations produced by bifidobacteria strains (Vazquez-Gutierrez *et al.*, 2016).

Significantly lower ammonia-nitrogen content and lower coliform abundance in BGS compared to XYO, suggested that the main origin of ammonia could have been under the expression of urease activity (Vince *et al.*, 1973). Above fact was further backed by the lower abundance of *C. perfringens* in BGS group, a prominent ammonia producer expressing urease activity, whose growth/proliferation might have been inhibited by lower cecal pH due to the fermentation of bagasse AXOS (Vince *et al.*, 1973; Montagne *et al.*, 2003).

5.3.5. Cecal mucin content

Mucin content in the cecal digesta in the BGS group was significantly higher ($p < 0.05$) than the CON group and similar to that of the XYO group (Fig. 5.7). Mucin is a highly structurally versatile polymeric glycoprotein secreted from the goblet cells in the intestinal epithelium and the major structural component of the mucus layer (Tailford *et al.*, 2015). Mucus lining along the gastrointestinal tract acts as a protective layer shielding the intestinal epithelia from physical, chemical and biological hazards (Montagne *et al.*, 2003; Tailford *et al.*, 2015). In the colon, the outer layer provides a nutrient-rich ecological niche for the

microbiota, while the inner layer is firmly attached to the epithelial surface which is free of microorganisms. Loss of integrity in the mucus bilayer is associated with deleterious physiological impairments, such as inflammatory bowel disease, colorectal cancer and susceptibility to infection by opportunistic pathogens (Chen *et al.*, 2012; Tailford *et al.*, 2015).

Mucus layers are in a dynamic equilibrium between the physical, chemical and enzymatic erosion on the luminal side and the mucin synthesis and secretion by the goblet cells in the epithelium (Montagne, Pluske and Hampson, 2003). Dietary fiber ingestion and increment of mucin synthesis in the intestine are considered to be repercussions of erosion driven recovery process of the mucus (Montagne *et al.*, 2003). Physical abrasion of the outer mucus layer is either caused by insoluble dietary fiber or swollen soluble fiber, enhancing the production and secretion of new mucins from the goblet cells on the epithelial side (Montagne *et al.*, 2003).

Thus, one of the reasons for the increased mucin synthesis influenced by BGS intake could be a result of a physical adaptation to the mechanical irritation caused by the swollen soluble fiber fraction in the BGS diet and resultant viscous luminal content as mentioned above (Montagne *et al.*, 2003). This could be attributed to the differences in physicochemical properties between xylobiose and xylotriose in XYO and AXOS in BGS diets (Montagne *et al.*, 2003). AXOS inherit a higher inherent viscosity due to the higher molecular weight (≥ 2500 g/mol) and are able to improve digesta viscosity due to both the higher molecular weight and the branched nature, which in turn causing a considerable mechanical irritation when fed BGS diet compared to small xylo-dimers and xylo-trimers (molecular weight 280-415 g/mol) in XYO diet (Montagne *et al.*, 2003; Charmet *et al.*, 2007).

Further, the abundance of *A. muciniphila* could be another major reason for the higher mucin contents observed in XYO and BGS groups compared to CON as discussed in section 5.3.3. A previous study had reported increased colonic mucus levels accompanied by the increased levels of *Akkermansia* in rats fed

prebiotic substrates, such as inulin or arabinoxylans, which is similar to the observations in the present study (Belzer & De Vos, 2012). This suggested that the secretion of mucin from goblet cells could have been influenced by the increased level of *A. muciniphila* (Belzer & De Vos, 2012). Thus, increased abundance of *A. muciniphila* in the XYO and BGS groups might implicate the presence of a healthy mucus layer, which had been frequently refreshed (Belzer and De Vos, 2012). Yet, BGS group had the highest mucin content with a lower abundance of *A. muciniphila* compared to XYO group, which can be attributed to the differences in the physicochemical properties of fermentable substrates in XYO and BGS diets as previously mentioned (Montagne *et al.*, 2003).

5.3.6. Cecal immunoglobulin A (IgA) content

Immunoglobulin A content was significantly ($p < 0.05$) higher in the XYO group followed by BGS, both of which had significantly higher IgA contents than the CON group (Fig. 5.8). Host secretory immune system is an important component of the gut barrier function that defines the structure of gut microbiota, which limits the opportunistic invasion by the pathogenic members of gut microbiota and protects the gut epithelial integrity (Thursby and Juge, 2017). Immunoglobulin A is the most abundant antibody isotype in the mucosal secretions, specialized in mucosal protection, which involves binding of IgA to the mucus layer to maintain immune homeostasis by limiting the exposure of bacteria to the epithelium (Gutzeit *et al.*, 2014; Thursby and Juge, 2017).

It has been reported that both probiotics and prebiotics influence gut homeostasis and improve gut barrier function via a set of multifactorial mechanisms (O'Flaherty *et al.*, 2010; Vieira *et al.*, 2013). Gut epithelial barrier functions of IgA enclose the maintenance of non-invasive commensals and neutralization of invasive pathogens, similar to the observations in BGS group for bifidobacteria, Coliform and *C.*

perfringens (Gutzeit *et al.*, 2014). But, the higher abundance of Coliform in XYO group was in discrepancy with the immune function of IgA, despite the higher abundance of bifidobacteria.

The underlying mechanisms of immune homeostasis of prebiotics are speculated to be due to the improved abundance of beneficial bacteria and subsequently the immunomodulatory effects of the effector molecules produced by those bacteria, such as SCFA, similarly observed in both XYO and BGS groups (O'Flaherty *et al.*, 2010). Various immunomodulatory mechanisms expressed by the gut microbiota involve, competition for niches, induction of antimicrobial peptide secretion from intestinal epithelial cells, regulation of differentiation and proliferation of epithelial cells, modulation of mucus production and induction of the production of IgA, which can be related to the observed microbial taxa in XYO and BGS groups such as, *Bifidobacterium*, *Blautia*, *R. faecis* and *A. muciniphila* (O'Flaherty *et al.*, 2010; Vieira *et al.*, 2013).

5.3.7. Fecal moisture and total lipid content

Fecal moisture content was significantly ($p < 0.05$) higher in XYO and BGS fed rats, while fecal dry weight was significantly lower in XYO followed by BGS, where the dry weight was significantly higher in the CON group (Table 5.5). Higher fecal moisture content implicated the higher water holding capacity of dietary fibers along the gastrointestinal tract, especially at the distal colon alleviating constipation and regulating normal bowel movement. Lowest fecal dry weight observed in the XYO group might indicate a higher cecal degradation of xylooligosaccharides, while in the BGS group there might be substrates that might not have been degraded completely. Higher fecal dry weight in CON group can be attributed to the higher non-fermentable fiber content in it.

Fecal total lipid excretion was significantly higher in both XYO and BGS groups compared to CON group and lipid excretion per day was significantly higher in the BGS group, while the other two groups exhibited

similar amounts (Table 5.5). Total fecal lipid constitutes of neutral sterol (cholesterol and coprostanol) and acidic sterols (bile acids). One mechanism of dietary fiber mediated fecal lipid excretion is in the form of bile acids. Cholesterol is converted into bile acid and excreted into the gastrointestinal tract to facilitate the digestive environment, which is later re-absorbed at ileum. Thus, bile acid production is a feed-forward dependent process that depends on the re-absorbed bile acid content. These bile acids are known to be bound to dietary fiber, thus, bound bile acid are not re-absorbed at ileum, resulting a lower turnover at the liver and as a repercussion more cholesterol is converted into bile acids. At the colon, the bound bile acids are released when fermentable dietary fibers are fermented and bile acids are also get converted to secondary bile acids by the activity of gut microbiota. Both secondary and primary bile acids are known to be bound to non-fermentable dietary fiber and get excreted via feces. This mechanism is known to play a key role in dietary fiber mediated lipid homeostasis in body.

5.3.8. Serum biochemical results

None of the serum biochemical parameters were significantly different at the end of the experimental period, except glutamic oxaloacetic transaminase (Table 5.6). Further, non-significant data obtained for zoometric parameters, organ weights (liver and adipose tissue) also might reflect these observations in serum. Thus, effector molecules of cecal fermentation of xylan based oligosaccharides might not have been involved in certain biochemical processes, such as body weight regulation, adipose tissue and liver function. Instead as reflected by the results, the effector molecules might have been mainly involved in immunomodulation (higher IgA and mucin contents).

5.4. Implications and Conclusions to Chapter 5

The present study revealed promising potentials of water soluble fraction of hydrothermally decomposed sugarcane bagasse as a prebiotic candidate. Significantly higher total SCFA, acetate contents, significantly lower ammonia-nitrogen content and similar cecal pH compared to the XYO group, suggested its superiority over xylobiose and xylotriose, well-characterized prebiotic xylooligosaccharides. Moreover, significantly higher mucin and IgA contents in the BGS group reflected its protective gut mechanical barrier and immune functions compared to XYO and CON, respectively.

Bacterial structure was clearly different between the XYO and BGS groups as reflected by the differences in microbial diversity and abundances. BGS group exhibited a higher diversity and richness compared to XYO group indicating its versatility as a substrate. Further, BGS and XYO diets influenced clearly different groups of microbiota, for example *B. producta*, *R. faecis*, in BGS group and *Bifidobacterium* strains in XYO group, again might have been due to the differences in the physicochemical structure of the two substrates.

Observed differences between BGS and XYO groups might reflect the physicochemical and structural differences in the two fermentable substrates in the two groups. Branched xylooligosaccharides with different types of branch chains such as arabinofuranosyl residues or 4-O-methyl derivatives of α -D-glucopyranosyl uronic acid groups as in the case of sugarcane bagasse xylan, possess different biological properties compared to their linear counterparts, which might explain the different fermentation capacities of the two xylooligosaccharide sources in this study.

For example, linear and low molecular weight (282-414 g/mol) xylooligosaccharides in the XYO diet and high molecular weight (≥ 2500 g/mol) branched xylooligosaccharides in the BGS diet might have selectively influenced the members of colonic microbiota in different degrees. It is a well-established fact

that the DP or molecular weight and the chain structure (linear or branched) affect the fermentability of xylooligosaccharides, as they determine the selectivity of microbial degraders depending on the metabolic capacities of different microbial species. For example, lower abundance of bifidobacteria in the BGS group can be attributed to its metabolic limitations in utilizing the branched xylooligosaccharides, where they were found to prefer low substituted linear structures such as xylobiose and xylotriose in the XYO group, reflected by their higher abundance in this group.

Further, high molecular weight, branched oligosaccharides are known to possess a higher inherent viscosity due to enhanced water holding capacity. Thus, feeding of BGS diet might have been able to improve digesta viscosity due to both the higher molecular weight and the branched nature, which in turn might have improved mucin synthesis, facilitated a higher fecal moisture entrapment in the BGS fed rats. Abundance of immunomodulatory bacteria, such as *Bifidobacterium*, *Akkermansia*, higher SCFA production, lower cecal pH in the two xylooligosaccharides groups, might have improved the immunoglobulin A secretion in these groups.

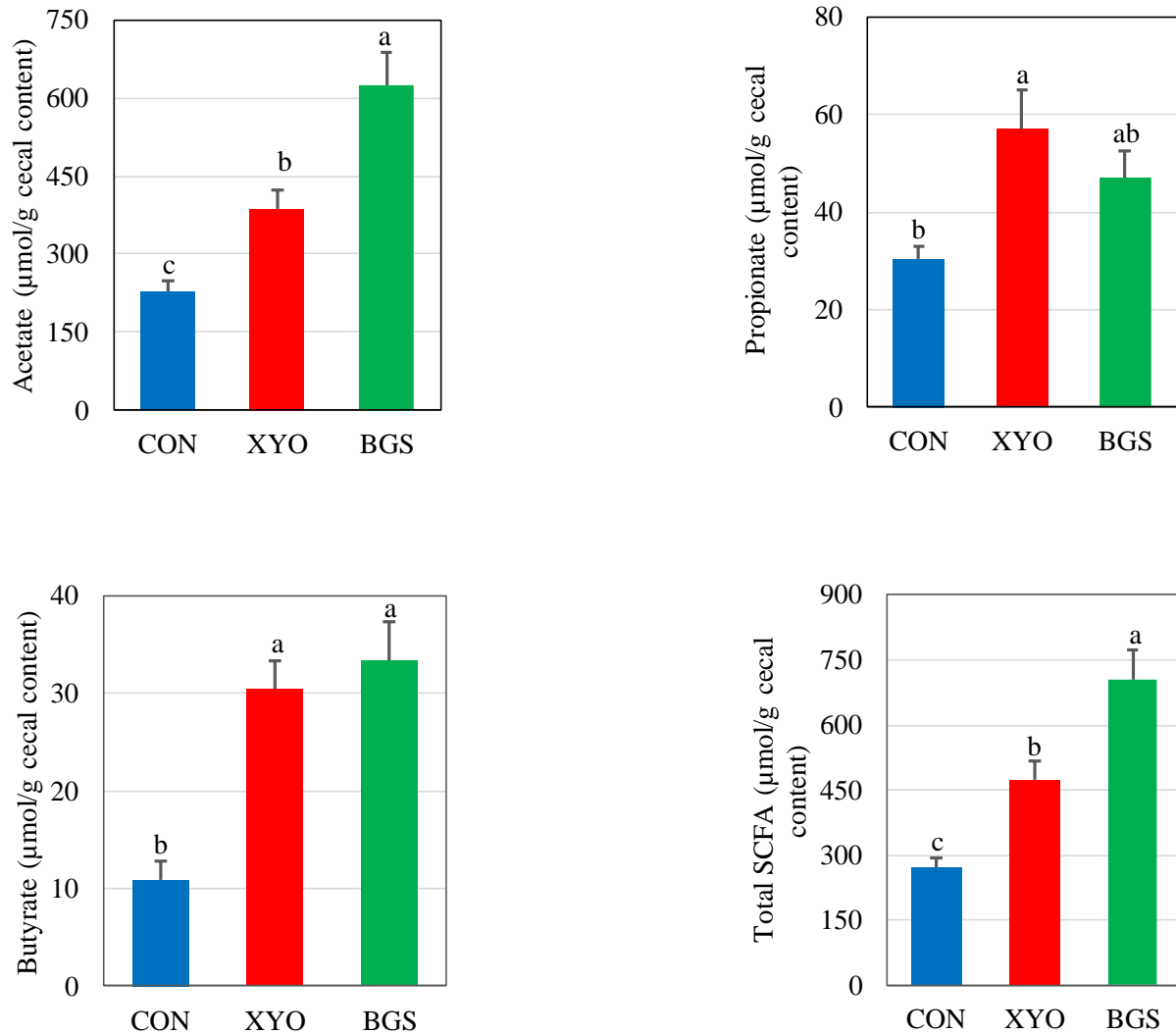
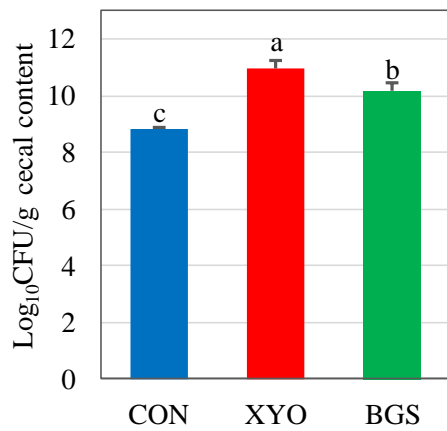


Fig. 5.1. Short chain fatty acid concentrations in the cecal content of rats.

Data presented are mean \pm SE (n=6) and different letters represent significant differences among the diet groups at $p < 0.05$. (CON, α -corn starch; XYO, commercial xylooligosaccharides (DP 2-3); BGS, water soluble fiber fraction of sugarcane bagasse).

(a)



(b)

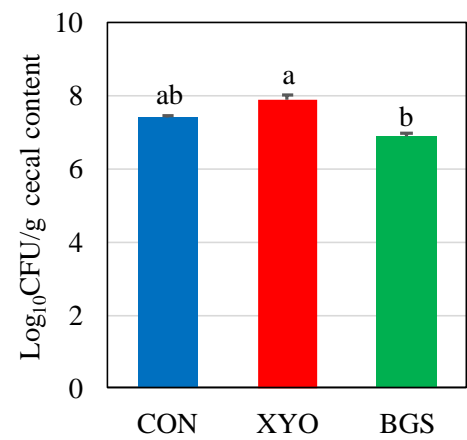


Fig. 5.2. Viable plate counts of (a) Anaerobes (b) Coliform in the cecal content of rats.

Data presented are mean ± SE (n=6) and different letters represent significant differences among the diet groups at $p < 0.05$. (CON, α -corn starch; XYO, commercial xylooligosaccharides (DP 2-3); BGS, water soluble fiber fraction of sugarcane bagasse).

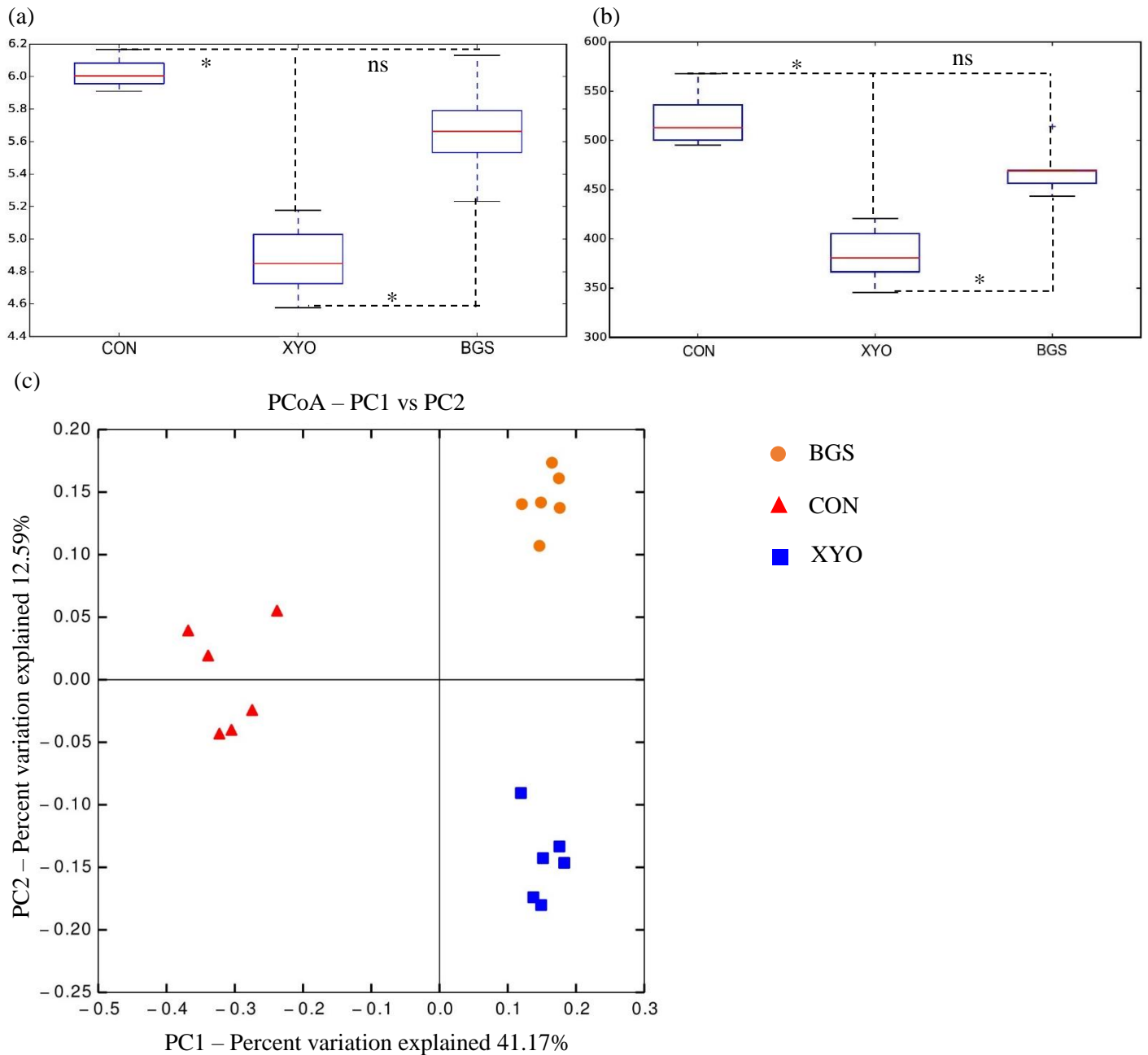


Fig. 5.3. Box and whisker plots of (a) Shannon's diversity index and (b) Observed species index (c) Weighted UniFrac PCoA plot for the β -diversity.

For (a) and (b), values presented are mean \pm SE (n=6) and statistical significance was determined by ANOVA (post hoc Tukey's test); ($p < 0.05$). β -diversity was determined by the weighted UniFrac distance metric in QIIME. (CON, α -corn starch; XYO, commercial xylooligosaccharides (DP 2-3); BGS, water soluble fiber fraction of sugarcane bagasse).

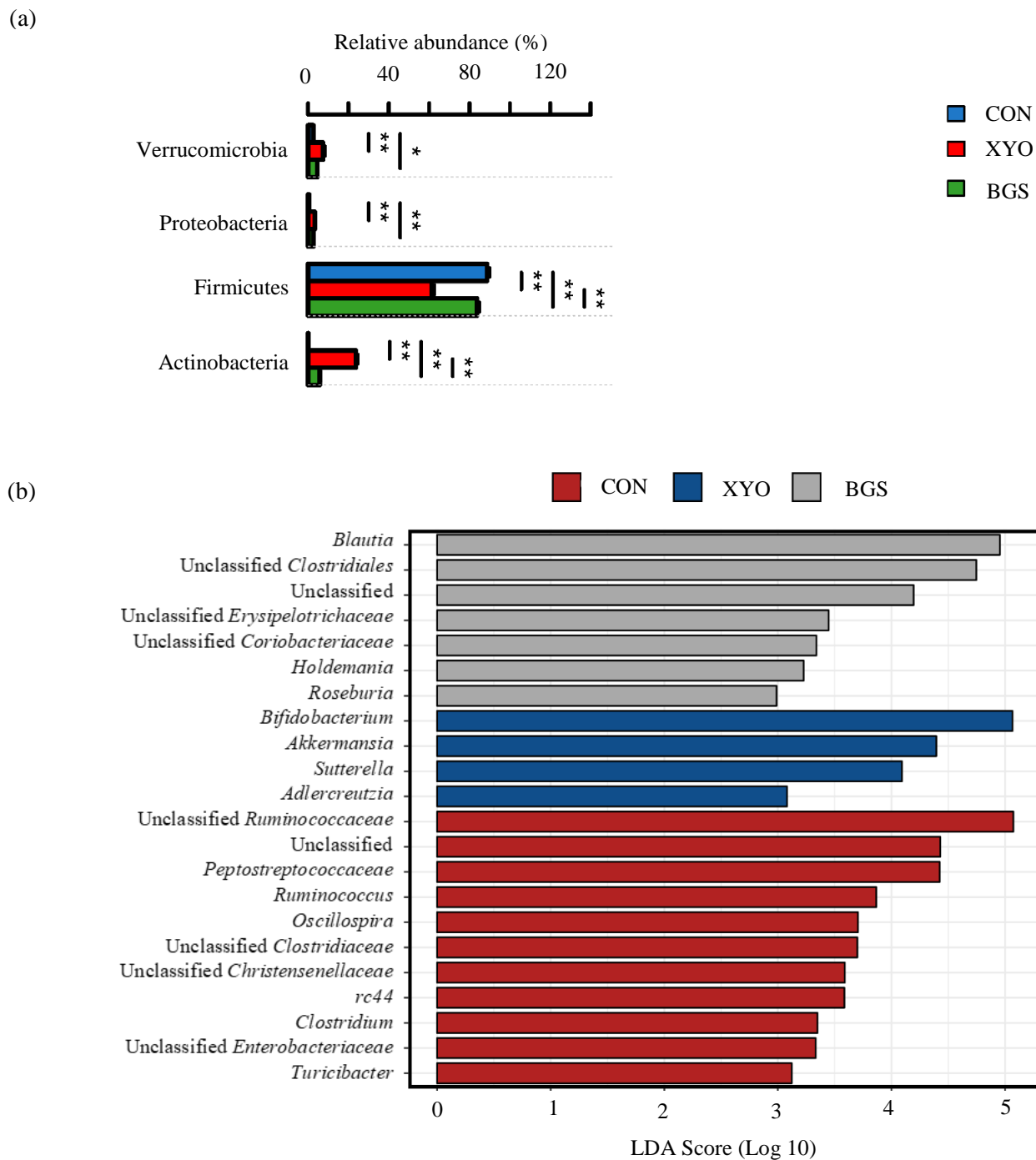


Fig. 5.4. (a) Rank test bar charts for the relative abundance of dominant microbial phyla in the rat cecal digesta and (b) Linear discriminant analysis (LDA) effect size (LEfSe) plot at genus level.

Statistical significance was determined by Kruskal-Wallis H test in Calypso (version 8.72) ($*p < 0.05$; $**p < 0.01$). (CON, α -corn starch; XYO, commercial xylooligosaccharides (DP 2-3); BGS, water soluble fiber fraction of sugarcane bagasse).

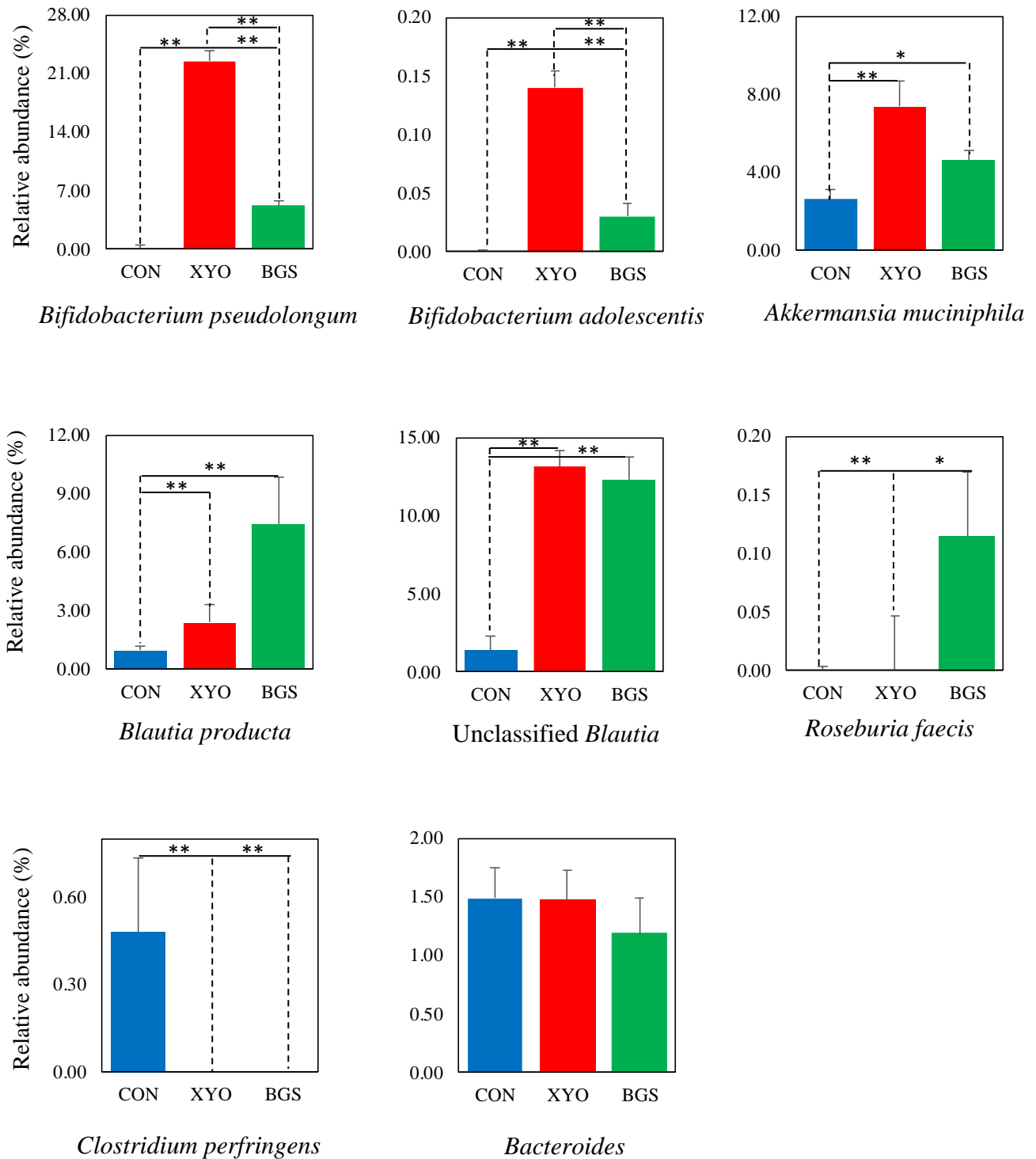


Fig. 5.5. Rank test bar charts for the relative abundance of selected microbial species in the rat cecal digesta.

Statistical significance was determined by Kruskal-Wallis H test in Calypso (version 8.72) (* $p < 0.05$; ** $p < 0.01$). (CON, α -corn starch; XYO, commercial xylooligosaccharides (DP 2-3); BGS, water soluble fiber fraction of sugarcane bagasse).

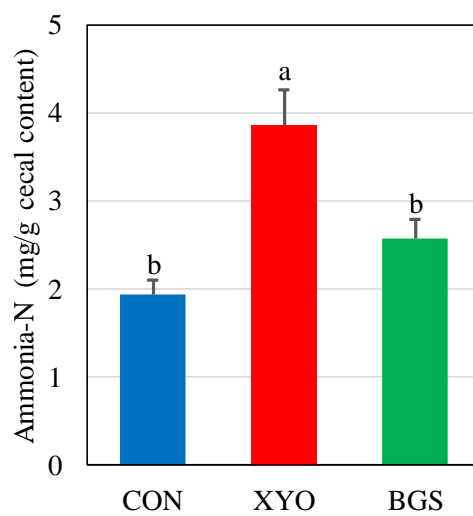


Fig. 5.6. Cecal ammonia-nitrogen content of rats.

Data presented are mean \pm SE (n=6) and different letters represent significant differences among the diet groups at $p < 0.05$. (CON, α -corn starch; XYO, commercial xylooligosaccharides (DP 2-3); BGS, water soluble fiber fraction of sugarcane bagasse).

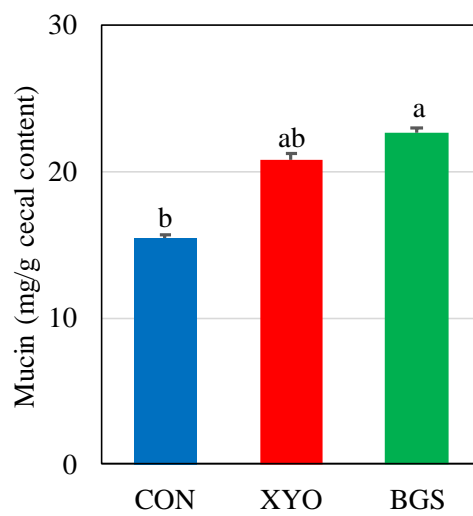


Fig. 5.7. Cecal mucin content of rats.

Data presented are mean \pm SE (n=6) and different letters represent significant differences among the diet groups at $p < 0.05$. (CON, α -corn starch; XYO, commercial xylooligosaccharides (DP 2-3); BGS, water soluble fiber fraction of sugarcane bagasse).

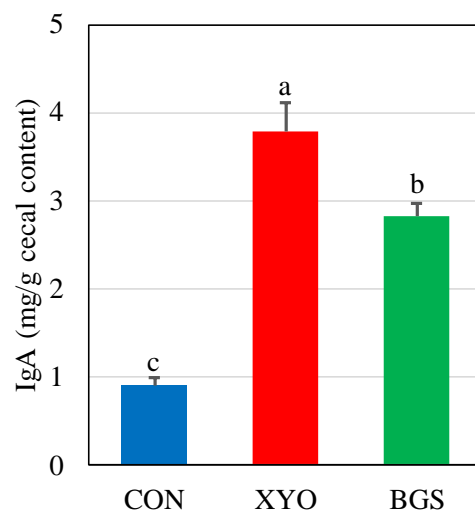


Fig. 5.8. Cecal Immunoglobulin A (IgA) content of rats.

Data presented are mean \pm SE (n=6) and different letters represent significant differences among the diet groups at $p < 0.05$. (CON, α -corn starch; XYO, commercial xylooligosaccharides (DP 2-3); BGS, water soluble fiber fraction of sugarcane bagasse).

Table 5.1. Proximate composition of hydrothermally decomposed bagasse water soluble fraction.

Component	% dwb
Carbohydrate	73.76
Dietary fiber	22.28
Oligosaccharides	51.49
Protein	17.08
Fat	0.25
Ash	8.91

Values presented are % dry weight basis (% dwb) in the concentrated suspension

Table 5.2. Experimental diet composition.

Ingredients (g/kg diet)	Dietary group		
	CON	XYO	BGS
Casein	200	200	200
L-Cystine	3	3	3
Sucrose	100	100	100
Soybean oil	70	70	70
<i>t</i> -Butylhydroquinone	0.014	0.014	0.014
Mineral Mix (AIN-93G-MX)	35	35	35
Vitamin Mix (AIN-93G-VX)	10	10	10
Choline bitartrate	2.5	2.5	2.5
Cellulose	50	0	0
Xylo-oligo 95P	0	50	0
Bagasse soluble fraction	0	0	50
α -Cornstarch	529.486	529.486	529.486
Sum	1000	1000	1000

Abbreviations: CON, α -corn starch; XYO, commercial xylooligosaccharides (DP 2-3); BGS, water soluble fraction of hydrothermally decomposed bagasse containing diet.

Table 5.3. Random groups prepared at the end of the acclimatization period.

Group	G1	G2	G3
	174.4	174.2	173.9
	170.6	172.0	173.2
	170.2	170.1	169.8
	167.9	168.0	169.1
	167.9	167.9	167.8
	166.6	166.7	166.8
Average	169.6	169.8	170.1
SD	2.80	2.85	2.87

Table 5.4. Feed intake, zoometric parameters, organ weight parameters and cecal pH in rats.

Parameter	CON			XYO			BGS		
Feed intake (g/28 days)	379.00	± 7.61	a	351.00	± 4.61	b	363.00	± 5.16	ab
Body weight gain (g/28 days)	68.20	± 3.77	ns	60.30	± 2.31	ns	61.00	± 2.93	ns
Final body weight (g)	237.81	± 4.16	ns	230.14	± 2.99	ns	231.11	± 2.73	ns
Liver weight (g)	8.37	± 0.18	ns	8.05	± 0.23	ns	8.17	± 0.25	ns
Perirenal adipose tissue weight (g)	4.71	± 0.22	ns	4.36	± 0.21	ns	4.68	± 0.20	ns
Epididymal adipose tissue weight (g)	4.79	± 0.23	ns	4.31	± 0.23	ns	4.82	± 0.17	ns
Cecal weight (g)	3.40	± 0.38	b	4.53	± 0.23	a	4.23	± 0.23	ab
Cecal content weight (g)	2.81	± 0.30	ns	3.68	± 0.22	ns	3.49	± 0.21	ns
Cecal tissue weight (g)	0.59	± 0.09	b	0.85	± 0.03	a	0.74	± 0.05	ab
pH	7.69	± 0.06	a	6.66	± 0.08	b	6.58	± 0.07	b

Abbreviations: CON, α -corn starch; XYO, commercial xylooligosaccharides (DP 2-3); BGS, water soluble fraction of hydrothermally decomposed bagasse containing diet; ns; not significant

Values presented are mean \pm SE (n=6); different lowercase letters represent significant differences among the diet groups at $p < 0.05$.

Table 5.5. Fecal fresh and dry weights, moisture content and total lipid content in rats.

Parameter	CON			XYO			BGS		
Fecal fresh weight (g/4 days)	1.38	± 0.13	a	0.6	± 0.04	c	0.98	± 0.06	b
Fecal moisture (% dwb)	25.2	± 3.4	b	39.8	± 1.8	a	39.0	± 3.0	a
Fecal dry weight (g/4 days)	1.02	± 0.05	a	0.36	± 0.02	c	0.59	± 0.02	b
Fecal total lipid (mg/g dry feces)	43.2	± 1.7	b	114.8	± 3.4	a	106.1	± 2.7	a
Fecal total lipid (mg/day)	43.8	± 2.0	b	41.6	± 1.7	b	62.6	± 1.8	a

Abbreviations: CON, α -corn starch; XYO, commercial xylooligosaccharides (DP 2-3); BGS, water soluble fraction of hydrothermally decomposed bagasse containing diet. Values presented are mean \pm SE (n=6); different lowercases letters represent significant differences among the diet groups at $p < 0.05$.

Table 5.6. Serum biochemical parameters at the end of the experimental period in rats.

Parameter	Feed groups											
	CON			XYO			BGS					
Total cholesterol (mmol/L)	1.66	±	0.07	ns	1.54	±	0.06	ns	1.66	±	0.09	ns
HDL-C (mmol/L)	0.48	±	0.02	ns	0.47	±	0.01	ns	0.46	±	0.03	ns
Non-HDL-C (mmol/L)	1.18	±	0.06	ns	1.06	±	0.05	ns	1.19	±	0.06	ns
Triglycerides (mmol/L)	0.98	±	0.04	ns	0.82	±	0.13	ns	0.83	±	0.05	ns
Free Fatty Acids (mmol/L)	10.15	±	0.67	ns	8.91	±	1.02	ns	9.01	±	0.91	ns
Glucose (mmol/L)	5.70	±	0.32	ns	6.63	±	0.24	ns	6.64	±	0.28	ns
Total protein (g/L)	7.43	±	0.07	ns	7.49	±	0.08	ns	7.56	±	0.07	ns
Albumin (g/L)	4.79	±	0.05	ns	4.77	±	0.05	ns	4.87	±	0.04	ns
Alkaline phosphatase (U/L)	732.83	±	18.29	ns	741.17	±	7.30	ns	726.00	±	23.36	ns
GOT (U/L)	165.33	±	4.54	a	169.33	±	10.28	a	131.83	±	5.76	b
GPT (U/L)	37.50	±	0.72	ns	39.17	±	1.51	ns	36.83	±	0.79	ns
Creatine (mg/L)	0.27	±	0.01	ns	0.30	±	0.01	ns	0.29	±	0.00	ns

Abbreviations: HDL-C, high density lipoprotein cholesterol; GOT, Glutamic oxaloacetic transaminase; GPT, Glutamic pyruvic transaminase; ns, not significant. Values presented are mean ± SE (n=6); different lowercase letters represent significant differences among the diet groups at $p < 0.05$.

General Conclusions

In the Chapter 1, it was clearly mentioned that the primary objective of this study was to evaluate agricultural products and by-products for their potential in colonic fermentation and suitability as prebiotic substrates. In this sense, a neglected cereal-sorghum, representing the group of “agricultural products” and sugarcane bagasse, a largely discarded waste material representing “agricultural by-product” class were chosen and studied further.

The *in vitro* study using ileal enzyme resistant fraction of sorghum (ERF) exhibited moderate colonic fermentation ability with moderate levels of SCFAs and higher ammonia-nitrogen production with a higher pH, which were considered as not favorable. Yet, ERF media were characterized by a higher abundance of lactic acid bacteria, exhibiting inconsistency between the known general probiotic effects of lactic acid bacteria and the observations. Thus, using an *in vivo* model, the effects of dietary intervention with raw sorghum was evaluated to confirm the findings of the *in vitro* study and further to observe the effects on physiological parameters. *In vivo* study also revealed similar observations for SCFA, ammonia-nitrogen, pH and microbial abundance as the *in vitro* study. Based on the observations, it was hypothesized that despite the very high RS contents in raw sorghum, due to the recalcitrant nature of sorghum protein fraction, RS might not be accessible for bacterial utilization. Rooting on that, it was aimed to examine the effect of cooking of sorghum on the colonic fermentation potential, as it has been previously revealed that cooking of sorghum further improved RS content. Favorably, cooked sorghum exhibited improved colonic fermentation potentials with improved SCFA production, higher mucin and IgA production and higher RS and dietary fiber utilizing bacterial abundance. Thus, cooking of sorghum improved its potential and suitability as a prebiotic substrate.

On the other hand, water soluble fiber fraction extracted from sugarcane bagasse hemicellulose (predominantly xylan), exhibited significantly and comparatively superior colonic fermentation

characteristics over a well-characterized prebiotic xylooligosaccharides substrate, with significantly higher acetate and total SCFA content, higher mucin and IgA contents, lower cecal pH, abundance of distinctively different microbial classes, etc. The observed differences between bagasse fiber and the commercial xylooligosaccharides were attributed to the distinctively different physicochemical properties in the two xylooligosaccharides substrates.

Thus, with reference to the primary objective, which was, “to evaluate different indigestible plant materials originated from different sources of agricultural products and by-products on their potential to be fermented and to extend beneficial health promoting effects on host”, it was clear that the indigestible plant materials from different botanical sources (agricultural products and by-products), differed in the nature of colonic fermentation, metabolite content and mediated benefits, attributed to their inherent physicochemical properties and processing history. Thus, evaluating the inherent physicochemical properties and processing history of a plant-based food or material might provide an approximate account of its suitability, prior to choosing it as a prebiotic substrate.

References

1. Aachary, A. A. and Prapulla, S. G. (2011). Xylooligosaccharides (XOS) as an emerging prebiotic: Microbial Synthesis, utilization, structural characterization, bioactive properties and applications. *Comprehensive Reviews in Food Science and Food Safety*, 10(1), pp. 2–16.
2. Aarathi, A., Urooj, A. and Puttaraj, S. (2003). In vitro starch digestibility and nutritionally important starch fractions in cereals and their mixtures. *Starch - Stärke*. 55(2), pp. 94–99.
3. Abbeele, P. Van Den., Gérard, P., Rabot, S., Bruneau, A., Aidy, S. E., Derrien, M., Kleerebezem, M., Zoetendal, E. G., Smidt, H., Verstraete, W., Wiele, T. Van de and Possemiers, S. (2011). Arabinoxylans and inulin differentially modulate the mucosal and luminal gut microbiota and mucin-degradation in humanized rats. *Environmental Microbiology*, 13(10), pp. 2667–2680.
4. Ajouz, H., Mukherji, D. and Shamseddine, A. (2014). Secondary bile acids: An underrecognized cause of colon cancer. *World Journal of Surgical Oncology*, 12(1), pp. 1–5.
5. Ashwar, B. A., Gani, A., Wani, I. A., Shah, A., Masoodi, F. A. and Saxena, D. C. (2016). Production of resistant starch from rice by dual autoclaving-retrogradation treatment: Invitro digestibility, thermal and structural characterization. *Food Hydrocolloids*, 56, pp. 108–117.
6. Axtell, J. D., Kirleis, A. W., Hassen, M. M., Mason, N. D'Croze, Mertz, E. T. and Munck, L. (1981). *Proceedings of the National Academy of Sciences of the United States of America-Applied Biology*, 78(3), pp. 1333–1335.
7. Bajaj, J. S., Hylemon, P. B., Ridlon, J. M., Heuman, D., M., Daita, K., White, M. B., Monteith, P., Noble, N. A., Sikaroodi, M. and Gillevet, P. M. (2012). Colonic mucosal microbiome differs from stool microbiome in cirrhosis and hepatic encephalopathy and is linked to cognition and inflammation. *American Journal of Physiology: Gastrointestinal and Liver Physiology*, 303(6), pp. G675–G685.
8. Barcelo, A., Claustre, J., Toumi, F., Burlet, G., Chayvialle, J-A., Cuber, J-C. and Plaisancié, P. (2001). Effect of bile salts on colonic mucus secretion in isolated vascularly perfused rat colon. *Digestive Diseases and Sciences*, 46(6), pp. 1223–1231.
9. Barczynska, R., Jurgoński, A., Silzewska, K., Juśkiewicz, J. and Kapusniał, J. (2017). Effects of potato dextrin on the composition and metabolism of the gut microbiota in rats fed standard and high-fat diets. *Journal of Functional Foods*, 34, pp. 398–407.
10. Benmoussa, M., Suhendra., Aboubacar, A. and Hamaker, B. R. (2006). Distinctive sorghum starch granule morphologies appear to improve raw starch digestibility. *Starch-Staerke*, 58(2), pp. 92–

11. Belzer, C. and De Vos, W. M. (2012). Microbes inside-from diversity to function: The case of *Akkermansia*. *ISME Journal*, 6(8), pp. 1449–1458.
12. den Besten, G., Eunen, K., Groen, A. K., Venema, K., Reijngoud, D-J. and Bakker, B. M. (2013). The role of short-chain fatty acids in the interplay between diet, gut microbiota, and host energy metabolism. *Journal of Lipid Research*, 54(9), pp. 2325–2340.
13. Belton, P. S., Deldadillo, I., Halford, N. G. and Shewry, P. R. (2006). Kafirin structure and functionality. *Journal of Cereal Science*, 44(3), pp. 272–286.
14. Bigetti, K., Costabile, A., Flores, G., Garcia, S. and Gibson, G. R. (2016). *In vitro* fermentation of juçara pulp (*Euterpe edulis*) by human colonic microbiota. *Food Chemistry*, 196, pp. 251–258.
15. Bjørndal, B., Burri, L., Staalesen, V., Skorve, J. and Berge, R. K. (2011). Different adipose depots: Their role in the development of metabolic syndrome and mitochondrial response to hypolipidemic agents. *Journal of Obesity*, 2011(1), id 490650.
16. Birt, D. F., Boylson, T., Hendrich, S., Jane, J-L., Hollis, J., Li, L., McClelland, J., Moore, S., Phillips, G. J., Rowing, M., Schalinske, K., Scott, M. P. and Whitley, E. M. (2013). Resistant Starch : Promise for Improving Human Health. *Advances in Nutrition*, 4, pp. 587–601.
17. Blazek, J. and Gilbert, E. P. (2010). Effect of Enzymatic Hydrolysis on native starch granule structure. *Macromolecules*, 11(12), pp. 3275–3289.
18. Bovee-Oudenhoven, I. M. J., Termont, D. S. M. L. and Meer, R. Van der (1997). Increasing the intestinal resistance of rats to the invasive pathogen *Salmonella enteritidis*: Additive effects of dietary lactulose and calcium. *Gut*, 40(4), pp. 497–504.
19. Buléon, A., Colonna, P. and Ball, S. (1998). Starch granules: Structure and biosynthesis. *International Journal of Biological Macromolecules*, 23(2), pp. 85–112.
20. Brienzo, M., Carvalho, A. F. A., Figueiredo, F. C. and de Olivia Neto, P. (2016). Sugarcane bagasse hemicellulose properties , extraction technologies and xylooligosaccharides production, in Riley, G. L. (ed.) *Food Waste*. New York: Nova Science Publishers Inc., pp. 155-188.
21. Calabrò, S., Carciofi, A. C., Musco, N., Tudisco, R., Gomes, M. O. S. and Cutrignelli, M. I. (2012). Fermentation characteristics of several carbohydrate sources for dog diets using the *in vitro* gas production technique. *Italian Journal of Animal Science*, 12(1), pp. 21–27.
22. Carciofi, A. C., Takakura, F. S., de-Oliveira, L. D., Teshima, E., Jeremias, J. T., Brunetto, M. A. and Prada, F. (2008). Effects of six carbohydrate sources on dog diet digestibility and post-

- prandial glucose and insulin response. *Journal of Animal Physiology and Animal Nutrition*, 92(3), pp. 326–336.
23. Carlson, J. L., Erickson, J. M., Hess, J. M., Gould, T. J. and Slavian, J. L. (2017). Prebiotic dietary fiber and gut health: Comparing the *in vitro* fermentations of beta-glucan, inulin and xylooligosaccharide. *Nutrients*, 9(12), pp. 1360-1377.
 24. Carvalho, A. F. A., de Olivia Neto, P., da Silva, D. F. and Pastore, G. M. (2013). Xylooligosaccharides from lignocellulosic materials: Chemical structure, health benefits and production by chemical and enzymatic hydrolysis. *Food Research International*, 51(1), pp. 75–85.
 25. Saulnier, L., Sado, P-E., Branlard, G., Charmet, G. and Guillon, F. (2007). Wheat arabinoxylans: Exploiting variation in amount and composition to develop enhanced varieties. *Journal of Cereal Science*, 46, pp. 261–281.
 26. Chen, M.-H., Bowman, M. J., Dien, B. S., Rausch, K. D., Tumbleson, M. E. and Singh, V. (2013). Autohydrolysis of *Miscanthus x giganteus* for the production of xylooligosaccharides (XOS): Kinetics, characterization and recovery. *Bioresource Technology*, 155C, pp. 359–365.
 27. Chen, W., Liu, F., Ling, Z., Tong, X. and Xiang, C. (2012). Human intestinal lumen and mucosa-associated microbiota in patients with colorectal cancer. *PLoS ONE*, 7(6), pp. e39743.
 28. Chibber, B. A. K., Mertz, E. T. and Axtell, J. D. (1980). *In Vitro* digestibility of high-tannin sorghum at different stages of dehulling. *Journal of Agricultural and Food Chemistry*, 28(1), pp. 160–161.
 29. Chen, X., He, X., Fu, X. and Huang, Q. (2015). *In vitro* digestion and physicochemical properties of wheat starch/flour modified by heat-moisture treatment. *Journal of Cereal Science*, 63, pp. 109–115.
 30. Cho, G. S., Ritzmann, F., Eckstein, M., Huch, M., Briviba, K., Behnlian, D., Neve, H. and Franz, C. M. A. P. (2016). Quantification of *Slackia* and *Eggerthella* spp. in human feces and adhesion of representatives strains to Caco-2 cells. *Frontiers in Microbiology*, 7(May), pp. 1–10.
 31. Chung, H.-J., Liu, Q. and Hoover, R. (2009). Impact of annealing and heat-moisture treatment on rapidly digestible, slowly digestible and resistant starch levels in native and gelatinized corn, pea and lentil starches. *Carbohydrate Polymers*, 75(3), pp. 436–447.
 32. Collado, M. C., Isolauri, E., Laitinen, K. and Salminen, S. (2008). Distinct composition of gut microbiota during pregnancy in overweight and normal-weight women. *American Journal of Clinical Nutrition*, 88(August), pp. 894–899.

33. Conlon, M. A. and Bird, A. R. (2015). The impact of diet and lifestyle on gut microbiota and human health. *Nutrients*, 7(1), pp. 17–44.
34. Cox R. A., Mario, R. and Palmieri, G. (1990). Cholesterol, Triglycerides, and Associated Lipoproteins, in Walker, H. K., Hall, W. D., Hurst, J. W. (ed.) *Clinical Methods: The History, Physical, and Laboratory Examinations*. Boston: Butterworths.
35. Crittenden, R., Karpunen, S., Ojanen, S., Tenkanen, M., Fagerström, R., Mättö, J., Saarela, M., Mattila-Sandholm, T. and Poutanen, K. (2002). *In vitro* fermentation of cereal dietary fibre carbohydrates by probiotic and intestinal bacteria. *Journal of the Science of Food and Agriculture*, 82(8), pp. 781–789.
36. Crost, E. H., Tailford, L. E., Monestier, M., Swarbreck, D., Henrissat, B., Crossman, L. C. and Juge, N. (2016). The mucin-degradation strategy of *Ruminococcus gnavus*: The importance of intramolecular trans-sialidases. *Gut Microbes*, 7(4), pp. 302–312.
37. Crost, E. H., Tailford, L. E., Gall, G. L., Fons, M., Henrissat, B. and Juge, N. (2013). Utilisation of mucin glycans by the human gut symbiont *Ruminococcus gnavus* is strain-dependent. *PLoS ONE*, 8(10), pp. e76341.
38. Crowther, R. S. and Wetmore, R. F. (1987). Fluorometric assay of O-linked glycoproteins by reaction with 2-cyanoacetamide. *Analytical Biochemistry*, 163(1), pp. 170–174.
39. Dai, Z. L., Wu, G. and Zhu, W. Y. (2011). Amino acid metabolism in intestinal bacteria: Links between gut ecology and host health. *Frontiers in Bioscience*, 16(5), pp. 1768–1786.
40. Davila, A.M., Blachier, F., Gotteland, M., Andriamihaja, M., Benetti, P. H., Sanz, Y. and Tomé D. (2013). Intestinal luminal nitrogen metabolism: Role of the gut microbiota and consequences for the host. *Pharmacological Research*, 68(1), pp. 95–107.
41. Dawson, A. M. (1978). Regulation of blood ammonia. *Gut*, 19(6), pp. 504–509.
42. Derrien, M., Baarlen, P. V., Hooiveld, G., Norin, E., Müller, M. and de Vos, W. M. (2011). Modulation of mucosal immune response, tolerance, and proliferation in mice colonized by the mucin-degrader *Akkermansia muciniphila*. *Frontiers in Microbiology*, 2(August), pp. 1–14.
43. Donaldson, G. P., Lee, S. M. and Mazmanian, S. K. (2017). Gut biogeography of the bacterial microbiota. *Nature Reviews Microbiology*, 14(1), pp. 20–32.
44. Duodu, K. G., Taylor, J. R. N., Belton, P. S. and Hamaker, B. R. (2003). Factors affecting sorghum protein digestibility. *Journal of Cereal Science*, 38(2), pp. 117–131.
45. Ebringerová, A., Hromádková, Z. and Heinze, T. (2005). Hemicellulose. *Advances in Polymer*

Science, 186, pp. 1–67.

46. Egshatyan, L. V., Kashtanova, D., Popenko, A., Tkacheva, O., Tyakht, A., Alexeev, D., Karamnova, N., Kostryukova, E., Babenko, V., Vakhitova, M. and Boytsov, S. (2015). Gut microbiota and diet in patients with different glucose tolerance. *Endocrine Connections*, 5, pp. 1-9.
47. Eichele, D. D. and Kharbanda, K. K. (2017). Dextran sodium sulfate colitis murine model: An indispensable tool for advancing our understanding of inflammatory bowel diseases pathogenesis. *World Journal of Gastroenterology*, 23(33), pp. 6016–6029.
48. Elkalifa, A. E. O., Bernhardt, R., Bonomi, F., Lametti, S., Pagani, M. A. and Zardi, M. (2006). Fermentation modifies protein/protein and protein/starch interactions in sorghum dough. *European Food Research and Technology*, 222, pp. 559–564.
49. Emmambux, M. N. and Taylor, J. R. N. (2009). Properties of heat-treated sorghum and maize meal and their prolamin proteins. *Journal of Agricultural and Food Chemistry*, 57(3), pp. 1045–1050.
50. Wolpert, E., Phillips, S. F. and Summerskill, W. H. (1971). Transport of urea and ammonia production in the human colon. *The Lancet*, 298(7739), pp. 1387–1390.
51. Eren, A. M., Sogin, M. L., Morrison, H. G., Vineis, J. H., Fisher, J. C., Newton, R. J. and McLellan, S. L. (2015). A single genus in the gut microbiome reflects host preference and specificity. *ISME Journal*, 9(1), pp. 90–100.
52. Ezeogu, L., Duodu, G. and Taylor, J. R. N. (2005). Effects of endosperm texture and cooking conditions on the *in vitro* starch digestibility of sorghum and maize flours. *Journal of Cereal Science*, 42(1), pp. 33–44.
53. Fernández, J., Redondo-Blanco, S., Gutiérrez-del-Río, I., Miguélez, E. M., Villar, C. J. and Lombó, F. (2016). Colon microbiota fermentation of dietary prebiotics towards short-chain fatty acids and their roles as anti-inflammatory and antitumour agents: A review. *Journal of Functional Foods*, 25, pp. 511–522.
54. Finn-eirik, J., Pekna, M., Norderhaug, I. N., Haneberg, B., Hietala, M. A., Krajci, P., Betsholtz, C. and Brandtzaeg, P. (1999). Absence of epithelial immunoglobulin a transport, with increased mucosal leakiness, in polymeric immunoglobulin receptor/secretory component-deficient mice. *Journal of Experimental Medicine*, 190(7), pp. 915–921.
55. Folch, J., Lees, M. and Stanley, G. H. S. (1957). A simple method for the isolation and purification of total lipids from animal tissues. *Journal of Biological Chemistry*, 222, pp. 497-509.

56. Frohnert, B. I., Jacobs Jr., D. R., Steinberger, J., Moran, A., Steffen, L. M. and Sinaiko, A. R. (2013). Relation between serum free fatty acids and adiposity, insulin resistance, and cardiovascular risk factors from adolescence to adulthood. *Diabetes*, 62(September), pp. 3163–3169.
57. Fukuda, S., Toh, H., Hase, K., Oshima, K., Nakanishi, Y., Yoshimura, K., Tobe, T., Clarke, J. M., Topping, D. L., Suzuki, T., Taylor, T. D., Itoh, K., Kikuchi, J., Morita, H., Hattori, M. and Ohno, H. (2011). Bifidobacteria can protect from enteropathogenic infection through production of acetate. *Nature*, 469(7331), pp. 543–547.
58. Ghaffarzadegan, T., Zhong, Y., Hållenius, F. F. and Nyman, M. (2018). Effects of barley variety, dietary fiber and β -glucan content on bile acid composition in cecum of rats fed low- and high-fat diets', *Journal of Nutritional Biochemistry*, 53, pp. 104–110.
59. Gibson, G. R., Probert, H. M., Loo, J. V., Rastall, R. A. and Roberfroid, M. B. (2004). Dietary modulation of the human colonic microbiota: updating the concept of prebiotics. *Nutrition Research Reviews*, 17(2), pp. 259-275.
60. Giuberti, G., Gallo, M., Moschini, M. and Masoero, F. (2013). *In vitro* production of short-chain fatty acids from resistant starch by pig faecal inoculum. *Animal*, 7(9), pp. 1446–1453.
61. Gobinath, D., Madhu, A. N., Prashant, G., Sirinivasan, K. and Prapulla, S. G. (2010). Beneficial effect of xylo-oligosaccharides and fructo-oligosaccharides in streptozotocin-induced diabetic rats. *British Journal of Nutrition*, 104(1), pp. 40–47.
62. Goldsmith, F., Guice, J., Page, R., Welsh, D. A., Taylor, C. M., Blanchard, E. E., Luo, M., Raggio, A. M., Stout, R. W., Carvajal-Aldaz, D., Gaither, A., Pelkman, C., Ye, J., Martin, R. J., Geaghan, J., Durham, H. A., Coulon, D. and Keenan, M. (2017). Obese ZDF rats fermented resistant starch with effects on gut microbiota but no reduction in abdominal fat. *Molecular Nutrition & Food Research*, 61(1), pp. 1–9 (1501025).
63. Grundy, S. M., Ahrens, E. H. and Miettinen, T. A. (1965). Quantitative isolation and gas-liquid chromatographic analysis of total fecal bile acids. *Journal of lipid research*, 6, pp. 397–410.
64. Grootaert, C., Delcour, J. A., Courtin, C. M., Broekaert, W. F., Verstraete, W. and Van de Wiele, T. (2007). Microbial metabolism and prebiotic potency of arabinoxylan oligosaccharides in the human intestine. *Trends in Food Science and Technology*, 18(2), pp. 64–71.
65. Guergoletto, K. B., Costabile, A., Flores, G., Garcia, S. and Gibson, G. R. (2016). *In vitro* fermentation of juçara pulp (*Euterpe edulis*) by human colonic microbiota. *Food Chemistry*. 196,

pp. 251–258.

66. Gutzeit, C., Magri, G. and Cerutti, A. (2014). Intestinal IgA production and its role in host-microbe interaction. *Immunological Reviews*, 260(1), pp. 1–23.
67. Hamaker, B. R., Mohamed, A. A., Habben, J. E., Huang, C. P. and Larkins, B. A. (1995). Efficient method for extracting maize and sorghum kernel proteins reveals higher prolamin contents than the conventional method. *Cereal Chemistry*, 72, pp. 583–588.
68. Hamaker, B. R., Kirleis, A. W., Butler, L. G., Axtell, J. D. and Mertz, E. T. (1987). Improving the *in vitro* protein digestibility of sorghum with reducing agents. *Proceedings of the National Academy of Sciences*, 84(3), pp. 626–628.
69. Han, K-H., Lee, C-H., Kinoshita, M., Oh, C-H., Shimada, K. and Fukushima, M. (2016). Spent turmeric reduces fat mass in rats fed a high-fat diet. *Food and Function*, 7(4), pp. 1814–1824.
70. Han, K-H., Azuma, S. and Fukushima, M. (2014). *In vitro* fermentation of spent turmeric powder with a mixed culture of pig faecal bacteria. *Food and Function*, 5(10), pp. 2446–2452.
71. Han, X. Z., Benmoussa, M., Gray, J. A., BeMiller, J. N. and Hamaker, B. R. (2005). Detection of proteins in starch granule channels. *Cereal Chemistry*, 82(4), pp. 351–355.
72. Hara, H. (2002). Physiological effects of short-chain fatty acid produced from prebiotics in the colon. *Bioscience and Microflora*, 21(1), pp. 35–42.
73. Haralampu, S. G. (2000). Resistant starch—a review of the physical properties and biological impact of RS 3. *Carbohydrate Polymers*, 41(3), pp. 285–292.
74. Hatzioanou, D., Mayer, M. J., Duncan, S. H., Flint, H. J. and Nisbaid, A. (2013). A representative of the dominant human colonic Firmicutes, *Roseburia faecis* M72/1, forms a novel bacteriocin-like substance. *Anaerobe*, 23, pp. 5–8.
75. Hegyi, P., Maléth, J., Walters, J. R., Hofmann, A. F. and Keely, S. J. (2018). Guts and gall: Bile acids in regulation of intestinal epithelial function in health and disease. *Physiological Reviews*, 98(4), pp. 1983–2023.
76. Hernández, M. A. G., Canfora, E. E., Jocken, J. W. E. and Blaak, E. E. (2019). The Short-Chain Fatty Acid Acetate in Body Weight Control and Insulin Sensitivity. *Nutrients*, 11(8), pp. 1943–1951.
77. Hopkins, M. J., Cummings, J. H. and Macfarlane, G. T. (1998). Inter-species differences in maximum specific growth rates and cell yields of bifidobacteria cultured on oligosaccharides and other simple carbohydrate sources. *Journal of Applied Microbiology*, 85(2), pp. 381–386.

78. Hsu, C-K., Liao, J-W., Chung, Y-C., Hsieh, C-P. and Chan, Y-C. (2004). Xylooligosaccharides and fructooligosaccharides affect the intestinal microbiota and precancerous colonic lesion development in rats. *Journal of Nutrition*, 134(December), pp. 1523–1528.
79. Huazano-García, A., Shin, H. and López, M. G. (2017). Modulation of gut microbiota of overweight mice by agavins and their association with body weight loss. *Nutrients*, 9(9), pp. 1-13 (2017070026).
80. Illumina (2013). 16S Metagenomic Sequencing Library', *Illumina.com*, (B), pp. 1–28. http://support.illumina.com/content/dam/illumina-support/documents/documentation/chemistry_documentation/16s/16s-metagenomic-library-prep-guide-15044223-b.pdf.
81. Kaur, A., Tuncil, Y. E., Sikaroodi, M., Gillevet, P., Patterson, J. A., Keshavarzian, A. and Hamaker, B. R. (2018). Alterations in the amounts of microbial metabolites in different regions of the mouse large intestine using variably fermentable fibres. *Bioactive Carbohydrates and Dietary Fibre*, 13(January), pp. 7-13.
82. Kaur, J. (2014). A comprehensive review on metabolic syndrome. *Cardiology Research and Practice*, 2014(March), pp. 1-21 (943162).
83. Kieffer, D. A., Martin, R. J. and Adams, S. H. (2016). Impact of dietary fibers on nutrient management and detoxification organs : Gut, Liver, Kidney. *Advances in Nutrition*, 7, pp. 1111–1121.
84. Kim, B. R., Shin, J., Guevarra, R. B., Lee, J. H., Kim, D. W., Seol, K-H., Lee, J-H., Kim, H. B. and Isaacson, R. E. (2017). Deciphering diversity indices for a better understanding of microbial communities. *Journal of Microbiology and Biotechnology*, 27(12), pp. 2089–2093.
85. Kimura, I., Ozawa, K., Inoue, D., Imamura, T., Kimura, K., Maeda, T., Terasawa, K., Kashihara, D., Hirano, K., Tani, T., Takahashi, T., Miyauchi, S., Shioi, G., Inoue, H. and Tsujimoto, G. (2013). The gut microbiota suppresses insulin-mediated fat accumulation via the short-chain fatty acid receptor GPR43. *Nature Communications*, 4(May), pp. 1–12 (1829).
86. Koh, A., Vadder, F. D., Kovatcheva-Datchary, P. and Bäckhed, F. (2016). From dietary fiber to host physiology: Short-chain fatty acids as key bacterial metabolites. *Cell*, 165(6), pp. 1332–1345.
87. LeBoeuf, R. C., Caldwell, M. and Kirk, E. (1994). Regulation by nutritional status of lipids and apolipoproteins A-I, A-II, and A-IV in inbred mice. *Journal of Lipid Research*, 35(1), pp. 121–133.

88. Li, L., Ma, L. and Fu, P. (2017). Gut microbiota – derived short-chain fatty acids and kidney diseases. *Drug Design, Development and Therapy*, 11, pp. 3531–3542.
89. Li, X., Watanabe, K. and Kimura, I. (2017). Gut microbiota dysbiosis drives and implies novel therapeutic strategies for diabetes mellitus and related metabolic diseases. *Frontiers in Immunology*, 8(December), pp. 1–7.
90. Lichtenwalner, R. E., Ellis, E. B. and Rooney, L. W. (1978). Effect of incremental dosages of the waxy gene of sorghum on digestibility. *Journal of Animal Science*, 46(4), pp. 1113–1119.
91. Liu, H., Guo, X., Li, W., Wang, X., Iv, M., Peng, Q. and Wang, M. (2015). Changes in physicochemical properties and in vitro digestibility of common buckwheat starch by heat-moisture treatment and annealing. *Carbohydrate Polymers*, 132, pp. 237–244.
92. Liu, C., Finegold, S. M., Song, Y. and Lawson, P. A. (2008). Reclassification of *Clostridium coccooides*, *Ruminococcus hansenii*, *Ruminococcus hydrogenotrophicus*, *Ruminococcus luti*, *Ruminococcus productus* and *Ruminococcus schinkii* as *Blautia coccooides* gen. nov., comb. nov., *Blautia hansenii* comb. nov., *Blautia hydrogenotrophica* comb. nov., *Blautia luti* comb. nov., *Blautia producta* comb. nov., *Blautia schinkii* comb. nov. and description of *Blautia wexlerae* sp. nov., isolated from human faeces. *International Journal of Systematic and Evolutionary Microbiology*, 58(8), pp. 1896–1902.
93. Liu, Q. *et al.* (2002). Phase transition in potato starch-water system I. Starch gelatinization at high moisture level. *Food Research International*, 35(4), pp. 397–407.
94. Louis, P. and Flint, H. J. (2009). Diversity, metabolism and microbial ecology of butyrate-producing bacteria from the human large intestine. *FEMS Microbiology Letters*, 294(1), pp. 1–8.
95. Lozupone, C. A., Stombaugh, J. I., Gordon, J. I., Jansson, J. K. and Knight, R. (2012). Diversity, stability and resilience of the human gut microbiota. *Nature*, 489(7415), pp. 220–230.
96. Lu, Y., Fan, C., Li, P., Lu, Y., Chang, X. and Qi, K. (2016). Short chain fatty acids prevent high-fat-diet-induced obesity in mice by regulating g protein-coupled receptors and gut Microbiota. *Scientific Reports*, 6(October), pp. 1–13 (37589).
97. Lv, Z-H., Ma, P., Luo, W., Xiong, H., Han, L., Li, S-W., Zhou, X. and Tu, J-C. (2014). Association between serum free fatty acid levels and possible related factors in patients with type 2 diabetes mellitus and acute myocardial infarction. *BMC Cardiovascular Disorders*, 14(November), pp. 1–7 (159).
98. Macfarlane, G. T. and Macfarlane, S. (2012). Bacteria, colonic fermentation, and gastrointestinal

- health. *Journal of AOAC International*, 95(1), pp. 50–60.
99. Macfarlane, G. T., Cummings, J. H. and Allison, C. (1986). Protein degradation by human intestinal bacteria. *Journal of Genetic Microbiology*, 132(6), pp. 1647–1656.
100. Madhukumar, M. S. and Muralikrishna, G. (2012). Fermentation of xylo-oligosaccharides obtained from wheat bran and Bengal gram husk by lactic acid bacteria and bifidobacteria. *Journal of Food Science and Technology*, 49(6), pp. 745–752.
101. Mantis, N. J., Rol, N. and Corthésy, B. (2011). Secretory IgA's complex roles in immunity and mucosal homeostasis in the gut. *Mucosal Immunology*, 4(6), pp. 603–611.
102. Martínez, I., Kim, J., Duffy, P. R., Schlegel, V. L. and Walter, J. (2010). Resistant starches types 2 and 4 have differential effects on the composition of the fecal microbiota in human subjects. *PLoS ONE*, 5(11), pp. 1-11 (e15046).
103. Matsubara, Y., Sawabe, A. and Iizuka, Y. (1990). Structures of new limonoid glycosides in lemon (*Citrus limon* BURM. f.) Peelings. *Agricultural and Biological Chemistry*, 54(5), pp. 1143–1148.
104. de Mesa-Stonestreet, N. J., Alavi, S. and Bean, S. R. (2010). Sorghum proteins: The concentration, isolation, modification, and food applications of kafirins. *Journal of Food Science*, 75(5), pp. R90-R104.
105. Montagne, L., Pluske, J. R. and Hampson, D. J. (2003). A review of interactions between dietary fibre and the intestinal mucosa, and their consequences on digestive health in young non-ruminant animals. *Animal Feed Science and Technology*, 108, pp. 95–117.
106. Morales, J., Pérez, J. F., Martín-Orúe, S. M., Fondevila, M. and Gasa, J. (2002). Large bowel fermentation of maize or sorghum–acorn diets fed as a different source of carbohydrates to Landrace and Iberian pigs. *British Journal of Nutrition*, 88(5), pp. 489–497.
107. Müntz, K. (1996). Proteases and proteolytic cleavage of storage proteins in developing and germinating dicotyledonous seeds. *Journal of Experimental Botany*, 47(298), pp. 605–622.
108. Saravanabavan, S. N., Shivanna, M. M. and Bhattacharya, S. (2013). Effect of popping on sorghum starch digestibility and predicted glycemic index. *Journal of Food Science and Technology*, 50(2), pp. 387–392.
109. Neis, E. P. J. G., Dejong, C. H. C. and Rensen, S. S. (2015). The role of microbial amino acid metabolism in host metabolism. *Nutrients*, 7, pp. 2930–2946.
110. Niba, L. L. and Hoffman, J. (2003). Resistant starch and β -glucan levels in grain sorghum

- (*Sorghum bicolor* M.) are influenced by soaking and autoclaving. *Food Chemistry*, 81(1), pp. 113–118.
111. O’Callaghan, A. and van Sinderen, D. (2016). Bifidobacteria and their role as members of the human gut microbiota. *Frontiers in Microbiology*, 7(June), pp. 1-23 (925).
 112. O’Flaherty, S., Saulnier, D. M., Pot, B. and Versalovic, J. (2010). How can probiotics and prebiotics impact mucosal immunity?. *Gut Microbes*, 1(5), pp. 293–300.
 113. Oria, M. P., Hamaker, B. R. and Shull, J. M. (1995). Resistance of Sorghum α -, β -, and γ -Kafirins to pepsin digestion. *Journal of Agricultural and Food Chemistry*, 43(8), pp. 2148–2153.
 114. Ottman, N., Geerlings, S. Y., Aalvink, S., de Vos, W. M. and Belzer, C. (2017). Action and function of *Akkermansia muciniphila* in microbiome ecology, health and disease. *Best Practice and Research: Clinical Gastroenterology*, 31(6), pp. 637–642.
 115. Ottman, N., Smidt, H., de Vos, W. M. and Belzer, C. (2012). The function of our microbiota: who is out there and what do they do?. *Frontiers in cellular and infection microbiology*, 2(August), pp. 1-11 (104).
 116. Pantaleão, L. C., Murata, G., Teixeira, C. J., Payolla, T. B., Santos-Silva, J. C., Duque-Guimaraes, D. E., Sodré, F. S., Lellis-Santos, C., Vieira, J. C., de Souza, D. N., Gomes, P. R., Rodrigues, S. C., Anhe, G. F. and Bordin, S. (2017). Prolonged fasting elicits increased hepatic triglyceride accumulation in rats born to dexamethasone-Treated mothers. *Scientific Reports*, 7(1), pp. 1–11 (10367).
 117. Pelpolage, S. W., Kyuho, H., Koaze, H., Hamamoto, T., Hoshizawa, M. and Fukushima, M. (2019). Influence of enzyme-resistant fraction of sorghum (*Sorghum bicolor* L.) flour on gut microflora composition , short chain fatty acid production and toxic substance metabolism. *Journal Of Food And Nutrition Research*, 58(2), pp. 135–145.
 118. Pelpolage, S., Nakata, K., Shinbayashi, Y., Murayama, D., Tani, M., Yamauchi, H. and Koaze, H. (2016). Comparison of pasting and thermal properties of starches isolated from four processing type potato varieties cultivated in two locations in Hokkaido. *Food Science and Technology Research*, 22(5), pp. 687-693.
 119. Perera, A., Meda, V. and Tyler, R. T. (2010). Resistant starch: A review of analytical protocols for determining resistant starch and of factors affecting the resistant starch content of foods. *Food Research International*, 43(8), pp. 1959–1974.
 120. Pessione, E. (2012). Lactic acid bacteria contribution to gut microbiota complexity: lights and

- shadows. *Frontiers in cellular and infection microbiology*, 2(June), pp. 1-15 (86).
121. Poquette, N. M., Gu, X. and Lee, S-O. (2014). Grain sorghum muffin reduces glucose and insulin responses in men. *Food and Function*, 5(5), pp. 894–899.
 122. Qi, Y., Jiang, C., Cheng, J., Krausz, K. W., Li, T., Ferrell, J. M., Gonzalez, F. J. and Chiang, J. Y. L. (2015). Bile acid signaling in lipid metabolism: Metabolomic and lipidomic analysis of lipid and bile acid markers linked to anti-obesity and anti-diabetes in mice. *Biochimica Biophysica Acta*, 1851(1), pp. 19–29.
 123. Rafii, F. (2015). The role of colonic bacteria in the metabolism of the natural isoflavone daidzin to equol. *Metabolites*, 5(1), pp. 56–73.
 124. Ragaee, S., Abdel-Aal, E. S. M. and Noaman, M. (2006). Antioxidant activity and nutrient composition of selected cereals for food use. *Food Chemistry*, 98(1), pp. 32–38.
 125. Ridlon, J. M., Kang, D. J., Hylemon, P. B. and Bajaj, J. S. (2014). Bile acids and the gut microbiome. *Current Opinion in Gastroenterology*, 30(3), pp. 332–338.
 126. Ríos-Covián, D., Ruas-Madiedo, P., Margolles, A., Gueimonde, M., de los Reyes-Gavilán, C. G. and Salazar, N. (2016). Intestinal short chain fatty acids and their link with diet and human health. *Frontiers in Microbiology*, 7(February), pp. 1–9 (185).
 127. Rivière, A., Selak, M., Lantin, D., Leroy, F. and Vuyst, L. D. (2016). Bifidobacteria and butyrate-producing colon bacteria: Importance and strategies for their stimulation in the human gut. *Frontiers in Microbiology*, 7(June), pp. 1-21 (979).
 128. Rodríguez, J. M., Murphy, K., Stanton, C., Ross, R. O., Kober, O. I., Juge, N., Avershina, E., Rudi, K., Narbad, A., Jenmalm, M. C., Marchesi, J. R. and Collado, M. C. (2015). The composition of the gut microbiota throughout life, with an emphasis on early life. *Microbial Ecology in Health and Disease*, 26(), pp. 1-17 (26050).
 129. Rooney, L. W. and Pflugfelder, R. L. (1986). Factors affecting starch digestibility with special emphasis on sorghum and corn. *Journal of animal science*, 63(5), pp. 1607–1623.
 130. Roura, E., Koopmans, S-J., Lallès, J-P., Huerou-L., de Jager, N., Schuurman, T. and Val-Laillet, D. (2016). Critical review evaluating the pig as a model for human nutritional physiology. *Nutrition Research Reviews*, 29(1), pp. 60–90.
 131. Rowland, I., Gibson, G., Heinken, A., Scott, K., Swann, J., Thiele, I. and Tuohy, K. (2018). Gut microbiota functions: metabolism of nutrients and other food components. *European Journal of Nutrition*, 57(1), pp. 1–24.

132. Sajilata, M. G., Singhal, R. S. and Kulkarni, P. R. (2006). Resistant starch-A review. *Comprehensive Reviews in Food Science and Food Safety*, 5(1), pp. 1–17.
133. Samanta, A. K., Jayapal, N., Jayaram, C., Roy, S., Kolte, A. P., Senani, S. and Sridar, M. (2015). Xylooligosaccharides as prebiotics from agricultural by-products: Production and applications. *Bioactive Carbohydrates and Dietary Fibre*, 5(1), pp. 62–71.
134. Samanta, A. K., Jayapal, N., Kolte, A. P., Senani, S., Sridar, M., Suresh, K. P. and Sampath, K. T. (2012). Bioresource Technology Enzymatic production of xylooligosaccharides from alkali solubilized xylan of natural grass (*Sehima nervosum*). *Bioresource Technology*, 112, pp. 199–205.
135. Sang, Y., Bean, S., Seib, P. A., Pedersen, J. and Shi, Y-C. (2008). Structure and functional properties of sorghum starches differing in amylose content. *Journal of Agricultural and Food Chemistry*, 56(15), pp. 6680–6685.
136. Seung, J. C., Woo, H. D., Ko, S. H. and Moon, T. W. (2008). Confocal laser scanning microscopy to investigate the effect of cooking and sodium bisulfite on in vitro digestibility of waxy sorghum flour. *Cereal Chemistry*, 85(1), pp. 65–69.
137. Scott, K. P., Gratz, S. W., Sheridan, P. O., Flint, H. J., Duncan, S. H. (2013). The influence of diet on the gut microbiota. *Pharmacological Research*, 69, pp. 52–60.
138. Shen, R. L., Zhang, W-L., Dong, J-L., Ren, G-X. and Chen, M. (2015). Sorghum resistant starch reduces adiposity in high-fat diet-induced overweight and obese rats via mechanisms involving adipokines and intestinal flora. *Food and Agricultural Immunology*, 26(1), pp. 120–130.
139. Sheridan, P. O., Martin, J. C., Lawley, T. D., Browne, H. P., Harris, H. M. B., Bernailler-Donadille, A., Duncan, S. H., O'Toole, P. W., Scott, K. P. and Flint, H. J. (2016). Polysaccharide utilization loci and nutritional specialization in a dominant group of butyrate-producing human colonic Firmicutes. *Microbial Genomics*, 2(2), pp. 1-16 (e000043).
140. Shewry, P. R. and Tatham, A. S. (1990). The prolamin storage proteins of cereal seeds: structure and evolution. *Biochemical Journal*, 267(1), pp. 1–12.
141. Shull, J. M., Watterson, J. J. and Kirleis, A. W. (1991). Proposed nomenclature for the alcohol-soluble proteins (kafirins) of *Sorghum bicolor* (L. Moench) based on molecular weight, solubility, and structure. *Journal of Agricultural and Food Chemistry*, 39(1), pp. 83–87.
142. Smiricky-Tjardes, M., Flickinger, E. A., Grieshop, C. M., Bauer, L. L., Murphy, M. R. and Fahey, G. C. (2003). *In vitro* fermentation characteristics of selected oligosaccharides by swine fecal microflora. *Journal of Animal Science*, 81, pp. 2505–2514.

143. Souilah, R., Djabali, D., Belhadi, B., Mokrane, H., Boudries, N. and Nadjemi, B. (2014). *In vitro* starch digestion in sorghum flour from Algerian cultivars. *Food Science and Nutrition*, 2(3), pp. 251–259.
144. Taciak, M., Barszcz, M., Tu nio, A. and Pastuszewska, B. (2015). Interactive effects of Indigestible carbohydrates , protein Type , and protein level on biomarkers of large intestine health in rats. *PLoS ONE*, pp. 1–17.
145. Tailford, L. E., Crost, E. H., Kavanaugh, D. and Juge, N. (2015). Mucin glycan foraging in the human gut microbiome. *Frontiers in Genetics*, 6(March), pp. 1-18 (81).
146. Taghipour, N., Molaei, M., Mosaffa, N., Rostami-Nejad, M., Aghdaei, H. A., Anissian, A., Azimzadeh, P. and Zali, M. R. (2016). An experimental model of colitis induced by dextran sulfate sodium from acute progresses to chronicity in C57BL/6: Correlation between conditions of mice and the environment. *Gastroenterology and Hepatology from Bed to Bench*, 9(1), pp. 45–52.
147. Tan, L. R., Zhao, S., Zhu, W., Wu, L., Li, J., Shen, M., Lei, l., Chen, X. and Peng, C. (2018). The *Akkermansia muciniphila* is a gut microbiota signature in psoriasis. *Experimental Dermatology*, 27(2), pp. 144–149.
148. Teixeira, N. D. C., Queiroz, V. A. V., Rocha, M. C., Amorim, A. C. P., Soares, T. O., Monteiro, M. A. M., de Menezes, C. B., Schaffert, R. E., Garcia, M. A. V. T. and Junqueira, R. G. (2016). Resistant starch content among several sorghum (*Sorghum bicolor*) genotypes and the effect of heat treatment on resistant starch retention in two genotypes. *Food Chemistry*, 197, pp. 291–296.
149. Toden, S., Bird, A. R., Topping, D. L. and Conlon, M. A. (2007). Differential effects of dietary whey, casein and soya on colonic DNA damage and large bowel SCFA in rats fed diets low and high in resistant starch. *British Journal of Nutrition*, 97(3), pp. 535–543.
150. Thursby, E. and Juge, N. (2017). Introduction to the human gut microbiota. *Biochemical Journal*, 474(11), pp. 1823–1836.
151. Tsuiki, K., Fujisawa, H., Itoh, A., Sato, M. and Fujita, N. (2016). Alterations of starch structure lead to increased resistant starch of steamed rice: Identification of high resistant starch rice lines. *Journal of Cereal Science*, 68, pp. 88–92.
152. Upadhyaya, B., McCormack, L., Fardin-Kia, A. R., Juenemann, R., Nichenamelta, S., Clapper, J., Specker, B. and Dey, M. (2016). Impact of dietary resistant starch type 4 on human gut microbiota and immunometabolic functions. *Scientific Reports*, 6, pp. 1–12 (28797).
153. Valdes, A. M., Walter, J., Segal, E. and Spector, T. D. (2018). Role of the gut microbiota in

- nutrition and health. *British Medical Journal*, 361, pp. 36–44.
154. Van Laere, K. M. J., Hartemink, R., Bosveld, M., Schols, H. A. and Voragen, A. G. J. (2000). Fermentation of plant cell wall derived polysaccharides and their corresponding oligosaccharides by intestinal bacteria. *Journal of Agricultural and Food Chemistry*, 48(), pp. 1644–1652.
 155. Vasquez, N., Suau, A., Magne, F., Pochart, P. and Pélissier, M-A. (2009). Differential effects of *Bifidobacterium pseudolongum* strain patronus and metronidazole in the rat gut. *Applied and Environmental Microbiology*, 75(2), pp. 381–386.
 156. Vazquez-Gutierrez, P., de Wouters, T., Werder, J., Chassard, C. and Lacroix, C. (2016). High iron-sequestering bifidobacteria inhibit enteropathogen growth and adhesion to intestinal epithelial cells *in vitro*. *Frontiers in Microbiology*, 7(September), pp. 1–12 (1480).
 157. Vieira, A. T., Teixeira, M. M. and Martins, F. S. (2013). The role of probiotics and prebiotics in inducing gut immunity. *Frontiers in Immunology*, 4(December), pp. 1–12 (445).
 158. Vince, A., Dawson, A. M., Park, N. and O'Grady, F. (1973). Ammonia production by intestinal bacteria. *Gut*, 14(3), pp. 171–7.
 159. Vu, T. H., Bean, S., Hsieh, C-F. and Shi, Y-C. (2017). Changes in protein and starch digestibility in sorghum flour during heat–moisture treatments. *Journal of the Science of Food and Agriculture*, 97(14), pp. 4770–4779.
 160. Wall, J. S. and Blessin, C. W. (1969). Composition and structure of sorghum grains. *Cereal Science Today*, 14(8), pp. 264-271.
 161. Waterschoot, J., Gomand, S. V., Fierens, E. and Delcour, J. A. (2015). Production, structure, physicochemical and functional properties of maize, cassava, wheat, potato and rice starches. *Starch-Staerke*, 67, pp. 14–29.
 162. Watterson, J. J., Shull, J. M. and Kirleis, A. W. (1993). Quantiation of α -, β -, and γ -kafirins in vitreous and opaque endosperm of *Sorghum bicolor*. *Cereal Chemistry*, 70(4), pp. 452–457.
 163. Williams, B. A., Verstegen, M. W. A. and Tamminga, S. (2001). Fermentation in the large intestine of single-stomached animals and its relationship to animal health. *Nutrition Research Reviews*, 14(2), pp. 207-227.
 164. Wong, J. H., Lau, T., Cai, N., Singh, J., Pedersen, J. F., Vensel, W. H., Hurkman, W. J., Wilson, J. D., Lemaux, P. G. and Buchanan, B. B. (2009). Digestibility of protein and starch from sorghum (*Sorghum bicolor*) is linked to biochemical and structural features of grain endosperm. *Journal of Cereal Science*, 49(1), pp. 73–82.

165. Xiao, J., Chen, L., Johnson, S., Yu, Y., Zhang, X. and Chenn, J. (2018). Predictive modeling of microbiome data using a phylogeny-regularized generalized linear mixed model. *Frontiers in Microbiology*, 9(June), pp. 1-14 (1391).
166. Yamashita, H., Maruta, H., Jozuka, M., Kimura, R., Iwabuchi, H., Yamato, M., Saito, T., Fujisawa, K., Takahashi, Y., Kimoto, M., Hiemori, M. and Tsuji, H. (2009). Effects of acetate on lipid metabolism in muscles and adipose tissues of type 2 diabetic otsuka long-evans tokushima fatty (OLETF) Rats. *Bioscience, Biotechnology and Biochemistry*, 73(3), pp. 570–576.
167. Yang, W., Huang, L., Gao, J., Wen, S., Tai, Y., Chen, M., Huang, Z., Liu, R., Tang, C. and Li, J. (2017). Betaine attenuates chronic alcohol-induced fatty liver by broadly regulating hepatic lipid metabolism. *Molecular Medicine Reports*, 16(4), pp. 5225–5234.
168. Yatsunencko, T., Rey, F. E., Manary, M. J., Trehan, I., Dominguez-Bello, M. G., Contreras, M., Magris, M., Hidalgo, G., Baldassano, R. N., Anokhin, A. P., Heath, A. C., Warner, B., Reeder, J., Kuczynski, J., Caporaso, J. G., Lozupone, C. A., Lauber, C., Clemente, J. C., Knights, D., Knight, R. and Gordon, J. I. (2012). Human gut microbiome viewed across age and geography. *Nature*, 486(June), pp. 222–228.
169. Zakrzewski, M., Proietti, C., Ellis, J. J., Hasan, S., Brion, M-J., Berger, B. and Krause, L. (2017). Calypso: A user-friendly web-server for mining and visualizing microbiome-environment interactions. *Bioinformatics*, 33(5), pp. 782–783.
170. Zhang, J., Zhao, Y., Xu, C., Hong, Y., Lu, H., Wu, J. and Chen, Y. (2014). Association between serum free fatty disease : a cross-sectional study. *Scientific Reports*, 4(), pp. 1-6 (5832).
171. Zhu, F. (2014). Structure, physicochemical properties, modifications, and uses of sorghum starch. *Comprehensive Reviews in Food Science and Food Safety*, 13(4), pp. 597–610.

Summary

Introduction & Objectives: Some components of the plant-based foods that are consumed, are not digested by the native digestive enzymes in animals, which are prominently known as “Dietary Fiber” or resistant proteins. Albeit, the indigestible plant matter (IPMs) skip digestion by the native hydrolytic enzymes, they are known to be disintegrated by the versatile amylolytic and proteolytic enzyme repertoire of the gut microbiota, which overcast the hosts’ capabilities to unlock the substrates in IPMs. Microbiota mediated hydrolysis of IPMs is known as “colonic fermentation” in omnivores and herbivores (other than ruminants). This anaerobic catabolic process mainly produces, short-chain fatty acids (SCFA) and gases. These SCFA are known to mediate beneficial biochemical, biological and physiological benefits on hosts, for example, regulating host energy metabolism, inhibiting carcinogen synthesis and pathogenic microbial activity, reducing the risk of developing colorectal cancers and improving gut physical and immunological barrier functions, highlighting their importance in the well-being of the host. The composition and the amount of SCFA produced upon fermentation, mainly depends on the diet, by extension on the type and the amount of IPMs reaching the colon and the availability of specific microbial members to hydrolyze them. Thus, the main objective was to evaluate different IPMs originated from different sources of agricultural products and by-products on their potential to be fermented and to extend beneficial health promoting effects on host.

Materials & Methods: In Chapter 2, the digestive enzyme resistant fractions (ERFs) prepared from whole (Wh) and refined (Rf) sorghum (*Sorghum bicolor* L.) were fermented in laboratory scale simulator fermenters for 48 h. Samples obtained from fermenter media at 0, 6, 12, 24 and 48 h points were analyzed for SCFA (HPLC), ammonia-nitrogen (commercial assay kit) and microbial composition (viable plate count method and 16S rRNA gene sequencing by Illumina MiSeq) (Pelpolage *et al.*, 2019; Journal of Food and Nutrition Research). Chapters 3, 4 & 5 were short-term (4 weeks) feeding trials using Fischer 344 male rats (6 rats/ group) using raw sorghum flour (30% w/w), cooked sorghum flour (30% w/w) and sugarcane (*Saccharum officinarum* L.) bagasse water soluble fiber (BGS) diets (5% w/w) prepared according to AIN 93G diet guidelines. The two sorghum experiments were tested against α -corn starch (CON) and high amylose starch (HAS), while the sugarcane bagasse soluble fiber study was tested against a commercial xylooligosaccharides (degree of polymerization, 2-3; 95% purity) (XYO). Zoometric parameters, organ weights, serum and cecal digesta biochemical/ microbiological analyses were

conducted accordingly (Pelpolage *et al.*, 2019, Journal of Nutritional Science and Vitaminology; Pelpolage *et al.*, 2019, Food Chemistry).

Results & Discussion:

Chapter 2: Both ERF-Wh and ERF-Rf exhibited an increased rate of SCFA production between 12-24 h period, where propionate, butyrate and total SCFA contents were significantly higher in the sorghum groups compared to the negative control group. On the contrary, the content of ammonia-nitrogen, a by-product of protein fermentation showed an increasing trend 12 h onwards in the sorghum groups, where cecal pH followed a similar trend as ammonia-nitrogen, due to the basifying effect of ammonia. Moreover, the characteristic microbial genera in the two sorghum groups were dominated by probiotic lactic acid bacteria. The observations in this study suggested that the higher SCFA production in sorghum groups could have been due to the resistant protein fermentation by some members of lactic acid bacteria.

Chapter 3: Cecal SCFA contents (individual and total) in the two sorghum fed groups were significantly lower than the positive control (HAS) and similar to that of the negative control (CON). Cecal pH and ammonia-nitrogen content followed the same trend observed in the Chapter 2, suggesting a prominent protein fermentation. Similarly, microbial composition also further supported the protein fermentation hypothesis by the higher abundance of potential protein fermenters in the sorghum fed groups, in contrast to the resistant starch fermenters in the positive control group. But the secondary data obtained from Pearson's correlation analysis exhibited several important trends related to colonic fermentation, for example, positive correlation between total SCFA content and cecal weight and negative correlations between total SCFA content and pH.

Chapter 4: Cooked refined sorghum fed rats cecal SCFA contents were comparatively higher compared to both whole sorghum and control (CON) diet fed rats, especially the butyrate content was statistically similar to that of the positive control group (HAS). Compared to raw sorghum fed groups (Chapter 3), the SCFA production was improved in the cooked sorghum fed groups. Further, the gut microbiota of cooked sorghum fed rats were dominated by genus *Ruminococcus* prominently known to utilize resistant starch and dietary fiber. Mucin and immunoglobulin A (IgA) synthesis were also improved in the cooked sorghum groups compared to their raw counterparts and were either comparatively or significantly higher than that of the positive control. Moreover, several beneficial trends such as lower final body weight, body

weight gain, feed intake, visceral fat mass and higher fecal bile excretion were observed in the cooked sorghum fed groups compared to the negative control.

Chapter 5: SCFA production in BGS fed rat cecum was significantly higher in terms of acetate content and butyrate content compared to the positive control (XYO) and the negative control (CON), respectively. Cecal pH and cecal weights also reflected the higher SCFA production in BGS group. Mucin and IgA synthesis were also significantly higher in the BGS group suggesting its beneficial effects on the gut barrier function. These beneficial effects were further supported by the gut microbial composition, where the BGS group was dominated by *Blautia*, an acetogenic bacteria and with a higher abundance of *Akkermansia*, a mucin utilizing bacteria known to improve mucin synthesis. BGS showed either comparatively or significantly higher fermentation ability compared to the positive control group.

General Conclusions: As observed in Chapters 2 and 3, sorghum exhibited a moderate influence on colonic fermentation, and effects on microbiological and physiological benefits. On the other hand, cooking of sorghum improved its potential to be fermented in the colon and also the mediated beneficial effects, such as improved SCFA production, higher mucin and IgA production and beneficial microbial member abundance. Sugarcane bagasse soluble fiber exhibited a superior colonic fermentation ability in comparison to a well-established commercial prebiotic. With reference to the primary objective, which was, “to evaluate different IPMs originated from different sources of agricultural products and by-products on their potential to be fermented and to extend beneficial health promoting effects on host”, it was clear that the IPMs from different botanical sources (agricultural products and by-products), differed in the nature of colonic fermentation, metabolite content and mediated benefits, attributed to their inherent physicochemical properties and processing history.

学 位 論 文 要 旨

背景と目的：植物由来のいくつかの成分は動物の消化酵素では消化されず、それらは“食物繊維”もしくは“難消化性タンパク質”として知られている。非消化性の植物成分（IPMs）は加水分解酵素で消化されないが、腸内細菌叢の酵素によって分解される。雑食動物や草食動物において、腸内細菌叢による IPMs の加水分解は腸内発酵として知られている（その他に反芻動物など）。この嫌気的な異化作用は主に短鎖脂肪酸（SCFA）やガスを産生する。SCFA は、宿主のエネルギー代謝の調節、発がん物質合成や病原菌活性の阻害、大腸がん発症のリスク低減、腸の物理的免疫学的バリア機能の向上など、有益な生化学的、生物学的、生理学的な影響を宿主に与えることが知られている。大腸発酵により産生される SCFA の組成や量は、主に大腸に届く IPMs の種類および量や、それらを加水分解する特定の細菌の能力に依存する。したがって、本研究の目的は様々な農産物および農産副産物由来の異なる IPMs の発酵特性や宿主への有益な健康促進効果を評価することである。

材料と方法：Chapter 2 において、全粒（Wh）および精白（Rf）されたソルガム（*Sorghum bicolor* L.）から難消化性画分（ERFs）を調製して、それを培養槽で 48 時間発酵させた。0,6,12,24,48 時間経過後に培養液を採取して SCFA、アンモニア態窒素および細菌叢組成（寒天培地法および 16S rRNA 遺伝子シーケンス）の分析に使用した。Chapters 3, 4, 5 では、Fischer 344 雄性ラット（1 群 6 匹）を用いて AIN93G 準拠の生ソルガム食（30% w/w）、湿熱処理ソルガム食（30% w/w）、サトウキビ（*Saccharum officinarum* L.）バガス水溶性繊維（BGS）食（5% w/w）を 4 週間給餌した。2 つのソルガム試験では対照として α -コーンスターチとハイアミローススターチ（HAS）が使用され、サトウキビバガス水溶性繊維試験ではキシロオリゴ糖（重合度 2-3; 95%純度）（XYO）が対照として使用された。

結果と考察：

Chapter 2：ERF-Wh と ERF-Rf の両試験区は培養 12-24 時間の間の SCFA 産生を増加させ、プロピオン酸、酪酸および総 SCFA 産生は両ソルガム試験区で対照区より有意に増加した。タンパク質発酵の副産物であるアンモニア態窒素産生は、両ソルガム試験区で培養 12 時間以降に増加傾向が示され、アンモニアの塩基性のために pH が上昇した。さらに、両ソルガム試験区で乳酸生成菌が優勢となった。本試験における知見は、ソルガム試験区での高い SCFA 産生はいくつかの乳酸菌による難消化性タンパク質の発酵によるものである可能性を示唆した。

Chapter 3 : 両ソルガム群の盲腸内 SCFA 量は HAS 群より有意に低く、コントロール群と同程度であった。盲腸 pH とアンモニア態窒素量は Chapter 2 と同様の傾向であり、タンパク質発酵による影響が示唆された。同様に、両ソルガム群でタンパク質分解菌の占有率が高かったことから、細菌叢組成もタンパク質発酵の仮説を裏付けた。しかし、ピアソンの相関分析は総 SCFA 量と盲腸重量との間に正の相関を示し、総 SCFA 量と pH の間に負の相関を示した。

Chapter 4 : 湿熱処理した精白ソルガムを摂取したラット盲腸 SCFA 量は、全粒ソルガム群およびコントロール群より高く、特に酪酸量は HAS 群と統計的に同程度であった。生のソルガム摂取と比較して (Chapter 3)、SCFA 産生は湿熱処理ソルガムの摂取により向上された。さらに、湿熱処理ソルガム摂取ラットの腸内細菌叢は、難消化性デンプンおよび食物繊維を利用することが知られる *Ruminococcus* 属が優勢であった。ムチンおよび免疫グロブリン A (IgA) 合成は湿熱処理ソルガム群で生ソルガム群より向上し、HAS 群と同等以上であった。さらに、最終体重、体重増加量、摂食量、脂肪組織重量の低下および糞中胆汁酸排泄の増加などのいくつかの有益な傾向が、コントロール群と比べて両湿熱処理ソルガム群でみられた。

Chapter 5 : BGS 群の盲腸酢酸および酪酸産生は、XYO 群およびコントロール群よりそれぞれ有意に増加した。BGS 群の盲腸 pH と盲腸重量は高い SCFA 産生を反映した。ムチンと IgA 合成は BGS 群で有意に増加し、腸管バリア機能における有益な効果が示唆された。これらの有益な効果は腸内細菌叢組成の結果からも支持され、BGS 群では酢酸産生菌の *Blautia* 属や、ムチンを利用しムチン合成を向上させる *Akkermansia* 属が優勢となった。また BGS は XYO と比較して同等以上の高い発酵特性を示した。

まとめ : Chapter 2 および 3 でみられたように、ソルガムは細菌叢や生理的特性に有益な影響を示した。一方で、ソルガムの湿熱処理は大腸での発酵を向上させ、SCFA、ムチンおよび IgA 産生の向上や有益な細菌の増加などを示した。Chapter 5 では、BGS は有益なプレバイオティクスと比較してもより優れた腸内発酵特性を示した。“様々な農産物および農産副産物由来の異なる IPMs の発酵特性や宿主への有益な健康促進効果を評価すること”とした目的で行った今回の試験結果では、異なる植物原料由来の IPMs (農産物および農産副産物) はそれら固有の物理化学特性や加工のされ方に起因して、腸内発酵特性、代謝産物およびそれらに関連する有益な効果を変化させることが明らかになった。